Asymmetric Catalysis of Ionic 1,2-Rearrangements

HARVARD UNIVERSITY
Graduate School of Arts and Sciences

DISSERTATION ACCEPTANCE CERTIFICATE

The undersigned, appointed by the

Department of Chemistry & Chemical Biology

have examined a dissertation entitled:

Asymmetric Catalysis of Ionic 1,2-Rearrangements

presented by: Hayden Anil Sharma

candidate for the degree of Doctor of Philosophy and hereby certify that it is worthy of acceptance.

Signature _____
Typed name: Professor Eric N. Jacobsen

Signature _____
Typed name: Professor Emily P. Balskus

Signature _____
Typed name: Professor Brian B. Liau

Date: 16 November 2021

Asymmetric Catalysis of Ionic 1,2-Rearrangements

A dissertation presented by

Hayden Anil Sharma

to

The Department of Chemistry and Chemical Biology

in partial fulfillment of the requirements

for the degree of

Doctor of Philosophy

in the subject of

Chemistry

Harvard University

Cambridge, Massachusetts

November 2021

Dissertation Advisor: Eric N. Jacobsen *Hayden Anil Sharma*

Asymmetric Catalysis of Ionic 1,2-Rearrangements

Abstract

In Chapter 1, we report the development and study of an aryl-iodide-catalyzed Wagner–Meerwein rearrangement reaction. This process converts styrenes bearing cumyl, *t*-butyl, and *i*-propyl substitution into enantioenriched 1,3-difluorinated molecules. Hammett analysis, KIE experiments, and DFT calculations revealed that these reactions proceed through distinct selectivity-determining steps that depend on the nature of the migrating group. Substrates bearing aryl migrating groups proceed via selectivity-determining rearrangement, whereas those with methyl migrating groups proceed via selectivity-determining fluorination. Both mechanisms are controlled with high selectivity by the same chiral aryl-iodide catalyst, providing a compelling illustration of generality across reaction mechanisms in asymmetric catalysis.

In Chapter 2, we detail the discovery of a catalytic strategy for controlling Matteson rearrangements with enantioselectivity. These reactions transform dichloromethane and organoboron pinacol esters into α-chloro boronic esters, versatile carbon building blocks that can undergo two stereospecific elaborations to afford molecules bearing trisubstituted stereocenters with myriad substitution patterns. While initial explorations centered around the use of hydrogen-bond donors (HBDs) as catalysts, we discovered that lithium-isothiourea-boronate complexes—formed via reaction of thioureas with the substrate in initial optimization studies—catalyze the rearrangement with extraordinary levels of enantioselectivity. These lithium boronate salts were characterized by NMR, IR, and solid-state studies to reveal a well-defined structure featuring a

five-membered lithium chelate with the cation located in a highly dissymmetric pocket. Supported by NMR and DFT experiments, the catalyst is proposed to promote rearrangement through a dual–lithium-induced chloride abstraction mechanism.

In Chapter 3, we disclose the application of a new method for the measurement of ^{13}C Kinetic Isotope Effects (KIEs) at natural abundance using ^{1}H NMR. This method leverages single quantum suppression in the ^{1}H spectrum (SQUASH) to effectively delete the main ^{1}H–^{12}C peak from the proton spectrum, enabling accurate and precise measurements of the integrals of the ^{1}H–^{13}C satellite peaks. KIEs were calculated using relative integrations of the ^{12}C–H parent peak, measuring using standard ^{1}H NMR, and ^{13}C–H satellite peaks, measured using SQUASH. Three reactions—phenol methylation, benzaldehyde reduction, and cinnamate epoxidation—were analyzed to showcase the general utility of this tool. As ^{1}H NMR sensitivity is approximately 64-fold greater than that of ^{13}C, this method potentially enables up to a 4,096-fold reduction in acquisition time, potentially transforming natural abundance carbon KIE experiments into routine experiments to employ in fundamental mechanistic studies.

Table of Contents

Acknowledgements

First and foremost, I would like to thank Eric Jacobsen. I feel immeasurably blessed to have had the opportunity to work with Eric these past five years. He is a fantastic thinker and scholar, and his critical approach to problem selection and data interpretation has become ingrained in my head (so much so that now I use the phrase “consistent with” far more often than the average person). I appreciate that Eric established the framework to succeed while encouraging me to figure out what to do independently. I am grateful that he has cultivated an environment filled with numerous talented and helpful people; because of Eric’s leadership and personnel selection process, the Jacobsen lab is a chemist’s paradise—a place for critical, creative, mechanistically minded chemists to come together driven purely by their passion for chemistry. Moreover, I am thankful for the specific efforts that Eric put into mentoring me; he has lavished genuine encouragement and praise mixed with sharp criticism and guidance at every point of this journey. His commitment to clarity in communication paired with his honest feedback on my presentations have been crucial to my growth as a scientist. He has poured many hours into helping me be a better mentor and teacher, both by sharing the wisdom he has accrued as an advisor and by providing a direct example. Most of all, I appreciate how much Eric embraced the role of a mentor in counseling me through painful parts of my life, asking me for help and advice when needed, retelling great stories of times past, sharing in/embracing the fun/humorous parts of lab life (i.e. pcl cat), and always trying to support the growth of me as a person. I cherish Eric’s kindness and our rapport, and I can only hope to leave such an impact on those I mentor in the future. I will be forever grateful, Eric.

I would like to think Professors Brian Liau, Emily Balskus, and Ted Betley for serving on my thesis committee. Each one of them has provided helpful guidance, whether it be specific experiments to try that helped us uncover the nature of the LIT boronate catalysts, advice for constructing proposals, and tips for doing a postdoc in a completely different area of science. It is a gift to be able to learn from such talented scientists, and I appreciate the time they have taken to mentor me. On a different note, I also thank Ted for giving me the confidence to embrace the bald-and-bearded aesthetic. I will take all these lessons forward with me in my career.

Nicole Minotti is a stellar admin who keeps this ship running. She has made doing research in this lab an incredibly smooth process, and I am thankful that she has been a consistent presence throughout my PhD. Moreover, Nicole is a deeply engaging and caring human being. I fondly remember hours of conversation thinking about life, psychoanalyzing the lab, and just generally goofing around together. She is the cheese fairy every researcher needs in their life. Thank you for a great five years, Nicole.

This time would mean nothing without the great people who have taught me and showed me love these past five years. I have been blessed with the squad of Dennis, Amanda Waterbury, Josh Cox, Alex Peterson, Allison Siegenfeld, and Dan Pollack. Dennis is one of the people who set the tone for the lab with his pure love for chemistry paired with his desire to make the lab (and world) into a more peaceful place. The amount of laughs and general hijinks (some of which I know will come out during the roast) we shared provided me with immense joy these past few years. It's been a really real ride, starting at our Princeton visit weekend and hopefully continuing on through our careers. It will be sad moving away, but I know we will always be brothers. Amanda is a driven, indefatigable, inquisitive scientist who has taught me some biology, but even more than that, has enriched my time here with her kindness, snark, and friendship. Josh has always brought fun and general chaos into my life, and I have appreciated our goofing off as well as our consistent philosophy phridays/Sundays. Alex is a sharp scientist who has provided much needed bro influence in my life. I am thankful for our chats about chemical biology, our times drinking beer and eating meat, and 4+ great years of living together. Allison and Dan are two of the sweetest people with whom I have spent these past few years, and I am grateful for their sincere and unswerving kindness as well as their infectious sense of humor.

When I was younger, there were many older students and postdocs who befriended me and helped me grow in ways that I cannot repay. I am thankful for my mentor Katrina, who gave me a project to work on and pushed me to do my best. She provided good advice while also giving me to space to grow from my own mistakes. Much appreciation goes out to Sam Levi, who brought me under his wing during the rotation and was always there to provide advice, entertainment, and support during my first few years. He is one of the most generous people I know, and I am thankful that we've remained good friends since his graduation.

Mark Levin was crucial to my growth as a chemist and to my experience in the Jacobsen lab. Mark's ridiculous and hilarious sense of humor, sharp mind, and talent as a teacher made those first few years all the richer. His ability to critique an idea while simultaneously making you feel like the smartest person in the world is something I can only strive to implement. Eugene Kwan taught me a lot about being curious while asking fundamental questions. As a young student, I was inspired by Eugene's meticulous, patient approach to interesting mechanistic problems, which I have tried my best to emulate ever since. I consider myself fortunate enough to have collaborated with him directly on multiple occasions, and I am grateful for the hours he poured into teaching me how to think and write. I am thankful for Dan Strassfeld, who is one of the most critical and passionate scientists I know, and who planted the seeds of rigorous physical-organic analysis in my mind. I often find myself asking "what would Dan say" during mechanistic discussions (sometimes to my chagrin). I am grateful for Andrew Mayfield, who often followed up after failed subgroups of mine with gentle nudges or challenges; his willingness to help a much younger, completely confused student learn to communicate ideas shaped my approach to how I talk about my work. Alison and Zach were examples of successful scientists who were always willing to give guidance and lend excitement; I distinctly remember how enthusiastic Alison got after I shared the initial boronate rearrangement "hit" with her, which was a huge encouragement to younger, uncertain me.

In many ways, the best part of grad school has been getting to know, work with, and learn from the younger students. I am indebted to my one-time mentee and teammate Jake, who decided to go all-in with a chaotic, still green 3rd year on an exciting, perplexing project. Jake brought a unique determination and set of chemical insights that were crucial for the success of the boron project, and I am excited to see where these gifts take him in the future. His hawk-like attention to detail was a blessing during multiple parts of this project, especially at the end. In a different vein, I am particularly thankful for the grace Jake showed me in the process of learning how to be a mentor (a process that is still very much ongoing) and the patience he exercised during the frustrating portions of our project. Jake is a kind man who wants to see good done, and I eagerly await to see the impact his inquisitive, tender soul has on the world. It was a gift to embrace Jake as a true partner for so many years.

I felt so lucky when Sam decided to join the B-hive, and I still feel that way as I write this now. Sam has a special blend of chemical ability, communication skills, and fun attitude that have carried her far and make it a joy to work with her. She learns from every experience, even the hard ones, displaying her resilience and humility. Additionally, Sam understands the importance of living a balanced life; her ability to iteratively make new scientific discoveries while pursuing this balance is a skill that I hope continues to bring her success and happiness. I am thankful for the time we've had together, for the ways in which we've been able to push each other, and for her patience and advice for me as a mentor. While she is still young, it is clear that she will continue to accomplish great things in her career.

I am grateful to have spent much time surrounded by talented, wise, and kind younger students. John (who, along with Liz, is not much younger) is both critical and perpetually helpful. He has a knack for bringing out the best ideas and for pushing projects in just the right way—I harken back to our lunch convo that birthed the boron project, the synthetic suggestions that became key examples in our paper, and other helpful one-on-one conversations. I am also thankful for the ways in which John has sacrificed to steer the lab. One example of his leadership comes from the pandemic; during a time of confusion, purposelessness, and isolation, he worked hard to keep our little community safe, productive, and connected. I am excited to see how his chemical insight and servant leadership impact his career and the field. Liz is a fun, passionate, orderly presence who provided much needed balance in chaotic M202c. She is a smart chemist who can learn just about anything, a trait that will carry her through her career. I am thankful for the global impact Katherine has had on my time in the group. She has an insatiable curiosity paired with an inexorable drive that propels her forward through the ether of chemistry, something that I will forever attempt to imitate. She may work on her project alone, but she is very collaborative in providing clever ideas, criticism, and encouragement for any who ask. She showers the lab with baked goods and enthusiastic comic relief and provides a reliable and kind ear. Endless hours of conversation with her have taught me much about chemistry, human nature, and myself, things that I will hold onto tightly for the rest of my life. Martin has been integral to my PhD in many ways. He is a smart, curious soul who brings a level of questioning that demands thoughtful answers. Martin also has a kindness and desire to be helpful—he

has fixed so many different machines and resolved so many different computer problems. Corin is one of the most thoughtful and mature people I know, and I am thankful for the friendship we have built during the crepuscular time of my PhD. His brilliance is manifold, and his contributions to the lab are myriad. He is incisively critical, intellectually agile, and refreshingly original, which makes conversations about chemistry and life both fun and rewarding. I also appreciate Corin's generosity, wisdom, and earnest friendliness, which I have leaned on much this past year. Petra is deeply inquisitive and industrious; her drive to unravel the way things work is inspirational. Additionally, her relentless, upstanding commitment to keeping the group running smoothly (e.g. returning NMR tubes from the autosampler to the owner, fixing and maintaining cryocools, etc.) has been a huge blessing to me throughout my time in the group. I am thankful to have overlapped with Peyton, who is a chill, curious, and unstoppable scientist. His ability to learn about something and then turn around and ask great questions is a gift to him and those around him. It was a ton of fun to hang with Nour (whose nickname bears the initials "dr" even though she is not a doctor), who is a bundle of joy, snark, and memes. She embodies all the best aspects of a trumpeter. If she brings her energy and intellect with her to everything she tries, I know she will succeed.

Even as I have gotten older, I have been blessed to be surrounded with senior chemists who have continued to teach me numerous skills and enrich my time. I am grateful for Joe, who has taught me much these past few years. Joe's thoughtful, measured, clear style of communication showcases how deeply he thinks about problems while also effectively engaging his listener. Whenever I am having trouble explaining something, I ask myself "how would Joe explain this?" and it *always* helps. I also appreciate Joe's commitment to "ruling-out" experiments and critical mechanistic analysis in general. Orthogonally, he is cleverly able to string together different parts of his brain to come up with compelling, creative ideas. It will be cool to see all these skills come together as a prof. Mel is both incisively critical and deeply kind; her ability to dole out constructive feedback in such an affirming, caring way provides a model that I will try to follow the rest of my career. I am grateful for the conversations we've had about both of our projects as well as for her feedback on this thesis. She is astute, observant, and persistent, and I am excited to see where she ends up next. I am thankful for Elias, who has been a well of unyielding kindness, good-natured

fun, and chemical insight these past few years. I've learned a lot from (and been seriously pushed by) his synthetic mindset and acumen, and I'm excited for his students to get to absorb his intellect and skills. Diego embodies the ideal of a kind mentor and of a hardworking, creative chemist. His willingness to teach anyone anything he knows is inspiring, and his patient pursuit of his clever ideas provides a great example of confidence and resilience. Mayuko's combination of hard work, chemical intuition, and charming sweetness makes it a joy to share the lab with her. I appreciate that she always wants to share the most exciting things! I am thankful for Gabe's support for the boron project as well as his general effervescence, both which were crucial in finishing and communicating the boron work. He is an excited researcher with a drive to succeed.

In addition to the chemists in the Jacobsen Lab, I am also thankful for my undergraduate mentor, Dr. Todd Hovey. Todd taught the fundamentals while also letting me make my own mistakes. He is patient and kind while also being incredibly smart and passionate about chemistry. Todd's manifest desire to innovate and create provided an early spark of curiosity for me that has grown into a full-fledged passion for chemistry. I am very excited to see his career at Abbvie grow!

My family is my rock. Thank you for always calling me, welcoming me back home, caring for me when times were hard, celebrating with me when times were good, joking around, working through life and relationships together, sending me small gifts/cards/notes, and much more. Thank you especially to my parents for your steadfast love and support, for raising me to value myself by things other than my performance or the opinions of others, and for always encouraging and enabling me to pursue my passions. There are endless things that I appreciate about my family that I do not have the space to share in this format.

I am overwhelmed with thankfulness for my non-Harvard friends who've provided a continual source of love, companionship, support, and humor, among other things. Michael (Big Mike) and Shelby, Phil and Julia, Nikhil, Chelsea, and many others have all been key figures these past 5+ years. I would not be the person I am today without you all. Thank you for helping me through the best and worst of times in grad school, I will forever have a place for you all in my heart.

List of Abbreviations

9BBN	9-borabicyclo[3.3.1]nonane
$[\alpha]_D^T$	specific rotation at T (°C) and 589 nm
Å	Angstrom
Ac	acetyl
aq.	aqueous
alk	alkyl
Ar	aryl
B3LYP	Becke-3-Lee-Yang-Parr
Bn	benzyl
BRSM	based on recovered starting material
Bu	butyl
Bz	benzoyl
˚C	degree Celsius
c	centi
cis	on the same side
Conv.	conversion
CPA	chiral phosphoric acid
CPME	cyclopentyl methyl ether
cy	cyclohexyl
d	chemical shift in parts per million
d	day(s); doublet (spectral)
Δ	change
d.r.	diastereomeric ratio
DCM	dichloromethane

DFT	density functional theory
(DHQD)2PHAL	hydroquinidine 1,4-phthalazinediyl diether
DIPEA	*N*,*N*-diisopropylethylamine, Hünig's base
DMAP	4-(N,N-dimethylamino)pyridine
DMSO	dimethyl sulfoxide
dppf	bis(diphenylphosphino)ferrocene
E	*Ger., entegen*, opposite
e.e.	enantiomeric excess
ent	enantiomeric
Equiv.	equivalents
e.r.	enantiomer ratio
ESI	electrospray ionization
Et	ethyl
EtOAc	ethyl acetate
eq.	equivalent
FT	Fourier-transform
FTIR	Fourier-transform infrared spectroscopy
g	gram
gem	geminal
h, hr	hour(s)
HBD	hydrogen-bond donor
HMDS	hexamethyldisilazide
HPLC	high performance liquid chromatography
HRMS	high resolution mass spectrometry
Hz	hertz

i	iso
IR	infrared
J	coupling constant
k	rate constant
KIE	kinetic isotope effect
L	liter(s)
LG	leaving group
m	micro
m	meta
m	meter; milli; multiplet(spectral)
M	molar
M06-2X	Minnesota 2006 hybrid meta density functional theory
Me	methyl
min	minute(s)
mol	mole
MQF	multiple quantum filtered ^{19}F NMR
MS	mass spectrometry
MTBE	methyl *tert*-butyl ether
n	normal
$NABH_4$	sodium borohydride
NMR	nuclear magnetic resonance
Neop	Neopentyl glycol
o	ortho
OTf	trifluoromethanesulfonate
p	para

Ph	phenyl
Pin	pinacol
PMB	*para*-methoxybenzyl
Pr	propyl
q	quartet (spectral)
R	rectus
r.r.	regioisomeric ratio
rt	room temperature
S	sinister
salen	2,2'-ethylenebis(nitrilomethylidene)diphenol, N,N' ethylenebis(salicylimine)
S_N1	unimolecular nucleophilic substitution
S_N2	bimolecular nucleophilic substitution
SQUASH	single quantum suppression ^{1}H NMR
STAB	sodium triacetoxyborohydride
t	*tert*, tertiary
t	time
T	temperature
TEA	triethylamine
TFA	trifluoroacetic acid
TMEDA	*N*,*N*,*N*',*N*'-tetramethylethylenediamine
trans	on the opposite side
TBAF	tetrabutylammonium fluoride
TfOH	triflic acid
THF	tetrahydrofuran
TMS	trimethylsilyl

Ts	tosyl
TS	transition state
xantphos	4,5-Bis(diphenylphosphino)-9,9-dimethylxanthene
Z	*Ger. zusammen*, together

Chapter 1

Enantioselective Aryl-Iodide-Catalyzed Wagner–Meerwein Rearrangements[1]

1.1 Introduction

Hypervalent-iodine compounds are widely employed reagents and catalysts that leverage the highly reactive, transition-metal-like character of I(III) or I(V) centers.[2] In this project, we exploit the cationic nature of alkene-iodonium complexes and alkyl iodane intermediates to effect catalytic, enantioselective carbocationic rearrangements. The developed reactions provide a rare example of Wagner–Meerwein rearrangements involving non-heteroatom-stabilized carbocations,

[1] This work was done in collaboration with Dr. Katrina Mennie and Dr. Eugene Kwan. Portions of this chapter have been reproduced or adapted from: Sharma, H. A.; Mennie, K. M.; Kwan, E. E.; Jacobsen, E. N. Enantioselective Aryl-Iodide-Catalyzed Wagner–Meerwein Rearrangements. *J. Am. Chem. Soc.* 2020, 142, 16090–16096.

[2] Yoshimura, A.; Zhdankin, V. V. Advances in Synthetic Applications of Hypervalent Iodine Compounds. *Chem. Rev.* **2016**, *116*, 3328–3435.

highlighting the extreme activating power of iodonium species. Hammett and kinetic isotope effect studies, in combination with computational investigations, reveal that two different mechanisms are operative in these rearrangement reactions, with the pathway depending on the identity of the migrating group. In reactions involving alkyl-group migration, intermolecular fluoride attack is product- and enantio-determining. In contrast, reactions in which aryl rearrangement occurs proceed through an enantiodetermining intramolecular 1,2-migration prior to fluorination. The fact that both pathways are promoted by the same chiral aryl iodide catalyst with high enantioselectivity provides a compelling illustration of generality across reaction mechanisms in asymmetric catalysis.

1.2 Background: Enantioselective Alkene Fluorofunctionalization Reactions Catalyzed by Chiral Hypervalent Aryl Iodides

Hypervalent-iodine compounds are strong π-acids that can coordinate to alkenes and render them electrophilic for attack by nucleophiles, including weak nucleophiles such as fluoride (Fig. 1.1A). The first report of alkene fluorination mediated by hypervalent iodine reagents was disclosed by Dimroth and Bockemüller in 1931, which involved the difluorination of a 1,1-diphenyl-substituted alkene (Fig. 1.1B).[3] However, Dimroth and Bockemüller initially misassigned the product of this reaction as a 1,2-difluoride, and it was not until 1963 that Borstein and coworkers correctly assigned the structure of the product as the 1,1-difluoride. [4,5] This product

[3] Dimroth, O; Bockemüller, W. Versuche zur Fluorierung organischer Verbindungen, I. Die Einwirkung von Blei(IV)-fluorid auf einige organische Verbindungen *Ber.* **1931,** *64*, 516–522.

[4] Borstein, J.; Borden, M. R.; Nunes, F.; Tarlin, H. I. Rearrangement Accompanying the Addition of Fluorine to 1,1-Diarylethylenes. J. Am. Chem. Soc. **1963**, *85*, 1609–1615.

[5] Carpenter, W. Aryliodosodifluorides. *J. Org. Chem.* **1966**, *31*, 2688–2689.

putatively arises from the competitive attack of the phenyl ring on the alkyl iodane formed after the initial fluorination, which gives rise to a phenonium that can be opened by fluorine at the original site of fluorination. The actual 1,2-difluorination of alkenes was not discovered until 1998, when Yoneda and Hara disclosed the difluorination of aliphatic alkenes which undergo sequential fluorinations rather than a fluorination-rearrangement-fluorination sequence (Fig. 1.1C). [6]

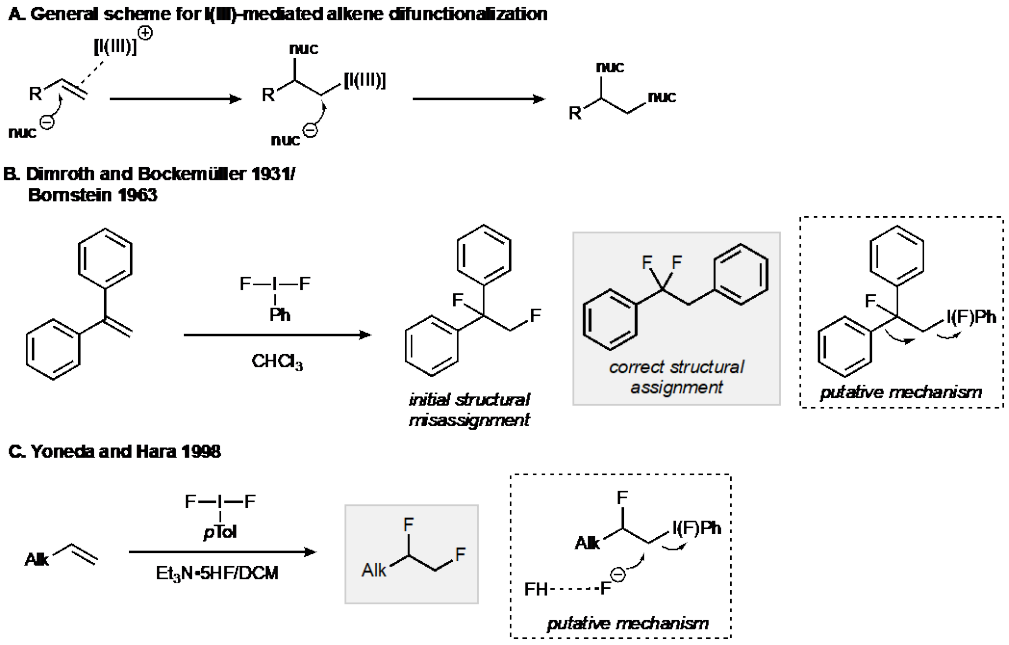

Figure 1.1 Seminal examples of alkene 1,1- and 1,2-difluorinations mediated by aryliodosodifluorides

In principle, only catalytic quantities of the hypervalent iodine compound or precursor are necessary if a stoichiometric terminal oxidant is employed. Achieving catalysis in this manner would require the oxidant to preferentially react with the iodane/iodane rather than the substrate.

[6] Hara, S.; Nakahigashi, J.; Ishi-I, K.; Sawaguchi, M.; Sakai, H.; Fukuhara, T.; Yoneda, N. Difluorination of Alkenes with Iodotoluene Difluoride. Synlett **1998**, 495–496.

This goal was initially achieved by the labs of Kita[7] and Ochiai[8] in the catalytic oxidation of phenols and ketones, respectively, which used *m*CPBA as the terminal oxidant (Fig. 1.2). The Yan lab reported the extension of this principle to alkenes in 2009 in the form of a catalytic oxy-sulfonylation.[9]

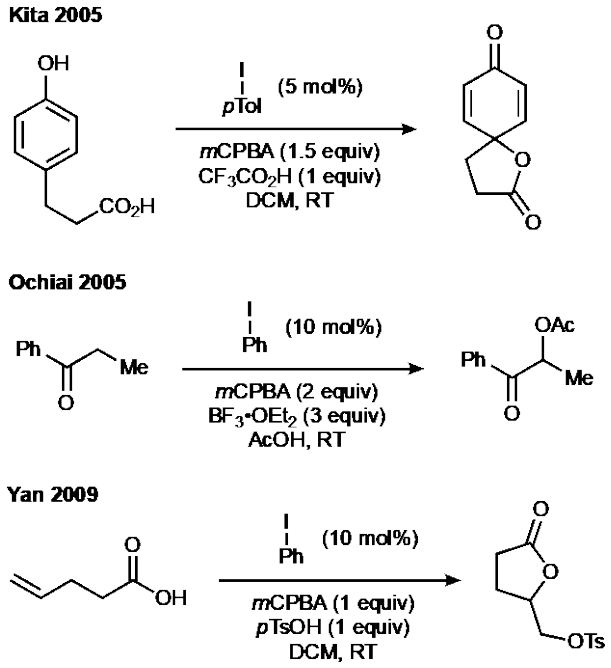

Figure 1.2 Seminal examples of catalytic I(III)-mediated oxidation reactions

Despite the longstanding history of I(III)-mediated fluorinations and the relatively similar catalytic principles, I(III)-mediated alkene difluorination reactions were not rendered catalytic until more recently. Initial reports of aryl-iodide-catalyzed alkene 1,2-difluorination were

[7] Dohi, T.; Maruyama, A.; Yoshimura, M.; Morimoto, K.; Tohma, H.; Kita, Y. Versatile Hypervalent-Iodine(III)-Catalyzed Oxidations with m-Chloroperbenzoic Acid as a Cooxidant. *Angew. Chem. Int. Ed.* **2005**, *44*, 6193 –6196.

[8] Ochiai, M.; Takeuchi, Y.; Katayama, T.; Sueda, T.; Miyamoto, K. *J. Am. Chem. Soc.* **2005**, *127*, 12244 – 12245.

[9] Yan, J.; Wang, H.; Yang, Z.; He, Y. An Efficient Catalytic Sulfonyloxylactonization of Alkenoic Acids Using Hypervalent Iodine(III) Reagent. *Synlett* **2009**, *16*, 2669–2672.

disclosed independently by the labs of Jacobsen[10] and Gilmour[11] in 2016 (Fig. 1.3A). These reactions leveraged simple aryl iodide precatalysts, *m*CPBA as the stoichiometric oxidant, and either py(HF)$_9$ or Et$_3$N(HF)$_3$ as the fluoride source/acid activator. The Jacobsen lab also discovered that these reactions give rise to 1,2-difluorinated products in fair to excellent diastereoselectivities, either via stereospecific displacement of the nascent alkyl iodane by fluoride or by anchimeric assistance (i.e. trapping by an amide) followed by displacement of the trapping group by fluoride (Fig. 1.3B).

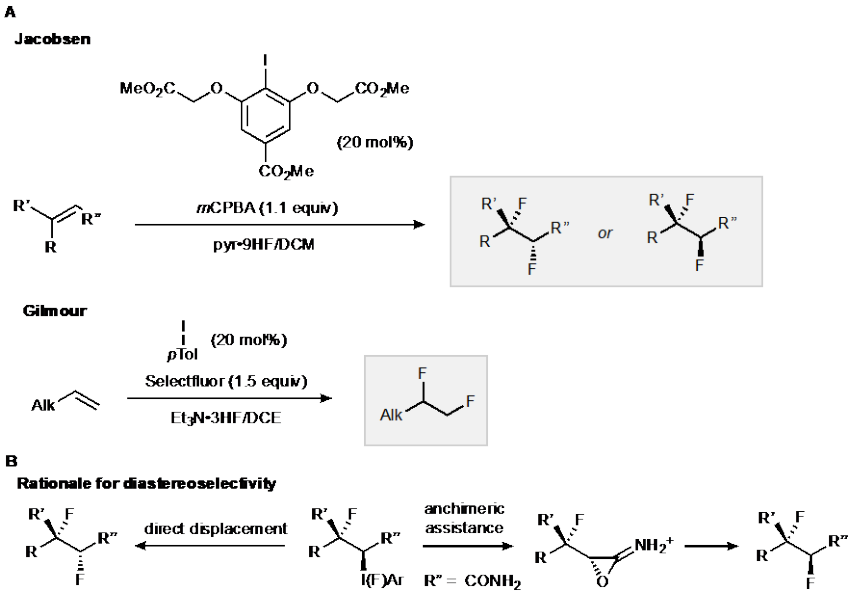

Figure 1.3 Seminal reports of I(III)-catalyzed alkene difluorination reactions

The development of aryl-iodide-catalyzed reactions makes the use of valuable iodoarene derivatives more cost-effective, enabling the application of chiral hypervalent-iodine species to facilitate catalytic, enantioselective difunctionalization reactions. The most common catalyst

[10] Banik, S. M.; Medley, J. W.; Jacobsen, E. N. Catalytic, Diastereoselective 1,2-Difluorination of Alkenes. *J. Am. Chem. Soc.* **2016**, *138*, 5000–5003.

[11] Molnár, I. G.; Gilmour, R. Catalytic Difluorination of Olefins. *J. Am. Chem. Soc.* **2016**, *138*, 5004–5007.

scaffold that effectively mediates many types of I(III)-catalyzed oxidation reactions was first reported by Ishihara for the catalytic oxidation of 1-naphthols (Fig. 1.4).[12,13] This C2-symmetric aryl iodide derivative has been broadly applied to alkene fluorination reactions, and was first used in superstoichiometric quantities for an enantioselective intramolecular aminofluorination reaction reported by Nevado.[14] The Jacobsen lab extended this work to the enantioselective 1,1- and 1,2-difluorination of cinnamamide and styrene derivatives, respectively (Fig. 1.5).[15] Key to this extension was the use of α-benzyl-substituted catalysts, which afforded products in significantly higher levels of selectivity than the previously reported α-methyl-substituted catalysts.

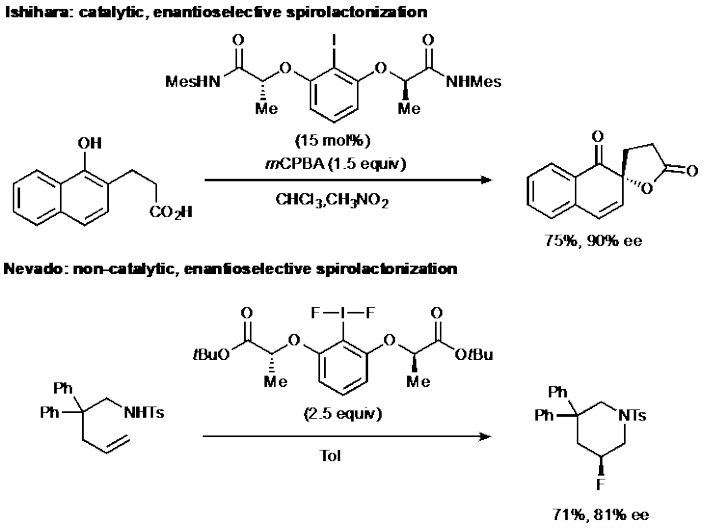

[12] Uyanik, M.; Yasui, T.; Ishihara, K. Enantioselective Kita Oxidative Spirolactonization Catalyzed by In Situ Generated Chiral Hypervalent Iodine(III) Species. *Angew. Chem., Int. Ed.* **2010**, *49*, 2175–2177.

[13] Uyanik, M.; Yasui, T.; Ishihara, Y. K. Chiral hypervalent iodine-catalyzed enantioselective oxidative Kitaspirolactonization of 1-naphthol derivatives and one-pot diastereo-selectiveoxidation to epoxyspirolactones. *Tetrahedron* **2010**, *66*, 5841–5851.

[14] Kong, W.; Feige, P.; de Haro, T.; Nevado, C. Regio- and Enantioselective Aminofluorination of Alkenes. *Angew. Chem. Int. Ed.* **2013**, *52*, 2469–2473.

[15] Banik, S. M.; Medley, J. W.; Jacobsen, E. N. Catalytic, asymmetric difluorination of alkenes to generate difluoromethylated stereocenters. *Science* **2016**, *353*, 51–54.

Figure 1.4 Inspiring precedent for enantioselective I(III)-catalyzed alkene fluorinations

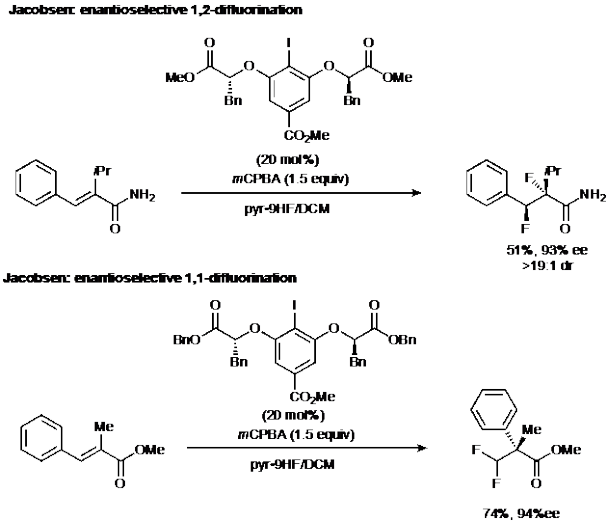

Figure 1.5 Initial reports of enantioselective I(III)-catalyzed alkene fluorinations

Since the disclosure of this initial work, a multitude of other catalytic, enantioselective alkene difluorinations and fluorofunctionalizations have been reported by Jacobsen and Gilmour (Fig. 1.6). Jacobsen developed an intramolecular fluorolactonization reaction that leverages the nucleophilicity of a pendant methyl ester to trap the nascent alkyl iodane stereospecifically.[16] Following up on the Nevado precedent, Jacobsen reported an intramolecular aminofluorination reaction that affords enantio- and diastereoenriched fluorinated aziridine or pyrrolidine derivatives.[17] Gilmour[18] and Jacobsen[19] reported more general catalytic, enantioselective 1,2-

[16] Woerly, E. M.; Banik, S. M.; Jacobsen, E. N. Enantioselective, Catalytic Fluorolactonization Reactions with a Nucleophilic Fluoride Source. *J. Am. Chem. Soc.* **2016**, *138*, 13858–13861.

[17] Mennie, K. M.; Banik, S. M.; Reichert, E.; Jacobsen, E. N. Catalytic Diastereo- and Enantioselective Fluoroamination of Alkenes. *J. Am. Chem. Soc.* **2018**, *140*, 4797–4802.

[18] Scheidt, F.; Schäfer, M; Sarie, J. C.; Daniliuc, C. G.; Molloy, J. J.; Gilmour, R. Enantioselective, Catalytic Vicinal Difluorination of Alkenes. *Angew. Chem. Int. Ed.* **2018**, 57, 16431–16435.

[19] Haj, M. K.; Banik, S. M.; Jacobsen, E. N. Catalytic, Enantioselective 1,2-Difluorination of Cinnamamides. *Org. Lett.* **2019**, *21*, 4919–4923.

difluorination reactions that proceed either via direct displacement of the alkyl iodane by fluoride or via an amide-trapping mechanism, respectively. Jacobsen has also reported a variant of the 1,1-difluorination reaction involving the migration of bromine, rather than an arene.[20] This report also disclosed the development of a more robust and selective catalyst, which features electron-poor benzyl esters that are more resistant to dealkylation-based degradation pathways. Finally, Gilmour has reported the development of an enantioselective intramolecular fluoroarylation, which leverages Friedel–Crafts-type alkylation to displace the nascent alkyl iodane.[21]

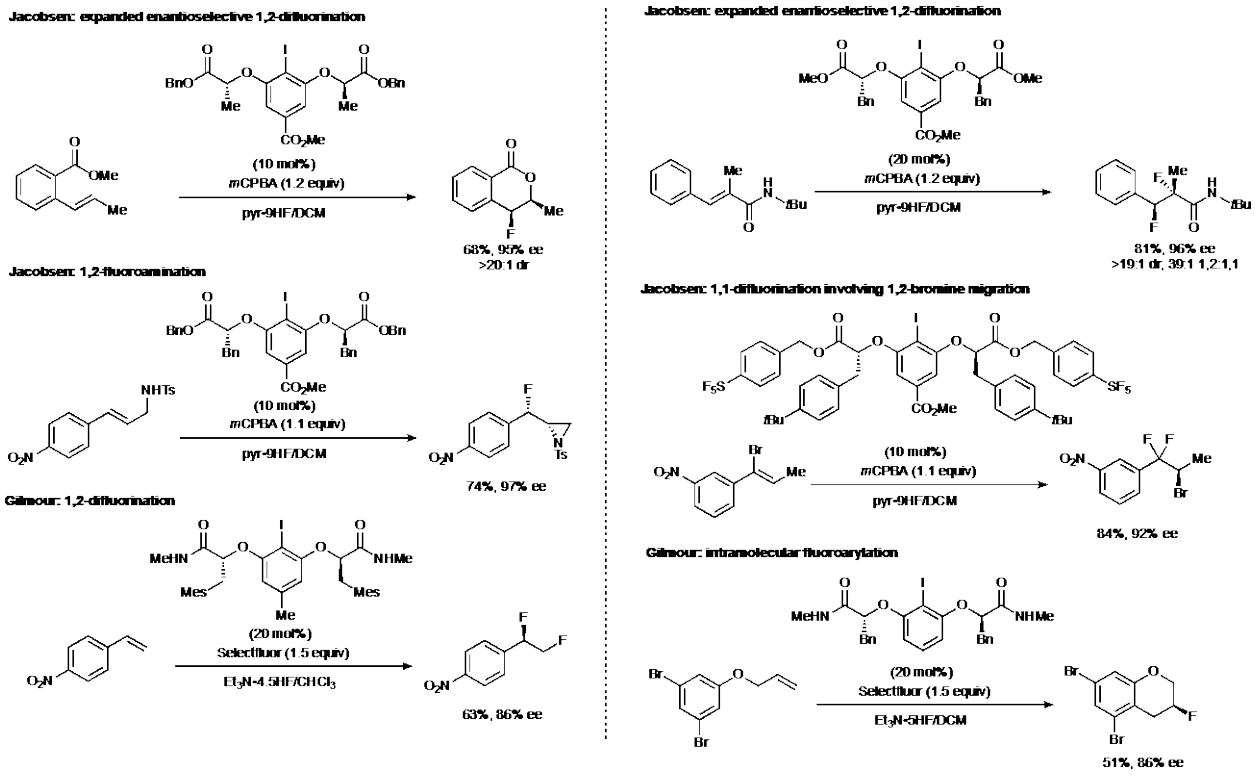

Figure 1.6 Summary of I(III)-catalyzed enantioselective fluorofunctionalizations

[20] Levin, M. D.; Ovian, J. M.; Read, J. A.; Jacobsen, E. N. Catalytic Enantioselective Synthesis of Difluorinated Alkyl Bromides. *J. Am. Chem. Soc.* **2020**, *142*, 14831–14837.

[21] Sarie, J. C.; Thiehoff, C.; Neufeld, J.; Daniliuc, C. G.; Gilmour, R. Enantioselective Synthesis of 3-Fluorochromanes via Iodine(I)/Iodine(III) Catalysis. *Angew. Chem. Int. Ed.* **2020**, *59*, 15069–15075.

Inherent to many of these reactions, as well as to numerous other I(III)-mediated reactions, is the existence of multiple reasonable mechanistic possibilities.[22] Despite the widespread interest in I(III)-catalyzed reactions, conclusive mechanistic studies have not been conducted, and basic questions pertaining to chemo- and regio-selectivity of functionalization as well as step reversibility persist. These mechanistic uncertainties are highlighted in the catalytic alkene fluorofunctionalization reactions, which feature two distinct reasonable pathways involving initial attack of the alkene-iodonium complex by either fluoride or a pendant nucleophile (Fig. 1.7). In both cases, these pathways deliver stereodefined alkyl iodanes that can then undergo a second nucleophilic displacement event to afford identical products. While both mechanisms produce the same outcome, they differ in the identities of the enantiodetermining events as long as the alkene complexation event is reversible. Aside from this project, no experimental investigations into the ordering of these events have been reported for any enantioselective ArI-catalyzed difunctionalization reaction.

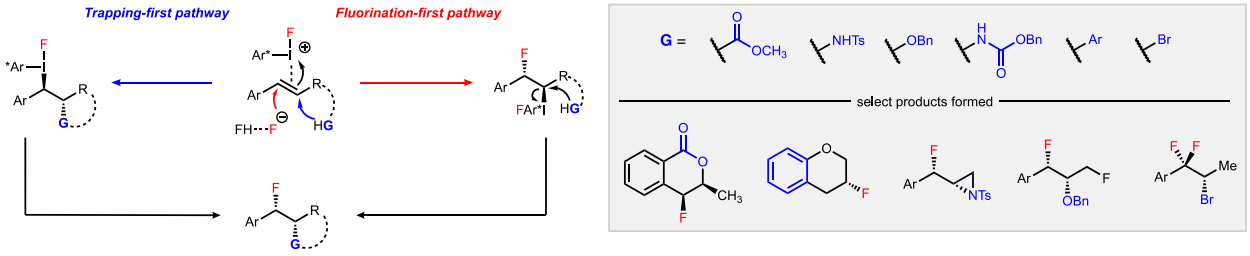

Figure 1.7 Mechanistic dichotomy prevalent in I(III)-catalyzed alkene fluorofunctionalization reactions

1.3 Background: Catalytic, Enantioselective Cationic Rearrangement Reactions

[22] Kong, W.; Merino, E.; Nevado, C. Divergent Reaction Mechanisms in the Aminofluorination of Alkenes. *CHIMIA* **2014**, *68*, 430–435.

Carbocations are highly reactive intermediates that can undergo skeletal rearrangements through the migration of strong C–C and C–H σ-bonds (Fig 1.8).[23] These types of rearrangements typically occur along the S_N1/S_N2 continuum and, as a result, are often stereoinvertive at the carbon center bearing the leaving group.[24,25] Alkyl, aryl, vinyl, and hydride groups undergo migration with varying relative rates. Migratory aptitude is generally correlated with the ability of the migrating group to stabilize cationic charge, although relative rates of migration also depend on the nature of the leaving groups and the degree of stabilization of the carbocation formed upon migration.

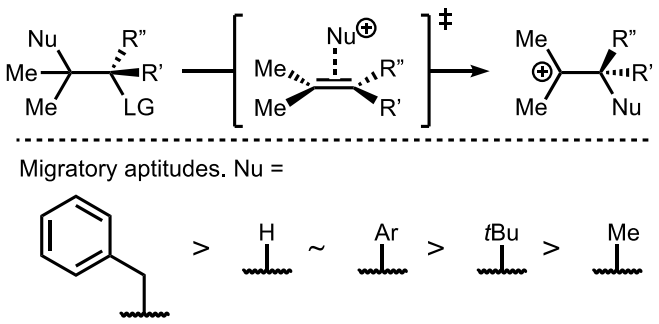

Figure 1.8 General scheme for Wagner–Meerwein rearrangements and relative migratory aptitudes for various substituents

[23] Zhang, X.-M.; Tu, Y.-Q.; Zhang, F.-M.; Chen, Z.-H.; Wang, S.-H. Recent applications of the 1,2-carbon atom migration strategy in complex natural product total synthesis. *Chem. Soc. Rev.* **2017**, *46*, 2272–2305.

[24] Suzuki, K.; Katayama, E.; Tsuchihashi, G. Asymmetric pinacol-type rearrangement of α-hydroxy methanesulfonates promoted by triethylaluminum — preparation of optically pure α-aryl and α-vinyl ketones. *Tet. Lett.* **1983**, *24*, 4997–5000.

[25] Cram, D. J. Phenonium Ions as Discrete Intermediates in Certain Wagner-Meerwein Rearrangements. *J. Am. Chem. Soc.* **1964**, *86*, 3767–3772.

The energetic barriers to σ-bond migrations in free carbocations are generally low,[26,27] so control over selectivity in such rearrangement pathways is intrinsically challenging. Numerous strategies for catalytic enantiocontrol over the rearrangement of β-hydroxy electrophiles, i.e. semi-pinacol rearrangements, have been reported.[28] Trost first reported the use of chiral palladium π-allyl complexes to facilitate the catalytic rearrangement of cyclopropanol and cyclobutanol derivatives (Fig 1.9).[29] Relevant to the fluorination work presented in this chapter, Tu[30] and Alexakis[31] respectively discovered that chiral dimeric cinchona alkaloid and phosphoric acid catalysts in tandem with stoichiometric "F+" sources promote the rearrangement of allyl carbinols. In general, catalytic, enantioselective semi-pinacol reactions leverage cationic transition-metal complexes, less-stabilized oxocarbeniums, and polarized alkene-halonium complexes to promote rearrangements.[32] The weakly electrophilic nature of these transient cationic intermediates requires the generation of even more stable oxocarbenium or iminium ions to drive rearrangement. As such, none of these strategies have been extended to the catalysis of classical Wagner–

[26] Anslyn, E. V.; Dougherty, D. A. *Modern Physical Organic Chemistry*; University Science Books: Sausalito, 2006; p 658.

[27] Sieber, S.; Buzek, P. Schleyer, P. v. R.; Koch, W.; de M. Carneiro, J. W. The tert-butyl cation (C4H9+) potential energy surface. *J. Am. Chem. Soc.* **1993**, *115*, 259–270.

[28] Zhang, X.-M.; Li, B.-S.; Wang, S.-H.; Zhang, K.; Zhang, F.-M.; Tu, Y.-Q. Recent development and applications of semipinacol rearrangement reactions. *Chem. Sci.* **2021**, 12*,* 9262–9274.

[29] Trost, B. M.; Yasukata, T. A Catalytic Asymmetric Wagner-Meerwein Shift. *J. Am. Chem. Soc.* **2001**, *123*, 7162–7163.

[30] Chen, Z.-M.; Yang, B.-M.; Chen, Z.-H.; Zhang, Q.-W.; Wang, M.; Tu, Y.-Q. Organocatalytic Asymmetric Fluorination/Semipinacol Rearrangement: An Efficient Approach to Chiral b-Fluoroketones. *Chem. Eur. J.* **2012**, *18*, 12950–12954.

[31] Romanov-Michailidis, F.; Guénée, L.; Alexakis, A. Enantioselective Organocatalytic Fluorination-Induced Wagner–Meerwein Rearrangement. *Angew. Chem. Int. Ed.* **2013**, *52*, 9266–9270.

[32] Wang, S.–H.; Li, B.–S.; Tu, Y.–Q. Catalytic asymmetric semipinacol rearrangements. *Chem. Comm*. **2014**, *50*, 2393–2408.

Meerwein rearrangements, which form more uphill, non-heteroatom-stabilized carbocationic intermediates. We envisioned that alkyl iodonium species, which feature leaving group abilities roughly 10^{12}–10^{14} times that of alkyl chlorides,[33] might be sufficiently electrophilic to induce Wagner–Meerwein rearrangements to form non-heteroatom-stabilized carbocations.

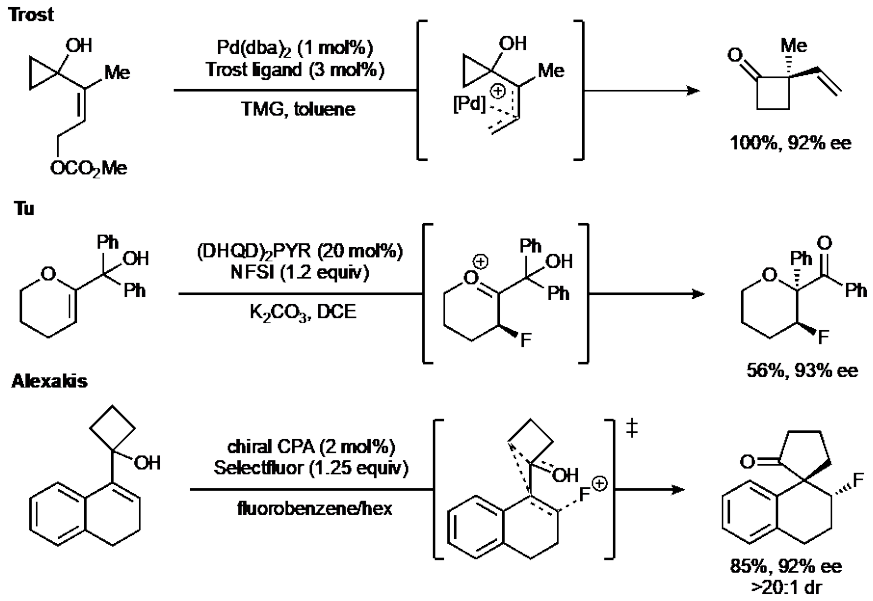

Figure 1.9 Representative reactive intermediates/transition states involved in catalytic, enantioselective semi-pinacol rearrangements

1.4 Development and Scope of Catalytic, Enantioselective Wagner–Meerwein Rearrangements

We envisioned that the alkyl iodane/iodonium species generated via hypervalent iodine catalysis might induce Wagner–Meerwein rearrangements. Specifically, fluoroiodination of styrene derivatives bearing cumyl, *tert*-butyl, or isopropyl substitution would deliver stereodefined

[33] Ochiai, M. Reactivities, Properties and Structures. In *Hypervalent Iodine Chemistry: Modern Developments in Organic Synthesis*; Wirth, T., Ed.; Springer-Verlag: Berlin, Heidelberg, 2003; pp 17–18.

secondary iodonium intermediates that might trigger migration of a neighboring aryl, methyl, or hydride group (Fig. 1.10).

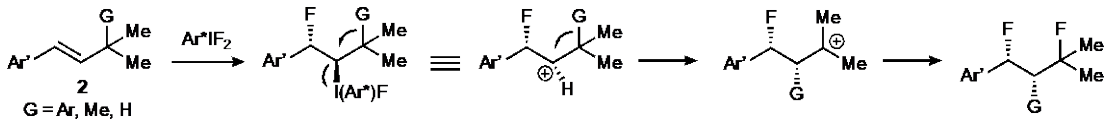

Figure 1.10 Design hypothesis for proposed Wagner–Meerwein rearrangements

The β-cumyl styrene derivative **2c** was evaluated as a model substrate for the proposed Wagner–Meerwein rearrangement (Fig 1.11). In the presence of the chiral aryl-iodide catalyst **1a**, *m*CPBA as a stoichiometric oxidant, and pyr·9HF (20–100 equiv of HF) as the fluoride source, **2c** was observed to undergo selective oxidation to generate the corresponding 1,3-difluorinated product **3c** as the anti-diastereomer (confirmed by scxrd) in 89% e.e. (Figure 1.11). The use of other commonly employed catalysts (**1b-d**) led to either lower or no change in ee or minimal observed product.

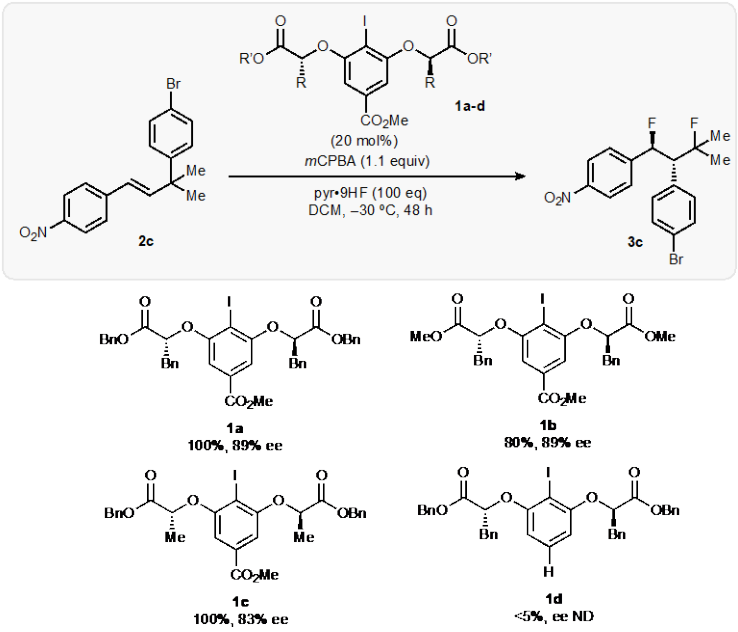

Figure 1.11 Effect of catalyst structure on the aryl rearrangement reaction

We then turned to examine the scope of migrating and stationary arenes in the developed rearrangement reaction (Fig 1.12). Substrates bearing a range of electron-poor to modestly electron-rich migrating arenes underwent rearrangement to give products in moderate to high levels of enantioselectivity. A larger excess of HF-pyridine (100 equiv) was required to reach full conversion with substrates bearing electron-deficient migrating arenes. Substrates bearing strongly electron-rich migrating or stationary arenes were observed to undergo decomposition under the reaction conditions. The level of 1,2-anti-diastereoselectivity was found to be highly dependent on the electronic properties of the arenes, decreasing with more electron-deficient migrating arenes and more electron-rich stationary arenes.[34] Both the predominant 1,2-anti and minor 1,2-syn diastereomers of **3f** were generated with within 2% e.e. of each other.

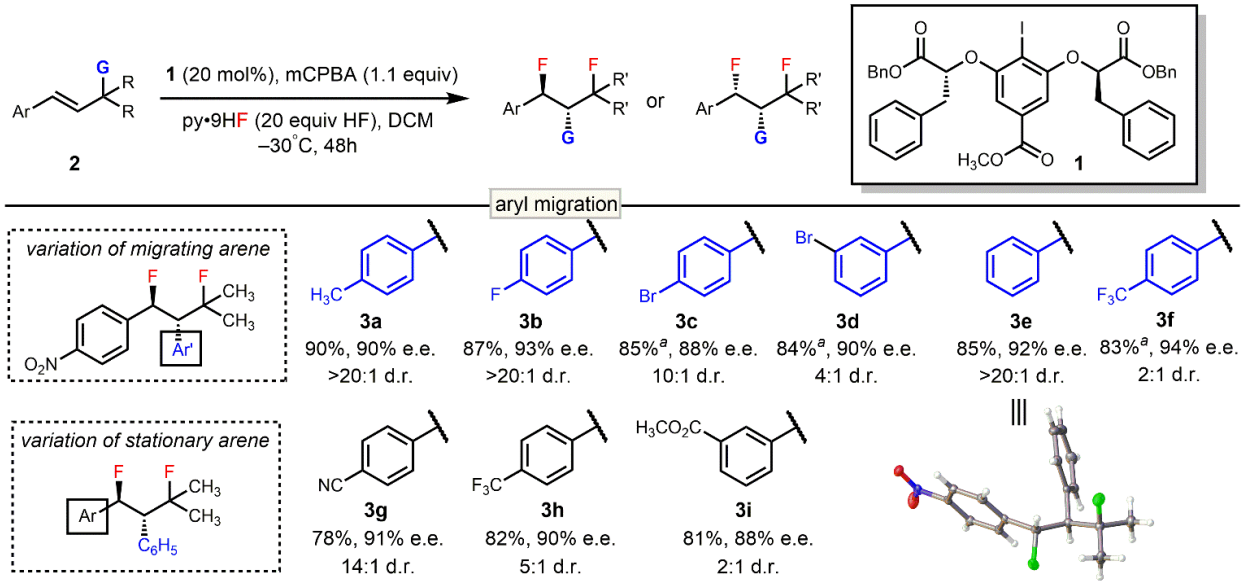

Figure 1.12 Scope of aryl rearrangement reaction a. using 100 equiv HF

[34] The dr and ee of the products were measured throughout the course of the reaction and found to not change over time. The products are stable under the reaction conditions.

The Wagner–Meerwein reactions catalyzed by **1a** were extended successfully to rearrangements involving non-aryl migrating groups (Fig 1.13). For example, β-*t*-butyl styrene derivatives underwent highly enantioselective 1,3-difluorination reactions involving methyl migration. In contrast to the aryl-migration reactions described above, uniformly high 1,2-syn, rather than 1,2-anti, diastereoselectivity was observed. A third substrate class bearing β-isopropyl-substitution was also shown to undergo hydride migration (**5a**), albeit with slightly diminished enantioselectivity. Use of a substrate bearing benzyl migrating group led to the highly selective yet unexpected formation of a trans indene, putatively through a Friedel–Crafts arylation/benzyl rearrangement sequence (Fig 1.14). Effective enantiocontrol was thus demonstrated for migrating groups spanning over three orders of magnitude of migratory aptitude.[35]

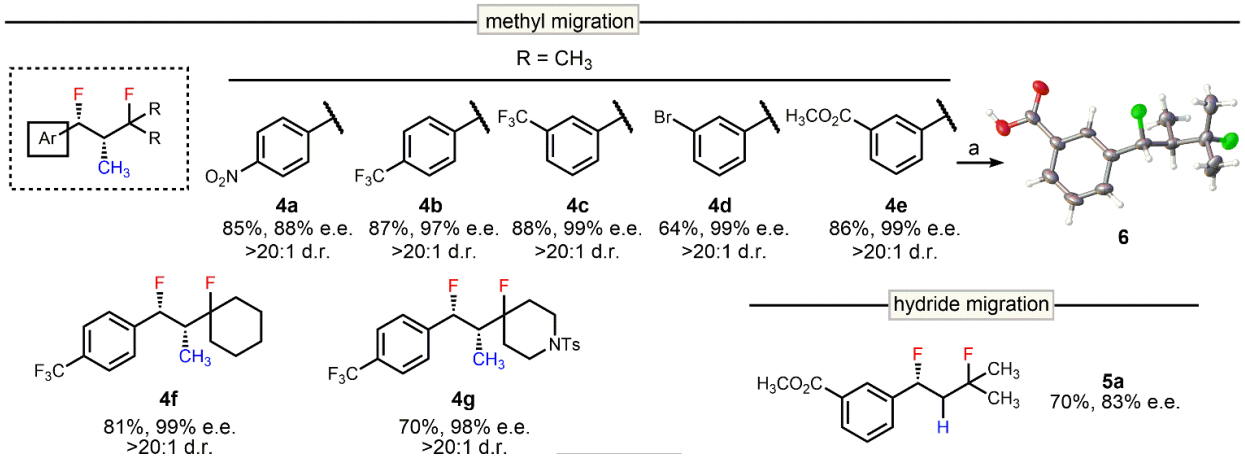

Figure 1.13 Scope of methyl and hydride migration reactions a. TMSOK, THF

[35] Saunders, W. H. Jr.; Paine, R. H. Phenyl vs. Methyl Migration Aptitudes in Some Carbonium Ion Reactions of Neophyl Derivatives. *J. Am. Chem. Soc.* **1961**, *83*, 882–885.

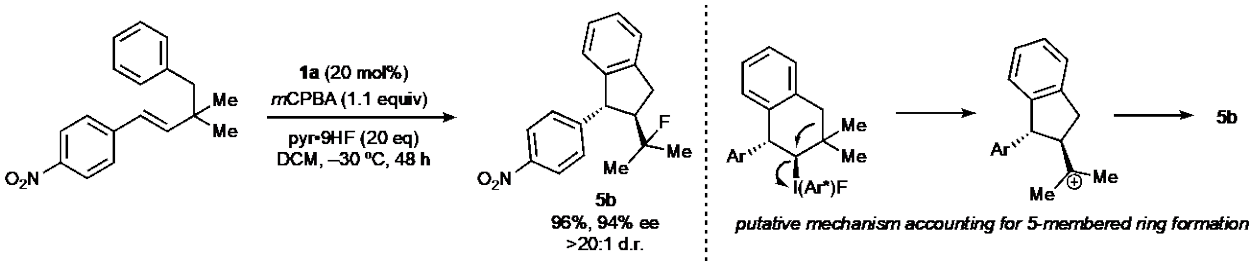

Figure 1.14 Rearrangement involving an arylation/rearrangement sequence

The 1,3-difluorinated products of these Wagner–Meerwein rearrangements possess relatively simple structures, but they can be elaborated readily to more highly functionalized molecules. For example, chemoselective oxidation[36] of the more electron-rich phenyl ring of **2e** by RuCl3/NaIO4 afforded carboxylic acid **7** (Fig. 1.15). Selective substitution of the more labile tertiary fluoride[37] of **4a** under Lewis-acidic conditions followed by subsequent trapping by azide resulted in the formation of the versatile chiral 1,3-fluoroazide **8**.

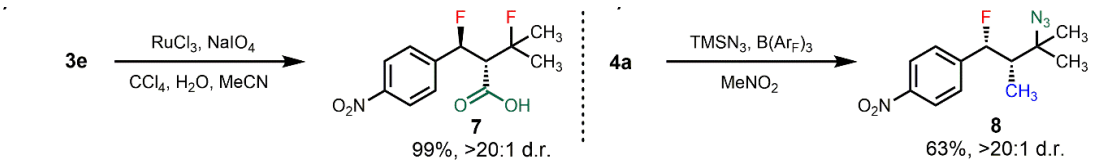

Figure 1.15 Elaboration of 1,3-difluorinated products

1.5 Hammett Studies on the Aryl-Migration Reaction

The mechanistic dichotomy outlined previously (Fig. 1.7) is manifest in the aryl migration reactions as fluoride-first and migration-first pathways (Fig. 1.16). The fluoride-first pathway

[36] Nunez, M. T.; Martin, V. S. Efficient oxidation of phenyl groups to carboxylic acids with ruthenium tetraoxide. A simple synthesis of (R)-gamma-caprolactone, the pheromone of Trogoderma granarium. *J. Org. Chem.* **1990**, *55*, 1928–1932.

[37] Dryzhakov, M.; Richmond, E.; Li, G.; Moran, J. Catalytic B(C6F5)3H2O-promoted defluorinative functionalization of tertiary aliphatic fluorides. *J. Fluor. Chem.* **2017**, *193*, 45–51.

involves attack of the styrenyl-iodonium π-complex **A** by fluoride to deliver an anti-1,2-fluoroiodane. Subsequent migration of the aryl group should occur invertively via a bridging phenonium[38] intermediate, which would be opened by fluoride at the more substituted position to give the 1,3-difluorinated product. In the migration-first scenario, the activated styrenyl-iodonium π-complex would undergo invertive displacement by the migrating arene to generate a phenonium intermediate with an adjacent benzylic iodane. This putative intermediate possesses two electrophilic sites disposed to fluoride substitution to generate the 1,3-difluoride product. Substitution could occur in either order, with the syn diastereomer expected based on either sequence if all migrations and substitutions are invertive. However, if fluoride attack occurs first on the phenonium ion (pathway b), then the resulting intermediate **C** would be poised to form a second phenonium ion (**D**), as has been documented in other I(III) mediated reactions. Opening of this phenonium intermediate by fluoride at the benzylic position would be expected to lead to the anti-diastereomer of 1,3-difluoride.

The anti-diastereomer of aryl-migration product **3** is observed to predominate for all substrates examined, so the experimental stereochemical outcomes are thus more readily reconciled with the migration-first mechanism involving phenonium ion intermediates **B** and **D**. The minor syn diastereomer could arise through any of the alternative pathways outlined in Figure 1.16. Alternatively, non-stereospecific displacement of the highly labile benzylic C–I(III) bond in intermediates **B** or **C** could also lead to mixtures of syn and anti-products. The participation of such S_N1 pathways is consistent with the observed electronic effect of the stationary aryl group

[38] Cram, D. J. Studies in Stereochemistry. I. The Stereospecific Wagner–Meerwein Rearrangement of the Isomers of 3-Phenyl-2-butanol. *J. Am. Chem. Soc*. **1949**, *71*, 3863–3870.

(**3e**, **g-i**) wherein lower diastereomeric ratios are observed with more electron-donating substituents.

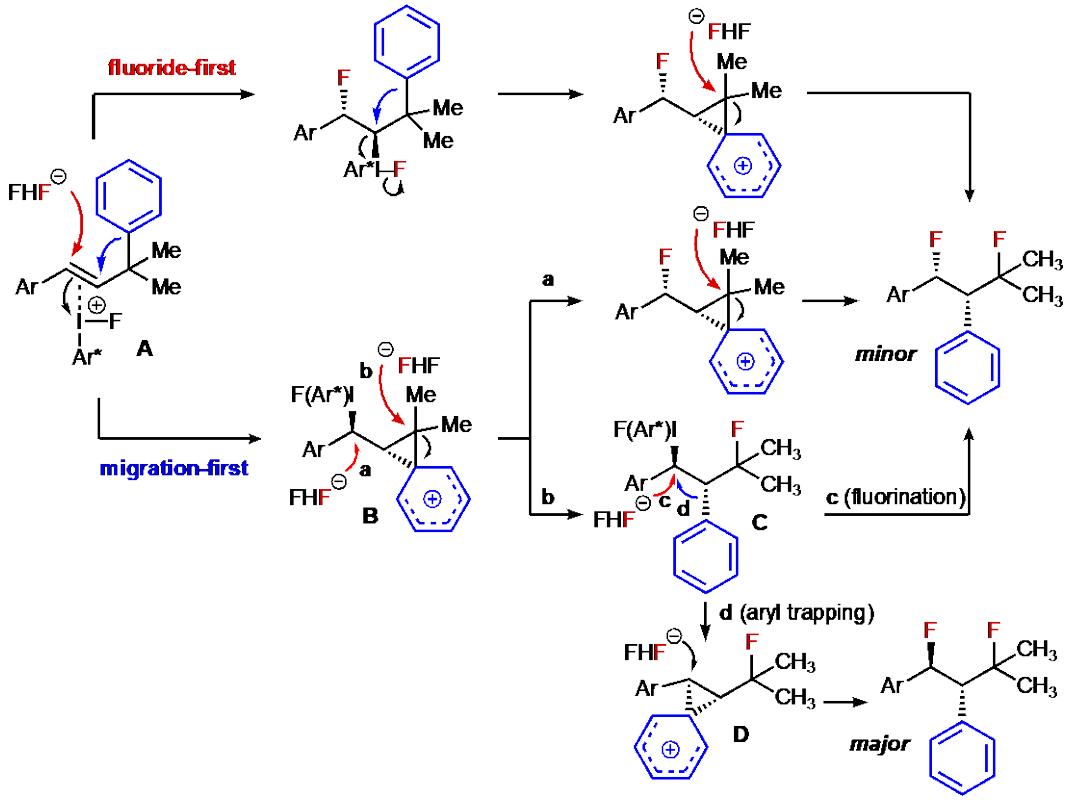

Figure 1.16 Aryl-rearrangement mechanistic possibilities

The impact of the electronic properties of the migrating aryl group was analyzed in a Hammett study (Fig. 1.17). Relative rates of reaction of substrates bearing different substituents on the migrating aryl group were determined in one-pot competition experiments. Such one-pot competitions allow assessment of the highest kinetic barrier involving the substrate, even if a step such as catalyst reoxidation that does not involve the substrate is rate-determining. Analysis of the relative rates of **2a** and **2c–f** revealed that substrates bearing electron-rich migrating arenes were consumed more rapidly, with excellent Hammett correlations obtained with both σ ($\rho = -3.7$, $R^2 = 0.99$) and σ+ values ($\rho+ = -2.9$, $R^2 = 0.96$) (Fig 1.18). The large, negative ρ value is consistent with phenonium ion formation accompanied by a high degree of positive charge development in

the migrating arene in the first irreversible step involving substrate. Similar correlations have been observed in semi-pinacol rearrangements of tetraaryl diols (ρ+ = –3.0), where aryl migration is rate-determining.[39,40] This analysis thus rules out both the fluorination-first pathway and substrate-committing π-complex formation and is consistent instead with a migration-first pathway involving irreversible, and thus enantiodetermining, arene migration.

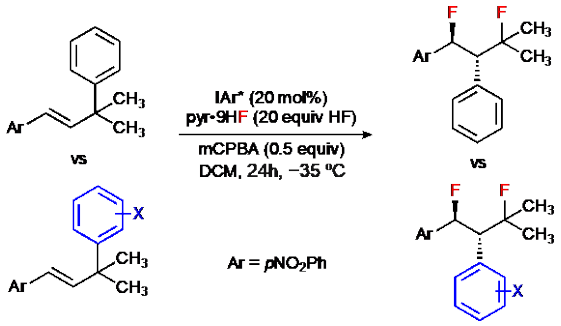

Figure 1.17 Hammett competition experiments

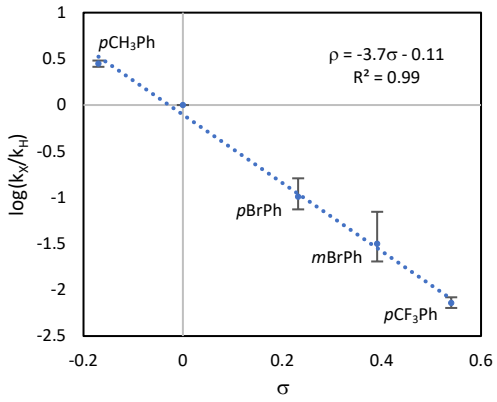

Figure 1.18 Hammett plot for aryl-rearrangement reaction competition experiments

[39] Bachmann, W. E.; Mosher, F. H. The Pinacol-Pinacolin Rearrangement. The Relative Migration Aptitudes of Aryl Groups. J. Am. Chem. Soc. **1932**, *54*, 1124–1133.

[40] Bachmann, W. E.; Ferguson, J. W. The Pinacol—Pinacolone Rearrangement. VI. The Rearrangement of Symmetrical Aromatic Pinacols. *J. Am. Chem. Soc.* **1934**, *56*, 2081–2084.

1.6 KIE Studies on the Alkyl-Migration Reactions

In contrast to the aryl migration reactions analyzed above, the methyl migration reactions involve a significantly less nucleophilic, sp^3-hybridized migrating group that cannot form a metastable bridged intermediate, a lack of dependence of d.r. on the nature of the stationary arene (Fig. 1.19), and uniformly high selectivity for the syn diastereomer is obtained in each of the cases examined (**4a-g**). The latter observation is consistent with a sequence of stereospecific steps in the overall process, but it does not allow distinction between fluoride-first or migration-first scenarios.

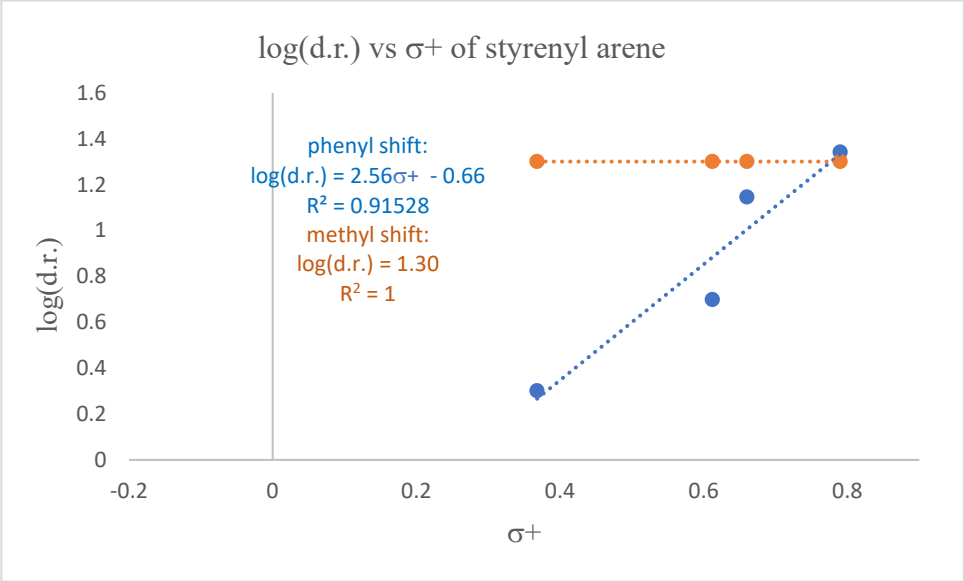

Figure 1.19 Difference in dependence of d.r. on stationary arene electronics between arene- vs methyl-migration reactions

The timing of bond-forming and bong-breaking events in the methyl-migration reactions was probed through a set of $^{12}C/^{13}C$ kinetic isotope effect (KIE) studies. The bond between the allylic C2 and the migrating carbon C1 is cleaved in the substrate-committing step in the migration-first mechanism, but it is left essentially unperturbed in the substrate-committing step in the fluoride-first mechanism (Fig. 1.20). Therefore, a primary intermolecular KIE on C1 is expected

in the former case, while a negligible KIE (ca. 1.00) is expected in the latter. As a useful benchmark, a primary KIE on migrating methyl groups of 1.027 was reported in the rearrangement of neopentyl tosylate systems, where methyl migration is rate-determining.[41]

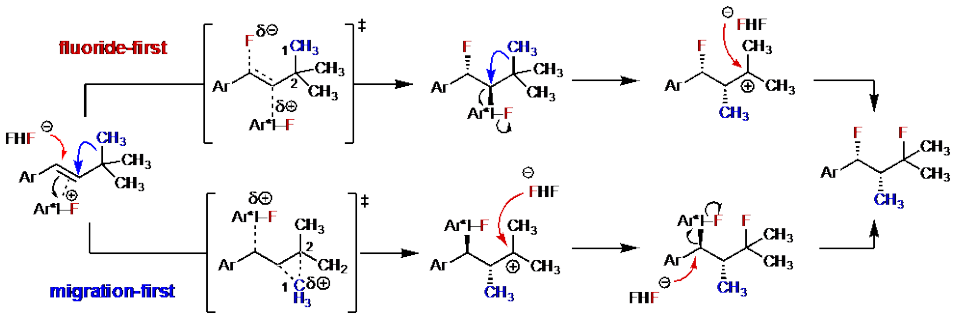

Figure 1.20 Plausible pathways for methyl-shift reaction

The intermolecular KIE in the Wagner–Meerwein methyl rearrangement was evaluated with a β-t-butyl styrene derivative at natural isotopic abundance, where all substrate can be considered to be unlabeled or singly ^{13}C labelled at the C1 or C2 positions (Fig. 1.21). Isotopic enrichment was assessed from fractionation measurements obtained using the DEPT method reported recently by our group.[42] In this manner, a KIE of 0.996(2) (average of two independent measurements of 0.991(2) and 1.001(2)) was determined, consistent with a fluoride-first pathway and inconsistent with substrate-committing methyl migration. A KIE of 0.999 (average of two independent measurements of 0.996(2) and 1.003(3)) was also determined at C2 using the MQF method recently reported by our group; this negligible KIE is similarly consistent with no change in the C1-C2 bond during the substrate-committing step. The intrinsic primary KIE for the methyl

[41] Ando, T.; Yamataka, H.; Kuramochi, J.; Yamawaki, J.; Yukawa, Y. Neighboring group participation in solvolysis. VI. Methyl participation in acetolysis of neopentyl p-nitrobenzenesulfonate. *Tet. Lett.* **1976**, *17*, 1879–1880.

[42] Kwan, E. E.; Park, Y.; Besser, H. A.; Anderson, T. L.; Jacobsen, E. N. Sensitive and Accurate 13C Kinetic Isotope Effect Measurements Enabled by Polarization Transfer. *J. Am. Chem. Soc.* **2017**, *139*, 43–46.

migration was determined in an intramolecular KIE experiment and found to be in the expected range (1.026).

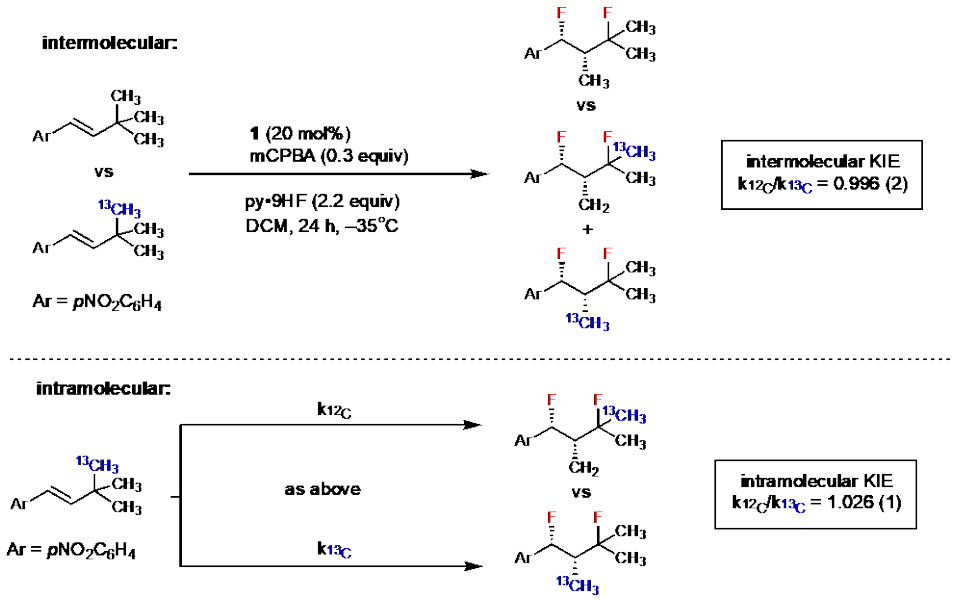

Figure 1.21 KIE study on the methyl-migration reaction

The possibility that formation of the alkene-iodonium complex – which is common to both the fluoride-first and migration-first mechanisms – might be the substrate-committing step in the methyl migration reactions was assessed by determining the KIEs at the alkene carbons. A value of 1.007 (average of two independent measurements of 01.009(1) and 1.005(1)) for the benzylic carbon was determined. Computational modeling of these steps (B3LYP-D3(BJ)/6-31G*/ LANL2DZ/PCM) predicts significant KIEs of 1.01–1.02 for the fluoride-first mechanism, but negligible KIEs for alkene-iodonium complexation (<1.003). It should be added that the rate of π-complexation is expected to be similar for the aryl and methyl rearrangement substrates, and rate-limiting π-complexation was ruled out in the arene migrations by the observation of a large electronic effect of the arene substituents on reaction rate. Thus, all of the available data are most

consistent with reversible complexation followed by irreversible, substrate-committing fluoride addition in the methyl migration reactions.

1.7 Summary of Mechanistic Studies

On the basis of the studies outlined above, two distinct catalytic mechanisms need to be invoked for the aryl-iodide-promoted methyl and aryl rearrangement reactions (Fig. 1.22). In the methyl rearrangement reaction, the observed syn product results from π-complexation of the substrate followed by irreversible substrate-committing and enantio-determining fluoride attack to form the 1,2-fluoroiodinated adduct. This highly electrophilic intermediate undergoes stereospecific methyl migration to form a tertiary carbocation that is then quenched with fluoride to deliver the observed product. Conversely, in the aryl rearrangement reaction, the experimental observations are only consistent with substrate-committing and enantiodetermining aryl migration. The observed anti selectivity can be rationalized by the intermediacy of a second phenonium intermediate, which is opened at the benzylic position by fluoride to give the observed product.

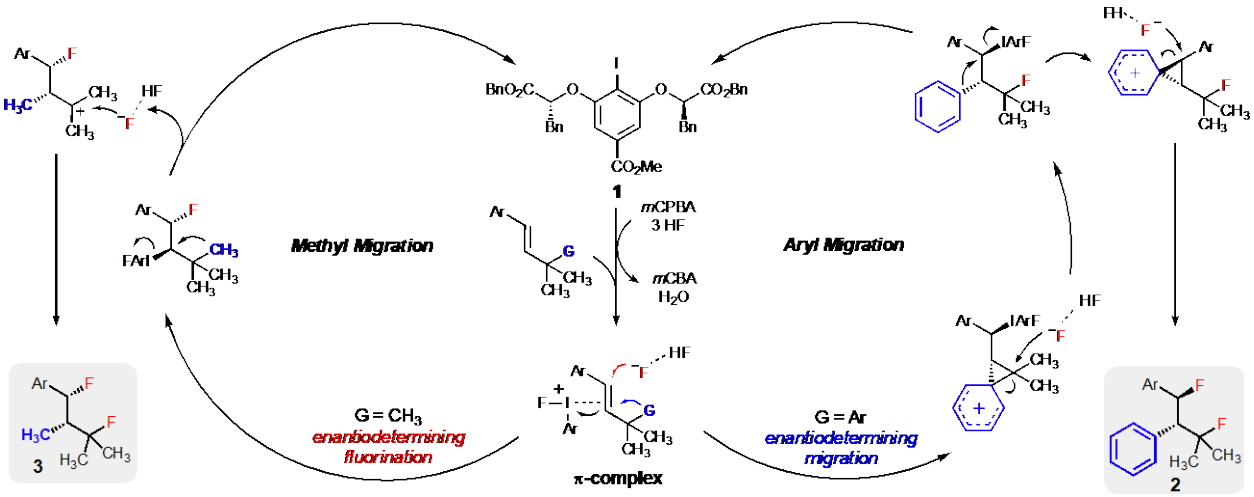

Figure 1.22 Proposed catalytic cycles based on Hammett, KIE, and computational analyses

1.8 Conclusion

The C2-symmetric aryl iodide **1a** was shown to catalyze Wagner–Meerwein rearrangements involving aryl, alkyl, hydride, and benzyl migrations to afford a variety of 1,3-difluorinated products in good yields and high enantio- and diastereoselectivities. These reactions provide new and compelling illustrations of the high electrophilicity and versatile reactivity of the intermediate alkene-iodonium π-complexes and alkyl iodanes. The biggest takeaway, however, is that the mechanism of catalysis and identity of the enantiodetermining event are dependent on the nature of the intramolecular nucleophile. In reactions involving alkyl trapping groups, intermolecular fluoride attack is product- and enantio-determining. In reactions involving more nucleophilic, sp2-based aryl trapping groups, intramolecular 1,2-migration is product- and enantiodetermining. These two different pathways are operative despite the nearly identical nature of the two substrate classes and aryl iodide catalyst used. This study provides an example of the generality of this class of C2-symmetric aryl iodides and emphasizes the importance of physical-organic tools in assigning mechanistic pathways in I(III)-catalyzed reactions.

1.9 Experimental

General experimental procedures. All reactions for the preparation of substrates were performed in standard, dry glassware fitted with rubber septa under an inert atmosphere of nitrogen unless otherwise described. All difluorination reactions were performed in low density polyethylene tubes sealed with a low density polyethylene cap under an atmosphere of air. Reported concentrations refer to solution volumes at room temperature. Concentration of organic solutions under reduced pressure was performed using house vacuum (ca. 40 mm Hg) at 30 °C. Column chromatography was performed with ZEOprep® 60 (40–63 micron) silica gel from American Scientific. Thin layer chromatography (TLC) was used for reaction monitoring and product detection was performed

using pre-coated glass plates covered with 0.20 mm silica gel with fluorescent indicator; plates were visualized by exposure to UV light (λ_{ex} = 254 nm) or by staining with potassium permanganate or ninhydrin.

CAUTION: Pyridine•9HF is a corrosive and toxic substance that will etch glassware. Safe handling can be conducted with plastic syringes and metal needles, with $NaHCO_3$ (aq.) or NaOH (aq.) employed to quench excess HF. Though reactions should not be conducted in glassware when employing pyridine•9HF, glassware may be used to quench reactions provided sufficient quantities of base are present. Always handle pyridine•9HF while wearing gloves and in a fumehood. As a precautionary measure, have calcium gluconate gel nearby and apply immediately and liberally on skin exposed to HF.

Materials. Reagents were purchased in reagent grade from commercial suppliers and used as received, unless otherwise described. Anhydrous solvents (dichloromethane, diethyl ether, tetrahydrofuran, and toluene) were prepared by passing the solvent through an activated alumina column.

Instrumentation. Proton nuclear magnetic resonance (^{1}H NMR) spectra were recorded on a Varian Mercury-400 or an Inova-500 spectrometer, are reported in parts per million downfield from tetramethylsilane, and are referenced to the residual protium resonances of the NMR solvent ($CDCl_3$: 7.26 [$CHCl_3$]). Proton-decoupled carbon-13 nuclear magnetic resonance (^{13}C {^{1}H} NMR) spectra were recorded on an Inova-500 spectrometer, are reported in parts per million

downfield from tetramethylsilane, and arhue referenced to the carbon resonances of the NMR solvent ($CDCl_3$: 77.23). Chemical shifts for fluorine-19 nuclear magnetic resonance (^{19}F NMR) were recorded on an Inova-500 spectrometer and are reported in parts per million downfield from chlorotrifluoromethane, and are referenced to the fluorine resonance of chlorotrifluoromethane ($\delta = 0$). Data are represented as follows: chemical shift, multiplicity (br = broad, s = singlet, d = doublet, t = triplet, q = quartet, quin = quintet, sext = sextet, sept = septet, m = multiplet), coupling constants in Hertz (Hz), integration. Infrared spectra were recorded using a Bruker Tensor 27 FT-IR spectrometer. Data are represented as follows: frequency of absorption (cm^{-1}), intensity of absorption (s = strong, m = medium, w = weak, br = broad). High resolution mass spectrometric data were obtained on an Agilent 6210 time-of-flight HPLC/MS spectrometer (ESI-TOF). GC analysis was performed using an Agilent 7890A GC system using commercially available columns. Chiral HPLC analysis was performed using an Agilent 1200 series quaternary HPLC system using commercially available CHIRALCEL analytical columns (4.6 x 250 mm).

Optimization Experiments.

General procedure for catalyst optimization

Catalyst (5.20 μmol, 20.0 mol%), *t*-butyl or cumyl styrene derivative (52.0 μmol, 1.00 equiv) and dichloromethane (0.30 mL) were combined in a polyethylene tube. The reaction mixture was cooled to −78 ˚C. Pyridinium poly(hydrogen fluoride) (pyr•9HF, 70% hydrogen fluoride by weight, 28 or 140 μL, 20 or 100 equiv hydrogen fluoride) was added *via* micropipette followed by *m*-chloroperbenzoic acid (*m*CPBA, 77% by weight, 12.8 mg, 57.2 μmol, 1.10 equiv). The reaction

was warmed to −30 ˚C and stirred for 48 hours at that temperature. The reaction was cooled to −78 ˚C and basic alumina (approximately 400 mg) was added slowly. The reaction was allowed to warm to room temperature with stirring and was filtered. The crude mixture was analyzed by ^{1}H NMR using mesitylene or fluorobenzene as an internal standard to determine the conversion of starting material or yield of product and by chiral HPLC to determine the enantioselectivity.

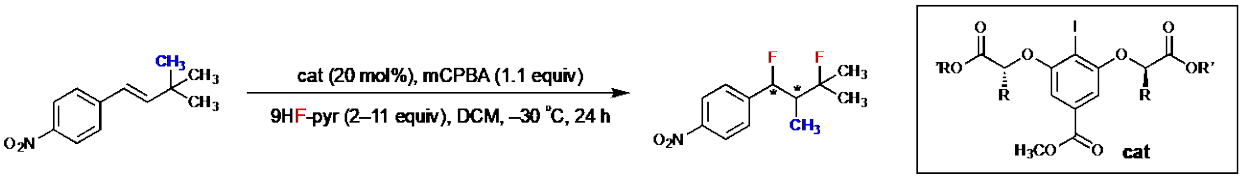

entry	equiv 9pyr-HF	R, OR'	conversion (%)[A]	ee (%)[B]
1	100	Bn, OBn	100	86
2	20	Bn, OBn	70	88
3[C]	20	Bn, OBn	100	88
4[D]	20	Bn, OBn	56	88
5[E]	20*	Bn, OBn	0	-
6	100	Bn, OMe	100	86
7	20	Bn, OMe	65	88
8	100	Me, OBn	100	86
9	20	Me, OBn	71	86

A. determined via 19F NMr relative to fluorobenzene internal standard B. Determined by chiral HPLC using method included in product analysis section C. Run for 48 hours D. run using 10 mol % catalyst loading E. run using 4.5HF-pyridine

Figure 1.23. Conditions optimization for methyl migration reaction.

Synthesis and Characterization of Substrates.

General Procedure A:

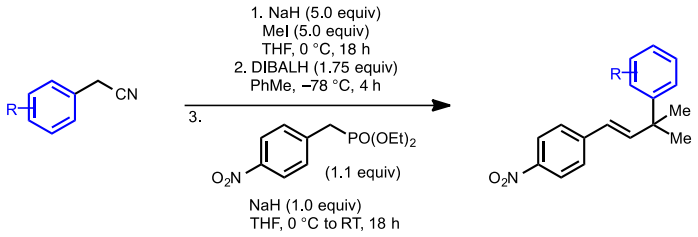

To a solution of arylacetonitrile (5.00 mmol, 1 equiv) in anhydrous THF (5 mL) at 0 ˚C under $N_{2(g)}$ was added NaH (60%, 1.00 g, 25.0 mmol, 5 equiv). The suspension was stirred at 0 ˚C for

30 m before the addition of iodomethane (1.55 mL, 25.0 mmol, 5 equiv). The reaction mixture was allowed to warm to room temperature and stirred overnight. The reaction was quenched with quenched with 1 M $HCl_{(aq)}$ (5 mL). The organic and aqueous layers were separated. The aqueous layer was extracted with Et_2O (3 x 20 mL). The combined organic layers were washed with brine (5 mL), dried over Na_2SO_4, filtered and concentrated *in vacuo*. To a solution of the crude residue in anhydrous toluene (10 mL) at –78 ˚C under $N_{2(g)}$ was added diisobutyl aluminum hydride (1 M in toluene, 8.75 mL, 8.75 mmol, 1. 75 equiv). After 4 hours at –78 ˚C, the reaction mixture was quenched with 1:1 sat. Rochelle $salt_{(aq)}$: ethyl acetate (20 mL) and stirred vigorously for 1 hour. The The organic and aqueous layers were separated. The aqueous layer was extracted with Et_2O (3 x 20 mL). The combined organic layers were washed with brine (5 mL), dried over Na_2SO_4, filtered, concentrated *in vacuo* and purified by silica gel column chromatography (0 to 30% Et_2O/hexanes). To a solution of diethyl (4-nitrobenzyl)phosphonate (1.50 g, 5.50 mmol, 1.1 equiv) in anhydrous tetrahydrofuran (20 mL) at 0 °C was added sodium hydride (60% by weight, 199 mg, 5.00 mmol, 1.0 equiv). The reaction mixture was allowed to stir at 0 °C for 30 minutes before the addition of a solution of the crude residue. The reaction mixture was allowed to warm to room temperature. After 18 hours, the reaction was quenched with 1 M $HCl_{(aq)}$ (5 mL). The organic and aquoeus layers were separated and the aqueous layer was extracted with ethyl acetate (2 x 20 mL). The combined organic layers were washed with brine (10 mL), dried over $NaSO_4$, filtered, concentrated *in vacuo* and purified by silica gel column chromatography (0 to 5% Et_2O/hexanes).

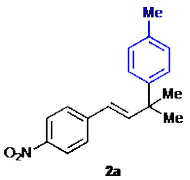

2a (E)-1-methyl-4-(2-methyl-4-(4-nitrophenyl)but-3-en-2-yl)benzene. Prepared according to general procedure A using 4-methylbenzyl cyanide (655 mg, 5.00 mmol) to give **2a** (1.06 g, 75%) as a yellow solid. ^{1}H NMR (500 MHz, $CDCl_3$) δ 8.27 – 8.12 (m, 2H), 7.58 – 7.48 (m, 2H), 7.35 – 7.28 (m, 2H), 7.21 (d, *J* = 7.9 Hz, 2H), 6.67 (d, *J* = 16.2 Hz, 1H), 6.50 (d, *J* = 16.1 Hz, 1H), 2.39 (s, 3H), 1.59 (s, 6H); ^{13}C NMR (125.7 MHz, $CDCl_3$) δ 146.6, 145.5, 144.7, 144.5, 135.8, 129.1, 126.7, 126.1, 124.4, 124.0, 40.9, 28.5, 21.0; HRMS (ESI-TOF) Calc'd for $C_{18}H_{19}NO_2$ $[M+H]^+$: 282.1489; found 282.1480.

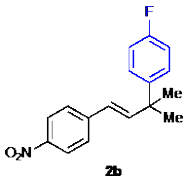

2b (E)-1-fluoro-4-(2-methyl-4-(4-nitrophenyl)but-3-en-2-yl)benzene. Prepared according to general procedure A using 4-fluorophenylacetonitrile (676 mg, 5.00 mmol) to give **2b** (1.11 g, 78%) as a yellow solid. ^{1}H NMR (500 MHz, $CDCl_3$) δ 8.16 (dd, *J* = 8.8, 1.9 Hz, 2H), 7.56 – 7.45 (m, 2H), 7.34 (ddd, *J* = 9.1, 5.0, 1.8 Hz, 2H), 7.02 (td, *J* = 8.6, 1.8 Hz, 2H), 6.60 (dt, *J* = 16.1, 1.4 Hz, 1H), 6.45 (dd, *J* = 16.1, 1.7 Hz, 1H), 1.55 (d, *J* = 1.9 Hz, 6H); ^{13}C NMR (125.7 MHz, $CDCl_3$) δ 161.4 (d, *J* = 245.0 Hz), 146.7, 145.0, 144.2, 143.4 (d, *J* = 3.2 Hz), 127.9 (d, *J* = 7.8 Hz), 126.8, 124.8, 124.1, 115.1 (d, *J* = 20.9 Hz), 40.9, 28.7; ^{19}F NMR (470.4 MHz, $CDCl_3$) δ -117.1 (tt, *J* = 8.8, 5.3 Hz); HRMS (ESI-TOF) Calc'd for $C_{17}H_{16}FNO_2$ $[M+H]^+$: 286.1238; found 286.1236.

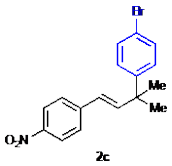

2c

(E)-1-bromo-4-(2-methyl-4-(4-nitrophenyl)but-3-en-2-yl)benzene. Prepared according to general procedure A using 4-bromophenylacetonitrile (980 mg, 5.00 mmol) to give **2c** (1.25 g, 72%) as a yellow solid. ^{1}H NMR (500 MHz, $CDCl_3$) δ 8.17 (dd, J = 8.8, 1.9 Hz, 2H), 7.53 – 7.48 (m, 2H), 7.48 – 7.43 (m, 2H), 7.27 (dd, J = 8.6, 1.9 Hz, 2H), 6.59 (dd, J = 16.1, 1.8 Hz, 1H), 6.46 (dd, J = 16.2, 1.8 Hz, 1H), 1.55 (s, 3H); ^{13}C NMR (125.7 MHz, $CDCl_3$) δ 146.8, 146.7, 144.5, 144.1, 131.5, 128.2, 126.8, 125.0, 124.0, 120.3, 41.1, 28.5; HRMS (ESI-TOF) Calc'd for $C_{17}H_{16}BrNO_2$ $[M+H]^+$: 346.0437; found 346.0430.

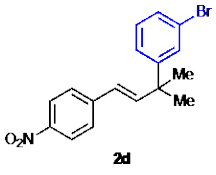

2d

(E)-1-bromo-3-(2-methyl-4-(4-nitrophenyl)but-3-en-2-yl)benzene. Prepared according to general procedure A using 3-bromophenylacetonitrile (980 mg, 5.00 mmol) to give **2d** (1.32 g, 76%) as a yellow solid. ^{1}H NMR (500 MHz, $CDCl_3$) δ 8.16 (dd, J = 8.8, 2.1 Hz, 2H), 7.58 – 7.45 (m, 3H), 7.36 (dd, J = 7.7, 2.1 Hz, 1H), 7.30 (dt, J = 7.9, 1.5 Hz, 1H), 7.21 (td, J = 7.9, 2.0 Hz, 1H), 6.64 – 6.53 (m, 1H), 6.52 – 6.39 (m, 1H), 1.53 (s, 6H); ^{13}C NMR (125.7 MHz, $CDCl_3$) δ 150.2, 146.8, 144.3, 144.0, 130.1, 129.5, 126.8, 125.1, 125.0, 124.0, 122.7, 41.3, 28.4; HRMS (ESI-TOF) Calc'd for $C_{17}H_{16}BrNO_2$ $[M+H]^+$: 346.0437; found 346.0427.

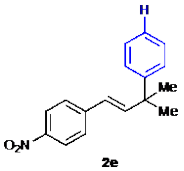

2e

(*E*)-1-(3-methyl-3-phenylbut-1-en-1-yl)-4-nitrobenzene. Prepared according to general procedure A using phenylacetonitrile (586 mg, 5.00 mmol) to give **2e** (949 mg, 71%) as a yellow solid. ^{1}H NMR (500 MHz, $CDCl_3$) δ 8.19 (dd, J = 8.8, 1.6 Hz, 2H), 7.52 (dd, J = 8.7,

1.7 Hz, 2H), 7.46 – 7.33 (m, 4H), 7.31 – 7.22 (m, 1H), 6.65 (dd, *J* = 16.2, 1.5 Hz, 1H), 6.54 – 6.45 (m, 1H), 1.58 (s, 6H); ^{13}C NMR (125.7 MHz, $CDCl_3$) δ 147.7, 146.7, 145.4, 144.4, 128.5, 126.8, 126.4, 126.3, 124.6, 124.1, 41.3, 28.5; HRMS (ESI-TOF) Calc'd for $C_{17}H_{17}NO_2$ $[M+H]^+$: 268.1332; found 268.1327.

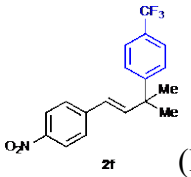

2f

(E)-1-(3-methyl-3-(4-(trifluoromethyl)phenyl)but-1-en-1-yl)-4-nitrobenzene.

Prepared according to general procedure A using 4-(trifluoromethyl)phenylacetonitrile (926 mg, 5.00 mmol) to give **2f** (1.09 g, 65%) as a yellow solid. ^{1}H NMR (500 MHz, $CDCl_3$) δ 8.16 (d, *J* = 8.8 Hz, 2H), 7.60 (d, *J* = 8.2 Hz, 2H), 7.56 – 7.44 (m, *J* = 8.9, 2.4 Hz, 4H), 6.62 (d, *J* = 16.2 Hz, 1H), 6.50 (d, *J* = 16.2 Hz, 1H), 1.59 (s, 6H); ^{13}C NMR (125.7 MHz, $CDCl_3$) δ 151.9, 146.8, 144.3 – 143.9 (m), 128.6 (q, *J* = 32.2 Hz), 126.8, 126.7, 125.5 – 125.2 (m), 124.0, 124.1 (q, *J* = 271.9 Hz), 41.45, 28.37; ^{19}F NMR (470.4 MHz, $CDCl_3$) δ -62.3 (s); HRMS (ESI-TOF) Calc'd for $C_{18}H_{16}F_3NO_2$ $[M+H]^+$: 336.1206; found 336.1203.

General Procedure B:

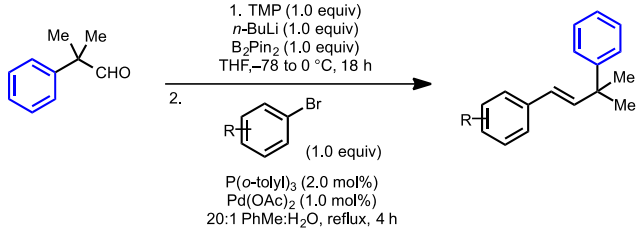

To a solution of 2,2,6,6-tetramethylpiperidine (0.89 mL, 5.25 mmol, 1 equiv) in anhydrous THF (14 mL) at 0 ˚C under $N_{2(g)}$ was added *n*-BuLi (2.5 M, 2.1 mL, 5.25 mmol, 1 equiv). The

resulting solution was stirred at 0 ˚C for 30 m. A solution of bis(pinacolato)diboron (1.33 g, 5.25 mmol, 1 equiv) in anhydrous THF (3 mL) was added and the reaction mixture cooled down to –78 ˚C. A solution of 2-methyl-2-phenylpropanal (778 mg, 5.25 mmol, 1 equiv) in anhydrous THF (3 mL) was added and the reaction mixture was allowed to warm to 0 ˚C. After 3 hours, the reaction was quenched with 1 M $HCl_{(aq)}$ (5 mL). The organic and aqueous layers were separated. The aqueous layer was extracted with Et_2O (3 x 10 mL). The combined organic layers were washed with brine (5 mL), dried over Na_2SO_4, filtered and concentrated *in vacuo* to give a yellow oil. To a suspension of the crude residue, aryl bromide (5.25 mmol, 1 equiv) and tri(*o*-tolyl)phosphine (32.0 mg, 0.105 mmol, 2 mol%) in toluene (25 mL) and deionized water (1.25 mL) was added palladium(II) acetate (12.71mg, 0.0525 mmol, 1 mol%). The reaction mixture was stirred under reflux for 4 hours. After cooling to room temperature, the reaction mixture was filtered through a plug of celite with Et_2O (200 mL), concentrated *in vacuo* and purified by silica gel column chromatography (0 to 5% Et_2O/hexanes).

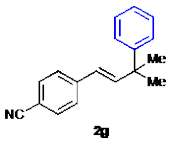

2g

(E)-4-(3-methyl-3-phenylbut-1-en-1-yl)benzonitrile. Prepared according to general procedure B using 4-bromobenzonitrile (956 mg, 5.25 mmol) to give **2g** (1.00 g, 77%) as a colorless oil. ^{1}H NMR (500 MHz, $CDCl_3$) δ 7.60 (dd, *J* = 8.3, 1.6 Hz, 2H), 7.51 – 7.45 (m, 2H), 7.43 – 7.34 (m, 4H), 7.30 – 7.23 (m, 1H), 6.60 (dd, *J* = 16.2, 1.5 Hz, 1H), 6.44 (dd, *J* = 16.1, 1.4 Hz, 1H), 1.57 (d, *J* = 1.6 Hz, 6H); ^{13}C NMR (125.7 MHz, $CDCl_3$) δ 147.8, 144.3, 142.3, 132.4, 128.4, 126.8, 126.2, 124.9, 119.2, 110.3, 41.2, 28.5; HRMS (ESI-TOF) Calc'd for $C_{18}H_{17}N$ $[M+H]^+$: 248.1434; found 248.1434.

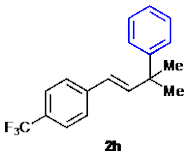

2h (E)-1-(3-methyl-3-phenylbut-1-en-1-yl)-4-(trifluoromethyl)benzene. Prepared according to general procedure B using 4-bromobenzotrifluoride (1.18 g, 5.25 mmol) to give **2h** (1.14 g, 75%) as a colorless oil. ^{1}H NMR (500 MHz, $CDCl_3$) δ 7.58 (d, *J* = 8.0 Hz, 2H), 7.49 (d, *J* = 8.1 Hz, 2H), 7.41 (d, *J* = 8.2 Hz, 2H), 7.39 – 7.33 (m, 2H), 7.26 (qd, *J* = 7.3, 6.1, 1.3 Hz, 1H), 6.56 (dd, *J* = 16.2, 1.3 Hz, 1H), 6.46 (d, *J* = 16.2 Hz, 1H), 1.56 (d, *J* = 1.3 Hz, 6H); ^{13}C NMR (125.7 MHz, $CDCl_3$) δ 148.3, 143.1, 141.4, 129.0 (q, *J* = 32.4 Hz), 128.5, 126.5, 126.3, 126.3, 125.6 (q, *J* = 3.9 Hz), 125.2, 124.1 (q, *J* = 271.6 Hz), 41.1, 28.7; ^{19}F NMR (376 MHz, $CDCl_3$) δ -62.4; HR-GC/MS (EI^+) Calc'd for $C_{18}H_{17}F_3$ $[M]^+$: 290.1277; found 290.1275.

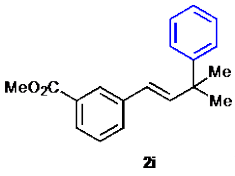

2i methyl (E)-3-(3-methyl-3-phenylbut-1-en-1-yl)benzoate. Prepared according to general procedure B using methyl 4-bromobenzoate (1.13 g, 5.25 mmol) to give **2i** (1.12 g, 76%) as a colorless oil. ^{1}H NMR (500 MHz, $CDCl_3$) δ 8.21 – 8.08 (m, 1H), 8.00 – 7.88 (m, 1H), 7.66 – 7.55 (m, 1H), 7.53 – 7.34 (m, 5H), 7.30 – 7.24 (m, 1H), 6.58 (d, *J* = 16.1 Hz, 1H), 6.50 (d, *J* = 16.2 Hz, 1H), 3.96 (s, 3H), 1.59 (s, 6H); ^{13}C NMR (125.7 MHz, $CDCl_3$) δ 167.1, 148.3, 141.5, 138.1, 130.6, 130.5, 128.6, 128.3, 128.1, 127.2, 126.2, 126.1, 125.3, 52.1, 40.9, 28.7; HRMS (ESI-TOF) Calc'd for $C_{19}H_{20}O_2$ $[M+H]^+$: 281.1536; found 281.1531.

General Procedure C:

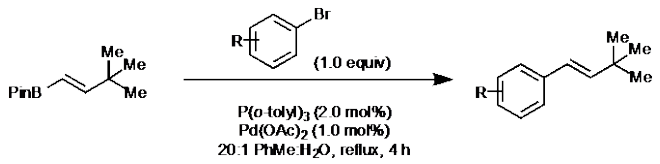

To a suspension of 2-[(1*E*)-3,3-dimethyl-1-buten-1-yl]-4,4,5,5-tetramethyl-1,3,2-dioxaborolane (1.10 g, 5.25 mmol 1 equiv), aryl bromide (5.25 mmol, 1 equiv) and tri(*o*-tolyl)phosphine (32.0 mg, 0.105 mmol, 2 mol%) in toluene (25 mL) and deionized water (1.25 mL) was added palladium(II) acetate (12.71mg, 0.0525 mmol, 1 mol%). The reaction mixture was stirred under reflux for 4 hours. After cooling to room temperature, the reaction mixture was filtered through a plug of celite with Et_2O (200 mL), concentrated *in vacuo* and purified by silica gel column chromatography (0 to 5% Et_2O/hexanes).

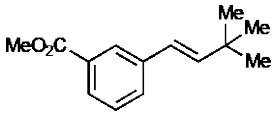

methyl (E)-3-(3,3-dimethylbut-1-en-1-yl)benzoate. Prepared according to general procedure C using methyl 4-bromobenzoate (1.13 g, 5.25 mmol) to give **2ae** (974 mg, 85%) as a colorless oil. ^{1}H NMR (500 MHz, $CDCl_3$) δ 8.05 (s, 1H), 7.84 (dd, J = 7.7, 1.5 Hz, 1H), 7.50 (ddd, J = 7.7, 1.9, 1.1 Hz, 2H), 7.39 – 7.22 (m, 2H), 6.42 – 6.21 (m, 2H), 3.89 (d, J = 1.1 Hz, 3H), 1.12 (d, J = 1.2 Hz, 9H); ^{13}C NMR (125.7 MHz, $CDCl_3$) δ 167.0, 143.0, 138.3, 130.4, 130.3, 128.4, 127.7, 127.0, 123.8, 51.9, 33.4, 29.5; HRMS (ESI-TOF) Calc'd for $C_{14}H_{18}O_2$ $[M+H]^+$: 219.1380; found 219.1380.

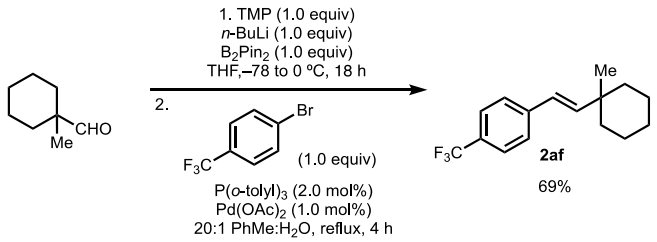

Preparation of (E)-1-(2-(1-methylcyclohexyl)vinyl)-4-(trifluoromethyl)benzene (**2af**). To a solution of 2,2,6,6-tetramethylpiperidine (0.89 mL, 5.25 mmol, 1 equiv) in anhydrous THF (14 mL) at 0 ˚C under $N_{2(g)}$ was added *n*-BuLi (2.5 M, 2.1 mL, 5.25 mmol, 1 equiv). The resulting solution was stirred at 0 ˚C for 30 m. A solution of bis(pinacolato)diboron (1.33 g, 5.25 mmol, 1 equiv) in anhydrous THF (3 mL) was added and the reaction mixture cooled down to –78 ˚C. A solution of 1-methyl-cyclohexanecarboxaldehyde (663 mg, 5.25 mmol, 1 equiv) in anhydrous THF (3 mL) was added and the reaction mixture was allowed to warm to 0 ˚C. After 3 hours, the reaction was quenched with 1 M $HCl_{(aq)}$ (5 mL). The organic and aqueous layers were separated. The aqueous layer was extracted with Et_2O (3 x 10 mL). The combined organic layers were washed with brine (5 mL), dried over Na_2SO_4, filtered and concentrated *in vacuo* to give a yellow oil. To a suspension of the crude residue, 4-bromobenzotrifluoride (1.18 g, 5.25 mmol, 1 equiv) and tri(*o*-tolyl)phosphine (32.0 mg, 0.105 mmol, 2 mol%) in toluene (25 mL) and deionized water (1.25 mL) was added palladium(II) acetate (12.7 mg, 0.0525 mmol, 1 mol%). The reaction mixture was stirred under reflux for 4 hours. After cooling to room temperature, the reaction mixture was filtered through a plug of celite with Et_2O (200 mL), concentrated *in vacuo* and purified by silica gel column chromatography (hexanes) to give **2af** (972 mg, 69%) as a colorless oil. ^{1}H NMR (500 MHz, $CDCl_3$) δ 7.64 – 7.55 (m, 2H), 7.50 (d, J = 8.1 Hz, 2H), 6.49 – 6.28 (m, 2H), 1.77 – 1.39 (m, 10H), 1.14 (d, J = 2.0 Hz, 3H); ^{13}C NMR (125.7 MHz, $CDCl_3$) δ 144.0, 142.0, 129.1 – 128.3 (m), 126.2, 125.5 (q, J = 3.9 Hz), 125.1, 124.1 (q, J = 271.6 Hz),

378.0, 36.6, 26.4, 22.6; ^{19}F NMR (376 MHz, $CDCl_3$) δ -62.3; HR-GC/MS (EI^+) Calc'd for $C_{16}H_{19}F_3$ $[M]^+$: 268.1433; found 268.1433.

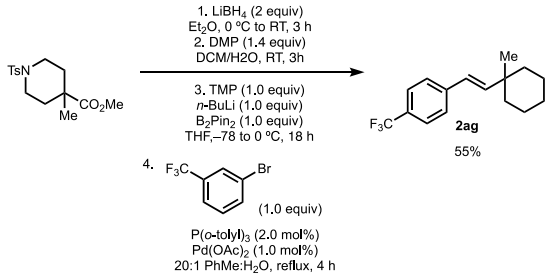

Preparation of (E)-4-methyl-1-tosyl-4-(4-(trifluoromethyl)styryl)piperidine (**1ag**). To a solution of 4-piperidinecarboxylic acid, 4-methyl-1-[(4-methylphenyl)sulfonyl]-, methyl ester (1.64 g, 5.25 mmol, 1 equiv) in anhydrous Et_2O (26 mL) at 0 ˚C under $N_{2(g)}$ was added lithium borohydride (230 mg, 10.6 mmol, 2.0 equiv). The resulting suspension was allowe to warm to room temperature. After 3 hours, the reaction was quenched with 1 M $HCl_{(aq)}$ (5 mL). The organic and aqueous layers were separated. The aqueous layer was extracted with Et_2O (3 x 10 mL). The combined organic layers were washed with brine (5 mL), dried over Na_2SO_4, filtered and concentrated *in vacuo*. The resulting crude residue was dissolved in dichloromethane (20 mL). Dess-Martin periodinane (3.10 g, 7.31 mmol, 1.4 equiv) and deionized water (0.25 mL) were added. The resulting suspension was stirred at room temperature. After 3 hours, 1:1 sat. $Na_2S_2O_{3(aq)}$:1 M $NaOH_{(aq)}$ (20 mL) was added. The organic and aqueous layers were separated. The aqueous layer was extracted with Et_2O (3 x 10 mL). The combined organic layers were washed with brine (5 mL), dried over Na_2SO_4, filtered and concentrated *in vacuo*. To a solution of 2,2,6,6-tetramethylpiperidine (0.89 mL, 5.25 mmol, 1 equiv) in anhydrous THF (14 mL) at 0 ˚C under $N_{2(g)}$ was added *n*-BuLi (2.5 M, 2.1 mL, 5.25 mmol, 1 equiv). The resulting solution was stirred at 0 ˚C for 30 m. A solution of bis(pinacolato)diboron (1.33 g, 5.25 mmol, 1 equiv) in

anhydrous THF (3 mL) was added and the reaction mixture cooled down to –78 ˚C. A solution of the crude aldehyde (5.25 mmol, 1 equiv) in anhydrous THF (3 mL) was added and the reaction mixture was allowed to warm to 0 ˚C. After 3 hours, the reaction was quenched with 1 M $HCl_{(aq)}$ (5 mL). The organic and aqueous layers were separated. The aqueous layer was extracted with Et_2O (3 x 10 mL). The combined organic layers were washed with brine (5 mL), dried over Na_2SO_4, filtered and concentrated *in vacuo* to give a yellow oil. To a suspension of the crude residue, 4-bromobenzotrifluoride (1.18 g, 5.25 mmol, 1 equiv) and tri(*o*-tolyl)phosphine (32.0 mg, 0.105 mmol, 2 mol%) in toluene (25 mL) and deionized water (1.25 mL) was added palladium(II) acetate (12.7 mg, 0.0525 mmol, 1 mol%). The reaction mixture was stirred under reflux for 4 hours. After cooling to room temperature, the reaction mixture was filtered through a plug of celite with Et_2O (200 mL), concentrated *in vacuo* and purified by silica gel column chromatography (0 to 30% Et_2O/hexanes) to give **2ag** (1.22 g, 55%) as a white solid. ^{1}H NMR (500 MHz, $CDCl_3$) δ 7.64 (dd, *J* = 8.2, 1.5 Hz, 2H), 7.51 (d, *J* = 8.1 Hz, 2H), 7.37 (d, *J* = 8.1 Hz, 2H), 7.30 (d, *J* = 7.9 Hz, 2H), 6.30 (d, *J* = 16.4 Hz, 1H), 6.14 (dd, *J* = 16.5, 1.3 Hz, 1H), 3.21 – 2.97 (m, 4H), 2.40 (s, 3H), 1.82 (ddd, *J* = 12.1, 7.3, 4.2 Hz, 2H), 1.62 (ddd, *J* = 12.6, 7.5, 4.2 Hz, 2H), 1.04 (d, *J* = 1.4 Hz, 3H); ^{13}C NMR (125.7 MHz, $CDCl_3$) δ 143.5, 141.0, 133.6, 129.7, 129.0 (q, *J* = 32.4 Hz), 127.7, 126.5, 126.3, 125.5 (q, *J* = 3.8 Hz), 124.3 (q, *J* = 271.8 Hz), 42.7, 36.3, 34.4, 26.0, 21.6; ^{19}F NMR (470.4 MHz, $CDCl_3$) δ -62.4; HRMS (ESI-TOF) Calc'd for $C_{22}H_{24}F_3NO_2S$ $[M+H]^+$: 424.1553; found 424.1552.

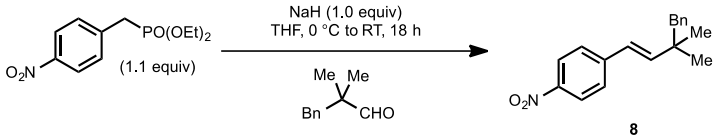

8

To a solution of diethyl (4-nitrobenzyl)phosphonate (1.50 g, 5.50 mmol, 1.1 equiv)[43] in anhydrous tetrahydrofuran (20 mL) at 0 °C was added sodium hydride (60% by weight, 199 mg, 5.00 mmol, 1.0 equiv). The reaction mixture was allowed to stir at 0 °C for 30 minutes before the addition of a solution of α,α-dimethyl-benzenepropanal (892 mg, 5.50 mmo, 1 equiv) in anhydrous THF (3 mL). The reaction mixture was allowed to warm to room temperature. After 18 hours, the reaction was quenched with 1 M $HCl_{(aq)}$ (5 mL). The organic and aquoeus layers were separated and the aqueous layer was extracted with ethyl acetate (2 x 20 mL). The combined organic layers were washed with brine (10 mL), dried over $NaSO_4$, filtered, concentrated *in vacuo* and purified by silica gel column chromatography (0 to 5% Et_2O/hexanes) to give **S2** (1.35 g, 87%) as a colorless oil. ^{1}H NMR (500 MHz, $CDCl_3$) δ 8.19 – 8.02 (m, 2H), 7.47 – 7.33 (m, 2H), 7.31 – 7.23 (m, 2H), 7.23 – 7.18 (m, 1H), 7.17 – 7.08 (m, 2H), 6.46 (ddd, *J* = 16.2, 3.2, 1.5 Hz, 1H), 6.25 (dt, *J* = 16.2, 2.2 Hz, 1H), 2.71 (t, *J* = 2.1 Hz, 2H), 1.23 – 1.08 (m, 6H); ^{13}C NMR (125.7 MHz, $CDCl_3$) δ 146.3, 145.1, 144.4, 138.1, 130.4, 127.6, 126.4, 126.1, 124.4, 123.8, 49.2, 37.7, 26.5; HRMS (ESI-TOF) Calc'd for $C_{18}H_{19}NO_2$ $[M+H]^+$: 282.1489; found 282.1481.

Synthesis and Characterization of Products.

General Procedure C:

[43] Pankova, A.S.; Sorokina, M.V.; Kuznetsov, M.A. Thermal rearrangement of 2,3-diaryl-1-phthalimidoaziridines. *Tet. Lett.* **2015**, *56*, 5381–5385.

To a solution of substrate (0.52 mmol, 1 equiv) and catalyst **Ar*I (1)** (80.0 mg, 0.104 mmol, 20 mol%) in dichloromethane (3 mL) in a low-density polyethylene tube at –78 °C was added HF•pyridine (py•9HF, 70% hydrogen fluoride by weight, 280 µL, 20 equiv hydrogen fluoride) followed by *m*CPBA (77% by weight, 128 mg, 0.57 mmol, 1.1 equiv). The reaction mixture was warmed to –35 °C and stirred at that temperature for 48 hours. The heterogeneous mixture was transferred carefully into a vigorously stirred suspension of basic alumina (4.0 g) in dichloromethane at –78 °C. The resulting suspension was allowed to warm to room temperature and filtered, washing with 200 mL dichloromethane. The combined filtrate was concentrated under reduced pressure.

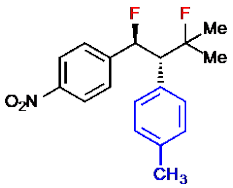

1-((1*S*,2*R*)-1,3-difluoro-3-methyl-1-(4-nitrophenyl)butan-2-yl)-4-methylbenzene.

3a was prepared according to the general procedure C using **2a** (146 mg, 0.52 mmol). The diastereomeric ratio of the crude residue after work-up was determined to be >20:1 by ^{1}H and ^{19}F NMR analysis. The crude residue was purified by silica gel column chromatography (0 to 5% diethyl ether in hexanes) to give **3a** (149 mg, 90%) as a white solid in 90% ee. ^{1}H NMR (500 MHz, $CDCl_3$) δ 7.97 (d, *J* = 8.4 Hz, 2H), 7.21 (d, *J* = 8.5 Hz, 2H), 6.92 (d, *J* = 7.8 Hz, 2H), 6.87

(d, J = 7.8 Hz, 2H), 6.02 (dd, J = 47.0, 9.5 Hz, 1H), 3.17 (ddd, J = 22.7, 12.7, 9.5 Hz, 1H), 2.19 (s, 3H), 1.61 (dd, J = 21.7, 2.4 Hz, 3H), 1.30 (d, J = 21.9 Hz, 3H); ^{13}C NMR (125.7 MHz, $CDCl_3$) δ 147.5 (d, J = 2.3 Hz), 146.3 (d, J = 20.7 Hz), 137.3, 133.4 (d, J = 8.5 Hz), 129.7 (d, J = 2.3 Hz), 129.3, 127.8 (d, J = 6.5 Hz), 123.1, 96.7 (d, J = 174.4 Hz), 93.7 (dd, J = 180.5, 4.7 Hz), 60.2 (t, J = 21.0 Hz), 27.8 (dd, J = 24.9, 6.8 Hz), 27.5 (d, J = 24.3 Hz), 21.0; ^{19}F NMR (470.4 MHz, $CDCl_3$) δ -143.6 (dseptd, J = 22.0, 21.9, 10.0 Hz, 1F), -168.9 (dt, J = 47.1, 11.6 Hz, 1F); HR-GC/MS (EI$^+$) Calc'd for $C_{18}H_{19}F_2NO_2$ [M]$^+$: 319.1378; found 319.1380.

90% ee, Chiral HPLC (OD-H, 1% isopropanol in hexanes, 1.0 mL/min, λ = 230 nm); t_R(major) = 11.9 min, t_R(minor) = 13.5 min.

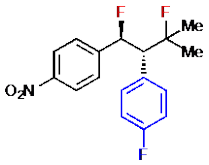

1-((1S,2R)-1,3-difluoro-2-(4-fluorophenyl)-3-methylbutyl)-4-nitrobenzene. **3b** was prepared according to the general procedure C using **2b** (148 mg, 0.52 mmol). The diastereomeric ratio of the crude residue after work-up was determined to be >20:1 by ^{1}H and ^{19}F NMR analysis. The crude residue was purified by silica gel column chromatography (0 to 5% diethyl ether in hexanes) to give **3b** (146 mg, 87%) as a white solid in >20:1 d.r. and 93% ee. ^{1}H NMR (500 MHz, $CDCl_3$) δ 8.04 – 7.97 (m, 2H), 7.23 (d, J = 8.4 Hz, 2H), 6.99 (dd, J = 8.3, 5.3 Hz, 2H), 6.83 (t, J = 8.8 Hz, 2H), 6.03 (dd, J = 46.8, 9.2 Hz, 1H), 3.22 (ddd, J = 24.3, 13.5, 9.3 Hz, 1H), 1.67 (dd, J = 21.7, 2.7 Hz, 3H), 1.28 (d, J = 21.8 Hz, 3H); ^{13}C NMR (125.7 MHz, $CDCl_3$) δ 162.0 (d, J = 247.3 Hz), 147.6 (d, J = 2.1 Hz), 145.9 (d, J = 20.9 Hz), 132.5 (dd, J = 9.3, 3.7 Hz), 131.4 (dd, J = 7.9, 3.0 Hz), 127.8 (d, J = 6.5 Hz), 123.3, 115.5 (d, J = 21.3 Hz), 96.6 (d, J = 174.6 Hz), 93.5 (dd, J = 180.7, 4.8 Hz), 59.9 (t, J = 21.2 Hz), 28.0 – 27.3 (m); ^{19}F

NMR (470.4 MHz, $CDCl_3$) δ -114.2 – -114.3 (m, 1F), -145.5 (dseptd, J = 21.8, 21.7, 7.6 Hz, 1F), -168.2 (dt, J = 46.8, 10.9 Hz, 1F); HRMS (ESI-TOF) Calc'd for $C_{17}H_{16}F_3NO_2$ $[M+H]^+$: 324.1206; found 324.1201.

93% ee, Chiral HPLC (OD-H, 2% isopropanol in hexanes, 1.0 mL/min, λ = 230 nm); t_R(major) = 10.5 min, t_R(minor) = 12.1 min.

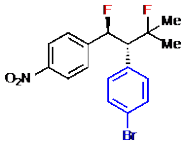

1-bromo-4-((1S,2R)-1,3-difluoro-3-methyl-1-(4-nitrophenyl)butan-2-yl)benzene. **3c** was prepared according to the general procedure C using **2c** (180 mg, 0.52 mmol) with the following modification: HF-pyridine (py-9HF, 70% hydrogen fluoride by weight, 1.4 mL, 100 equiv hydrogen fluoride) was employed. The diastereomeric ratio of the crude residue after work-up was determined to be 10:1 by ^1H and ^{19}F NMR analysis. The crude residue was purified by silica gel column chromatography (0 to 5% diethyl ether in hexanes) to give the major diastereomer of **3c** (154 mg, 77%) as a white solid in 90% ee. The overall yield of both diastereomers was 85%. ^1H NMR (500 MHz, $CDCl_3$) δ 8.03 (d, J = 8.6 Hz, 2H), 7.29 (d, J = 8.3 Hz, 2H), 7.25 (d, J = 8.4 Hz, 2H), 6.92 (d, J = 8.1 Hz, 2H), 6.04 (dd, J = 46.7, 9.2 Hz, 1H), 3.22 (ddd, J = 23.3, 13.5, 9.2 Hz, 1H), 1.68 (dd, J = 21.7, 2.7 Hz, 3H), 1.29 (d, J = 21.7 Hz, 3H); ^{13}C NMR (125.7 MHz, $CDCl_3$) δ 147.7, 145.6 (d, J = 20.7 Hz), 135.6 (d, J = 9.1 Hz), 131.7, 131.5 (d, J = 2.7 Hz), 127.8 (d, J = 6.3 Hz), 123.3, 121.7, 96.4 (d, J = 174.9 Hz), 93.2 (dd, J = 180.6, 4.8 Hz), 60.0 (t, J = 21.3 Hz), 27.8 (d, J = 21.3 Hz), 27.7 – 27.4 (m); ^{19}F NMR (470.4 MHz, $CDCl_3$) δ -145.1 (dseptd, J = 22.1, 22.0, 7.6 Hz, 1F), -168.2 (dt, J = 47.0, 10.3 Hz, 1F); HR-GC/MS (EI^+) Calc'd for $C_{17}H_{16}BrF_2NO_2$ $[M]^+$: 383.0327; found 383.0327.

90% ee, Chiral HPLC (IA, 2% isopropanol in hexanes, 1.0 mL/min, λ = 210 nm); t_R(major) = 11.6 min, t_R(minor) = 13.5 min.

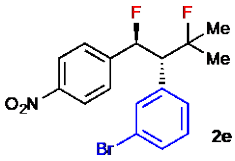

2e 1-bromo-3-((1S,2R)-1,3-difluoro-3-methyl-1-(4-nitrophenyl)butan-2-yl)benzene. **3d** was prepared according to the general procedure C using **2d** (180 mg, 0.52 mmol) with the following modification: HF-pyridine (py-9HF, 70% hydrogen fluoride by weight, 1.4 mL, 100 equiv hydrogen fluoride) was employed. The diastereomeric ratio of the crude residue after work-up was determined to be 4:1 by ^{1}H and ^{19}F NMR analysis. The crude residue was purified by silica gel column chromatography (0 to 5% diethyl ether in hexanes) to give the major diastereomer of **3d** (134 mg, 67%) as a white solid in 91% ee. The overall yield of both diastereomers was 84%. ^{1}H NMR (500 MHz, $CDCl_3$) δ 8.03 (d, *J* = 8.2 Hz, 2H), 7.31 – 7.18 (m, 4H), 7.01 (t, *J* = 7.9 Hz, 1H), 6.92 (d, *J* = 7.7 Hz, 1H), 6.03 (dd, *J* = 46.6, 9.1 Hz, 1H), 3.29 – 3.08 (m, 1H), 1.68 (dd, *J* = 21.7, 2.7 Hz, 3H), 1.30 (d, *J* = 21.7 Hz, 3H); ^{13}C NMR (125.7 MHz, $CDCl_3$) δ 147.7, 145.6 (d, *J* = 20.7 Hz), 139.0 (d, *J* = 8.8 Hz), 132.8 (d, *J* = 3.3 Hz), 130.9, 130.1, 128.7 (d, *J* = 2.6 Hz), 127.8 (d, *J* = 6.4 Hz), 123.4, 122.6, 96.4 (d, *J* = 175.2 Hz), 93.3 (dd, *J* = 180.7, 5.0 Hz), 60.7 – 60.1 (m), 27.9 (d, *J* = 24.8 Hz), 27.8 – 27.5 (m); ^{19}F NMR (470.4 MHz, $CDCl_3$) δ -145.2 (dseptd, *J* = 22.1, 22.0, 7.2 Hz, 1F), -168.3 – -168.7 (m, 1F); HRMS (ESI-TOF) Calc'd for $C_{17}H_{16}BrF_2NO_2$ $[M+H]^+$: 384.0405; found 384.0397.

91% ee, Chiral HPLC (OD-H, 2% isopropanol in hexanes, 1.0 mL/min, λ = 254 nm); t_R(major) = 10.0 min, t_R(minor) = 11.1 min.

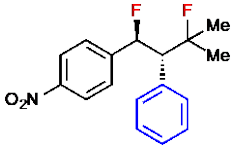

1-((1S,2R)-1,3-difluoro-3-methyl-2-phenylbutyl)-4-nitrobenzene. **3e** was prepared according to the general procedure C using **2e** (139 mg, 0.52 mmol). The diastereomeric ratio of the crude residue after work-up was determined to be >20:1 by ^{1}H and ^{19}F NMR analysis. The crude residue was purified by silica gel column chromatography (0 to 5% diethyl ether in hexanes) to give **3e** (135 mg, 85%) as a white solid in >20:1 d.r. and 92% ee. ^{1}H NMR (500 MHz, $CDCl_3$) δ 7.99 (d, J = 8.5 Hz, 2H), 7.23 (d, J = 8.5 Hz, 2H), 7.17 – 7.11 (m, 3H), 7.06 – 6.96 (m, 2H), 6.07 (dd, J = 47.0, 9.4 Hz, 1H), 3.22 (ddd, J = 24.0, 13.0, 9.4 Hz, 1H), 1.67 (dd, J = 21.7, 2.5 Hz, 3H), 1.32 (d, J = 21.8 Hz, 3H); ^{13}C NMR (125.7 MHz, $CDCl_3$) δ 147.5 (d, J = 2.5 Hz), 146.2 (d, J = 20.6 Hz), 136.6 (d, J = 9.5 Hz), 129.9 (d, J = 2.8 Hz), 128.6, 127.8 – 127.6 (m), 123.1, 96.6 (d, J = 174.8 Hz), 93.7 (dd, J = 180.6, 4.8 Hz), 60.7 (t, J = 21.0 Hz), 28.0 – 27.7 (m), 27.8 – 27.5 (m); ^{19}F NMR (470.4 MHz, $CDCl_3$) δ -144.2 (septdd, J = 22.0, 21.9, 9.3 Hz, 1F), -169.0 (dt, J = 47.1, 11.4 Hz, 1F); HRMS (ESI-TOF) Calc'd for $C_{17}H_{17}F_2NO_2$ $[M+Na]^+$: 328.1120; found 328.1104.

92% ee, Chiral HPLC (OD-H, 2% isopropanol in hexanes, 1.0 mL/min, λ = 230 nm); t_R(major) = 9.4 min, t_R(minor) = 10.8 min.

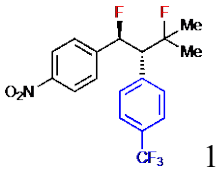

1-((1*S*,2*R*)-1,3-difluoro-3-methyl-1-(4-nitrophenyl)butan-2-yl)-4-(trifluoromethyl)benzene. **3f** was prepared according to the general procedure C using **2f**

(174 mg, 0.52 mmol) with the following modification: HF-pyridine (py-9HF, 70% hydrogen fluoride by weight, 1.4 mL, 100 equiv hydrogen fluoride) was employed. The diastereomeric ratio of the crude residue after work-up was determined to be 2:1 by ^{1}H and ^{19}F NMR analysis. The crude residue was purified by silica gel column chromatography (0 to 5% diethyl ether in hexanes) to give the major diastereomer of **3f** (107 mg, 55%) as a white solid in 95% ee. The overall yield of both diastereomers was 83%. ^{1}H NMR (500 MHz, $CDCl_3$) δ 8.02 (d, J = 8.4 Hz, 2H), 7.42 (d, J = 8.0 Hz, 2H), 7.24 (d, J = 8.5 Hz, 2H), 7.16 (d, J = 8.0 Hz, 2H), 6.08 (dd, J = 46.6, 9.1 Hz, 1H), 3.31 (ddd, J = 23.4, 13.8, 9.1 Hz, 1H), 1.70 (dd, J = 21.7, 2.7 Hz, 3H), 1.27 (d, J = 21.7 Hz, 3H); ^{13}C NMR (125.7 MHz, $CDCl_3$) δ 147.8 (d, J = 2.4 Hz), 145.4 (d, J = 20.7 Hz), 140.8 (d, J = 8.7 Hz), 130.4 (d, J = 2.9 Hz), 130.0 (q, J = 32.8 Hz), 127.8 (d, J = 6.3 Hz), 125.5 (d, J = 3.7 Hz), 123.4, 123.9 (q, J = 272.0 Hz), 96.4 (d, J = 175.4 Hz), 93.2 (dd, J = 180.7, 4.9 Hz), 61.5 – 59.5 (m), 28.0 (d, J = 24.4 Hz), 27.6 (dd, J = 24.7, 7.3 Hz);^{19}F NMR (470.4 MHz, $CDCl_3$) δ -62.7 (s, 3F), -145.1 – -145.5 (m, 1F), -168.2 – -168.6 (m, 1F); HR-GC/MS (EI^+) Calc'd for $C_{18}H_{16}F_5NO_2$ $[M]^+$: 373.1096; found 373.1094.

95% ee, Chiral HPLC (OD-H, 2% isopropanol in hexanes, 1.0 mL/min, λ = 230 nm); t_R(major) = 10.6 min, t_R(minor) = 12.8 min.

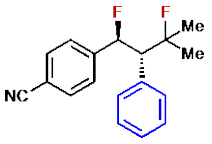

4-((1S,2R)-1,3-difluoro-3-methyl-2-phenylbutyl)benzonitrile. **3g** was prepared according to the general procedure C using **2g** (129 mg, 0.52 mmol). The diastereomeric ratio of the crude residue after work-up was determined to be 14:1 by ^{1}H and ^{19}F NMR analysis. The crude residue was purified by silica gel column chromatography (0 to 5% diethyl ether in

hexanes) to give **3g** (116 mg, 78%) as a colorless oil in 14:1 d.r and 91% ee. Major Diastereoisomer: ^{1}H NMR (500 MHz, $CDCl_3$) δ 7.42 (d, *J* = 8.0 Hz, 2H), 7.18 – 7.11 (m, 5H), 7.01 – 6.97 (m, 2H), 6.00 (dd, *J* = 47.0, 9.5 Hz, 1H), 3.18 (ddd, *J* = 23.7, 12.9, 9.4 Hz, 1H), 1.65 (dd, *J* = 21.7, 2.6 Hz, 3H), 1.31 (d, *J* = 21.8 Hz, 3H); ^{13}C NMR (125.7 MHz, $CDCl_3$) δ 144.2 (d, *J* = 20.6 Hz), 136.7 (d, *J* = 8.9 Hz), 131.8, 129.9 (d, *J* = 2.6 Hz), 128.5, 127.9 – 127.3 (m), 118.6, 112.0 (d, *J* = 2.4 Hz), 96.6 (d, *J* = 175.0 Hz), 93.9 (dd, *J* = 180.2, 4.8 Hz), 60.7 (t, *J* = 20.9 Hz), 28.0 – 27.5 (m); ^{19}F NMR (470.4 MHz, $CDCl_3$) δ -144.2 (septdd, *J* = 22.5, 22.0, 10.7 Hz, 1F), -169.2 (dt, *J* = 46.9, 11.2 Hz, 1F); HRMS (ESI-TOF) Calc'd for $C_{18}H_{17}F_2N$ $[M+H]^+$: 286.1402; found 286.1402.

92% ee, Chiral HPLC (OD-H, 2% isopropanol in hexanes, 1.0 mL/min, λ = 230 nm); t_R(major) = 14.1 min, t_R(minor) = 16.2 min.

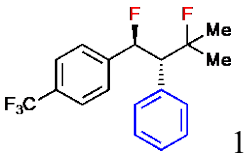

1-((1S,2R)-1,3-difluoro-3-methyl-2-phenylbutyl)-4-(trifluoromethyl)benzene.

3h was prepared according to the general procedure C using **2h** (151 mg, 0.52 mmol). The diastereomeric ratio of the crude residue after work-up was determined to be 5:1 by ^{1}H and ^{19}F NMR analysis. The crude residue was purified by silica gel column chromatography (0 to 5% diethyl ether in hexanes) to give **3h** (140 mg, 82%) as a colorless oil in 5:1 d.r and 90% ee. Major Diastereoisomer: ^{1}H NMR (500 MHz, $CDCl_3$) δ 7.45 – 7.42 (m, 2H), 7.25 – 7.21 (m, 2H), 7.20 – 7.15 (m, 3H), 7.08 – 7.04 (m, 2H), 6.13 – 6.01 (m, 1H), 3.28 (ddd, *J* = 23.2, 12.4, 9.5 Hz, 1H), 1.70 (dd, *J* = 21.6, 2.4 Hz, 3H), 1.38 (d, *J* = 21.9 Hz, 3H); ^{13}C NMR (125.7 MHz, $CDCl_3$) δ 143.1 (d, *J* = 20.6 Hz), 137.0 (d, *J* = 9.6 Hz), 130.1 (q, *J* = 32.8 Hz), 130.0 (d, *J* = 2.4 Hz), 128.5,

127.5, 127.3 (d, J = 6.3 Hz), 125.0 (d, J = 3.8 Hz), 123.9 (q, J = 272.0 Hz), 96.7 (d, J = 174.2 Hz), 94.2 (dd, J = 179.4, 4.8 Hz), 60.8 (t, J = 21.1 Hz), 28.0 – 27.6 (m);^{19}F NMR (376 MHz, $CDCl_3$) δ -62.7 (s, 3F), -143.7 (dseptd, J = 21.9, 21.7, 10.9 Hz, 1F), -168.4 (dt, J = 46.8, 11.4 Hz, 1F); HR-GC/MS (EI$^+$) Calc'd for $C_{18}H_{17}F_5$ $[M]^+$: 328.1245; found 328.1242.

90% ee, Chiral HPLC (?, 0.3% isopropanol in hexanes, 1.0 mL/min, λ = 230 nm); t_R(major) = 5.8 min, t_R(minor) = 6.2 min.

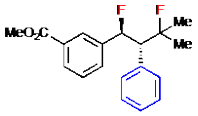

methyl 3-((1S,2R)-1,3-difluoro-3-methyl-2-phenylbutyl)benzoate. **3i** was prepared according to the general procedure C using **2i** (146 mg, 0.52 mmol). The diastereomeric ratio of the crude residue after work-up was determined to be 2:1 by ^{1}H and ^{19}F NMR analysis. The crude residue was purified by silica gel column chromatography (0 to 5% diethyl ether in hexanes) to give **3i** (89 mg, 54%) as a colorless oil in 2:1 d.r and 88% ee. The overall yield of both diastereomers was 81%. Major Diastereoisomer: ^{1}H NMR (500 MHz, $CDCl_3$) δ 7.85 – 7.84 (m, 1H), 7.81 (dd, J = 6.9, 1.7 Hz, 1H), 7.23 – 7.15 (m, 2H), 7.10 (tdd, J = 7.0, 5.6, 2.5 Hz, 3H), 7.01 (d, J = 7.1 Hz, 2H), 6.01 (ddd, J = 46.9, 9.7, 1.2 Hz, 1H), 3.88 (s, 1H), 3.28 (ddd, J = 22.6, 12.4, 9.7 Hz, 1H), 1.66 (d, J = 21.7 Hz, 3H), 1.33 (d, J = 21.8 Hz, 3H); ^{13}C NMR (125/7 MHz, $CDCl_3$) δ 166.8, 139.6 (d, J = 20.6 Hz), 137.3 (d, J = 9.1 Hz), 131.6 (d, J = 5.7 Hz), 130.1, 130.0 (d, J = 2.4 Hz), 129.4 (d, J = 2.2 Hz), 128.4, 128.2 (d, J = 6.2 Hz), 128.1, 127.3, 96.7 (d, J = 173.2 Hz), 94.4 (dd, J = 178.6, 4.7 Hz), 60.6 (t, J = 21.2 Hz), 52.3, 28.0 – 27.6 (m); ^{19}F NMR (470.4 MHz, $CDCl_3$) δ -143.8 (septdd, J = 22.1, 22.0, 11.1 Hz, 1F), -166.3 (dt, J = 46.9, 11.2 Hz, 1F); HRMS (ESI-TOF) Calc'd for $C_{19}H_{20}F_2O_2$ $[M+Na]^+$: 341.1324; found 341.1322.

88% ee, Chiral HPLC (AS-H, 1% isopropanol in hexanes, 1.0 mL/min, λ = 210 nm); t_R(major) = 8..8 min, t_R(minor) = 10.3 min.

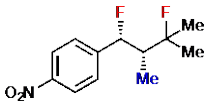

1-((1R,2R)-1,3-difluoro-2,3-dimethylbutyl)-4-nitrobenzene. **4a** was prepared according to the general procedure C using (E)-1-(3,3-dimethylbut-1-en-1-yl)-4-nitrobenzene (107 mg, 0.52 mmol) with the following modification: 20 equiv of HF was used instead. The diastereomeric ratio of the crude residue after work-up was determined to be >20:1 by 1H and 19F NMR analysis. The crude residue was purified by silica gel column chromatography (0 to 5% diethyl ether in hexanes) to give **4a** (108 mg, 85%) as a colorless oil in 88% e.e. 1H NMR (500 MHz, CDCl3) δ 8.22 (d, J = 8.7 Hz, 1H), 7.46 (d, J = 8.7 Hz, 1H), 6.04 (d, J = 48.4 Hz, 1H), 2.14 – 1.97 (m, 1H), 1.48 (dd, J = 22.1, 2.0 Hz, 2H), 1.43 (d, J = 22.4 Hz, 2H), 0.84 (dd, J = 7.3, 1.5 Hz, 2H); 19F NMR (470.4 MHz, CDCl3) δ -134.1 (heptd, J = 11.9, 4.6 Hz), -200.5 (dd, J = 15.7, 8.9 Hz); 13C NMR (126 MHz, CDCl3) δ 147.6, 125.6, 123.5, 97.4, 90.9, 49.5, 26.6, 23.1, 7.3. HRMS (ESI-TOF) Calc'd for C12H15F2NO2 [M+H]+: 244.1144; found 244.1143.

88% e.e., chiral HPLC (OD-H, 2% isopropanol in hexanes, 1.0 mL/min, λ = 254 nm); t_R(major) = 9.2 min, t_R(minor) = 10.3 min.

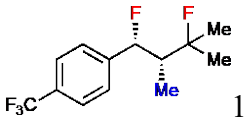

1-((1R,2R)-1,3-difluoro-2,3-dimethylbutyl)-4-(trifluoromethyl)benzene. **4b** was prepared according to the general procedure C using (*E*)-1-(3,3-dimethylbut-1-en-1-yl)-4-(trifluoromethyl)benzene (119 mg, 0.52 mmol). The diastereomeric ratio of the crude residue after work-up was determined to be >20:1 by ^{1}H and ^{19}F NMR analysis. The crude residue was purified by silica gel column chromatography (0 to 5% diethyl ether in hexanes) to give **4b** (120 mg, 87%) as a colorless oil in 97% ee. ^{1}H NMR (500 MHz, $CDCl_3$) δ 7.64 (d, *J* = 8.2 Hz, 2H), 7.42 (d, *J* = 8.1 Hz, 2H), 6.03 (d, *J* = 48.4 Hz, 1H), 2.17 – 1.98 (m, 1H), 1.51 (dd, *J* = 22.1, 2.0 Hz, 3H), 1.45 (d, *J* = 22.4 Hz, 3H), 0.87 (dd, *J* = 7.3, 1.5 Hz, 3H); ^{13}C NMR (125.7 MHz, $CDCl_3$) δ 144.6 (d, *J* = 21.6 Hz), 130.0 (q, *J* = 32.4 Hz), 125.5 – 125.3 (m), 125.2, 125.1, 123.8 (d, *J* = 272.0 Hz), 100.4 – 95.7 (m), 91.3 (dd, *J* = 178.9, 7.3 Hz), 49.8, 26.7 (dd, *J* = 24.3, 2.0 Hz), 23.3 (dd, *J* = 25.1, 3.8 Hz), 7.5 – 7.2 (m); ^{19}F NMR (470.4 MHz, $CDCl_3$) δ -62.6 (s, 3F), -134.2 (septd, *J* = 22.1, 9.7 Hz, 1F), -200.9 (dd, *J* = 48.4, 33.1 Hz, 1F); HR-GC/MS (EI^+) Calc'd for $C_{13}H_{15}F_5$ $[M]^+$: 266.1088; found 266.1088.

98% e.e., chiral GC (β-Cyclosil, 130 ˚C, 14 psi); t_R(major) = 5.2 min, t_R(minor) = 5.3 min.

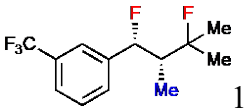

1-((1R,2R)-1,3-difluoro-2,3-dimethylbutyl)-3-(trifluoromethyl)benzene. **4c** was prepared according to the general procedure C using (E)-1-(3,3-dimethylbut-1-en-1-yl)-3-(trifluoromethyl)benzene (119 mg, 0.52 mmol). The diastereomeric ratio of the crude residue after work-up was determined to be >20:1 by ^{1}H and ^{19}F NMR analysis. The crude residue was purified by silica gel column chromatography (0 to 5% diethyl ether in hexanes) to give **4c** (121 mg, 88%) as a colorless oil in 99% ee. ^{1}H NMR (500 MHz, $CDCl_3$) δ 7.59 – 7.55 (m, 2H),

7.54 – 7.46 (m, 2H), 6.02 (d, J = 48.2 Hz, 1H), 2.16 – 1.98 (m, 1H), 1.51 (dd, J = 22.1, 1.9 Hz, 3H), 1.45 (d, J = 22.5 Hz, 3H), 0.87 (d, J = 7.2 Hz, 3H); ^{13}C NMR (125.7 MHz, $CDCl_3$) δ 141.7 (d, J = 21.6 Hz), 131.7 – 130.3 (m), 128.9 (d, J = 2.3 Hz), 128.2 (d, J = 9.5 Hz), 124.2 (q, J = 272.4 Hz), 124.5 (d, J = 3.8 Hz), 121.7 (dd, J = 10.2, 3.8 Hz), 100.7 – 95.4 (m), 91.3 (dd, J = 178.7, 7.3 Hz), 49.7 (t, J = 20.6 Hz), 26.7 (dd, J = 24.2, 2.0 Hz), 23.4 (dd, J = 24.9, 3.8 Hz), 7.4 (t, J = 8.1 Hz); ^{19}F NMR (470.4 MHz, $CDCl_3$) δ -62.7 (s, 3F), -134.2 (septd, J = 22.3, 10.0 Hz, 1F), -200.6 (dd, J = 48.2, 33.2 Hz, 1F); HR-GC/MS (EI^+) Calc'd for $C_{13}H_{15}F_5$ $[M]^+$: 266.1088; found 266.1089.

99% e.e., chiral GC (β-Cyclosil, 130 ˚C, 14 psi); t_R(major) = 4.3 min, t_R(minor) = 4.4 min.

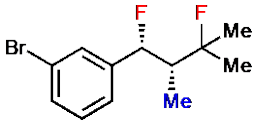

1-bromo-3-((1R,2R)-1,3-difluoro-2,3-dimethylbutyl)benzene. **4d** was prepared according to the general procedure C using (*E*)-1-bromo-3-(3,3-dimethylbut-1-en-1-yl)benzene (124 mg, 0.52 mmol). The diastereomeric ratio of the crude residue after work-up was determined to be >20:1 by ^{1}H and ^{19}F NMR analysis. The crude residue was purified by silica gel column chromatography (0 to 2% diethyl ether in hexanes) to give **4d** (92.2 mg, 64%) as a colorless oil in 99% ee. ^{1}H NMR (500 MHz, $CDCl_3$) δ 7.49 – 7.38 (m, 2H), 7.29 – 7.16 (m, 2H), 5.92 (d, J = 48.3 Hz, 1H), 2.36 – 1.89 (m, 1H), 1.48 (dd, J = 22.2, 1.9 Hz, 3H), 1.42 (d, J = 22.4 Hz, 3H), 0.86 (dd, J = 7.3, 1.4 Hz, 3H); ^{13}C NMR (126 MHz, $CDCl_3$) δ 142.9 (d, J = 21.5 Hz), 130.7, 130.0 (d, J = 1.7 Hz), 127.9 (d, J = 10.3 Hz), 123.4 (d, J = 9.5 Hz), 122.7 (d, J = 2.2 Hz), 97.7 (d, J = 167.3 Hz), 91.0 (dd, J = 179.0, 7.3 Hz), 49.7 (t, J = 20.7 Hz), 29.9, 26.7 (dd, J = 24.4, 1.9 Hz), 23.4 (dd, J = 25.0, 3.7 Hz), 7.6 – 7.3 (m); ^{19}F NMR (470.4 MHz, $CDCl_3$) δ -134.3

(septd, J = 22.3, 10.1 Hz), -200.3 (dd, J = 48.3, 33.2 Hz); HR-GC/MS (EI^+) Calc'd for $C_{12}H_{15}BrF_2$ $[M]^+$: 276.0320; found 276.0319.

98% e.e., chiral HPLC (IB, 100% hexanes, 1.0 mL/min, λ = 220 nm); t_R(minor) = 6.6 min, t_R(major) = 7.3 min.

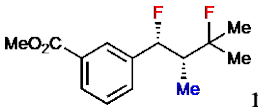

methyl 3-((1R,2R)-1,3-difluoro-2,3-dimethylbutyl)benzoate. **4e** was prepared according to the general procedure C using **2ae** (114 mg, 0.52 mmol). The diastereomeric ratio of the crude residue after work-up was determined to be >20:1 by ^1H and ^{19}F NMR analysis. The crude residue was purified by silica gel column chromatography (0 to 5% diethyl ether in hexanes) to give **4e** (115 mg, 86%) as a colorless oil in 99% ee. ^1H NMR (500 MHz, $CDCl_3$) δ 8.09 – 7.89 (m, 2H), 7.51 – 7.47 (m, 1H), 7.44 (t, J = 7.6 Hz, 1H), 5.99 (d, J = 48.2 Hz, 1H), 3.92 (d, J = 1.1 Hz, 3H), 2.18 – 1.95 (m, 1H), 1.51 (d, J = 1.9 Hz, 3H), 1.42 (d, J = 22.2 Hz, 3H), 0.85 (dd, J = 7.2, 1.3 Hz, 3H); ^{13}C NMR (125.7 MHz, $CDCl_3$) δ 166.9, 141.0 (d, J = 21.5 Hz), 130.4 (d, J = 1.8 Hz), 129.3 (d, J = 9.6 Hz), 128.8, 128.5 (d, J = 1.8 Hz), 125.9 (d, J = 9.6 Hz), 97.6 (d, J = 167.6 Hz), 91.4 (dd, J = 178.3, 7.3 Hz), 52.3, 49.6 (t, J = 20.7 Hz), 26.6 (dd, J = 24.5, 2.0 Hz), 23.5 (dd, J = 24.9, 3.7 Hz), 7.3 (d, J = 7.9 Hz); ^{19}F NMR (470.4 MHz, $CDCl_3$) δ -134.3 (septd, J = 22.3, 10.0 Hz), -200.3 (dd, J = 48.2, 33.3 Hz); HR-GC/MS (EI^+) Calc'd for $C_{14}H_{18}F_2O_2$ $[M]^+$: 256.1269; found 256.1269.

99% e.e., chiral GC (β-Cyclosil, 120 to 200 ˚C, 14 psi); t_R(major) = 50.1 min, t_R(minor) = 50.2 min.

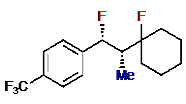

1-((1R,2R)-1-fluoro-2-(1-fluorocyclohexyl)propyl)-4-(trifluoromethyl)benzene. **4f** was prepared according to the general procedure C using **2af** (140 mg, 0.52 mmol). The

diastereomeric ratio of the crude residue after work-up was determined to be >20:1 by ^{1}H and ^{19}F NMR analysis. The crude residue was purified by silica gel column chromatography (0 to 2% diethyl ether in hexanes) to give **4f** (129 mg, 81%) as a colorless oil in 99% ee. ^{1}H NMR (500 MHz, $CDCl_3$) δ 7.64 (d, *J* = 8.1 Hz, 2H), 7.45 (d, *J* = 8.1 Hz, 2H), 5.99 (d, *J* = 48.1 Hz, 1H), 2.25 – 2.03 (m, 3H), 1.85 – 1.56 (m, 5H), 1.51 (dd, *J* = 22.0, 3.6 Hz, 3H), 1.33 – 1.20 (m, 1H), 1.20 – 1.07 (m, 1H), 1.07 – 0.95 (m, 1H); ^{13}C NMR (125.7 MHz, $CDCl_3$) δ 144.7 (d, *J* = 21.5 Hz), 129.9 (q, *J* = 32.3 Hz), 125.5 – 125.3 (m), 125.3 (d, *J* = 9.6 Hz), 122.1 (d, *J* = 272.1 Hz), 100.2 (dd, *J* = 167.1, 2.0 Hz), 91.8 (dd, *J* = 178.8, 2.0 Hz), 54.7 (dd, *J* = 22.0, 20.0 Hz), 41.6 (d, *J* = 23.2 Hz), 29.3 (d, *J* = 49.5 Hz), 23.34 (dd, *J* = 25.5, 4.4 Hz), 21.7 (d, *J* = 3.2 Hz), 21.3 (dd, *J* = 10.2, 6.7 Hz);^{19}F NMR (470.4 MHz, $CDCl_3$) δ -62.5 (s, 3F), -129.3 – -129.7 (m, 1F), -198.7 (ddd, *J* = 48.3, 35.9, 3.7 Hz, 1F); HR-GC/MS (EI^+) Calc'd for $C_{16}H_{19}F_5$ $[M]^+$: 306.1401; found 306.1399.

99% ee, Chiral GC (?, 130 ˚C, 14 psi); t_R(major) = 48.8 min, t_R(minor) = 50.2 min.

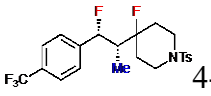

4-fluoro-4-((1R,2R)-1-fluoro-1-(4-(trifluoromethyl)phenyl)propan-2-yl)-1-tosylpiperidine. **4g** was prepared according to the general procedure C using **2ag** (220 mg, 0.52 mmol). The diastereomeric ratio of the crude residue after work-up was determined to be >20:1 by ^{1}H and ^{19}F NMR analysis. The crude residue was purified by silica gel column chromatography (0 to 30% diethyl ether in hexanes) to give **4g** (168 mg, 70%) as a white solid in 99% ee. ^{1}H NMR (500 MHz, $CDCl_3$) δ 7.70 – 7.65 (m, 2H), 7.61 (d, *J* = 8.0 Hz, 2H), 7.36 (d, *J* = 7.5 Hz, 2H), 7.34 (d, *J* = 8.6 Hz, 2H), 5.97 (d, *J* = 48.2 Hz, 1H), 3.76 (dddd, *J* = 12.1, 9.8, 4.8, 2.2 Hz, 2H), 2.69 – 2.53 (m, 2H), 2.43 (s, 3H), 2.22 – 1.83 (m, 4H), 0.81 (d, *J* = 7.3 Hz, 3H); ^{13}C

NMR (125.7 MHz, $CDCl_3$) δ 143.8, 143.7 (d), 133.3, 130.0 (q, J = 32.9 Hz), 127.8, 125.4 (d, J = 4.6 Hz), 125.1 (d, J = 9.6 Hz), 124.1 (q, J = 271.8 Hz), 95.2 (d, J = 174.1 Hz), 90.7 (dd, J = 179.3, 7.4 Hz), 48.7 (t, J = 20.3 Hz), 42.2 – 41.8 (m), 33.2 (d, J = 21.2 Hz), 30.5 (dd, J = 21.8, 4.0 Hz), 21.6, 7.0 (t, J = 7.7 Hz); ^{19}F NMR (470.4 MHz, $CDCl_3$) δ -62.6 (s, 3F), -160.3 (tq, J = 40.5, 9.4 Hz, 1F), -199.2 (dd, J = 48.2, 33.8 Hz, 1F); HRMS (ESI-TOF) Calc'd for $C_{22}H_{24}BrF_5NO_2S$ $[M+H]^+$: 462.1521; found 462.1520.

99% ee, Chiral HPLC (OD-H, 10% isopropanol in hexanes, 1.0 mL/min, λ = 210 nm); t_R(major) = 17.4 min, t_R(minor) = 18.5 min.

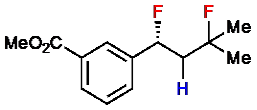

methyl (*R*)-3-(1,3-difluoro-3-methylbutyl)benzoate. **5a** was prepared according to the general procedure C using methyl (*E*)-3-(3-methylbut-1-en-1-yl)benzoate. (106 mg, 0.52 mmol). The crude residue was purified by silica gel column chromatography (0 to 3% diethyl ether in hexanes) to give **5a** (79.4 mg, 63%) as a colorless oil in 94% ee. ^{1}H NMR (500 MHz, $CDCl_3$) δ 8.04 – 7.98 (m, 2H), 7.55 (ddt, J = 8.4, 1.9, 0.9 Hz, 1H), 7.47 (tt, J = 7.6, 0.9 Hz, 1H), 5.77 (ddd, J = 48.5, 9.7, 2.1 Hz, 1H), 3.93 (s, 3H), 2.29 (dddd, J = 25.4, 18.4, 15.4, 9.7 Hz, 1H), 2.10 (dddd, J = 38.1, 15.3, 12.8, 2.1 Hz, 1H), 1.54 (dd, J = 21.7, 1.7 Hz, 3H), 1.45 (d, J = 21.7 Hz, 3H); ^{13}C NMR (125.7 MHz, $CDCl_3$) δ 166.8, 141.1 (d, J = 20.3 Hz), 130.7, 130.0 (d, J = 6.9 Hz), 129.7 (d, J = 1.7 Hz), 128.9, 126.7 (d, J = 7.1 Hz), 94.4 (d, J = 166.6 Hz), 90.6 (dd, J = 172.2, 6.0 Hz), 52.4, 48.8, 28.6 (d, J = 24.9 Hz), 26.4 (dd, J = 24.9, 3.0 Hz); ^{19}F NMR (470.4 MHz, $CDCl_3$) δ -136.6 – -137.0 (m, 1F), -173.8 – -174.2 (m, 1F); HRMS (ESI-TOF) Calc'd for $C_{13}H_{16}F_2O_2$ $[M+Na]^+$: 265.1011; found 265.1011.

94% ee, Chiral GC (Cyclosil-β, 100 ˚C, 14 psi); t_R(major) = 153.4 min, t_R(minor) = 156.8 min.

Friedel-Crafts Alkylation/rearrangement Product.

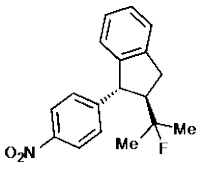

Prepared according to the general procedure C using **S2** (146 mg, 0.52 mmol). The diastereomeric ratio of the crude residue after work-up was determined to be >20:1 by ^{1}H and ^{19}F NMR analysis. The crude residue was purified by silica gel column chromatography (0 to 4% diethyl ether in hexanes) to give **S3** (149 mg, 96%) as a colorless oil in 94% ee. ^{1}H NMR (500 MHz, $CDCl_3$) δ 8.18 (d, *J* = 8.7 Hz, 2H), 7.37 (d, *J* = 8.7 Hz, 2H), 7.34 – 7.27 (m, 1H), 7.26 – 7.20 (m, 1H), 7.19 – 7.08 (m, 1H), 6.76 (d, *J* = 7.6 Hz, 1H), 4.57 (d, *J* = 7.7 Hz, 1H), 3.27 (dd, *J* = 16.2, 8.9 Hz, 1H), 3.05 (dd, *J* = 16.2, 8.2 Hz, 1H), 2.95 – 2.76 (m, 1H), 1.39 (d, *J* = 21.4 Hz, 3H), 1.33 (d, *J* = 21.5 Hz, 3H); ^{13}C NMR (125.7 MHz, $CDCl_3$) δ 153.96, 146.66, 145.35, 142.03, 129.41, 127.50, 127.12, 124.97, 124.48, 123.91, 96.79 (d, *J* = 168.8 Hz), 58.11 (d, *J* = 21.5 Hz), 52.66 (d, *J* = 3.7 Hz), 34.11 (d, *J* = 6.3 Hz), 26.61 (d, *J* = 24.5 Hz), 24.94 (d, *J* = 24.5 Hz); ^{19}F NMR (470.4 MHz, $CDCl_3$) δ -141.4 (septd, *J* = 21.4, 16.2 Hz); HR-GC/MS (EI^+) Calc'd for $C_{18}H_{19}F_2NO_2$ $[M]^+$: 319.1378; found 319.1380.

94% ee, Chiral HPLC (OD-H, 2% isopropanol in hexanes, 1.0 mL/min, λ = 230 nm); t_R(major) = 10.0 min, t_R(minor) = 13.9 min.

Product Elaborations.

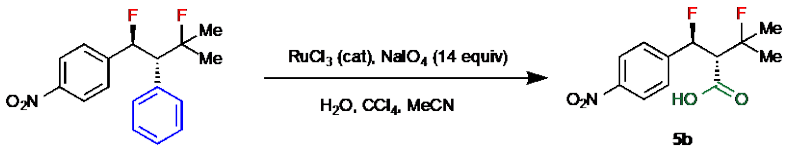

To a solution of **3e** (76.3 mg, 0.25 mmol, 1 equiv) in acetonitrile (0.65 mL) and carbon tetrachloride (0.65 mL) was added water (1.3 mL), sodium periodate (749 mg, 3.49 mmol, 14 equiv) and a catalytic amount of ruthenium(III) chloride hydrate were added. The reaction mixture was allowed to stir at room temperature under air. After 18 h, diethyl ether (10 mL) was added, and the aqueous and organic layers were separated. The aqueous layer was extracted with diethyl ether (3 x 10 mL), washed with brine (5 mL), dried over Na_2SO_4, filtered and concentrated to give **7** as a brown oil (63.5 mg, 93%). ^{1}H NMR (500 MHz, $CDCl_3$) δ 8.22 (d, *J* = 8.4 Hz, 2H), 7.54 (d, *J* = 8.3 Hz, 2H), 5.79 (dd, *J* = 46.7, 10.2 Hz, 1H), 3.27 (td, *J* = 10.0, 7.8 Hz, 1H), 1.76 – 1.54 (m, 6H); ^{13}C NMR (125.7 MHz, $CDCl_3$) δ 174.8 – 172.5 (m), 148.6, 143.6 (d, *J* = 20.4 Hz), 127.9 (d, *J* = 6.2 Hz), 124.0, 95.0 (d, *J* = 174.0 Hz), 90.9 (dd, *J* = 179.9, 7.0 Hz), 61.3 (t, *J* = 24.2 Hz), 28.1 (dd, *J* = 23.9, 4.2 Hz), 25.5 – 23.4 (m); ^{19}F NMR (470.4 MHz, $CDCl_3$) δ -133.4 – -133.9 (m, 1F), -179.2 (d, *J* = 46.9 Hz, 1F); HRMS (ESI-TOF) Calc'd for $C_{12}H_{13}F_2NO_4$ $[M-H]^-$: 272.040; found 272.0753.

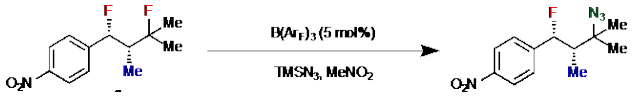

To a solution of **4a** (45 mg, 0.185 mmol, 1 equiv) and $TMSN_3$ (49 μL, 0.37 mmol, 2 equiv) in $MeNO_2$ (0.093 mL, 2M) was added $B(C_5F_5)_3$ (4.5 mg, 0.009 mmol, 0.05 equiv). The reaction mixture was stirred for 90 minutes, after which the solution was loaded onto silica using hexanes and purified by column chromatography using 2% to 6% diethyl ether in hexanes to give **8** (36.0 mg, 73%). 1H NMR (500 MHz, CDCl3) δ 8.23 (t, J = 9.4 Hz, 2H), 7.46 (t, J = 9.1 Hz, 2H), 6.05

(d, J = 48.4 Hz, 1H), 1.88 – 1.71 (m, 1H), 1.42 (d, J = 2.0 Hz, 3H), 1.40 (s, 3H), 0.85 (dd, J = 7.2, 1.6 Hz, 3H). ^{13}C NMR (125.7 MHz, $CDCl_3$) δ 150.5 – 149.9 (m), 128.2 – 128.1 (d, *J* = 10.0 Hz), 126.2 (d, *J* = 2.0 Hz), 95.0, 93.8, 66.9 (d, *J* = 1.5 Hz), 51.7 (d, *J* = 20.1 Hz), 28.0 (d, *J* = 1.7 Hz), 24.7 (d, *J* = 4.1 Hz), 9.6 (d, *J* = 8.1 Hz) ; 19F NMR (470.4 MHz, CDCl3) δ -200.38 (dt, J = 31.3, 23.8 Hz, 1F). Calc'd for $C_{12}H_{15}FN_4O_4$ $[M+H]^+$: 266.1179; found 266.1172.

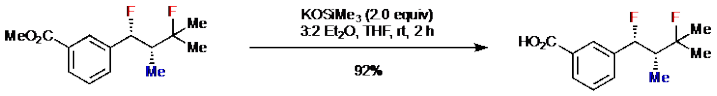

To a solution of **4e** (115 mg, 0.45 mmol, 1 equiv) in 3:2 Et_2O:THF (4.5 mL) under $N_{2(g)}$ was added potassium trimethylsilanoate (90%, 128 mg, 0.90 mmol, 2 equiv). The reaction mixture was stirred at room temperature. After 2 hours, the reaction was quenched with 1 M $HCl_{(aq)}$ (2 mL). The organic and aqueous layers were separated. The aqueous layer was extracted with Et_2O (3 x 5 mL). The combined organic layers were washed with brine (2 mL), dried over Na_2SO_4, filtered and concentrated *in vacuo* to give **6** as a white solid (100 mg, 92%). Crystals of **6** were grown by slow evaporation from Et_2O. ^{1}H NMR (500 MHz, $CDCl_3$) δ 8.10 – 8.00 (m, 2H), 7.57 (d, *J* = 7.8 Hz, 1H), 7.51 (td, *J* = 7.7, 2.2 Hz, 1H), 6.03 (d, *J* = 48.3 Hz, 1H), 2.20 – 2.01 (m, 1H), 1.52 (d, *J* = 21.9 Hz, 3H), 1.47 (d, *J* = 2.1 Hz, 3H), 0.88 (d, *J* = 7.0 Hz, 3H); ^{13}C NMR (125.7 MHz, $CDCl_3$) δ 171.9, 141.2 (d, *J* = 21.6 Hz), 130.3 (d, *J* = 9.4 Hz), 129.5, 128.7, 126.6 (d, *J* = 9.5 Hz), 97.7 (d, *J* = 167.5 Hz), 91.4 (dd, *J* = 178.5, 7.4 Hz), 49.6 (t, *J* = 20.7 Hz), 26.7 (d, *J* = 24.2 Hz), 23.5 (dd, *J* = 25.0, 3.7 Hz), 7.4 (t, *J* = 8.0 Hz); ^{19}F NMR (376 MHz, $CDCl_3$) δ -134.3 (septd, *J* = 22.2, 9.8 Hz, 1F), -200.3 (dd, *J* = 48.2, 33.4 Hz, 1F); HR-GC/MS (EI^+) Calc'd for $C_{13}H_{16}F_2O_2$ $[M-H]^-$: 241.1046; found 241.1056.

Impact of Stationary Arene Electronics on Diastereoselectivity

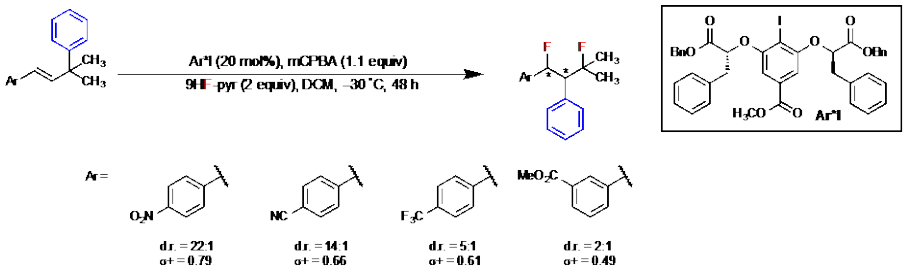

Figure 1.24. Impact of stationary arene on crude product d.r. for the aryl rearrangement reactions.

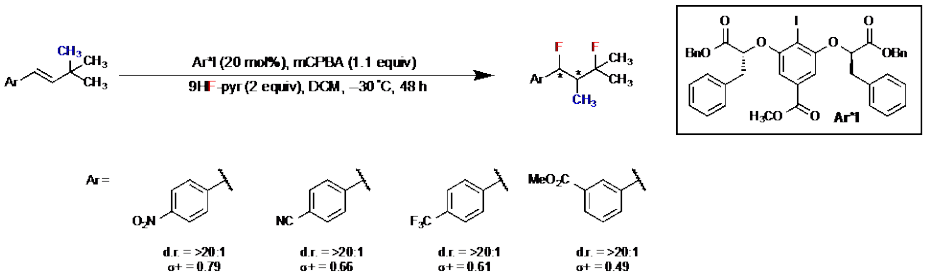

Figure 1.25. Impact of stationary arene on crude product d.r. for the methyl rearrangement reactions.

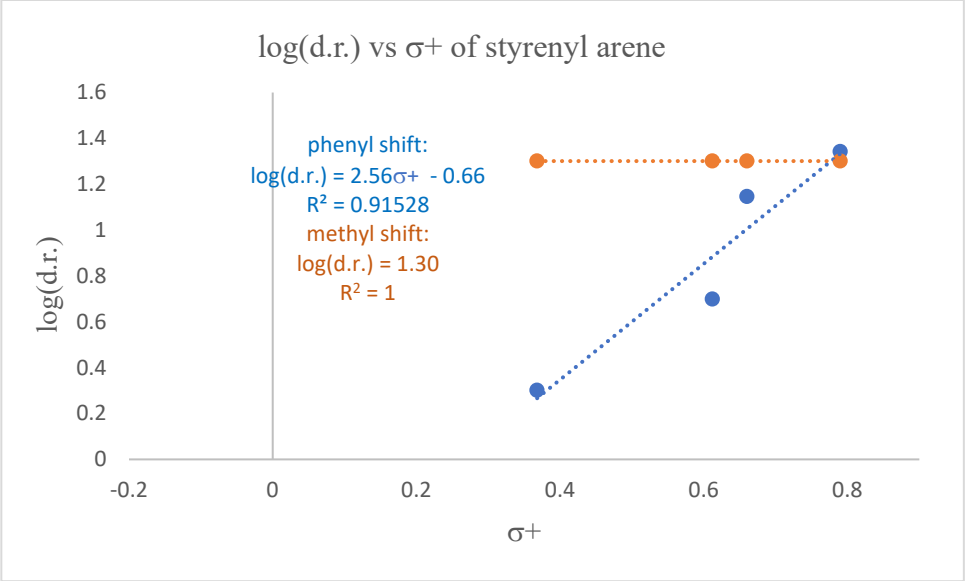

Ar	σ+	d.r.	log (d.r.)
Ph shift			
p-CN	0.66	14	1.1
p-CF3	0.61	5	0.70
p-NO2	0.79	22	1.3
m-CO_2Me	0.37	2	0.30
Me shift			
p-CN	0.66	20	1.3
p-CF3	0.612	20	1.3
p-NO2	0.79	20	1.3

m-CO_2Me	0.368	20	1.3

Figure 1.26. Hammett plot of log(d.r.) vs. σ+ of stationary arene for the methyl (orange) and phenyl (blue) migration reactions. For the phenyl rearrangement reaction, the measured ρ+ value of 2.56 is consistent with significant buildup of cationic charge at benzylic position (of the styrenyl arene) the in the product-determining step. For the methyl rearrangement reaction, the ρ+ value of 0 is consistent with minimal buildup of cationic charge at the benzylic position in the product-determining step.

Hammett Study on Relative Rate of Aryl Rearrangement Reactions

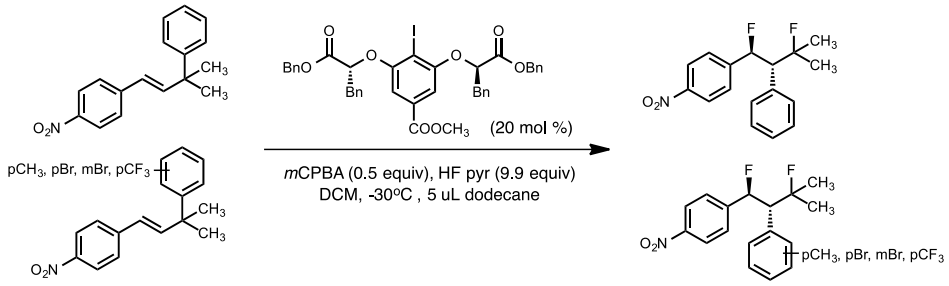

To a solution of phenyl-migration-substrate **2e** (.05 mmol, 1 equiv), substituted-aryl-migration-substrate **2a**, **2b**, **2c**, or **2d** (.05 mmol, 1 equiv), and catalyst (0.01 mmol, 20 mol%) in dichloromethane (0.3 mL) in a low-density polyethylene tube was added 5 µL dodecane as an internal standard. Alternatively, the slowly reacting substrate **2f** was mixed with **2d** instead of **2e** in order to compare more similar levels of conversions. The substrate, catalyst, solvent, and internal standard mixture was briefly stirred, and then 10 µL was removed and diluted with 1 mL of DCM as T_0 for conversion analysis. The mixture was cooled to –78 °C, followed by sequential addition of HF-pyridine (py-9HF, 70% hydrogen fluoride by weight, 140 µL, 90 equiv hydrogen fluoride) and *m*CPBA (77% by weight, 5 mg, 0.025 mmol, 0.5 equiv). The reaction mixture was warmed to –30 °C and stirred at that temperature for 48 hours. The heterogeneous mixture was

transferred carefully into a vigorously stirred suspension of basic alumina (1 g) in dichloromethane at –78 °C. The resulting suspension was allowed to warm to room temperature and filtered, washing with 10 mL dichloromethane. 2 mL of this solution was removed for GC analysis for the T_f measurement.

All conversions were determined by gas chromatography (achiral GC, 40 to 300 ˚C, ramp = 21ºC/min, 14 psi; t_R(Ph) = 7.92 min, t_R(*p*-CH_3Ar) = 7.92 min, t_R(*p*-BrAr) = 8.75 min, t_R(*m*-BrAr) = 8.66 min, t_R(*p*-CF_3Ar) = 7.87 min, t_R(dodecane) = 4.43 min). All samples were acquired with five GC runs, and the integration of relevant peaks was averaged.

Each competition experiment was run in either duplicate or triplicate, and the relative rate was calculated for all three experiments and then averaged. The standard deviation was derived from the spread of values obtained between the three experiments, and does not take into account the standard deviation from the measurement itself (the standard deviation between the five GC runs for each experiment), which is negligible. The equation used to determine the relative rate of consumption of the standard phenyl substrate **2e** vs substituted aryl substrate vs was:

$$\left|\frac{k_H}{k_X}\right| = \frac{\ln\left(1 - F_H\right)}{\ln\left(\left(1 - F_H\right)\left(\frac{R_F}{R_0}\right)\right)}$$

where

$$1 - F = 1 - conversion = starting\ material\ remaining = \frac{\frac{SM_F}{dod_F}}{\frac{SM_0}{dod_0}}$$

and

$$\frac{R_F}{R_0} = \frac{ratio\ of\ starting\ material\ X\ over\ starting\ material\ H\ at\ T_F}{ratio\ of\ starting\ material\ X\ over\ starting\ material\ H\ at\ T_0} = \frac{\frac{[SM_X]_F}{[SM_H]_F}}{\frac{[SM_X]_0}{[SM_H]_0}}$$

and

$$SM = integral\ of\ starting\ material;\ dod = integral\ of\ dodecane\ internal\ standard$$

Table 1. Relative rate measurements for one-pot competition experiments competing substrates 2a–d and 2f versus 2e.

Migrating aryl group substitution	σ+	σ	k_X/k_H	**log(k_X/k_H)**	**k_X/k_H lower bound**	**k_X/k_H upper bound**
H	0	0	1	0	0	0
p-Br	0.15	0.232	0.103	-0.993	0.0743	0.161
m-Br	0.405	0.391	0.0315	-1.50	0.0203	0.0699
p-CF3	0.612	0.54	0.00721	-2.14	0.00637	0.00830
p-Me	-0.311	-0.170	2.81	0.449	2.59	3.03

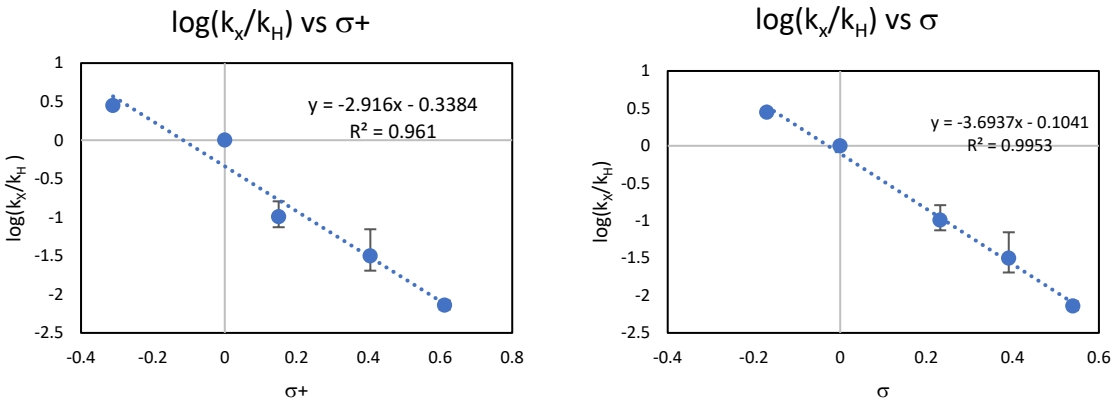

Figure 1.27. Hammett plots of σ^+ versus log(k_X/k_H) and σ versus log(k_X/k_H).

Table 2. Measurements of relative and absolute conversions of different aryl migrations substrates by GC. dod = integral of internal standard. pX or mX = integral of substituted aryl migration starting material. H = integral of phenyl starting material. F = conversion of starting material = (SMf/dodf)/(Sm0/dod0). kh/kX = relative rate of consumption of H vs X = ln(1–FH)/ln(1-FX).

	kpBr/kH
avg	0.1054
std dev	0.0211

Exp 1	dod	pBr	H		SM left	Relative rates
To	4486.8	3479.8	4896.6	1 – FH	0.553	0.0923
Tf	8499.3	6241.3	5131.3	1 – FpBr	0.947	

Exp 2	dod	pBr	H		SM left	Relative rates
To	2376.8	2210	1911.5	1 – FH	0.418	0.0888
Tf	8596	7397	2888	1 – FpBr	0.925	
Exp 3	dod	pBr	H		SM left	Relative rates
To	6713.8	12380	4711.3	1 – FH	0.835	0.135
Tf	5349.5	9626.8	3134	1 – FpBr	0.976	

	kmBr/ kH
avg	0.0407
std dev	0.0171

Exp 1	dod	mBr	H		SM left	Relative rates
To	1222	1003.3	374.75	1 – FH	0.053	0.0177
Tf	5145	4009	83.05	1 – FmBr	0.949	
Exp 2	dod	mBr	H		SM left	Relative rates
To	3975.3	3980.5	2460	1 – FH	0.441	0.0454
Tf	5688.5	5488.3	1553.3	1 – FmBr	0.964	
Exp 3	dod	mBr	H		SM left	Relative rates

To	2031	3609.4	1756.2	1 – FH	0.133	0.0588
Tf	3427.6	5409.8	394.28	1 – FmBr	0.888	

	kpCF3/ kmBr	**kpCF3/ kH**
avg	0.2377	0.0097
std dev	0.0448	

Exp 1	dod	pCF3	mBr		SM left	Relative rates
To	4363.2	3270	981	1 – FmBr	0.782	0.283
Tf	9161.8	6406.5	1611.8	1 – FpCF3	0.933	

Exp 2	dod	pCF3	mBr		SM left	Relative rates
To	2526.3	3328	1700.3	1 – FmBr	0.551	0.193
Tf	4030.2	4731.6	1493.4	1 – FpCF3	0.891	

	kpCH3/kH
avg	2.8104
std dev	0.2182

Exp 1	dod	H	pCH3		SM left	Relative rates

To	5192.7	8320.3	6040.3	1 – FpCH3	0.669	2.90
Tf	9391.7	13097	7303.7	1 – FH	0.87	
Exp 2	dod	H	pCH3		SM left	Relative rates
To	1344	1542.7	1475.3	1 – FpCH3	0.764	3.02
Tf	1425	1496.3	1195.3	1 – FH	0.915	
Exp 3	dod	H	pCH3		SM left	Relative rates
To	1676.4	2623.8	1362.8	1 – FpCH3	0.506	2.51
Tf	3959.8	4725.2	1629.4	1 – FH	0.762	

KIE experiments

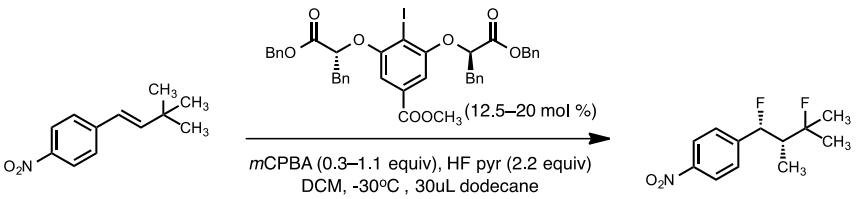

Full conversion:

To a solution of substrate (120mg, 0.58 mmol, 1 equiv) and catalyst (88.0 mg, 0.11 mmol, 20 mol%) in dichloromethane (3.5 mL) in a low-density polyethylene tube at –78 °C was added HF-pyridine (py-9HF, 70% hydrogen fluoride by weight, 360 µL, 20 equiv hydrogen fluoride)

followed by *m*CPBA (77% by weight, 140. mg, 0.63 mmol, 1.1 equiv). The reaction mixture was warmed to –35 °C and stirred at that temperature for 48 hours. The heterogeneous mixture was transferred carefully into a vigorously stirred suspension of basic alumina (4.0 g) in dichloromethane at –78 °C. The resulting suspension was allowed to warm to room temperature and filtered, washing with 100 mL dichloromethane. The combined filtrate was concentrated under reduced pressure and was purified by silica gel column chromatography (0 to 3.4% diethyl ether in hexanes).

Partial conversion:

To a solution of substrate (330 mg, 1.61 mmol, 1 equiv) and catalyst (154.0 mg, 0.2 mmol, 12.5 mol%) in dichloromethane (11 mL) in a low-density polyethylene tube was added 30 μL dodecane as an internal standard. This mixture was briefly stirred, and then 10 μL was removed as T_0 for conversion analysis. The mixture was cooled to –78 °C, followed by sequential addition of HF-pyridine (py-9HF, 70% hydrogen fluoride by weight, 1.06 mL, 20 equiv hydrogen fluoride) and *m*CPBA (77% by weight, 107 mg, 0.48 mmol, 0.30 equiv). The reaction mixture was warmed to –30 °C and stirred at that temperature for 48 hours. The heterogeneous mixture was transferred carefully into a vigorously stirred suspension of basic alumina (10 g) in dichloromethane at –78 °C. The resulting suspension was allowed to warm to room temperature and filtered, washing with 200 mL dichloromethane. 2 mL of this solution was removed for GC analysis for the T_f measurement. The combined filtrate was concentrated under reduced pressure and was purified by silica gel column chromatography (0 to 3.4% diethyl ether in hexanes).

Conversion (32.5%, 28.3%) was determined by quantitative gas chromatography spectra (achiral GC, 40 to 300 ˚C, ramp = 21°C/min, 14 psi; t_R(starting material) = 7.92 min, t_R(dodecane) = 4.43

min). All samples were acquired five times, and the integration of relevant peaks was averaged. The equation used to assess conversion was:

$$conversion = 1 - \frac{\frac{SM_F}{dod_F}}{\frac{SM_0}{dod_0}}$$

Where SM_F = the average integration of the starting material peak at the end of the reaction, SM_0 = the average integration of the starting material peak at the start of the reaction, dod_F = the average integration of the reference peak at the end of the reaction, and dod_F = the average integration of the reference peak at the start of the reaction.

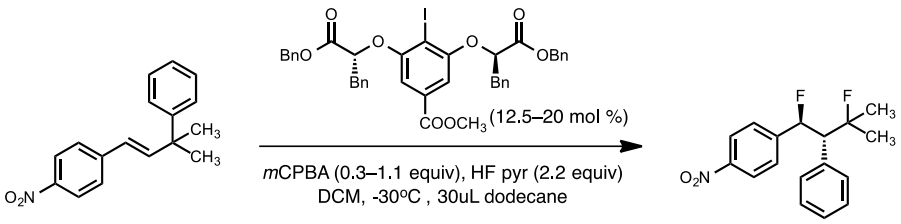

Full conversion:

To a solution of substrate (200mg, 0.75 mmol, 1 equiv) and catalyst (115.0 mg, 0.15 mmol, 20 mol%) in dichloromethane (4.5 mL) in a low-density polyethylene tube at –78 °C was added HF-pyridine (py-9HF, 70% hydrogen fluoride by weight, 460 µL, 20 equiv hydrogen fluoride) followed by *m*CPBA (77% by weight, 185. mg, 0.82 mmol, 1.1 equiv). The reaction mixture was warmed to –35 °C and stirred at that temperature for 48 hours. The heterogeneous mixture was

transferred carefully into a vigorously stirred suspension of basic alumina (5.0 g) in dichloromethane at –78 °C. The resulting suspension was allowed to warm to room temperature and filtered, washing with 100 mL dichloromethane. The combined filtrate was concentrated under reduced pressure and was purified by silica gel column chromatography (0 to 1.8% diethyl ether in hexanes).

Partial conversion:

To a solution of substrate (600 mg, 2.47 mmol, 1 equiv) and catalyst (230 mg, 0.30 mmol, 12.5 mol%) in dichloromethane (15 mL) in a low-density polyethylene tube was added 100 μL dodecane as an internal standard. This mixture was briefly stirred, and then 15 μL was removed as T_0 for conversion analysis. The mixture was cooled to –78 °C, followed by sequential addition of HF-pyridine (py-9HF, 70% hydrogen fluoride by weight, 1.5mL, 20 equiv hydrogen fluoride) and *m*CPBA (77% by weight, 169 mg, 0.75 mmol, 0.30 equiv). The reaction mixture was warmed to –30 °C and stirred at that temperature for 48 hours. The heterogeneous mixture was transferred carefully into a vigorously stirred suspension of basic alumina (10 g) in dichloromethane at –78 °C. The resulting suspension was allowed to warm to room temperature and filtered, washing with 200 mL dichloromethane. 2 mL of this solution was removed for GC analysis for the T_f measurement. The combined filtrate was concentrated under reduced pressure and was purified by silica gel column chromatography (0 to 1.8% diethyl ether in hexanes).

Conversion (26.2%, 23.3%) was determined by quantitative gas chromatography spectra (achiral GC, 40 to 300 ˚C, ramp = 21ºC/min, 14 psi; t_R(starting material) = 7.92 min, t_R(dodecane) = 4.43 min). All samples were acquired five times, and the integration of relevant peaks was averaged. The equation used to assess conversion is the same as used for analysis of the methyl migration reaction.

NMR Sample Preparation

Methyl migration reaction:

4 samples of product were prepared (60 mg of product in 650 μL of $CDCl_3$ containing 2 mM $Cr(acac)_3$). Two of the samples were full conversion samples (F = 100%) with respect to the starting material and two were partial conversion samples (F = 32.5% and 28.3%) with respect to the starting material. The samples were prepared in Wilmad 528-PP-9 NMR tubes and subsequently hermetically sealed under air at room temperature.

Phenyl migration reaction:

4 samples of product were prepared (120 mg of product in 650 μL of $CDCl_3$ containing 0.5 mM $Cr(acac)_3$). Two of the samples were full conversion samples (F = 100%) with respect to the starting material and two were partial conversion samples (F = 26.2% and 23.3%) with respect to the starting material. The samples were prepared in Wilmad 528-PP-9 NMR tubes and subsequently hermetically sealed under air at room temperature.

Collection and Processing Procedure

NMR data was collected and processed according to procedures previously reported methods for both DEPT (^1H) and MQF (^{19}F) techniquess. NMR data were processed using Python and the nmrglue package (www.nmrglue.com). NMR data were collected in blocks of 32 scans in a single experiment using the array command (e.g., array('nt',6,32,0) would set up 6 blocks of 32 scans). The methyl migration samples were acquired across three sets of 8–36 blocks and the phenyl migration sample was acquired with one set of 8–12 block. Each FID was zero-filled to four times the number of complex points, apodized with a line broadening of 0.25 Hz, and Fourier transformed. For each set of FIDs, one spectrum was manually referenced and phased. Regions of

integration were defined for each peak for each spectra, as detailed below. The regions were then centered individually on each peak. A first order baseline correction was calculated by fitting a linear function to the non-signal regions and then subtracting it from the entire spectrum. In the case of the 19F spectra, a second-order baseline correction was applied. Signal to noise ratios were calculated for each peak by dividing the signal intensity at half height by the rootmean-square deviation of the signal in a noisy region. Integrals were simply calculated by summing the signal intensities over the peak regions. After the integrals were obtained, KIEs and their associated errors were calculated using an Excel document (in the provided archive file).

Methyl rearrangement integration regions:

For the MQF spectra, the region of integration was defined with width 0.090 and 0.120 ppm for the downfield and upfield satellites, respectively, for the tertiary C-F. For the 1H spectra, the region of integration was defined with a width of 0.100 ppm for the benzylic C-H. For the DEPT spectra, the region of integration was defined with a width of 0.120 ppm for all CH_3 groups. The downfield member of the aryl proton doublet was chosen as the reference peak for the MQF measurement, and all other peaks were referenced to themselves.

Phenyl rearrangement integration regions:

For the MQF spectra, the region of integration was defined with width 0.100 and 0.175 ppm for the downfield and upfield satellites, respectively. For the 19F spectra, the region of integration was defined with width 0.900 for the tertiary C-F. The downfield member of the aryl proton doublet

was chosen as the reference peak for the MQF measurement, and all other peaks were referenced to themselves.

Calculation of KIEs and Error Bars

For both the aryl and alkyl migration reaction analyses, the KIE was calculated according to:

$$\frac{\log(1-F)}{\log\left(1-F\frac{R}{R_0}\right)}$$

where F is the fractional conversion, R is the 13C/12C ratio in the product, R0 is the ratio in the starting material, and log refers to the natural logarithm. R0 is experimentally determined by taking the reaction to 100% conversion and quantitating product because this minimizes errors caused by deviations in response factors. The propagated error in this formula was calculated in Mathematica (using

https://github.com/FlashTek/mathematica-error-propagation):

```
TeXForm[FullSimplify[ErrorProgataionPrintFormula[
 Log[1 - F]/Log[1 - F*R/Subscript[R, 0]], {F, R, Subscript[R, 0]}]]]
```

$$\sqrt{\frac{(F-1)^2F^2R^2\log^2(1-F)\sigma_{R_0}^2+(F-1)^2F^2R_0^2\log^2(1-F)\sigma_R^2+R_0^2\sigma_F^2\left((F-1)R\log(1-F)+(R_0-FR)\log\left(1-\frac{FR}{R_0}\right)\right)^2}{(F-1)^2R_0^2(R_0-FR)^2\log^4\left(1-\frac{FR}{R_0}\right)}}$$

KIE data

Table 3. Summary of KIE data for the methyl rearrangement reaction.

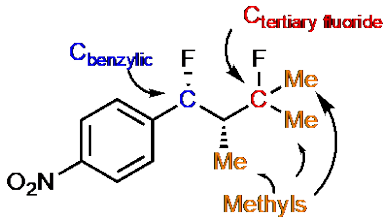

	$C_{benzylic}$ (MQF)		sum of methyls (DEPT)		tertiary C-F (MQF)	
	KIE	error	KIE	error	KIE	error
Sample A	1.009	0.001	0.991	0.002	0.996	0.002
Sample B	1.005	0.001	1.001	0.002	1.003	0.003
average	**1.007**		**0.996**		**0.999**	

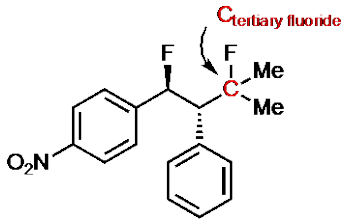

Table 4. Summary of KIE data for the aryl rearrangement reaction.

	KIE	std err
sample A	1.008	0.006
sample B	1.005	0.007
average	**1.007**	

Table 5. Methyl rearrangement reaction intermolecular KIE data and processing. 19F column = data derived from the standard 19F experiment, representing 12C. MQF column = data derived from the MQF experiment, representing 13C. R = (Area C13)/(Area C12) for partial conversion samples. R0 = (Area C13)/(Area C12) for the averaged full conversion samples.

	Cbenzylic (MQF)		**sum of methyls (DEPT)**		**tertiary C-F (MQF)**	
KIE	KIE	error	KIE	error	KIE	error
sample A	1.009	0.001	0.991	0.002	0.996	0.002
sample B	1.005	0.001	1.001	0.002	1.003	0.003
average	**1.007**		**0.996**		**0.999**	

Conversion	conversion	error
sample A	0.325	0.005
sample B	0.283	0.003

	benzylic (MQF)		sum of methyls (DEPT)		tertiary C-F (MQF)	
RAW INTEGRALS	C12	C13	C12	C13	C12	C13
Full conv sample A block 1	8.7376	9.8426	85.1412	79.040 7	36.3243	10.045 5
Full conv sample B block 1	10.2342	11.409 8	94.7573	91.843 1	41.497	11.671 9
Partial conv sample A block 1	9.0387	10.039 4	85.4997	81.359 5	36.7742	10.300 4
Partial conv sample B block 1	9.226	10.274 2	87.5041	82.557 8	37.6125	10.478 9
Full conv sample A block 2	8.565	9.5915	83.198	78.750 4	35.4966	8.7185
Full conv sample B block 2	9.9728	11.113 1	92.0642	90.427 9	40.2976	9.9444

Partial conv sample A				81.223		
block 2	8.8475	9.8111	83.36	9	35.848	8.8617
Partial conv sample B		10.089		82.650		
block 2	9.0744	9	85.6611	6	36.7792	9.0377
Full conv sample A				78.607		
block 3	8.6003	9.6358	83.5618	6	35.6372	8.7646
Full conv sample B		11.134		90.719		
block 3	10.0246	5	92.1989	7	40.3648	10.026
Partial conv sample A				80.996		
block 3	8.8587	9.8242	83.4884	5	35.8727	8.8777
Partial conv sample B		10.089		82.530		
block 3	9.0645	4	85.5959	9	36.7482	9.0463

FRACTIONATION	**benzylic (MQF)** **R = C13/C12**	**sum of methyls (DEPT)** **R = C13/C12**	**tertiary C-F (MQF)** **R = C13/C12**
Full conv sample A			
block 1	1.1265	0.9283	0.2766
Full conv sample A			
block 2	1.1198	0.9465	0.2456

Full conv sample A						
block 3	1.1204		0.9407		0.2459	
Full conv sample B						
block 1	1.1149		0.9692		0.2813	
Full conv sample B						
block 2	1.1143		0.9822		0.2468	
Full conv sample B						
block 3	1.1107		0.9840		0.2484	
	R = C13/C12	**R/R0**	**R = C13/C12**	**R/R0**	**R = C13/C12**	**R/R0**
Partial conv sample A						
block 1	1.1107	0.9911	0.9516	1.0029	0.2801	1.0043
Partial conv sample A						
block 2	1.1089	0.9937	0.9744	0.9944	0.2472	0.9989
Partial conv sample A						
block 3	1.1090	0.9927	0.9702	1.0104	0.2475	1.0041
Partial conv sample B						
block 1	1.1136	0.9954	0.9435	1.0005	0.2786	0.9981

Partial conv sample B block 2	1.1119	0.9941	0.9649	1.0081	0.2457	1.0013
Partial conv sample B block 3	1.1131	0.9978	0.9642	1.0019	0.2462	0.9960

	benzylic (MQF)		**sum of methyls (DEPT)**		**tertiary C-F (MQF)**	
AVERAGED FRACTIONATION	**R/R0**		**R/R0**		**R/R0**	
partial_A_avg_all_reps	0.9926		1.0071		1.0032	
partial_B_avg_all_reps	0.9956		0.9989		0.9977	

	benzylic (MQF)		**sum of methyls (DEPT)**		**tertiary C-F (MQF)**	
ERROR CALC	sample 1	sample 2	sample 1	sample 2	sample 1	sample 2
F	0.325	0.283	0.325	0.283	0.325	0.283
1-F	0.675	0.717	0.675	0.717	0.675	0.717
deltaF^2	2.50E-05	9.00E-06	2.50E-05	9.00E-06	2.50E-05	9.00E-06

R/R0	0.9926	0.9956	1.0071	0.9989	1.0032	0.9977
delta(R/R0)^2	4.30E-07	4.87E-07	3.59E-06	3.75E-06	4.03E-06	5.31E-06
A	-3.90E-01	-3.31E-01	-3.96E-01	-3.32E-01	-3.94E-01	-3.32E-01
w1	6.77E-01	7.18E-01	6.73E-01	7.17E-01	6.74E-01	7.18E-01
w2	-3.90E-01	-3.31E-01	-3.96E-01	-3.32E-01	-3.95E-01	-3.32E-01
B	1.03E-01	7.87E-02	1.06E-01	7.92E-02	1.05E-01	7.90E-02
C	-2.63E-01	-2.37E-01	-2.68E-01	-2.38E-01	-2.66E-01	-2.38E-01
D	7.01E-09	4.31E-09	5.86E-08	3.32E-08	6.57E-08	4.70E-08
E	1.06E-02	6.19E-03	1.12E-02	6.27E-03	1.10E-02	6.24E-03

(A/B - 1/C)^2 * deltaF^2	1.28E-09	1.33E-10	1.18E-09	7.78E-12	2.39E-10	3.77E-11
D/E	6.64E-07	6.97E-07	5.24E-06	5.29E-06	5.97E-06	7.54E-06

Table 6. Methyl rearrangement reaction intramolecular KIE.

DEPT			
RAW INTEGRALS	migrating Me (13C)	avg of non-migrating Mes (13C)	KIE = (13C migrating Me)/ (13C non-migrating Me)
Sample 1	29.515	30.214	1.0237
Sample 2	34.136	35.188	1.0308
Sample 3	30.383	31.099	1.0236
Sample 4	30.766	31.590	1.0268
		Average =	1.026

Table 7. Phenyl rearrangement reaction KIE: Raw and processed NMR integrations for the tertiary C-F carbon acquired using the MQF method. 19F column = data derived from the standard 19F experiment, representing 12C. MQF column = data derived from the MQF

experiment, representing 13C. R = (Area C13)/(Area C12) for partial conversion samples. R0 = (Area C13)/(Area C12) for the averaged full conversion samples.

KIE	KIE	std err
sample A	1.008	0.006
sample B	1.005	0.007
average	**1.007**	

Conversion	
sample A conversion	0.26
sample B conversion	0.23
est. error(conversion)	0.01

	19F	**MQF**
INTEGRALS	12C	13C
Full conv sample 1	9.5431	11.2598
Full conv sample 2	9.1369	10.7235
Part conv sample 1	8.2175	9.601
Part conv sample 2	8.441	9.8879
AVERAGES	12C	13C

Part conv sample 1	8.2175	9.6010
Part conv sample 2	8.4410	9.8879
Full conv samples avg	9.3400	10.9917
FRACTIONATION	R	R0
Part conv sample 1	1.1684	1.1768
Part conv sample 2	1.1714	1.1768
ERROR CALC		
	sample A	sample B
R/R0	9.93E-01	9.95E-01
(deltaR/R)^2	1.45E-05	2.47E-05
(deltaR0/R0)^2	1.11E-05	1.11E-05
delta(R/R0)^2	2.56E-05	3.58E-05
A	-2.99E-01	-3.00E-01
w1	7.42E-01	7.41E-01
w2	-2.99E-01	-2.99E-01
B	6.61E-02	6.65E-02
C	-2.21E-01	-2.22E-01

D	1.57E-07	2.19E-07
E	4.37E-03	4.42E-03
(A/B - 1/C)^2 * deltaF^2	3.60E-09	1.47E-09
D/E	3.58E-05	4.96E-05

Chapter 2

Highly Enantioselective Matteson Homologations Catalyzed by Lithium Isothiourea Boronates[1]

2.1 Introduction

Organoboron compounds are valuable synthetic targets with applications as functional groups in bioactive small molecules and as versatile synthetic intermediates.[2,3,4,5] Two FDA-approved drugs, Bortezomib and Vaborbactam, contain α-amino boronic acids and serve as proteasome and beta lactamase inhibitors, respectively (Fig. 2.1A). While a variety of other

[1] This work was done in collaboration with Jake Z. Essman.. Portions of this chapter have been reproduced or adapted from: Sharma, H. A.‡; Essman, J. Z.‡; Jacobsen, E. N. Enantioselective Catalytic 1,2-Boronate Rearrangements. *Science* **2021**, *374*, 752–757.

[2] Xu, L.; Sawamura, M.; Ping, Y.; Pineschi, M.; Fernández, E.; Kubota, K.; Kitanosono, T.; Gong, T.-J.; Geetharani, K.; Aiken, S. G.; Carbó, J. J.; Clark, T. B.; Zhang, F.-L.; Yoshida, H.; Maseras, F.; Ahmed, E. -a. M. A.; Bateman, J. M.; Boldrini, C.; Bose, S. K.; Cho, H. Y.; Ito, H.; Kobayashi, S.; Ohmiya, H.; Wang, Y.-F.; Wu, C.; Wang, J.; Fu, Y.; Aggarwal, V. K.; Fernández, E. *Advances in Organoboron Chemistry towards Organic Synthesis* (Thieme Verlag, 2020; https://www.thieme-connect.de/products/ebooks/series/10.1055/b-00000101).

[3] Fernández, E.; Whiting, A. Eds., *Synthesis and Application of Organoboron Compounds* (Springer International Publishing, 2015; https://www.springer.com/gp/book/9783319130538), *Topics in Organometallic Chemistry*.

[4] Miyaura, N.; Yamamoto, Y. in *Comprehensive Organometallic Chemistry III*, Mingos, D. M. P.; Crabtree, R. H. Eds. (Elsevier, Oxford, 2007; https://www.sciencedirect.com/science/article/pii/B0080450474001126), pp. 145–244.

[5] Hall, D. G. *Boronic Acids: Preparation and Applications in Organic Synthesis, Medicine and Materials* (John Wiley & Sons, 2012).

organoboron compounds are being examined as therapeutics, these molecules mostly find use as versatile intermediates in the synthesis of complex molecules. This utility is enabled by the chemical versatility of the C–B bond, which can be transformed into C–C, C–O, C–N, and C–X bonds,[6,7] essentially serving as a "placeholder" functional group that can be swapped out later for desired substituents.

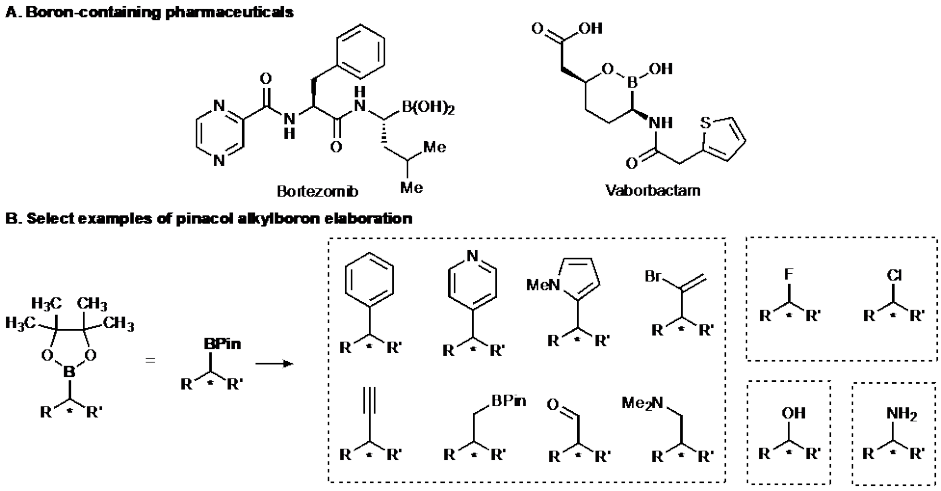

Figure 2.1 Utility of organoboron compounds

Recent efforts have focused on the development of methods to enable the stereospecific transformation of alkylboron *pinacol* esters into compounds bearing diverse substitution patterns (Fig. 2.1B).[8] Despite the prevalence and utility of these elaboration methods, there are still no general, highly modular strategies for the synthesis of enantioenriched alkylboron pinacol ester

[6] Carey, F. A.; Sundberg, R. J. in *Advanced Organic Chemistry: Part B: Reactions and Synthesis*, Carey, F. A.; Sundberg, R. J., eds (Springer US, Boston, MA, 2007; https://doi.org/10.1007/978-0-387-71481-3_9), *Advanced Organic Chemistry*, pp. 783–860.

[7] Chinnusamy, T.; Feeney, K.; Watson, C. G.; Leonori, D.; Aggarwal, V. K. in *Comprehensive Organic Synthesis II (Second Edition)*, Knochel, P. Ed. (Elsevier, Amsterdam, 2014; https://www.sciencedirect.com/science/article/pii/B9780080977423007266), pp. 692–718.

[8] Sandford, C.; Aggarwal, V. K. Stereospecific functionalizations and transformations of secondary and tertiary boronic esters. *Chem. Commun.* **2017**, *53*, 5481–5494.

derivatives. This chapter will mostly focus on the design, discovery, and mechanistic investigation of a catalytic method for controlling the rearrangement of dichloromethyl boronates with high ee and the application of this method to the general, modular synthesis of molecules bearing diverse tertiary stereocenters. Our investigations uncovered a new family of catalysts—lithium isothiourea (LIT) boronates—that mediate the rearrangement reaction and have the potential to control the additions of hard organometallics to other electrophiles.

2.2 Strategies for Controlling Boronate Rearrangement Reactions

By leveraging the known propensity of boronate species to undergo rearrangement processes, a number of methods have been developed to enable the stereoselective construction of enantioenriched alkylboron reagents. The first report of a boronate rearrangement of any kind was disclosed by Matteson in 1963 and detailed the displacement of a bromide geminal to a dibutyloxy boron by aryl and alkyl Grignard reagents (Fig. 2.2A).[9] The existence of the proposed boronate intermediate was corroborated in an alternate experiment involving the addition of sodium butyloxide to an analogous phenyl-substituted α-bromo boronic ester, which led to formation of the same product observed in the original experiment. While this result does not rule out direct substitution of the bromide by the phenyl Grignard in the original experiment, it clearly indicates the viability of the borylation/rearrangement sequence. In 1967, Rathke reported an extension of this methodology to dichloromethylboronates, which generate versatile chiral α-chloro boronic ester products upon rearrangement (Fig. 2.2B).[10] Matteson popularized the use of dichloromethylboronates for the synthesis of unsymmetric secondary boronic esters by

[9] Matteson, D. S. Neighboring Boron in Nucleophilic Displacement. *J. Am. Chem. Soc.* **1963**, 85, 2599.

[10] Rathke, M. W.; Chao, E.; Wu, G. The Preparation and Reactions of Esters of Dichloromethaneboronic acid. *J. Organomet. Chem.* **1976**, *122*, 145–149l

generalizing the two-step sequence of 1) formation/rearrangement of dichloromethylboronates and 2) subsequent boronate formation/rearrangement with organomagnesium and -lithium species to displace the remaining chloride.[11]

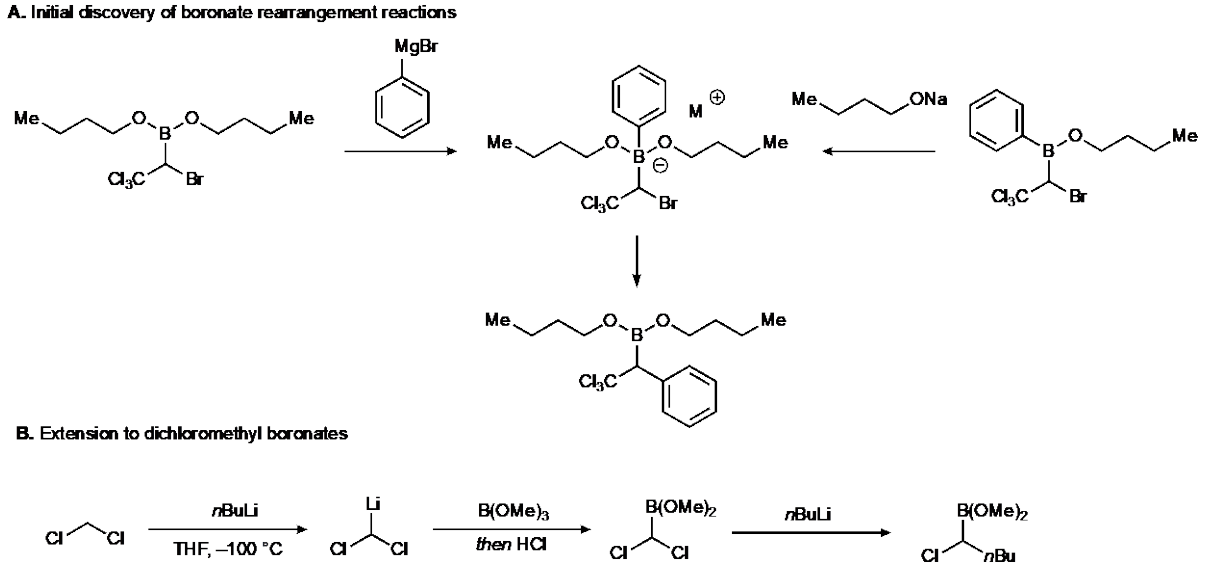

Figure 2.2 Initial discovery of boronate rearrangement reactions and extension to dichloromethyl boronates

The rearrangements of dichloromethyl boronates were rendered stereoselective by Matteson (reported on the following page of JACS as the previously discussed precedent) by using (+)- or (–)-pinanediol (pnd) or C2-symmetric 1,2-disubstituted ethanediols as a chiral auxiliary on boron (Fig. 2.3).[12] These pinanediol-controlled rearrangements afford α-chloro boronic ester products with high diastereomeric ratios employing a range of primary, secondary, α-heteroatom-bearing, and, in some cases, aryl boronic esters. Dichloroethyllithium can be used in place of

[11] Matteson, D. S.; Majumdar, D. α-Chloro Boronic Esters from Homologation of Boronic Esters. *J. Am. Chem. Soc.* **1980**, *102*, 7588–7590.

[12] Matteson, D. S.; Ray, R. Directed Chiral Synthesis with Pinanediol Boronic Esters. *J. Am. Chem. Soc.* **1980**, *102*, 7590–7591.

dichloromethyllithium to afford fully substituted products with variable, but typically low, levels of d.r.[13] The α-chloro products can be ~~generally~~ elaborated through displacement of the chloride with carbon- and heteroatom-based nucleophiles to deliver a variety of diastereoenriched secondary boronic esters. Typically, the pnd-bearing secondary boronic esters are oxidized to generate enantioenriched alcohols or are subjected to iterative diastereoselective/diastereospecific rearrangements to provide increasingly long, stereocomplex alkyl chains. This platform has enabled the stereoselective synthesis of numerous natural products and bioactive targets.

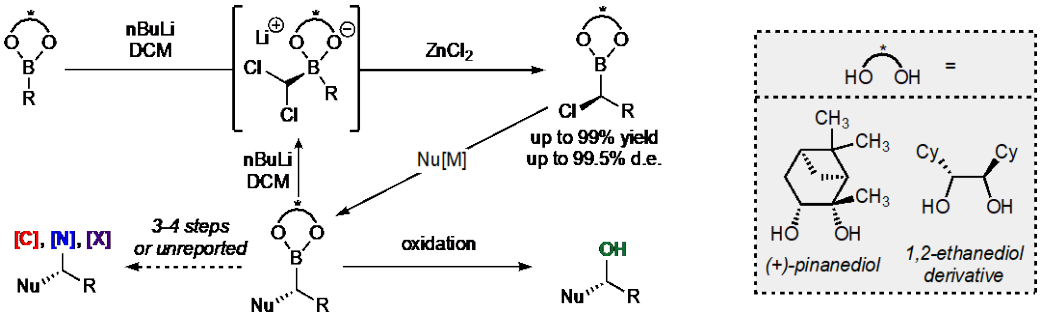

Figure 2.3 General scheme of Matteson homologation reactions

While the diastereoselective Matteson rearrangement methodology is an incredibly powerful tool, further application is limited by a few drawbacks. Removal of the pnd auxiliary is often a multi-step process, and most—if not all—abbreviated removal sequences lack generality (i.e. they require α-amido substitution). This is problematic for a few reasons. The Matteson methodology requires multiple steps when applied to the synthesis of the full complement of stereoisomers of complex alkyl chains, as the pnd will need to be removed and replaced with its enantiomer at least once to access more than 2 possible diastereomers. Additionally, most modern C–B elaboration reactions have been optimized for pinacol- or neopentyl glycol-bearing boronic

[13] Matteson, D. S.; Hurst, G. D. Heteroatom Chemistry 1990, 1, 65−74.

esters, rather than pnd-bearing boronic esters. Thus, to apply the Matteson technology to the synthesis of products that are not secondary alcohols, the pnd must first be installed to set the desired stereocenter, and then it must be cleaved and replaced before transforming the C–B bond, adding multiple synthetic steps to the reaction sequence. Despite these limitations, the pnd-based methodology provides a reliably selective, even if chemically inefficient, route to access diverse non-boron-containing products and stereocomplementary libraries of compounds bearing complex alkyl chains.

In addition to these diastereoselective approaches, numerous enantioselective approaches towards the synthesis of alkylboronic esters have leveraged rearrangement strategies. Building on the seminal work of Hoppe,[14] Aggarwal and coworkers have developed stoichiometric chiral lithium carbenoid reagents that enable the enantioselective synthesis of secondary and tertiary pinacol boronic ester products via stereospecific formation and rearrangement of chiral boronate derivatives (Figure 2.4).[15,16] These chiral carbenoids can be accessed either via enantioselective deprotonation of primary carbonates and carbamates by sparteine-*s*BuLi complexes or by enantiospecific deprotonation of chiral secondary carbonates and carbamates by TMEDA-*s*BuLi.

[14] Beckmann, E.; Desai, V.; Hoppe, D. Stereospecific Reaction of α-Carbamoyloxy-2-alkenylboronates and α-Carbamoyloxy-alkylboronates with Grignard Reagents - Synthesis of Highly Enantioenriched Secondary Alcohols. *Synlett* **2004**, *2004*, 2275–2280.

[15] Stymiest, J. L.; Dutheuil, G.; Mahmood, A.; Aggarwal, V. K.; Lithiated Carbamates: Chiral Carbenoids for Iterative Homologation of Boranes and Boronic Esters. *Angew. Chem. Int. Ed.* **2007**, *46*, 7491–7494.

[16] Stymiest, J. L.; Bagutski, V.; French, R. M.; Aggarwal, V. K. Enantiodivergent conversion of chiral secondary alcohols into tertiary alcohols. *Nature* **2008**, *456*, 778–782.

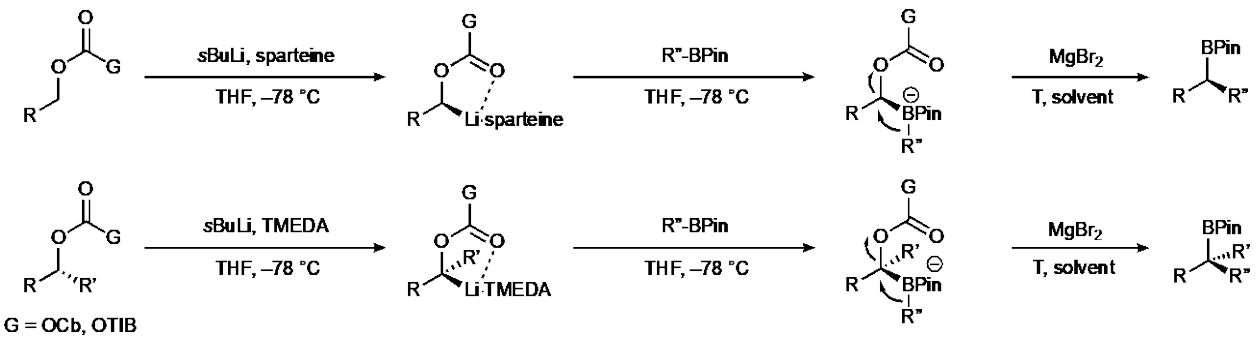

Figure 2.4 Stereospecific rearrangements of chiral boronates derived from chiral carbenoids

This carbenoid platform overcomes both major limitations of the Matteson approach. The relative sense of chirality of each stereogenic carbon center along a carbon chain can be controlled by the choice of carbenoid enantiomer rather than by the enantiomer of the ligand on boron. The Aggarwal lab has leveraged this advantage in the expedient synthesis of all isomers of incredibly complex natural products and conformationally interesting permethylated alkyl chains.[17] The second advantage of the Aggarwal approach is that it generates products bearing pinacol- or neopentyl glycol-substituted boronic esters, which can be directly elaborated to molecules featuring a wide variety of substitution on the stereogenic centers. While powerful, the Aggarwal approach has a few drawbacks, including the reliance on stoichiometric chiral information in the form of the sparteine ligand on *s*BuLi or the chiral alcohol starting materials. Additionally, the chiral carbenoid reagent must be independently prepared from the alcohol in a multi-step sequence. The use of high-purity, salt-free carbenoid derivatives is often necessary to achieve reproducibly high selectivities, which requires a three-step sequence of lithiation, organotin formation and recrystallization, and reversion back to the carbenoid by Sn-Li exchange. These two requirements make it more laborious to synthesize compounds with diverse substitution patterns or to prepare

[17] Leonori, D.; Aggarwal, V. K. Lithiation−Borylation Methodology and Its Application in Synthesis. *Acc. Chem. Res.* **2014**, *47*, 3174–3183.

libraries of products. Additionally, the Aggarwal method poorly controls the rearrangement of sp2-substituted carbenoids[18] and thus cannot be used to construct alkyl chains with sp2-based substitution.

In addition to this stoichiometric work involving displacement of geminal leaving groups, catalytic, highly enantioselective rearrangements of prochiral alkenylboronates have been developed (Fig. 2.5). These rearrangements are promoted via π-activation of the pendant alkene, either directly by a chiral catalyst or by a chiral electrophile-catalyst complex.[19] The Morken group has disclosed the use of both cationic palladium[20] and neutral nickel[21] species that facilitate the rearrangement of vinyl boronates. These reactions are three-component couplings that afford enantioenriched homobenzylic and homoallylic secondary organoboron compounds. This work was initially achieved using palladium catalysts, which link sp2-(pseudo)halides with either pinacol boron derivatives and vinyllithium or organolithium and -magnesium species and vinyl boronic esters. This strategy was extended to nickel catalysts, a change enabled by the use of vinylborates rather than vinylboronates. The Denmark lab reported a carbenosulfenylation of vinyl boronates facilitated by a chiral selenium-based catalyst (Fig. 2.5C).[22] The Ready lab detailed the use of chiral palladium π-allyl complexes that trigger the rearrangement of 2-indolyl boronates to

[18] Noble, A.; Roesner, S.; Aggarwal, V. K. Short Enantioselective Total Synthesis of Tatanan A and 3-epi- Tatanan A Using Assembly-Line Synthesis. *Angew. Chem. Int. Ed.* **2016**, *55*, 1–6.

[19] Namirembe, S.; Morken, J. P. Reactions of Organoboron Compounds Enabled by Catalyst-Promoted Metalate Shifts. *Chem. Soc. Rev.* **2019**, *48*, 3464–3474.

[20] Zhang, L.; Lovinger, G. J.; Edelstein, E. K.; Szymaniak, A. A.; Chierchia, M. P.; Morken, J. P. Catalytic Conjunctive Cross-Coupling Enabled by Metal-Induced Metallate Rearrangement. *Science* **2016**, *351*, 70–74.

[21] Chierchia, M. Law, C.; Morken, J. P. Nickel-Catalyzed Enantioselective Conjunctive Cross-Coupling of 9-BBN Borates. *Angew. Chem. Int. Ed.* **2017**, *56*, 11870–11874.

[22] Tao, Z.; Robb, K. A.; Panger, J. L.; Denmark, S. E. Enantioselective, Lewis Base-Catalyzed Carbosulfenylation of Alkenylboronates by 1,2-Boronate Migration. *J. Am. Chem. Soc.* **2018**, *140*, 15621–15625.

deliver enantioenriched 3-allylated indole derivatives (Fig. 2.5D).[23] Of all these methods, the Morken approach provides the most general, modular way to access homoallylic and homobenzylic organoboron compounds with synthetically useful ligands on boron. In general, the metal-catalyzed methods use commercially available ligands and relatively cost-effective metals, thus increasing their utility. However, these methods yield products with very specific substitution patterns and have limited application to the iterative construction of stereocomplex chains.

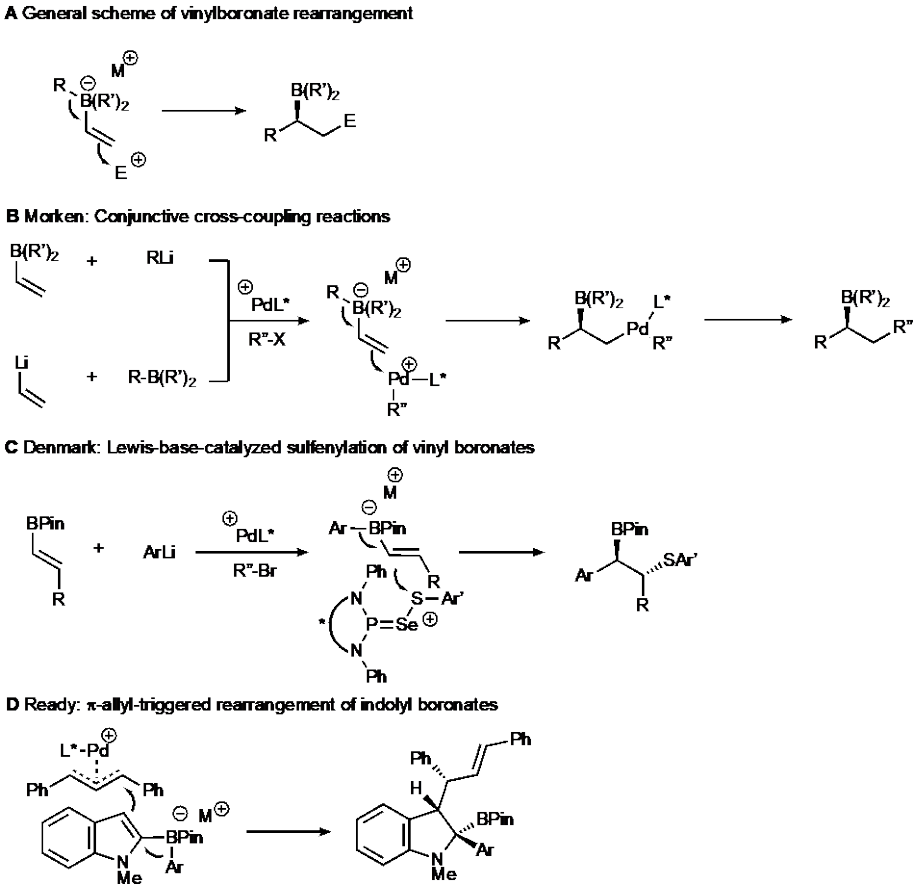

Figure 2.5 Catalytic, enantioselective rearrangement of vinyl boronates

[23] Panda, S.; Ready, J. M. Palladium Catalyzed Asymmetric Three-Component Coupling of Boronic Esters, Indoles, and Allylic Acetates. *J. Am. Chem. Soc.* **2017**, *139*, 6038–6041.

A distinct approach that does not proceed via a boronate rearrangement yet leverages a similar retrosynthetic disconnection involves the enantioconvergent nickel-catalyzed cross-coupling of racemic α-halo boronic ester derivatives with organozinc nucleophiles (Fig. 2.6). The first version of this reaction was reported by the Fu lab in 2016.[24] The Fu approach consists of a two-step sequence involving a racemic Matteson homologation of dichloromethyl boronates followed by an enantioselective cross-coupling with *n*-alkyl organozincs to transform dichloromethyl-BPin into optically active secondary boronic ester derivatives. This method effectively employs α-halo boronic esters bearing β-branching, which enables extension to the selective construction of diastereomeric products via an iterative homologation/cross-coupling sequence. However, as the stereoconvergent reaction requires the use of propylzinc reagents bearing only distal substitution, this approach lacks application to most natural product or pharmaceutical targets. More recently, the Martin lab reported an attempt to extend this chemistry to the use of aryl coupling partners.[25] This goal was successful in a racemic fashion, but the reaction afforded products in low levels of enantioselectivity with reported chiral ligands. These two papers represent a clever application of single-electron logic to the Matteson homologation reaction yet highlight the synthetic limitations of this approach.

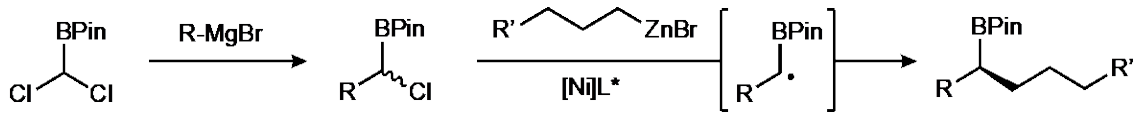

[24] Schmidt, J.; Choi, J.; Liu, A. T.; Slusarczyk, M.; Fu, G. C. A General, Modular Method for the Catalytic Asymmetric Synthesis of Alkylboronate esters. *Science* **2016**, *354*, 1265–1269.

[25] Sun, S.-Z.; Martin, R. Nickel-Catalyzed Umpolung Arylation of Ambiphilic α-Bromoalkyl Boronic Esters. *Angew. Chem. Int. Ed.* **2018**, *57*, 3622–3625.

Figure 2.6 Enantioconvergent synthesis of secondary boronic esters from racemic α-chloro boronic esters

The closest efforts toward an enantioselective, catalytic variant of the Matteson homologation are those reported by Jadhav and Man in the chiral Lewis acid-mediated rearrangement of a dichloromethyl-substituted *n*-butyl pinacol boronate (Fig. 2.7).[26] In this reaction, 55% ee was obtained using catalytic amounts of both $Yb(OTf)_3$ (20 mol%) and chiral bis(oxazoline) (BOX) ligand (50 mol%). Using pseudo-stoichiometric quantities of both metal salt and ligand (90% and 110%, respectively) increased the ee to 71%. However, the most beneficial modification for selectivity was increasing the loading of BOX ligand to superstoichiometric (500 mol%) quantities while keeping metal salt at 30 mol%, which led to formation of product in 88% ee. A followup study further examining the impact of $Yb(OTf)_3$ loading discovered that, with 50 mol% BOX ligand, the highest levels of selectivities were achieved *in the complete absence* of Ytterbium salt.[27] The authors additionally found that increases in BOX ligand loading up to 100 mol% led to increases in selectivity, although use of superstoichiometric loadings led to no further increase in ee. The necessity of stoichiometric loadings of BOX ligands and the increased selectivity upon removal of $Yb(OTf)_3$ are most consistent with a scenario where the ligand acts as an auxiliary on the boronate salt—perhaps on the lithium—rather than as a catalyst. In summary, it is unclear whether or not catalysis has been achieved in the enantioselective Matteson homologation reaction, as the data from these two

[26] Jadhav, P. K.; Man, H.-W. Enantiotopic Differentiation of pro-R or pro-S Chlorides in (Dichloromethyl)borates by Chiral Lewis Acids: Enantioselective Synthesis of (α-Chloroalkyl)boronates. *J. Am. Chem. Soc.* **1997**, *119*, 846–847.

[27] Smith, K.; Saleh, B. A.; Alshammari, M. B.; El-Hiti, G. A.; Elliott, M. C. Studies on a catalytic version of the Matteson asymmetric homologation reaction. *Org. Biomol. Chem.* **2021**, *19*, 4279–4284.

studies is most consistent with the chiral ligand facilitating the rearrangement with only one turnover.

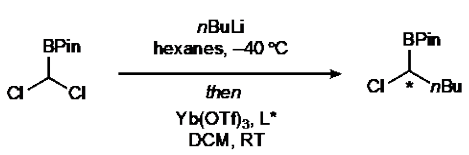

mol% [Yb]	mol% L*	% e.e.
20	50	55
90	110	71
30	500	88

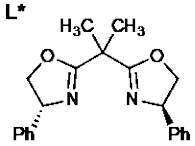

Figure 2.7 Attempts at a catalytic, enantioselective Matteson homologation

2.3 Reaction Design and Motivation

With the utility of chiral organoboron compounds and limitations to their accessibility in mind, I aimed to develop a catalytic variant of the Matteson homologation reaction. I hypothesized that the rearrangement of boronates bearing one or more geminal leaving groups might be accelerated by anion-abstraction catalysis. Weakly Brønsted acidic dual-hydrogen-bond-donor (HBD) catalysts have been applied broadly and successfully to promote stereoselective nucleophilic substitution reactions via chloride-abstraction pathways with alpha-chloro amines[28], designer neryl chlorides[29], and glycosyl chlorides[30]. In the envisioned boronate rearrangement reaction, the HBD would be required to preferentially abstract one enantiotopic chloride on the dichloromethyl boronate to facilitate an enantioselective desymmetrization (Figure 2.8).

[28] Bendelsmith, A. J.; Kim, S. C.; Wasa, M.; Roche, S. P.; Jacobsen, E. N. Enantioselective Synthesis of α-Allyl Amino Esters via Hydrogen-Bond-Donor Catalysis. *J. Am. Chem. Soc.* **2019**, *141*, 11414–11419.

[29] Kutateladze, D. A.; Strassfeld, D. A.; Jacobsen, E. N.; Enantioselective Tail-to-Head Cyclizations Catalyzed by Dual-Hydrogen-Bond Donors. *J. Am. Chem. Soc.* **2020**, *142*, 6951–6956.

[30] Park, Y.; Harper, K. C.; Kuhl, N.; Kwan, E. E.; Liu, R. Y.; Jacobsen, E. N. Macrocyclic bis-thioureas catalyze stereospecific glycosylation reactions. *Science*. **2017**, *355*, 162–166.

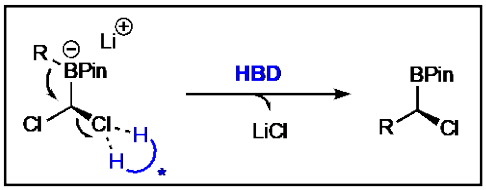

Figure 2.8 Design hypothesis for proposed catalytic boronate rearrangement reaction

From a synthetic perspective, the development of a catalytic, enantioselective rearrangement of pinacol-substituted dichloromethyl boronates could form the basis for a modular and highly general strategy for the synthesis of trisubstituted stereocenters (Figure 2.9). Such a reaction would afford chiral building blocks bearing chlorine and pinacol boronic ester substituents on a defined stereogenic carbon center that could be elaborated enantiospecifically through a second rearrangement sequence and a carbon-boron bond transformation. In addition to requiring only catalytic levels of a chiral source to achieve absolute stereocontrol, this strategy would leverage recent, powerful methods for the elaboration of carbon-boron bonds that primarily make use of pinacol boronic esters. The catalytic, enantiodetermining event would involve commitment to only one of the three ultimate substituents, thereby enabling immense versatility and potential generality in the enantioselective construction of trisubstituted carbon stereocenters from dichloromethane as the common starting material.

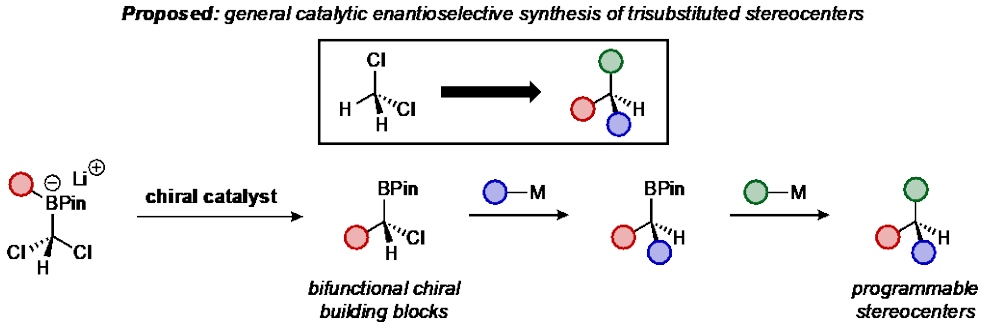

Figure 2.9 Proposed synthetic sequence to transform DCM into diverse 3° stereocenters

Apart from the synthetic utility, the proposed transformation could provide a strategy for using hard organometallics, such as organolithium reagents, as coupling partners in organocatalytic reactions. This might enable catalysis of new types of reactions and would allow for a common class of commercially available reagents to be used with HBDs. The proposed strategy would leverage boronic esters as reagents to capture and attenuate the extreme reactivity of organolithiums to levels that are compatible with hydrogen-bond-donor catalysis (Figure 2.10).

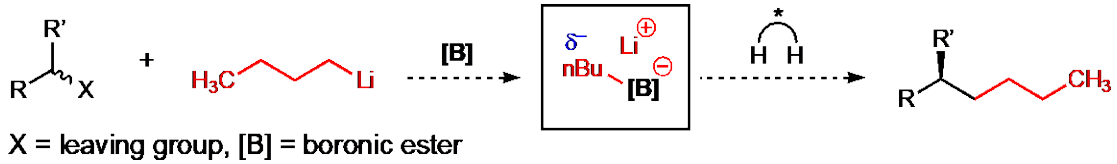

Figure 2.10 Envisioned model for using organolithiums as coupling partners in HBD catalysis by leveraging boronates as intermediates

Specifically, the attenuated basicity and C-nucleophilicity of organoboronate derivatives might be compatible with acidic, electrophilic catalysts, such as amide-bearing thioureas. The nucleophilicity of aryl-substituted alkylboronates is similar to that of other nucleophiles employed in HBD catalysis (figure 2.11).[31] These nucleophilicity parameters have been characterized by the labs of Aggarwal and Mayr, where they found that pinacol alkylboronates with aryl substituents on the boron feature nucleophilicity parameters from N = 6–12 (s_N = 0.6–0.8).[32] The main determinants of nucleophilicity are the nature of the aryl substituent, with bis-CF_3-phenyl-derived boronates featuring nucleophilicity parameters of N = 6–7 vs values of N = 9–11 for phenyl-derived

[31] Mayr, H.; Kempf, B.; Ofial, A. R. π-Nucleophilicity in Carbon−Carbon Bond-Forming Reactions. *Acc. Chem. Res.* **2003**, *36*, 66–77.

[32] Feeney, K.; Berionni, G.; Mayr. H.; Aggarwal, V. K. Structure and Reactivity of Boron-Ate Complexes Derived from Primary and Secondary Boronic Esters. *Org. Lett.* **2015**, *17*, 2614–2617.

boronates featuring similar substitution, and the nature of the diol, with neopentyl glycol-derived boronates featuring higher nucleophilicity than pinacol-derived boronates by N = +3–4. Based on these nucleophilicity parameters, pinacol boronates provide a reasonable starting point for our investigations. While a variety of reactions have been reported using this class of nucleophiles,[33,34] we decided to begin investigations with the Matteson homologation reaction.

Figure 2.11 Comparison of nucleophilicity of boronates to electrophiles commonly employed in HBD catalysis

2.4 Reaction Development

The rearrangement of lithium boronate substrate **3a** was selected as a model reaction (Fig. 2.12). This boronate can be accessed either via addition of *n*BuLi to DCM-BPin **1** or by addition of in situ-generated DCM-Li to *n*Bu-BPin **2a**. Initial optimization focused on the former of these two approaches due to its operational simplicity.

[33] Li, C.; Zhang, Y.; Sun, Q.; Gu, T.; Peng, H.; Tang, W. Transition-Metal-Free Stereospecific Cross-Coupling with Alkenylboronic Acids as Nucleophiles. *J. Am. Chem. Soc.* **2016**, *138*, 10774−10777.

[34] Mohiti, M; Rampalakos, C.; Feeney, K.; Leonori, D.; Aggarwal, V. K. Asymmetric addition of chiral boron-ate complexes to cyclic iminium ions. *Chem. Sci.* **2014**, *5*, 602–607.

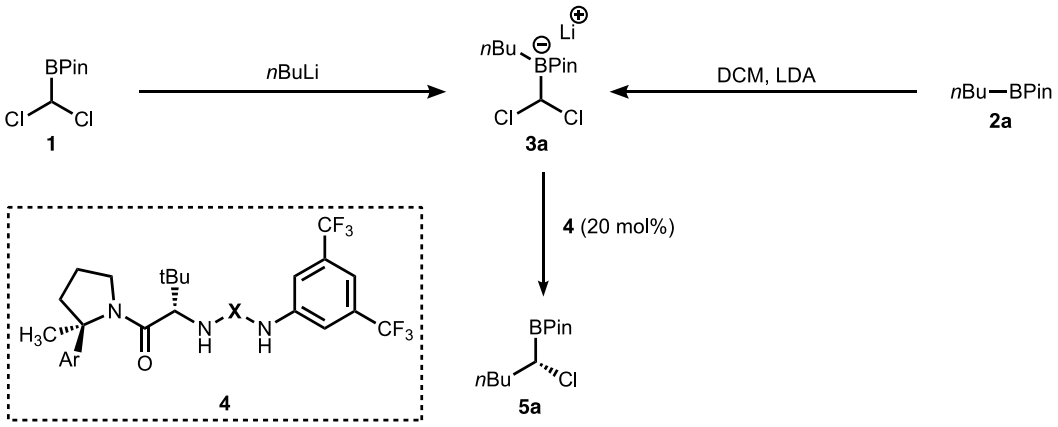

Figure 2.12 General reaction scheme

The arylpyrrolidine-*tert*-leucine-derived thiourea **4a** was observed to promote the formation of the α-chloro boronic ester product **5a** with modest levels of enantioselectivity (48% ee) when added to a pre-formed solution of **3a** (Fig. 2.13) . Use of catalyst analogue featuring a urea (**4a-Ur**) moiety in place of thiourea afforded product in 48% ee, consistent with the urea-based catalyst operating through a similar mechanism as the thiourea catalyst. Use of catalyst analogue featuring a squaramide (**4a-Sq**) moiety in place of thiourea afforded product in 5% ee; additionally, the reaction turned orange, consistent with squaramide-based catalyst undergoing deprotonation and thus giving low levels of selectivity by not being able to effectively operate via a hydrogen-bond-donor mechanism.

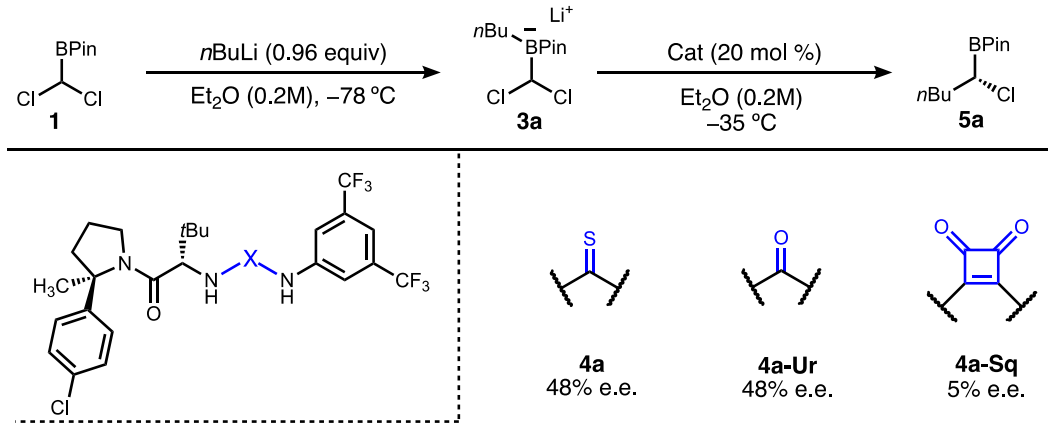

Figure 2.13 Initial optimization studies for rearrangement of *n*butyl-substituted boronic esters

Next, we turned to examine the order-of-addition of the *n*BuLi, the substrate **1**, and catalyst **4a** and **4a-ur** (Fig. 2.14). The initial goal of these experiments was to determine if it would be possible to use *n*BuLi in the presence of the HBD without deprotonating or degrading the catalyst. We hypothesized that the boronic ester would capture that *n*BuLi prior to deprotonation of the catalyst, as it has been previously shown that the addition of organolithium reagents to organoboron derivatives commonly outcompetes deprotonation events.[35] Unexpectedly, we found that **4a**, but not **4a-Ur** or **4a-Sq**, gave significantly higher levels of selectivity when added before *n*BuLi (but after **1**). We also discovered that adding thiourea immediately after adding *n*BuLi, rather than waiting 5 minutes, led to a substantial increase in enantioselectivity. Finally, we found that adding 1.4 equivalents of *n*BuLi after addition of **4a** led to formation of product in slightly higher levels of enantioselectivity. These results are consistent with deprotonation of **4a** being important for achieving high levels of selectivity and less consistent with the boronic ester fully capturing all of the organolithium. To summarize, the results of these order of addition experiments are consistent with chiral dual-hydrogen-bond-donor catalysts can promote the rearrangement of dichloromethyl boronates with moderate levels of selectivity, but that a non-HBD-mediated pathway is responsible for delivering products in high levels of selectivity.

[35] Fyfe, J. W. B.; Watson, A. J. B. Recent Developments in Organoboron Chemistry: Old Dogs, New Tricks. *Chem* **2017**, *3*, 31–55.

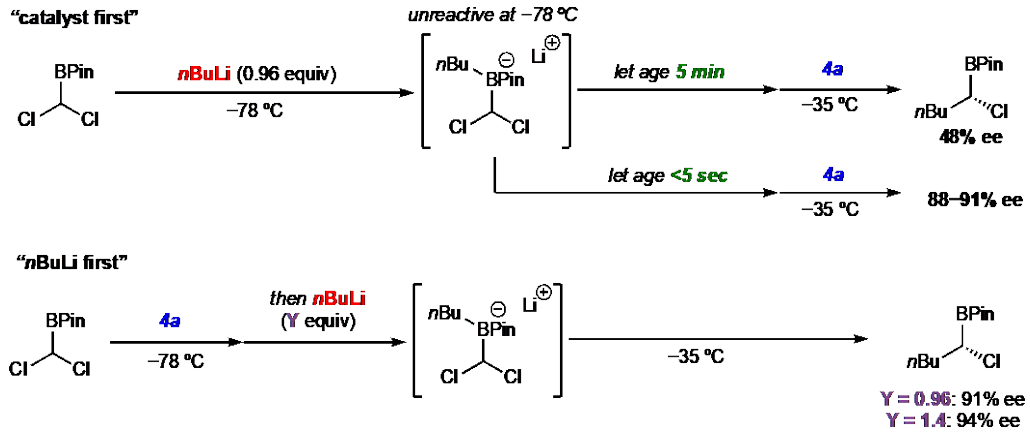

Figure 2.14 Order-of-addition and *n*BuLi equivalents experiments reveal an important role for thiourea deprotonation

With data indicative of a highly selective non-HBD-mediated pathway, we then turned to probe the unexpected boost to selectivity provided by lithiation of the catalyst. We first examined the fate of the catalyst under the reaction conditions. It was discovered that, under "*n*BuLi first conditions," the thiourea **4a** forms numerous boron-containing adducts that were initially challenging to purify and characterize by NMR. HRMS studies of the major **4b** (a brominated catalyst analogue)-boron adduct revealed a molecule that consists of one unit of thiourea **4b** and one unit of starting material **1** minus one unit of HCl. This mass, paired with the NMR spectrum, were consistent with 12+ different structural assignments (Fig 2.14). X-ray crystallography studies (Fig 2.15) of the major isolated adduct revealed that the major alkylated thiourea structure featured a sulfur-carbon bond resulting from S-displacement of the chloride to form **6a**.

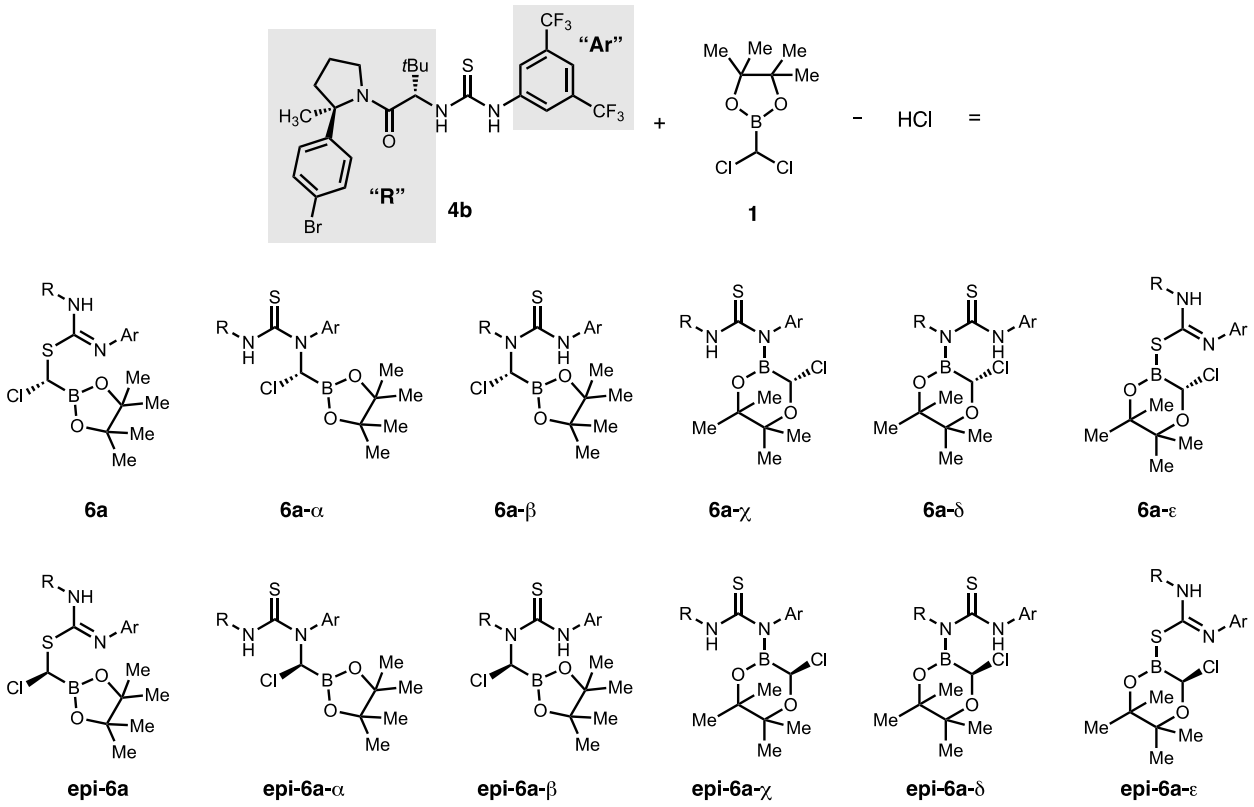

Figure 2.14 Plausible constitutional and stereochemical isomers accounting for NMR shifts and HRMS-acquired mass and isotopic pattern of isolated major thiourea-boron adduct

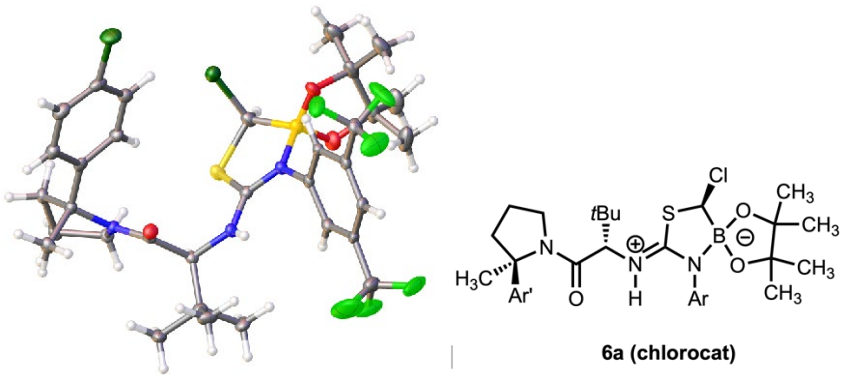

Figure 2.15 Solid-state structure of major thiourea-substrate adduct **6a** (chlorocat)

Additional minor thiourea-boron adducts were isolated and characterized. Depending on the reaction conditions, the thiourea formed unique transformation products (Fig. 2.16) by

attacking either **1**, **6a**, or **5a** through a putative mechanism detailed in Fig. 2.17. This gave rise to isothiourea boronate species **6a**, **epi-6a**, and **6b** as the major thiourea transformation products of the reaction employing **1** and *n*BuLi, and gave **6c** and **epi-6c** as the major products of the reaction employing **2a** and LDA/DCM.

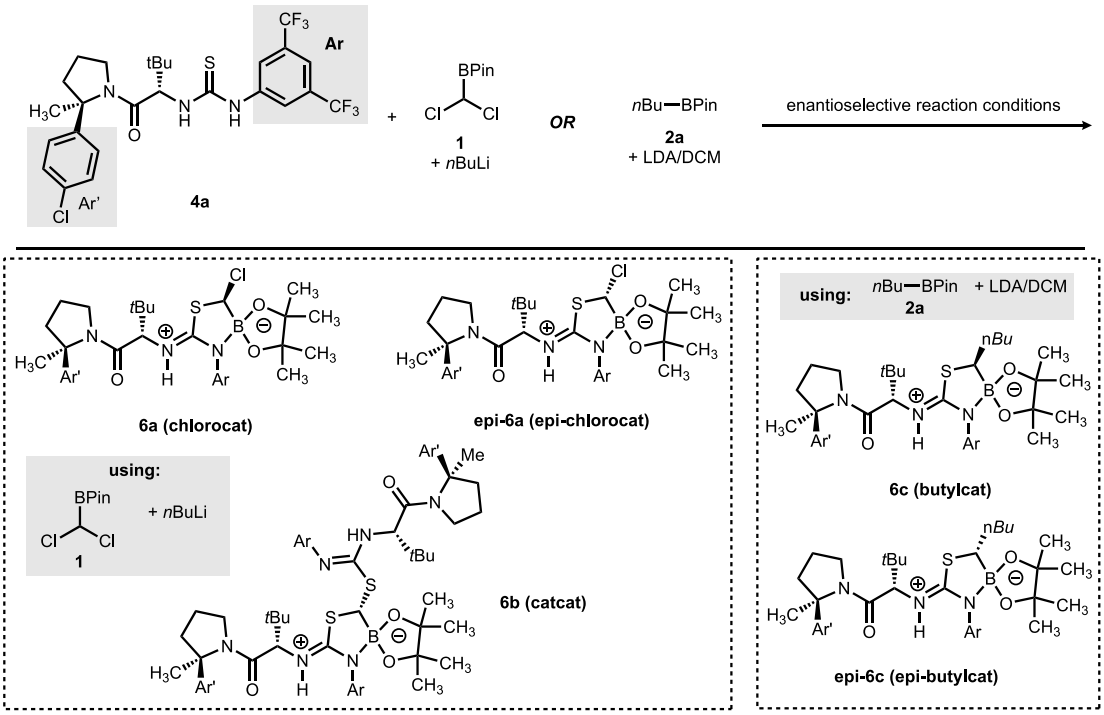

Figure 2.16 Thiourea-boron adducts isolated and characterized from catalytic reactions

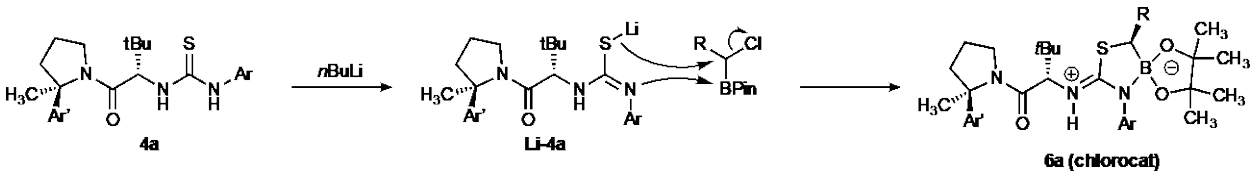

Figure 2.17 Mechanism of thiourea-adduct formation

Having identified an array of thiourea "degradation" products, we sought to examine the impact of each species on the boronate rearrangement reaction, with the hypothesis that the new species formed under the reaction condition might be catalytically active. Use of 20 mol%

isothiourea boronate **6a** ("chlorocat") in the rearrangement of *n*butyl boronate derived via addition of *n*BuLi to DCM-BPin **1** afforded product in varying ee depending on the order of addition (Fig. 2.18). When **6a** was added after *n*BuLi, product was afforded in in 21% ee, whereas product was afforded in 94% ee when **6a** was added prior to *n*BuLi. It was hypothesized that the dramatically higher level of selectivity observed in the latter experiment might be due to deprotonation of **6a** by *n*BuLi to form **Li-6a**, which in turn might be a highly efficient and selective catalyst. Deprotonation of **6a** by pre-mixing with lithium hexamethyldisilazide (LiHMDS) prior to use in the reaction led to unity in the order of addition experiments, with **Li-6a** affording product in 94% ee regardless of being added before or after *n*BuLi. Importantly, rearrangement of **3a** prepared either by addition of *n*-butyllithium to **1** or by addition of dichloromethyllithium (generated *in situ* via deprotonation of dichloromethane by lithium diisopropylamide (LDA)) to *n*-butyl boronic ester **2a** was promoted by **Li-6a** in 94–95% ee.

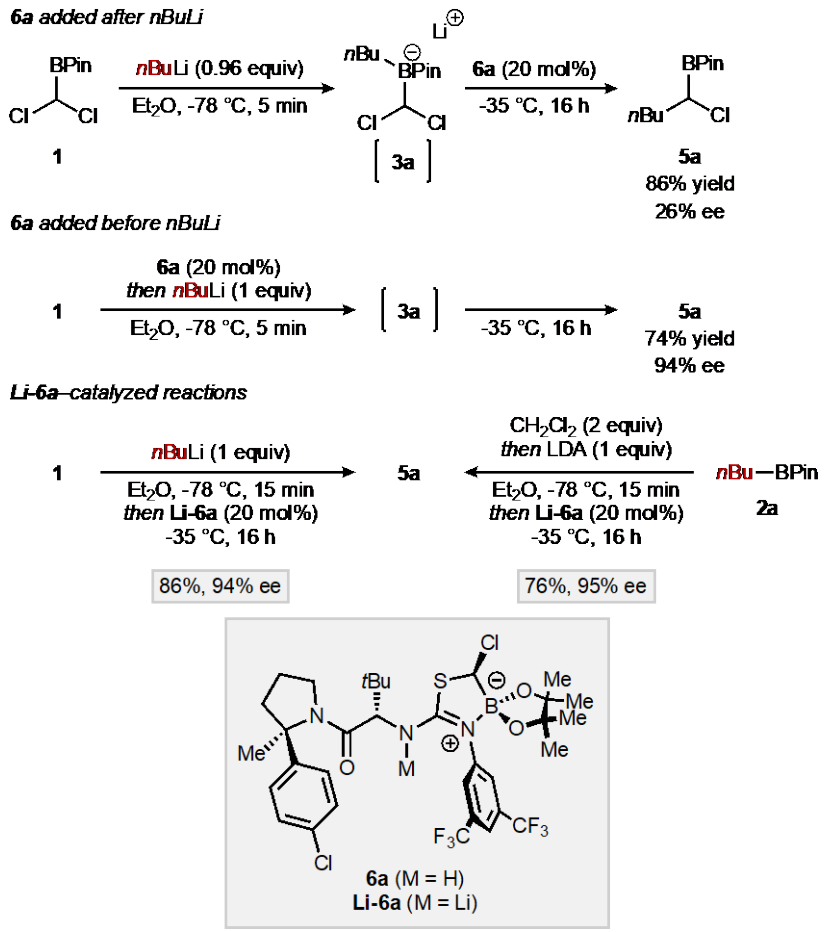

Figure 2.18 Lithiated isothiourea boronates catalyze the Matteson homologation

With the optimal procedure in hand, the selectivity of the remaining thiourea transformation species was assessed (Fig. 2.19). **Li-epi-6a** afforded product in 92% ee, **Li-6c** afforded product in 83% ee, **Li-epi-6c** afforded product in 47% ee, and, under slightly different reaction conditions, **Li-6b** afforded product in 82% ee. The takeaway from these experiments is that **Li-6a**, formed under the initial "*n*Buli after thiourea **4a**" reaction conditions, is an unexpected and highly active catalyst that mediates the rearrangement reaction with high levels of enantioselectivity.

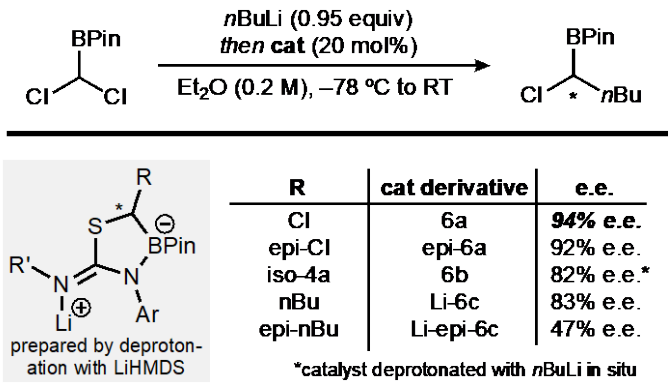

Figure 2.19 Activity of lithiated isothiourea boronate species

2.5 Structural Characterization of Lithium IsoThiourea (LIT) Boronate Catalysts

To better understand the nature of **Li-6a**, structural studies were conducted using ReactIR, DFT, and x-ray crystallography. Upon lithiation of precatalyst **6a** with LiHMDS, shifts were observed in the IR frequencies of both the isothiourea N–C–N stretch (1596 cm^{-1} to 1555 cm^{-1}, δ = -41 cm^{-1}) and the amide C–O stretch (1658 cm^{-1} to 1618 cm^{-1}, δ = -40 cm^{-1}), indicative of significant perturbations to both functional groups (Fig. 2.20). These shifts were fully reversible by addition of one equivalent of HCl. The observed IR spectral changes were interpreted as being due to deprotonation of the N-H of **6a** by LiHMDS with chelation of the lithium counterion by the exocyclic isothiourea nitrogen and the amide oxygen. In line with experimental observations, density-functional theory (DFT) calculations on **6a** and the proposed chelate structure of **Li-6a** predict a similar shift for both the isothiourea N–C–N stretch (1591 cm^{-1} to 1567 cm^{-1}, δ = -24 cm^{-1}) and the amide C–O stretch (1648 cm^{-1} to 1607 cm^{-1}, δ = -41 cm^{-1}). Deprotonation of **6c**, which bears an *n*butyl group in place of the α-chloride, resulted in similar spectral changes (Fig. 2.21). Intriguingly, this catalyst tolerated multiple equivalents of *n*BuLi without undergoing observable decomposition. Use of KHMDS in place of *n*BuLi for the deprotonation of **6c** afforded a ReactIR

trace with somewhat different spectral features (Fig. 2.22), as only the amide undergoes significant vibrational changes, consistent with DFT predictions.

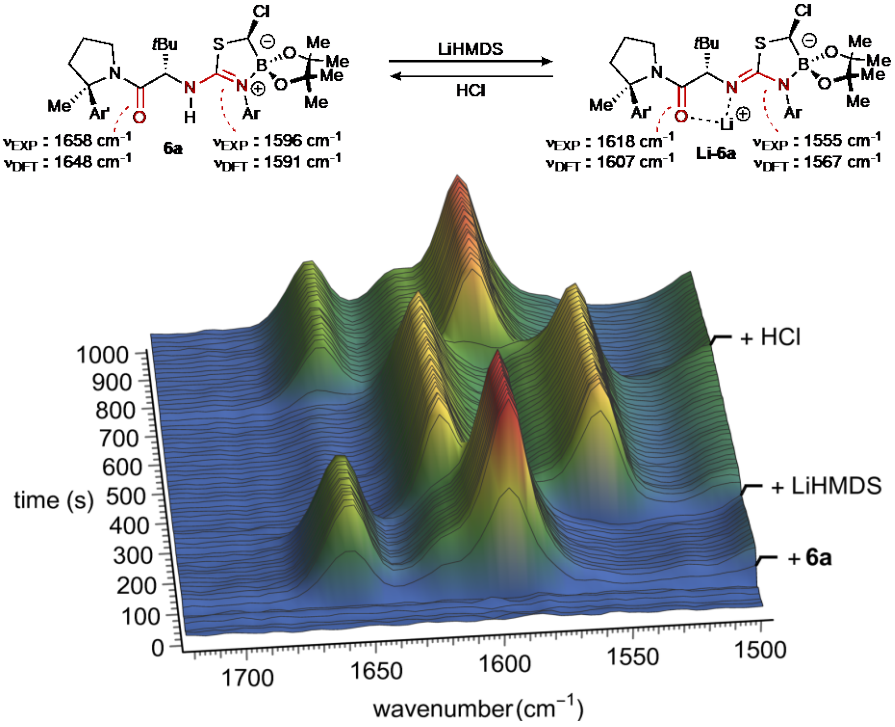

Figure 2.20 ReactIR monitoring of deprotonation of 6a with LiHMDS to form Li-6a

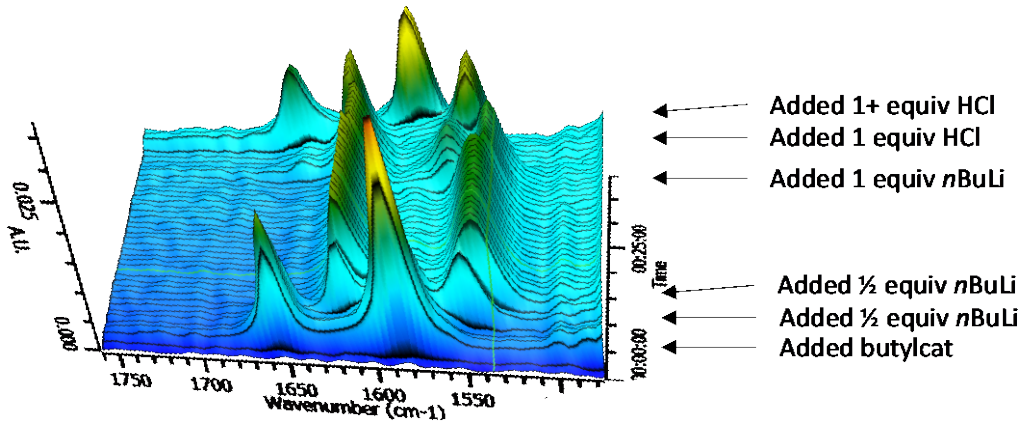

Figure 2.21 ReactIR monitoring of deprotonation of **6c** with LiHMDS

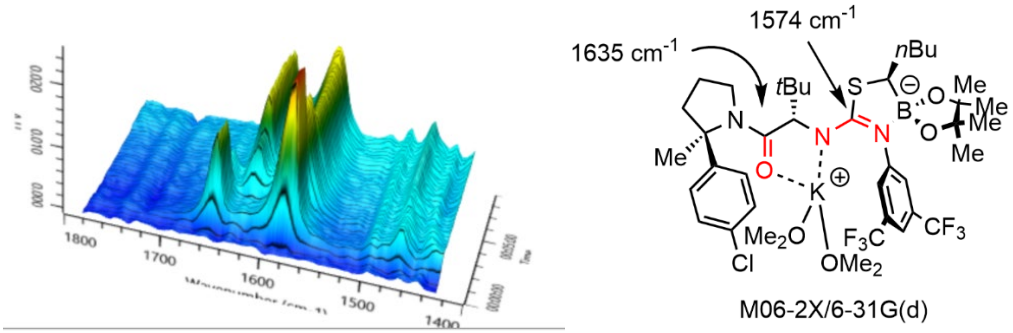

Figure 2.22 ReactIR monitoring of deprotonation of **6c** with KHMDS; DFT structure of **K-6c** with predicted IR frequencies

An x-ray crystal structure analysis of methyl analogue **Li-6d** provided additional experimental support for the chelate model (Fig. 2.23). Complex **Li-6d** displayed similar spectral characteristics to **Li-6a** but proved more amenable to crystallization; it also afforded similar but slightly diminished enantioinduction in the rearrangement of the model boronate **3a**. Taken together, these observations point to a catalyst structure featuring a 5-membered lithium chelate with the cation located in a highly dissymmetric pocket defined by the 4-chlorophenyl group, the *tert*-butyl group, the isothiourea-boronate heterocycle, and the 3,5-bis(trifluoromethyl)phenyl group, the last of which is rotated out of the plane of the heterocyclic core.

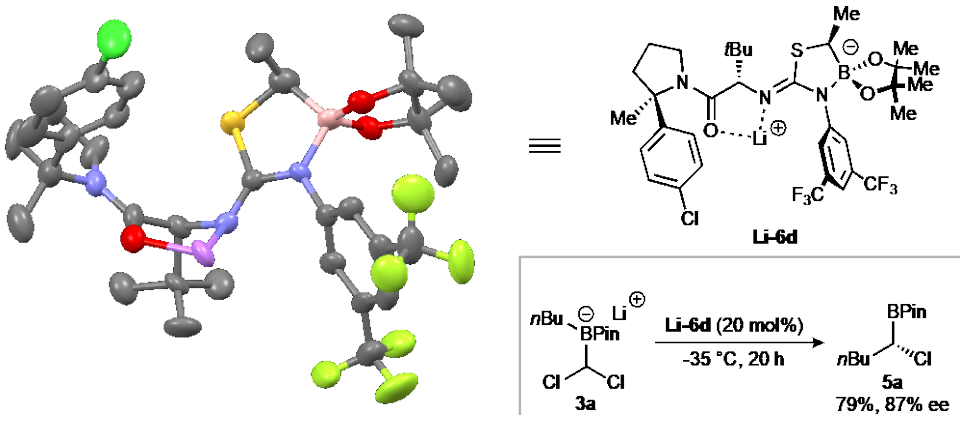

Figure 2.23 Crystal structure and catalytic activity of **Li-6d** (Li-methylcat)

2.6 Scope of Migrating Groups in Catalytic Rearrangement

With the identification and structural characterization of **Li-6a** as a highly enantioselective catalyst, the scope of migrating groups for the catalytic rearrangement was explored (Fig. 2.24). The efficacy of the catalytic reaction was assessed by measuring NMR yields and GC selectivities of the crude α-chloro boronic ester products, which were purified and fully characterized as the secondary boronic esters following stereospecific displacement of the remaining chloride with either phenethyl- or isopropyllithium. Excellent levels of enantioselectivity were achieved in rearrangements of boronates accessed by addition of dichloromethyllithium to readily available primary alkyl (**5a–j**) and unhindered secondary alkyl (**5k–m**) pinacol boronic ester derivatives bearing a variety of substitution and branching patterns. Compounds bearing mildly Lewis basic (**5c**,**h**,**i**) or base-sensitive (**5e**,**g**) functionality underwent the rearrangement effectively. Compounds bearing isotopically labeled stereocenters could be readily generated by employing commercially available CD_2Cl_2 (**5f-d$_1$**) and $^{13}CH_2Cl_2$ (**5b-^{13}C**).

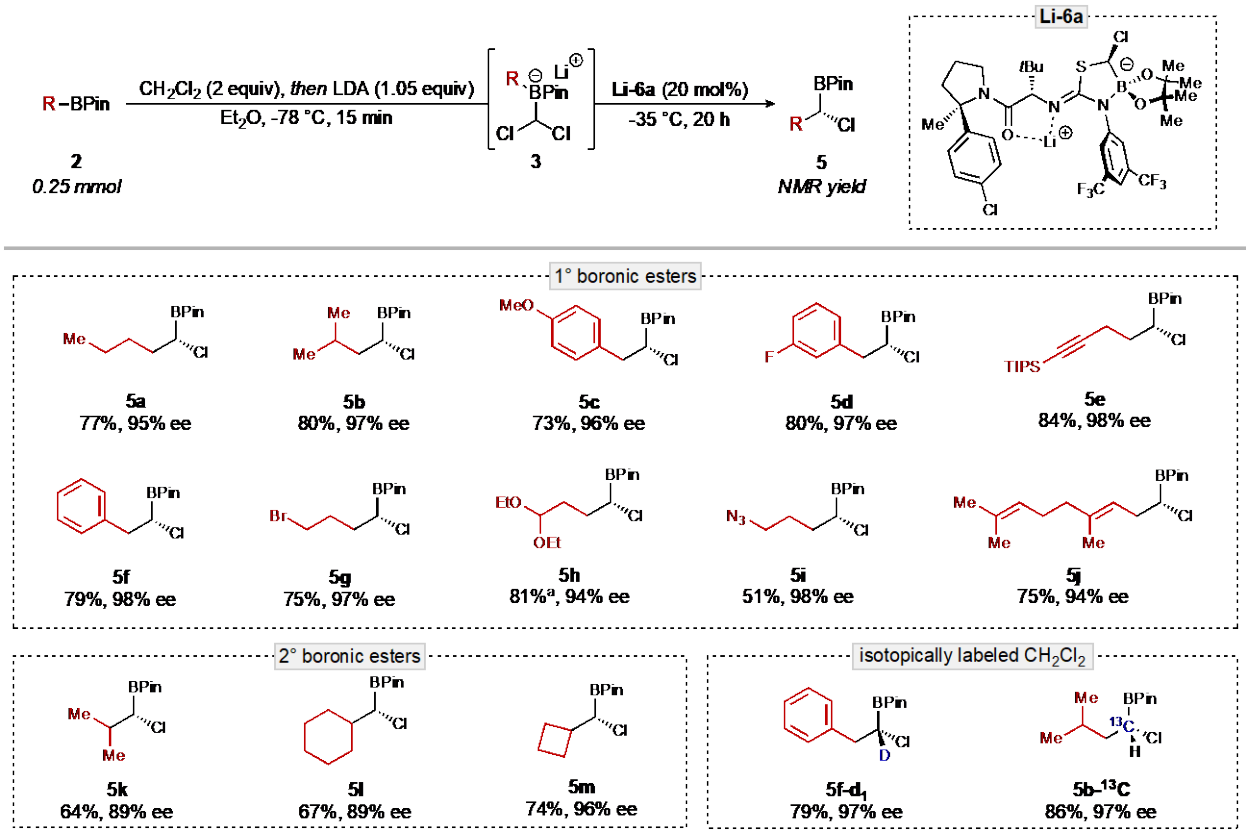

Figure 2.24 Scope of catalytic rearrangement reaction: successful substrates

Unfortunately, a number of substrates performed poorly in these rearrangement reactions, either by failing to undergo rearrangement or by doing so with variable levels of enantioselectivity (Fig. 2.25). These include substrates bearing moderate-to-strong Lewis basic functionality, aryl- and alkenylboronic esters, and sterically hindered alkylboronic esters. Particularly troublesome is the low levels of selectivity observed for secondary boronic esters featuring long branching chains, which suggests that direct application to iterative homologations will be challenging.

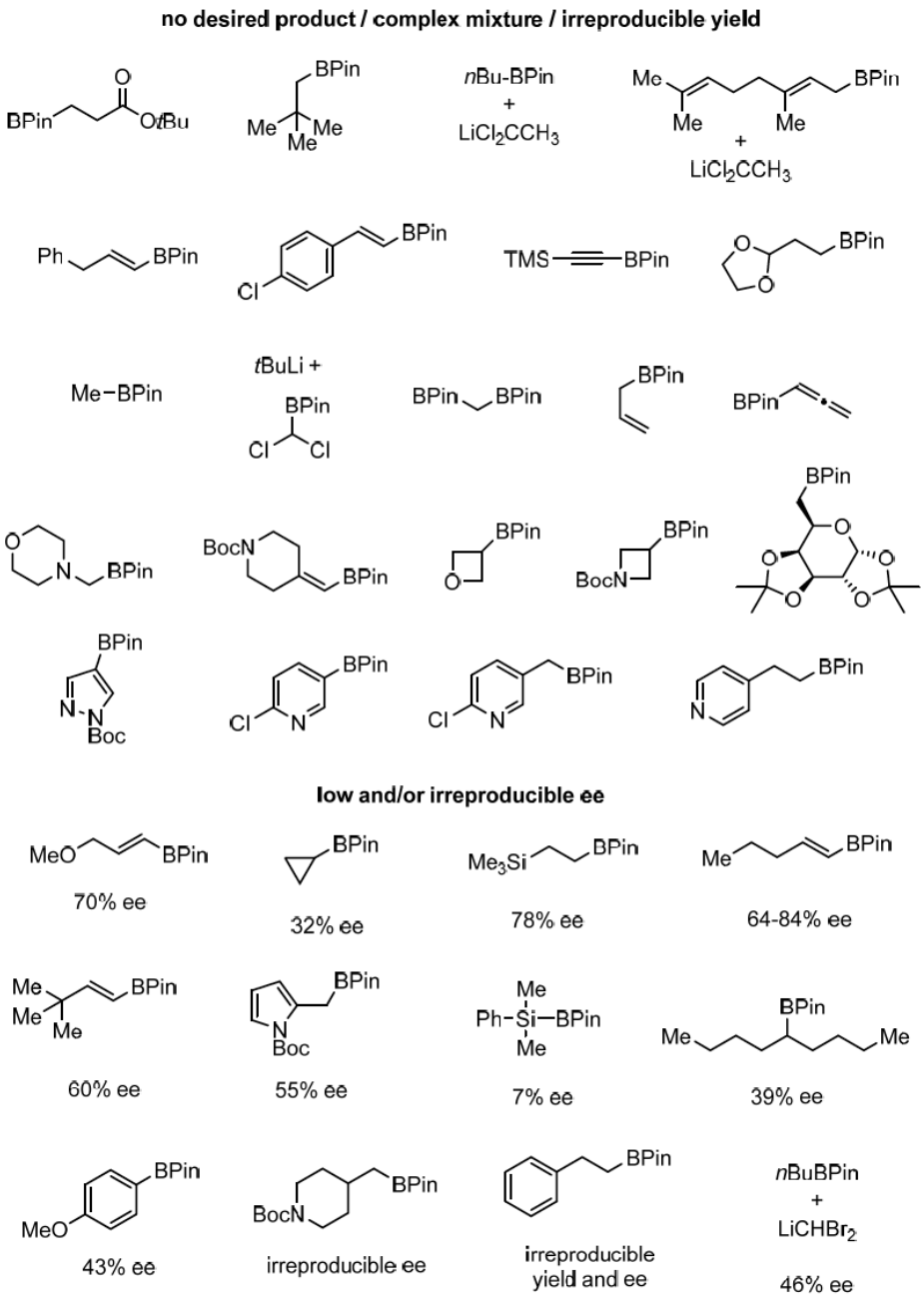

Figure 2.25 Scope of catalytic rearrangement reaction: unsuccessful substrates

2.7 Scope of Carbon-Chlorine and Carbon-Boron Elaboration Reactions

As noted in the original premise, the products of rearrangement of dichloromethyl boronates are bifunctional building blocks that can be elaborated sequentially and

stereospecifically to a broad array of stereodefined structural motifs (Fig. 2.26). To illustrate the synthetic utility of the enantioselective catalytic rearrangement reaction in the preparation of such compounds, we developed a two-step, telescoped procedure entailing the **Li-6a**-catalyzed rearrangement followed by a second, enantiospecific rearrangement to afford enantioenriched secondary boronic ester products directly. Grignard reagents bearing various substitution patterns were engaged in the second step to generate boronic ester products bearing primary alkyl (**7a**,**g**), secondary alkyl (**7b**,**f**,**h**), cyclic tertiary alkyl (**7c**),[36] aryl (**7d**), and alkenyl (**7e**,**i**) substitution in good yields over two steps and with complete enantiospecificity. Addition of heteroatomic nucleophiles to enantioenriched chloride building block **5b** afforded the corresponding ether (**7j**) and thioether (**7k**) products with high levels of enantiospecificity. Similarly, **5b-^{13}C** was elaborated to the α-boryl amine (**7l**) as the basis for an efficient route to an isotopically labeled analog of the proteasome inhibitor drug bortezomib.[37]

[36] Yu, S.; Jing, C.; Noble, A.; Aggarwal, V. K. 1,3-Difunctionalizations of [1.1.1]Propellane via 1,2-Metallate Rearrangements of Boronate Complexes. *Angew. Chem. Int. Ed.* **2020**, *59*, 3917–3921.

[37] Hinkes, S. P. A.; Klein, C. D. P. Virtues of Volatility: A Facile Transesterification Approach to Boronic Acids. *Org. Lett.* **2019**, *21*, 3048–3052.

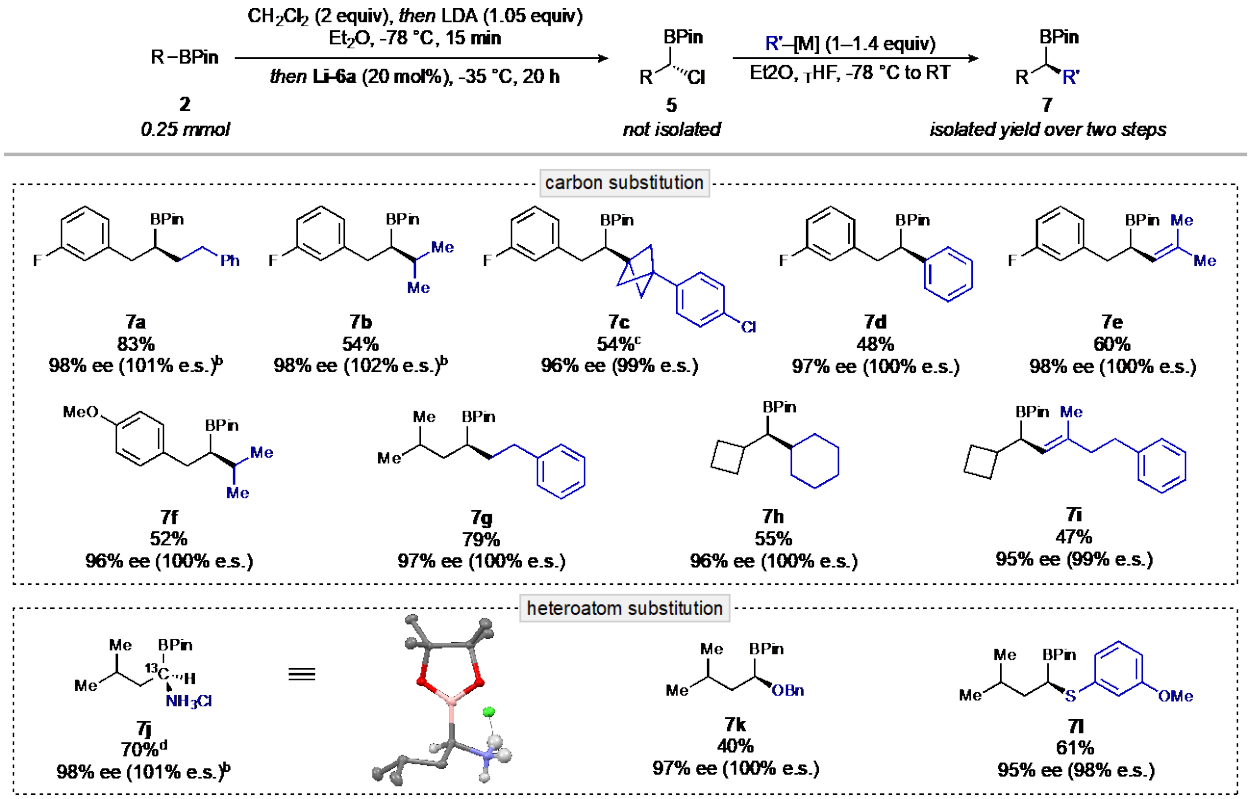

Figure 2.26 Scope of nucleophilic chloride displacement for the developed two-step sequence

The purified secondary boronic ester products obtained as outlined above were further elaborated to compounds bearing a diverse array of trisubstituted stereocenters using precedented carbon-boron bond transformations (Fig. 2.27). Boronic ester intermediates **7f–h** were thus transformed directly into products bearing a broad range of C–C, C–N, and C–O bonds in high

yields and enantiospecificities (**8a–e**,**h**,**i**).[38,39,40,41,42] Additionally, allylboronic ester intermediates **7e** and **7i** were elaborated selectively at the γ-position to afford fully substituted products bearing an α-tertiary amine (**8f**)[43] and a quaternary stereocenter (**8g**),[44] respectively.

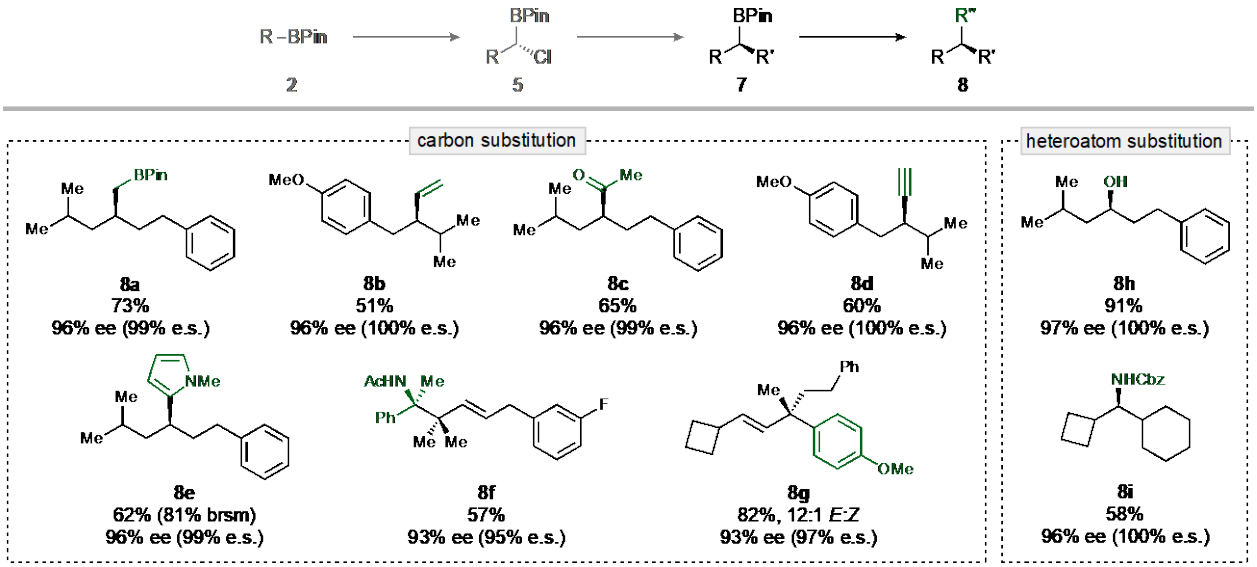

Figure 2.27 Scope of carbon-boron bond elaborations

[38] Sonawane, R. P.; Jheengut, V.; Rabalakos, C.; Larouche-Gauthier, R.; Scott, H. K.; Aggarwal, V. K. Enantioselective Construction of Quaternary Stereogenic Centers from Tertiary Boronic Esters: Methodology and Applications. *Angew. Chem. Int. Ed.* **2011**, *50*, 3760–3763.

[39] Pulis, A. P.; Blair, D. J.; Torres, E.; Aggarwal, V. K. Synthesis of Enantioenriched Tertiary Boronic Esters by the Lithiation/Borylation of Secondary Alkyl Benzoates. J. Am. Chem. Soc. **2013**, *135*, 16054–16057.

[40] Wang, Y.; Noble, A.; Myers, E. L.; Aggarwal, V. K. Enantiospecific Alkynylation of Alkylboronic Esters. *Angew. Chem. Int. Ed.* **2016**, *55*, 4270–4274.

[41] Odachowski, M.; Bonet, A.; Essafi, S.; Conti-Ramsden, P.; Harvey, J. N.; Leonori, D.; Aggarwal, V. K. Development of Enantiospecific Coupling of Secondary and Tertiary Boronic Esters with Aromatic Compounds. *J. Am. Chem. Soc.* **2016**, *138*, 9521–9532.

[42] Edelstein, E. K.; Grote, A. C.; Palkowitz, M. D.; Morken, J. P. A Protocol for Direct Stereospecific Amination of Primary, Secondary, and Tertiary Alkylboronic Esters. *Synlett*. **2018**, *29*, 1749–1752.

[43] Chen, J. L.-Y.; Aggarwal, V. K. Highly Diastereoselective and Enantiospecific Allylation of Ketones and Imines Using Borinic Esters: Contiguous Quaternary Stereogenic Centers. *Angew. Chem. Int. Ed.* **2014**, *53*, 10992–10996.

[44] Potter, B.; Edelstein, E. K.; Morken, J. P. Modular, Catalytic Enantioselective Construction of Quaternary Carbon Stereocenters by Sequential Cross-Coupling Reactions. *Org. Lett.* **2016**, *18*, 3286–3289.

2.8 Initial Extension to Iterative Rearrangements

Application of this methodology to iterative rearrangements was pursued with initial mixed results. The goal of this project is to deliver alkyl chains bearing multiple stereogenic centers where the sense of absolute and relative chirality can be controlled by the choice of the catalyst enantiomer for the enantioselective and diastereoselective steps, respectively (Fig. 2.28).

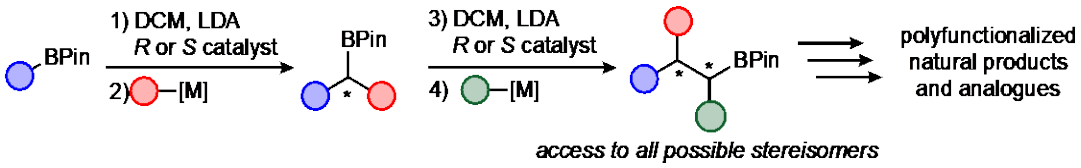

Figure 2.28 General scheme for iterative homologation sequence

Racemic secondary boronic ester **7m** was initially selected for investigation, partially because this substrate undergoes an unselective background rearrangement reaction (1.2:1 d.r.). In the presence of **Li-6a**, **7m** undergoes a modestly selective rearrangement reaction, with one enantiomer giving rise to product in 41:4 d.r. (~10:1) and the other enantiomer affording product in 43:12 d.r. (~4:1) (Fig. 2.29). More sterically congested starting material **7n** underwent less selective rearrangement to afford product in 41.5:8.75 d.r. (~4.7:1) or 34:15.75 d.r. (~2.2:1) depending on the enantiomer of starting material. These sets of experiments are flawed in that they subject equal quantities of enantiomeric compounds to the reaction conditions, which might lead to different selectivities than if an enantiomerically enriched mixture was used. In order to simplify the analysis, enantiopure (~97% ee) **(S)-7n** was subjected to the catalytic reaction conditions; rearrangement afforded product in slightly higher but still moderately low d.r. (2.7:1). To summarize the initial examinations into catalyst-controlled iterative rearrangements, one enantiomer of a sterically unencumbered substrate underwent rearrangement in 10:1 d.r., while the other enantiomer and both enantiomers of a bulkier substrate underwent less selective rearrangement. These results are

promising, but improvements to the catalyst and reaction conditions and identification of more interesting substrates will be crucial for transforming this endeavor into a working project.

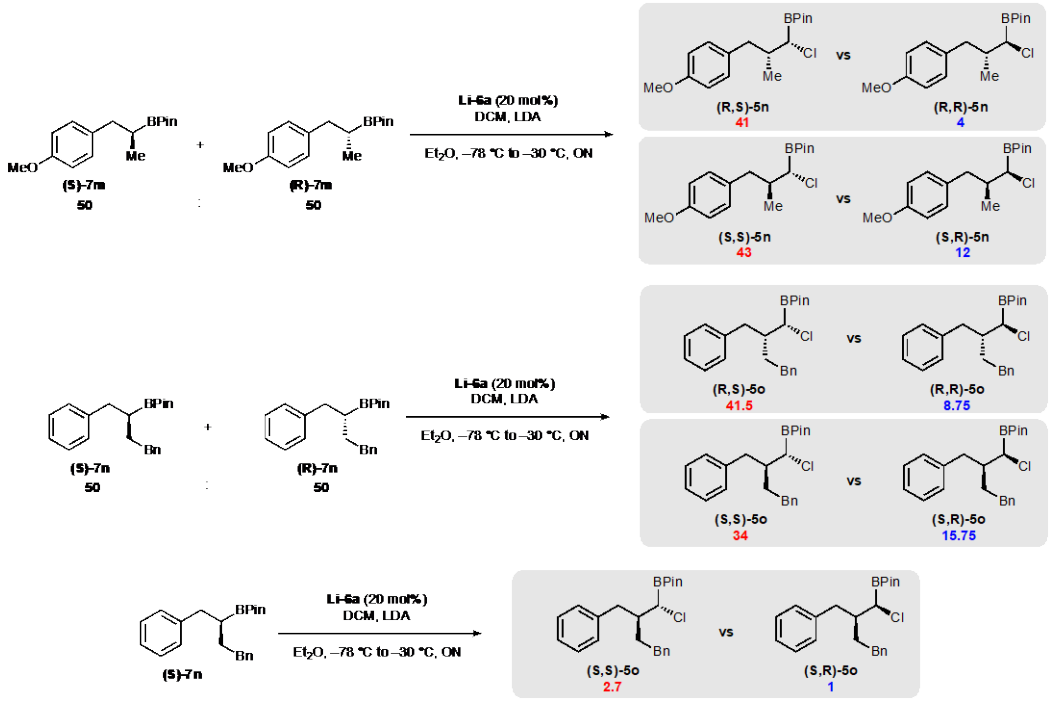

Figure 2.29 Catalytic, diastereoselective iterative homologations involving racemic or enantioenriched starting material

2.9 NMR- and DFT-Based Mechanistic Analysis

The effectiveness of lithium-isothiourea-boronate **Li-6a** in enantioselective 1,2-boronate rearrangements raises intriguing questions about the mode of catalysis and origin of enantioinduction. Given the absence of any potential H-bond-donor groups on the catalyst, the Lewis acidic lithium center represents the logical agent for chloride abstraction. We measured the Lewis acidity of these species, as well as of select common lithium species, by using the Gutmann–Beckett analysis (Fig. 2.30), which measures the δP of triethylphosphine oxide upon treatment

with the purported Lewis acid.[45,46,47] This analysis revealed that **Li-6a** possesses only moderate Lewis acidity, similar to that of other lithium salts and substantially lower than that of traditional Lewis acid catalysts such as $TiCl_4$. Most significantly, lithium boronate **Li-9**, which was designed to serve as a substrate mimic that cannot undergo rearrangement, displayed a slightly higher acceptor number (AN) than that obtained with **Li-6a**. Given the observed levels of enantioselectivity under catalytic conditions, **Li-6a** must be more reactive than the lithium boronate substrate **3** itself in promoting the rearrangement. While these observations do not rule out **Li-6a** acting as a chiral Lewis acid, the similar degree of Lewis acidity exhibited by lithium boronate substrate mimic **Li-9** precludes Lewis acidity alone as the only factor responsible for rate acceleration in the catalyst-mediated rearrangement.

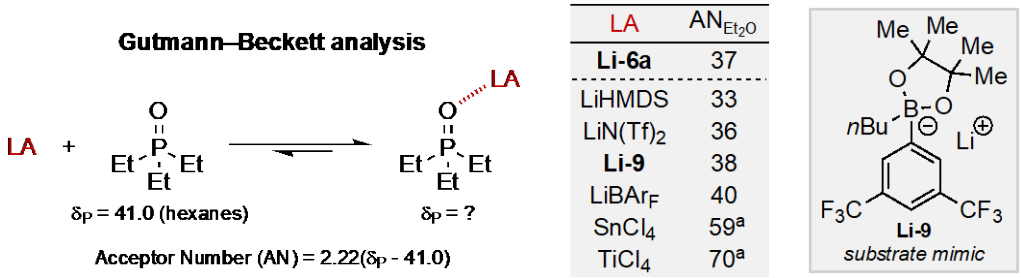

Figure 2.30 Gutmann–Beckett analysis

Valuable insight into the basis for the high reactivity of **Li-6a** in mediating the boronate rearrangement reaction was provided from DFT computational studies. In the initial investigations,

[45] Mayer, U.; Gutmann, V.; Gerger, W. The acceptor number — A quantitative empirical parameter for the electrophilic properties of solvents. *Monatshefte Für Chem. Chem. Mon.* **1975**, *106*, 1235–1257.

[46] Beckett, M. A.; Strickland, G. C.; Holland, J. R.; Sukumar Varma, K. A convenient n.m.r. method for the measurement of Lewis acidity at boron centres: correlation of reaction rates of Lewis acid initiated epoxide polymerizations with Lewis acidity. *Polymer* **1996**, *37*, 4629–4631.

[47] Beckett, M. A.; Brassington, D. S.; Coles, S. J.; Hursthouse, M. B. Lewis acidity of tris(pentafluorophenyl)borane: crystal and molecular structure of B(C6F5)3·OPEt3. Inorg. Chem. Commun. **2000**, *3*, 530–533.

a substrate:catalyst stoichiometry of 1:1 in the enantiodetermining transition states was assumed. The lowest-energy transition state structures reveal networks of attractive interactions involving the lithium ions and the boronate moieties of both the substrate and the catalyst (Fig. 2.31). In the putative enantiodetermining transition state leading to the major enantiomer in the **Li-6a**-catalyzed rearrangement of isobutyl-substituted lithium boronate **3b**, the anterior boronate oxygen and α-boryl chloride of **Li-6a** chelate the lithium ion of **3b** (depicted in blue in the graphic), while the posterior boronate oxygen of substrate **3b** is anchored by the lithium ion of the catalyst (depicted in red). In this geometry, both lithium ions are poised to promote abstraction of the departing chloride (shown in green) by a cooperative mechanism, with the Li–Cl bond distances for the catalyst and substrate lithium ions being 2.41 and 2.30 Å, respectively. In contrast, in the lowest energy transition state structure leading to the minor product enantiomer, the departing chloride resides proximal to the substrate lithium (2.29 Å) but distant from the catalyst lithium (4.81 Å); additionally, the substrate and catalyst lithium ions are both bound to the spectator chloride of the substrate. The modestly lower level of enantioselectivity observed in the rearrangement mediated by catalyst analogue **Li-6d** is consistent with the proposed attractive interaction between the α-boryl chloride of **Li-6d** and the substrate lithium ion being beneficial but not obligatory in the enantiodetermining event. Additionally, the catalyst amide oxygen is proximal to the dichloromethyl C–H in the major TS (2.29 Å) but not in the minor TS, consistent with a hydrogen-bond-accepting (HBA) interaction that might stabilize the loss of anionic charge on that hydrogen in the TS relative to the GS. This stabilizing HBA interaction has been previously observed in DFT studies on the $ZnCl_2$-catalyzed diastereoselective Matteson homologation, where Aggarwal and coworkers found a similar type of interaction between a catalyst chloride and the dichloromethyl

C–H.[48] Although a deeper analysis must await fuller characterization of the aggregation state and relative stoichiometry of the product-determining transition state, these results suggest a role for both the catalyst and substrate lithium ions in promoting chloride departure. Taken together, the NMR and DFT studies are consistent with lithium-isothiourea-boronate species **Li-6a** promoting the rearrangement reaction through a dual-lithium-induced chloride abstraction, aided by Lewis basic functionality on the rigid catalyst scaffold that orients both the catalyst and substrate lithium ions in a precise geometry.

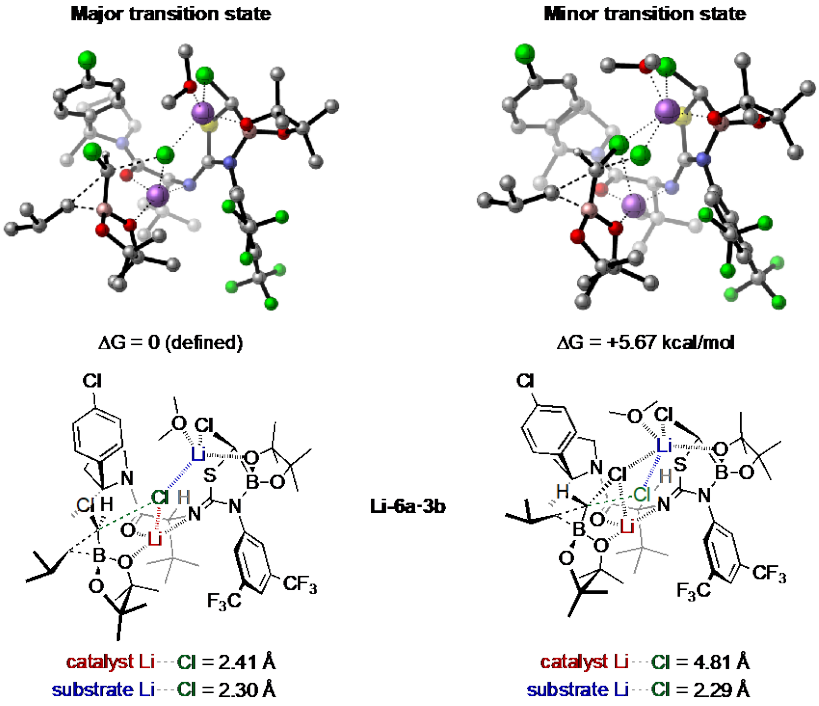

Figure 2.31 DFT pictures of Li-6a-catalyzed boronate rearrangement: lowest energy major and minor transition states

[48] Fasano, F.; Aggarwal, V. K. Origin of stereocontrol in the Matteson reaction: Importance of attractive electrostatic interactions. *Tetrahedron* **2021**, *78*, 131810.

2.10 Progress Towards Enantioselective, Catalytic Reactions Involving Hard Organometallic Reagents

One future direction is the development of new catalytic, enantioselective processes mediated by **Li-6**-type catalysts that proceed via a dual-lithium-bonding mechanism. We envisioned these catalysts could possibly mediate enantioselective reactions involving the direct coupling of organolithium reagents with electrophiles without the requirement for a "protective" intermediary such as an organoboron. This hypothesis is partially inspired by the previous discovery that **Li-6c** is robust to multiple equivalents of *n*BuLi at –78 °C.

Reports of catalytic, enantioselective reactions that employ organolithiums directly as coupling partners are rare, likely due to the challenge of selectively accelerating reactions with already low kinetic barriers, the presumed incompatibility of most chiral catalysts with strong, highly basic nucleophiles, and the difficulty of designing chiral ligands that preferentially bind the lithiated nucleophile rather than the lithiated product. The first of such reports detailed the enantioselective addition of phenyllithium to cyclohexene oxide (Fig. 2.32) catalyzed by a deprotonated chiral Schiff base of unknown structure or lithiation state.[49] A later report from the Tomioka lab divulged the enantioselective addition of 1-napthyllithium to 2-iminyl-1-fluoronapthalenes as catalyzed by chiral C2-symmetric ethane diethers.[50] This reaction proceeds via a dearomatizing, likely enantiodetermining conjugate addition, followed by ejection of lithium fluoride to restore aromaticity and deliver the atrop-chiral product. More recently, the Nakajima

[49] Oguni, N.; Miagi, Y.; Itoh, K. Highly Enantioselective Arylation of Symmetrical Epoxides with Phenyllithium Promoted by Chiral Schiff Bases and Salens. *Tet. Lett.* **1998**, *39*, 9023–9026.

[50] Tomioka, K. Asymmetric Reactions Based on Activation and Structure Control of Molecule—Asymmetric Reactions of Lithiated Nucleophiles. *Yakugaku Zasshi* **2004**, *124*, 43–53.

group reported the use of bis-lithiated BINOL-based catalysts to control the addition of lithiated phenyl acetylides to ketones.[51] In all cases, these reactions involve the use of lithiated or lithium-binding catalysts to control the addition of organolithium reagents to heteroatom-containing electrophiles, and thus provide a reasonable starting place for extension of the dual-lithium-binding hypothesis to other reactions using LIT boronate catalysts.

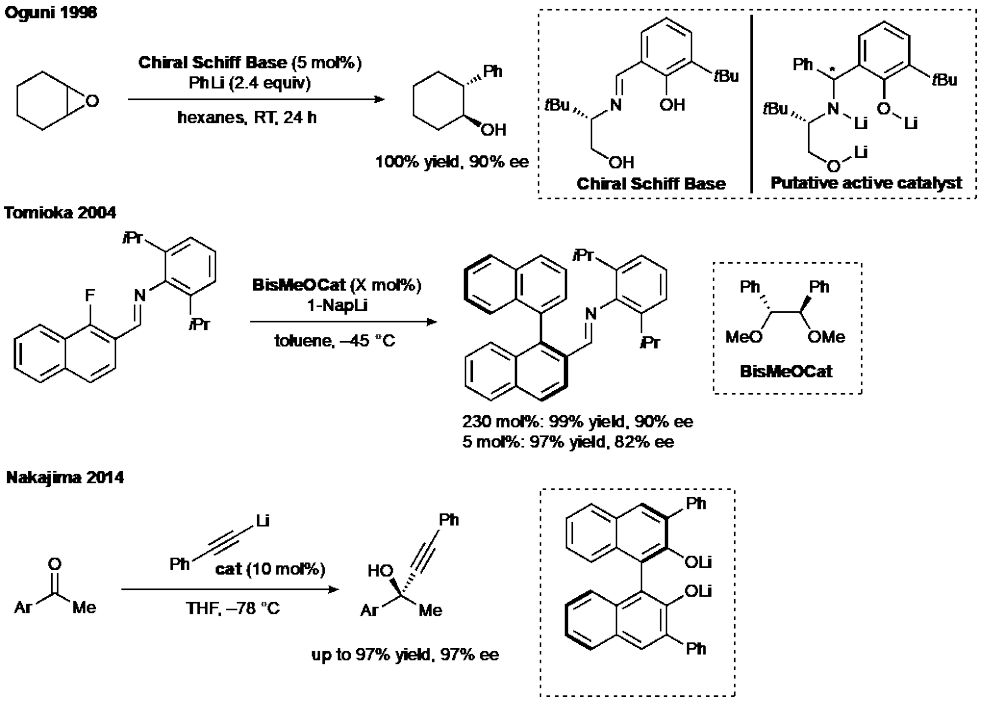

Figure 2.32 Literature reports of enantioselective addition of organolithiums to electrophiles

Initial investigations centered around controlling the addition of various hard organometallics such as phenyllithium and butyllithium or -magnesium bromide in coupling reactions with benzaldehyde, 4'-Cl-acetophenone, and cyclohexene oxide (Fig. 2.33).

[51] Kotani, S.; Kukita, K.; Tanaka, K.; Ichibakase, T.; Nakajima, M. Lithium Binaphtholate-Catalyzed Asymmetric Addition of Lithium Acetylides to Carbonyl Compounds. *J. Org. Chem.* **2014**, *79*, 4817–4825.

Figure 2.33 Scope of hard organometallics and O-based electrophiles surveyed in initial studies

I first explored addition of *n*butyl-derived organometallics to benzaldehyde facilitated by either **Li-6c** or **BrMg-6c** (Fig. 2.34; Table 2.1). The use of *n*BuMgBr and benzaldehyde **10a** in Et_2O paired with stoichiometric **Li-6c** resulted in the formation of chiral benzyl alcohol **11a** in variable but non-zero 18–35% ee. Use of *n*BuLi instead of *n*BuMgBr, **BrMg-6c** in place of **Li-6c**, or THF in place of Et_2O resulted in the formation of racemic product. The observation of any levels of enantioselectivity are encouraging; however, the largest challenge in this area of chemistry is the attainment of catalysis in this reactions, rather than high selectivity. As such, immediate next steps should prioritize screening for catalyst turnover by measuring enantioselectivities observed at various catalyst loadings.

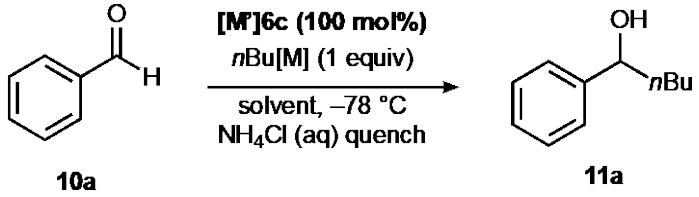

Figure 2.34 Addition of organometallics to benzaldehyde mediated by **[M']6c**

Table 2.1 Enantioselectivities observed for the reaction of organometallic additions to benzaldehyde mediated by **Li-6c or BrMg-6c**

[M]	MgBr	MgBr	Li	MgBr

Solvent	Et_2O	THF	Et_2O	Et_2O
Cat	**Li-6c**	**Li-6c**	**Li-6c**	**BrMg-6c**
Observed pdt?	Y	N	Y	Y
ee	18–35%	-	3%	1%

Parallel investigations into the catalytic opening of cyclohexene oxide with phenyllithium proved to be more promising, although the results were highly variable (Fig. 2.35). **Ent-Li-6c** facilitates the ring-opening reaction in variable yields and ee's, in some cases delivering product with incredibly high levels of enantioenrichment (Table 2.2). Attempts to reproduce these high selectivities or use slightly modified catalyst (**Li-6d**) resulted in much lower selectivities. In all of these cases, no reprotonated pre-catalyst was recovered. A survey of temperature and time revealed that the reaction is much slower than anticipated, consistent with a high kinetic barrier for epoxide opening. In these cases, some amount of catalyst was recovered, indicative of the robustness of the catalyst under shorter or consistently colder reaction conditions. The yields of all reactions were below 30%, including reactions without catalyst (Table 2.3). Unexpectedly, reactions that were run for longer durations afforded lower yields of product, consistent with a degradation pathway, which might contribute to the irreproducibility observed in the catalytic reaction. Taken together, these results suggest the existence of a highly enantioselective pathway for **Li-6c**-catalyzed opening of epoxides with phenyllithium and merit high-priority follow-up studies. Future examinations should focus on screening identical reactions in parallel, using purified and/or different meso-epoxides as well as salt-free aryllithium derivatives, increasing the

equivalents of aryllithium to achieve higher yields, and examining the effect of reaction time on yield and ee.

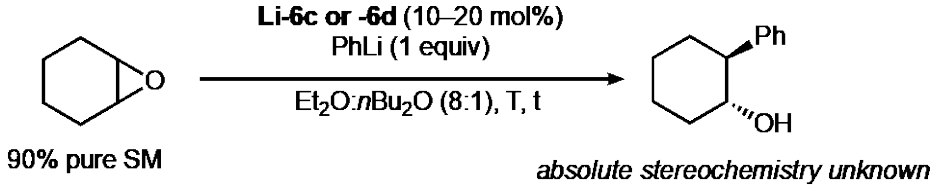

Figure 2.35 Catalytic ring-opening of cyclohexene oxide by phenyllithium

Table 2.2 Results for opening of cyclohexene oxide by phenyllithium catalyzed by **ent-Li-6c**

Mol % **ent-Li-6c**	10				10	10	20
t_{quench}	18h				0.5h	18h	18h
T	–78 °C to RT				RT	RT	4 °C
Yield	25%	30%	20%	20%	<5%	17%	15%
e.e.	–88%	–96%	–48%	20% (**Li-6d**)	–50–60%	–15%	–74%
Mol % cat remaining	0	0	0	0	6	0	7

Table 2.3 Results for uncatalyzed opening of cyclohexene oxide by phenyllithium

Mol % cat	0		
t_{quench}	0.5h	18h	32h

T	RT		
Yield	<2%	29%	15%
e.e.		N/A	

2.11 Conclusion

This chapter details the development of a catalytic, enantioselective Matteson homologation reaction. Consistent with the initial design hypothesis, the rearrangement is mediated by chiral thiourea and urea catalysts with moderate efficacy. However, more impactful is the discovery that lithium isothiourea boronate derivatives—formed via alkylation of thioureas with various intermediates involved in the reaction—catalyze the reaction with high levels of selectivity. The precise structure of these LIT catalysts was determined by NMR, HRMS, IR, and SCXRD, which reveal an isothiourea boronate bearing a lithium chelated by the isothiourea and amide and locked in a highly dissymmetric pocket. The products of this reaction are versatile building blocks that can be sequentially elaborated to afford molecules bearing tertiary and, in select cased, quaternary stereocenters with a range of substitution patterns, thus enabling a general construction of enriched chiral molecules from dichloromethane. Supported by DFT calculations, the rearrangement is proposed to proceed via a dual-lithium-induced (LiLi) chloride abstraction mediated by the catalyst. These LIT catalysts can potentially mediate other reactions via LiLi-induced mechanisms, with promising but variable levels of selectivity observed for the addition of phenyllithium to cyclohexene oxide.

2.12 Experimental

General Information

Methods:

Unless otherwise noted, all reactions for the preparation of substrates and catalysts were performed in standard, dry glassware, under a nitrogen atmosphere. Reported concentrations refer to solution volumes at room temperature. Concentration of organic solutions under reduced pressure was performed using house vacuum (40 torr) at 30 °C unless otherwise indicated. Column chromatography was performed with SiliaFlash P60 (230–400 mesh, SiliCycle) silica gel ("normal silica") or with deactivated C2 silica ("C2 silica") prepared as detailed below. Automated flash column chromatography was performed on a Biotage Isolera One. Thin layer chromatography (TLC) was used for reaction monitoring and product detection was performed using Silica Gel 60 F254 plates (EMD); plates were visualized by exposure to UV light (λ = 254 nm) or by staining with potassium permanganate, ninhydrin, or curcumin.

Materials and Reagents:

Reagents and solvents were purchased in reagent grade from Sigma-Aldrich, Alfa Aesar, Acros Organics, Strem, Oakwood, Matrix Scientific, Synthonix, Chem-Impex, Cambridge Isotope Laboratories, or TCI and used as received, unless otherwise indicated. Anhydrous solvents (dichloromethane, diethyl ether, tetrahydrofuran, toluene, 1,4-dioxane, and DMF) were prepared by passage through columns of activated alumina. Deuterated solvents were purchased from Cambridge Isotope Laboratories and were used as received, unless otherwise described.

Instrumentation:

All nuclear magnetic resonance (NMR) spectra were recorded on a Bruker AVANCE NEO 400, Bruker AVANCE NEO 400B, or JEOL ECZ400S spectrometer. Proton nuclear magnetic

resonance (^{1}H NMR) spectra are reported in parts per million (ppm) downfield from tetramethylsilane, and are referenced to the residual protium resonances of the NMR solvent ($CDCl_3$: 7.26 ppm; C_6D_6: 7.16 ppm; CD_3OD: 3.31 ppm). Proton-decoupled and proton-and-fluorine-decoupled carbon nuclear magnetic resonance (^{13}C-{^{1}H} and ^{13}C-{^{1}H}{^{19}F} NMR) spectra are reported in parts per million downfield from tetramethylsilane, and are referenced to the carbon resonances of the NMR solvent ($CDCl_3$: 77.16; C_6D_6: 128.06 ppm; CD_3OD: 49.00 ppm). Chemical shifts for fluorine nuclear magnetic resonance (^{19}F NMR) are reported in parts per million downfield from chlorotrifluoromethane ($\delta = 0$). Chemical shifts for boron nuclear magnetic resonance (^{11}B NMR) are reported in parts per million downfield from boron trifluoride diethyl etherate ($\delta = 0$). Data are represented as follows: chemical shift, multiplicity (br = broad, s = singlet, d = doublet, t = triplet, q = quartet, p = pentet, sext = sextet, sept = septet, m = multiplet), coupling constants in Hertz (Hz), integration. Mass spectral (MS) data were obtained by submission to the Harvard FAS Division of Science Small Molecule Mass Spectrometry facility. Optical rotations ([α]) were measured using a 1 mL cell with a 0.5 dm path length on a Jasco DIP 370 digital polarimeter at 589 nm (sodium D line) at room temperature. GC analysis was performed using an Agilent 7890A GC system using commercially available columns. Chiral HPLC analysis was performed using an Agilent 1200 series quaternary HPLC system using commercially available analytical columns. Chiral supercritical fluid chromatography (SFC) analysis was performed using a JASCO SFC-4000 SFC system with commercially available columns. In-situ IR experiments were carried out using a Mettler Toledo ReactIR™ iC 10 ATR FTIR spectrometer and a 9 mm AgX probe with a SiComp (silicon-based) window.

Synthesis and **Characterization** of Precatalyst 6a

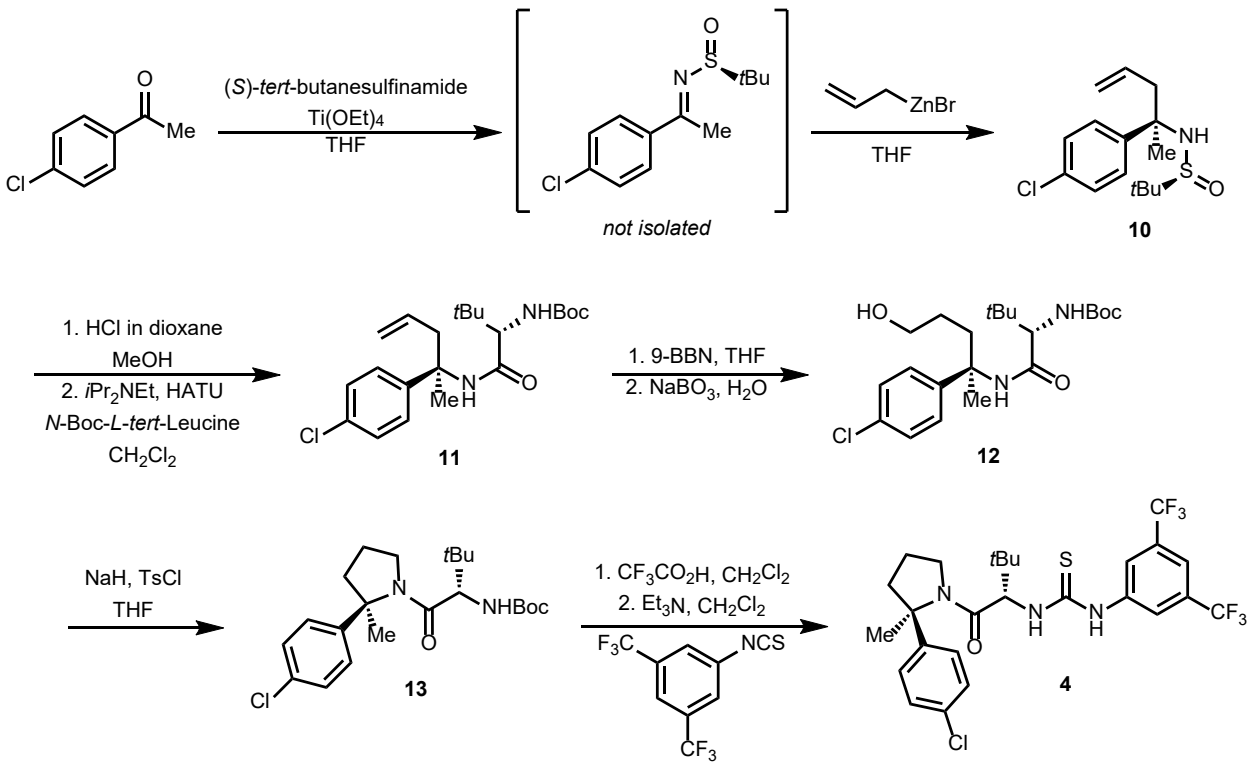

Figure 2.36. Synthesis of thiourea **4**, the direct precursor to isothiourea-boronate precatalyst **6a**.

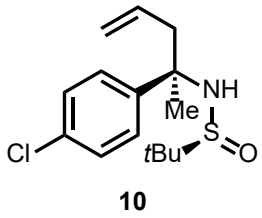

10

(*S*)-*N*-((*R*)-2-(4-chlorophenyl)pent-4-en-2-yl)-2-methylpropane-2-sulfinamide (10): Prepared according to the following method, adapted from a literature procedure previously reported by our group (*1*). A flame-dried 200 mL round-bottom flask equipped with a magnetic stir bar was charged with (*S*)-*tert*-butanesulfinamide (4.848 g, 40 mmol, 1 equiv) and THF (40 mL), then sealed with a rubber septum and put under a nitrogen atmosphere. The flask was charged with 4-chloroacetophenone (6.23 mL, 48 mmol, 1.2 equiv), followed by titanium (IV) ethoxide (16.8 mL, 80 mmol, 2 equiv). The reaction mixture was allowed to stir under positive nitrogen pressure at 70 °C for 7 hours. The reaction mixture was cooled to room temperature, then diluted with EtOAc (50 mL) and quenched with saturated aqueous Na_2SO_4 (9 mL). The heterogeneous mixture was stirred for 5 minutes at room temperature. Anhydrous $MgSO_4$ was added to the stirring mixture and stirring was continued for an additional 5 minutes. The reaction mixture was filtered through

Celite, rinsing with copious EtOAc, and the filtrate was concentrated under reduced pressure to afford the crude imine as a yellow oil. A flame-dried 250 mL round-bottom flask equipped with a magnetic stir bar was charged with zinc dust (3.4 g, 52 mmol, 1.3 equiv) and THF (100 mL), then sealed with a rubber septum and put under a nitrogen atmosphere. To the stirring suspension was added TMSCl (247 µL, 2 mmol, 0.05 equiv). The reaction mixture was allowed to stir for 5 minutes. Neat allyl bromide (4.5 mL, 52 mmol, 1.3 equiv) was added and the reaction mixture was allowed to stir for 1 hour to form the organozinc reagent. The crude imine was added to the reaction mixture as a solution in THF (20 mL), and the mixture was allowed to stir at room temperature for an additional 2 hours. The reaction mixture was diluted with EtOAc (50 mL) and quenched with saturated aqueous $NaHCO_3$. The organic and aqueous layers were separated, and the aqueous layer was extracted with EtOAc (2 x 50 mL). The combined organic layers were dried over $MgSO_4$, filtered, concentrated under reduced pressure, and purified by flash column chromatography on normal silica (70 to 100% Et_2O in hexanes) to afford **10** as a clear, faintly yellow syrup (9.0915 g, 76%). **^{1}H NMR** (400 MHz, $CDCl_3$) δ 7.40 – 7.35 (m, 2H), 7.33 – 7.29 (m, 2H), 5.55 (ddt, J = 17.4, 10.1, 7.4 Hz, 1H), 5.22 – 5.11 (m, 2H), 3.71 (s, 1H), 2.64 (d, J = 7.4 Hz, 2H), 1.76 (s, 3H), 1.22 (s, 9H); **^{13}C NMR** (101 MHz, $CDCl_3$) δ 143.9, 133.0, 132.7, 128.4, 128.0, 120.8, 59.7, 56.3, 49.1, 27.7, 22.8; **HRMS** (ESI) calculated for $C_{15}H_{23}ClNOS$ $[M+H]^+$: 300.1189; found: 300.1189. $[a]_D^{23}$ = +97.4° (c =10 mg/mL, CH_2Cl_2).

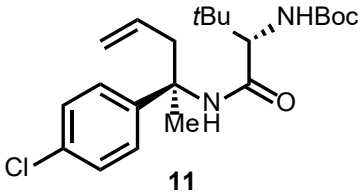

11

***tert*-butyl ((*S*)-1-(((*R*)-2-(4-chlorophenyl)pent-4-en-2-yl)amino)-3,3-dimethyl-1-oxobutan-2-yl)carbamate (11):**

Prepared according to the following method, adapted from a literature procedure previously reported by our group (*1*). A 100 mL round-bottom flask equipped with a magnetic stir bar was charged with sulfinamide **10** (9.0915 g, 30.3 mmol, 1

equiv) and MeOH (30 mL), and the stirring mixture was cooled to 0 °C. A solution of HCl (15.15 mL, 4.0 M in dioxane, 2 equiv) was added over 2 minutes, the cold bath was removed, and the reaction mixture was allowed to stir at room temperature for 1 hour. The reaction mixture was concentrated under reduced pressure to afford the crude amine hydrochloride salt, which was taken up in water and Et_2O. The organic and aqueous layers were separated, and the aqueous layer was extracted with Et_2O (3x). The aqueous layer was adjusted to pH 14 by addition of 2 M aqueous NaOH, then extracted with CH_2Cl_2 (5x). The combined CH_2Cl_2 extracts were dried over Na_2SO_4, filtered, and concentrated under reduced pressure to afford the crude amine. The amine was transferred to a 250 mL round-bottom flask equipped with a magnetic stir bar using CH_2Cl_2 (50 mL), and the solution was cooled to 0 °C. To the stirring solution was added *N*,*N*-diisopropylethylamine (7.9 mL, 45.5 mmol, 1.5 equiv), *N*-Boc-*L*-*tert*-Leucine (7.7 g, 33.3 mmol, 1.1 equiv), and HATU (12.7 g, 33.3 mmol, 1.1 equiv), and the reaction mixture was allowed to stir at 0 °C for an additional 15 minutes. The cold bath was removed and the reaction mixture was allowed to stir at room temperature for 20 hours. The reaction mixture was diluted with Et_2O and quenched with water. The organic and aqueous layers were separated, and the aqueous layer was extracted with Et_2O (3x). The combined organic layers were dried over $MgSO_4$, filtered, concentrated, and purified by flash column chromatography on normal silica (25% Et_2O in hexanes) to afford **11** as a white foam (10.8140 g, 87%). **^{1}H NMR** (400 MHz, $CDCl_3$) δ 7.26 (s, 4H), 6.06 (s, 1H), 5.60 (ddt, *J* = 14.7, 10.6, 7.3 Hz, 1H), 5.17 (dd, *J* = 16.3, 8.2 Hz, 3H), 3.77 (d, *J* = 9.4 Hz, 1H), 2.62 (dd, *J* = 13.5, 7.5 Hz, 1H), 2.47 (dd, *J* = 13.7, 7.1 Hz, 1H), 1.77 (s, 3H), 1.48 (s, 9H), 1.01 (s, 9H); **^{13}C NMR** (101 MHz, $CDCl_3$) δ 170.0, 156.2, 143.7, 132.6, 132.4, 128.4, 126.6, 120.2, 79.8, 62.8, 57.5, 48.1, 34.2, 28.3, 26.7, 24.9; **HRMS** (ESI)

calculated for $C_{22}H_{34}ClN_2O_3$ $[M+H]^+$: 409.2258; found: 409.2257. $[a]_D^{24} = +4.6°$ (c =10 mg/mL, CH_2Cl_2).

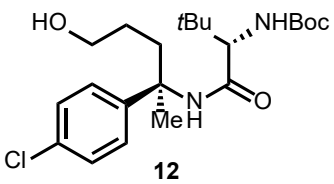

12

***tert*-butyl ((*S*)-1-(((*R*)-2-(4-chlorophenyl)-5-hydroxypentan-2-yl)amino)-3,3-dimethyl-1-oxobutan-2-yl)carbamate (12):** Prepared according to the following method, adapted from a literature procedure previously reported by our group (*2*). A flame-dried 500 mL round-bottom flask equipped with a magnetic stir bar was charged with carbamate **11** (10.8140 g, 26.4 mmol, 1 equiv) and THF (50 mL), sealed with a rubber septum, put under a nitrogen atmosphere, and cooled with stirring to 0 °C. A solution of 9-BBN (105.6 mL, 0.5 M in THF, 52.8 mmol, 2 equiv) was cannulated into the stirring solution over 10 minutes. The cold bath was removed, and the reaction was allowed to stir at room temperature for 2.5 hours before being cooled back to 0 °C. The septum was removed, and water (50 mL) and sodium perborate tetrahydrate (26.4 g, 171.6 mmol, 6.5 equiv) were added. The cold bath was removed, and the reaction was allowed to stir at room temperature for 16 hours. The reaction mixture was diluted with Et_2O and water. The organic and aqueous layers were separated, and the aqueous layer was extracted with Et_2O (3x). The combined organic layers were dried over $MgSO_4$, filtered, concentrated under reduced pressure, and purified by flash column chromatography on normal silica (25 to 50% EtOAc in hexanes) to afford **12** as a white foam (11.1430 g, 99%). **^{1}H NMR** (400 MHz, $CDCl_3$) δ 7.21 (s, 4H), 7.14 (s, 1H), 5.18 (d, J = 9.6 Hz, 1H), 3.73 (d, J = 9.8 Hz, 1H), 3.68 – 3.49 (m, 2H), 3.01 (s, 1H), 2.34 (s, 1H), 1.97 – 1.87 (m, 1H), 1.82 (dt, J = 14.0, 7.3 Hz, 1H), 1.75 (s, 3H), 1.45 (s, 9H), 1.42 – 1.34 (m, 1H), 0.99 (s, 9H); **^{13}C NMR** (101 MHz, $CDCl_3$) δ 170.2, 156.4, 143.9, 132.1, 128.2, 126.8, 80.0, 62.6, 62.2, 58.0, 40.6, 34.0, 28.3, 26.6, 26.5, 24.7; **HRMS** (ESI) calculated for $[M+H]^+$: 427.2358; found: 427.2367. $[a]_D^{23} = -15.2°$ (c =10 mg/mL, CH_2Cl_2).

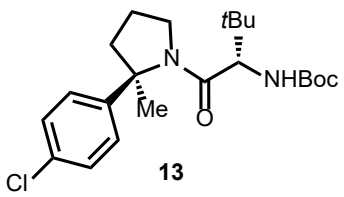

13

***tert*-butyl ((*S*)-1-((*R*)-2-(4-chlorophenyl)-2-methylpyrrolidin-1-yl)-3,3-dimethyl-1-oxobutan-2-yl)carbamate (13):**

Prepared according to the following method, adapted from a literature procedure previously reported by our group (*2*). A flame-dried 1 L round-bottom flask equipped with a large magnetic stir bar was charged with sodium hydride (4.14 g, 60% dispersion in mineral oil, 103.6 mmol, 4 equiv) and THF (400 mL), sealed with a rubber septum, put under a nitrogen atmosphere, and cooled to 0 °C with stirring. A solution of alcohol **12** (11.0624 g, 25.9 mmol, 1 equiv) in THF (40 mL) was added to the stirring suspension, rinsing the flask containing **12** with THF (2 x 20 mL), and the reaction mixture was allowed to stir for 30 minutes. The septum was removed and solid *p*-toluenesulfonyl chloride (5.93 g, 31.1 mmol, 1.2 equiv) was added in one portion. The septum was replaced, and the reaction mixture was allowed to stir for 16 hours, gradually warming to room temperature. The reaction was quenched with saturated aqueous NH_4Cl and allowed to stir for 10 minutes. The aqueous and organic layers were separated, and the aqueous layer was extracted with CH_2Cl_2 (3x). The combined organic layers were washed with brine, dried over $MgSO_4$, filtered, and concentrated under reduced pressure to a yellow solid. Trituration with Et_2O (4x) afforded **13** as a white powder (8.2924 g, 78%). **^{1}H NMR** (400 MHz, $CDCl_3$) δ 7.18 (d, *J* = 8.5 Hz, 2H), 7.09 (d, *J* = 8.5 Hz, 2H), 5.10 (d, *J* = 9.8 Hz, 1H), 4.31 – 4.19 (m, 2H), 3.77 (q, *J* = 7.8 Hz, 1H), 2.08 – 1.90 (m, 2H), 1.86 (s, 5H), 1.48 (s, 9H), 1.02 (s, 9H); **^{13}C NMR** (101 MHz, $CDCl_3$) δ 170.2, 156.6, 144.7, 131.7, 128.2, 126.3, 79.6, 66.9, 58.9, 49.9, 44.4, 34.5, 28.4, 26.5, 25.2, 22.4; **HRMS** (ESI) calculated for $C_{22}H_{34}ClN_2O_3$ $[M+H]^+$: 409.2252; found: 409.2255. $[a]_D^{24} = +20.4°$ (c =10 mg/mL, CH_2Cl_2).

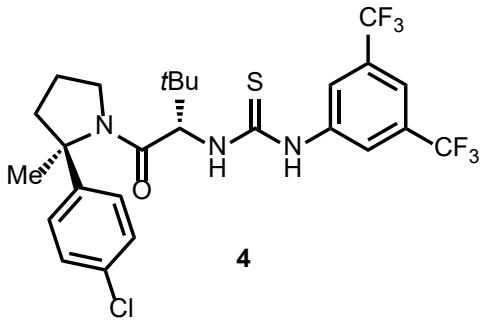

4

1-(3,5-bis(trifluoromethyl)phenyl)-3-((*S*)-1-((*R*)-2-(4-chlorophenyl)-2-methylpyrrolidin-1-yl)-3,3-dimethyl-1-oxobutan-2-yl)thiourea (4): A 250 mL round-bottom flask equipped with a magnetic stir bar was charged with **13** (8.1869 g, 20.0 mmol, 1 equiv) and CH_2Cl_2 (80 mL) and the stirring solution was cooled to 0 °C. Neat trifluoroacetic acid (30 mL) was added over 2 minutes and the reaction mixture was allowed to stir at room temperature for 2 hours. The reaction mixture was concentrated under reduced pressure to remove excess trifluoroacetic acid and the residue redissolved in CH_2Cl_2 (80 mL). To the stirring solution of ammonium salt was added triethylamine (16.7 mL, 120 mmol, 6 equiv). The reaction mixture was allowed to stir for 5 minutes before addition of 3,5-bis(trifluoromethyl)phenyl isothiocyanate (4.4 mL, 24 mmol, 1.2 equiv). The reaction mixture was stirred at room temperature for 16 hours, then quenched with 1:1 water:brine. The organic and aqueous layers were separated, and the aqueous layer was extracted with CH_2Cl_2 (3x). The combined organic layers were dried over $MgSO_4$, filtered, concentrated, and purified by flash column chromatography on normal silica (5 to 15% EtOAc in hexanes) to afford **4** as a white powder (11.6517 g, 100%). **^{1}H NMR** (400 MHz, $CDCl_3$) δ 9.53 (s, 1H), 7.83 (s, 2H), 7.63 (s, 2H), 7.01 (d, J = 8.6 Hz, 2H), 6.89 (d, J = 8.5 Hz, 2H), 5.33 (d, J = 9.3 Hz, 1H), 4.64 – 4.50 (m, 1H), 3.86 (q, J = 8.6 Hz, 1H), 2.09 – 1.95 (m, 1H), 1.87 (m, J = 6.0 Hz, 3H), 1.83 (s, 3H), 1.14 (s, 9H); **^{13}C NMR** (101 MHz, $CDCl_3$) δ 181.2, 170.0, 143.8, 139.4, 132.2 (q, J = 33.6 Hz), 131.6, 127.0, 126.2, 124.0, 123.0 (q, J = 272.9 Hz), 188.9, 67.7, 63.7, 50.3, 44.4, 35.6, 27.0, 25.1, 22.4; **^{19}F NMR** (376 MHz, $CDCl_3$) -62.80; **HRMS** (ESI) calculated for $C_{26}H_{29}ClF_6N_3OS$ $[M+H]^+$: 580.1624; found: 580.1623. $[a]_D^{24} = +7.2°$ (c =10 mg/mL, CH_2Cl_2). A crystal suitable for X-ray diffraction grew spontaneously upon allowing a saturated

solution of **4** in pentane/Et_2O to stand at 0 °C, allowing for the assignment of its structure and absolute configuration (see section **X-Ray Crystallography** for crystallographic details).

Preparation of C2 silica: Prepared according to the following method, adapted from a literature procedure (*3*). Normal silica (500 g) was suspended in $CHCl_3$ (1 L) with rapid overhead stirring. The suspension was put under a nitrogen atmosphere and cooled to 0 °C. To this suspension was added ethyltrichlorosilane (20.6 mL). The suspension was stirred at room temperature for 24 hours. The suspension was filtered on a frit, then washed with MeOH (1 L). The silica was washed with water until the filtrate was no longer acidic, then washed with additional MeOH (1 L). The resulting wet C2 silica was transferred to a 2 L round-bottom flask and heated to dryness on a rotary evaporator (95 °C, 40 torr), cooling to room temperature once water ceased distilling over. **Note:** used C2 silica may be cleaned and reused by following these washing and drying steps.

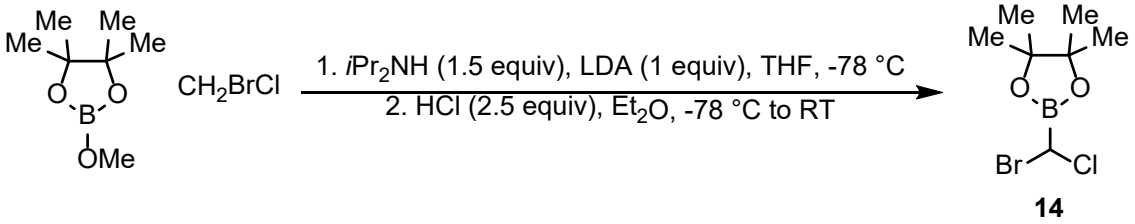

14

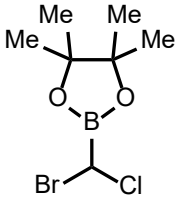

14

2-(bromochloromethyl)-4,4,5,5-tetramethyl-1,3,2-dioxaborolane, "bromochloromethyl-BPin" (14): A flame-dried 100 mL round-bottom flask equipped with a magnetic stir bar was charged with THF (50 mL), sealed with a rubber septum, and put through three rapid vacuum/nitrogen cycles to provide an N_2 atmosphere. To this flask was added diisopropylamine (9.5 mL, 67.5 mmol, 1.5 equiv), and the vessel was cooled to -78 °C. A solution of *n*-butyllithium (18.0 mL, 2.5 M in hexanes, 45 mmol, 1 equiv) was added over 5 minutes, and then the mixture was allowed to stir at -78 °C for

15 minutes to provide a cold LDA solution to be used later. A separate flame-dried 500 mL round-bottom flask equipped with a magnetic stir bar was charged with THF (100 mL), sealed with a rubber septum, and put through three rapid vacuum/nitrogen cycles to provide an inert atmosphere. To this flask was added bromochloromethane (3.5 mL, 54 mmol, 1.2 equiv) and 2-methoxy-4,4,5,5-tetramethyl-1,3,2-dioxaborolane (7.4 mL, 45 mmol, 1 equiv). The vessel was cooled to -78 °C, and then the cold LDA solution was cannulated into the reaction mixture over the course of 10 minutes. The reaction mixture was stirred at -78 °C for 20 minutes and then quenched with HCl (56.25 mL, 2.0 M in Et_2O, 112.5 mmol, 2.5 equiv) to produce a thick slurry. The reaction vessel was agitated by hand to provide thorough mixing and then was warmed to room temperature with rapid stirring. The vessel was then opened to air, and the reaction mixture was diluted with hexanes (200 mL) and then stirred rapidly for 5 minutes. The mixture was filtered through a pad of Celite (~ 4 cm thick) rinsing with Et_2O (300 mL), and the resulting cloudy solution was concentrated under reduced pressure. The concentrated yellow residue was resuspended in hexanes (100 mL) and filtered through a second pad of fresh Celite, rinsing with hexanes (300 mL). The resulting clear solution was concentrated to a clear yellow oil and subjected to flash column chromatography on C2 silica (0 to 5% Et_2O in hexanes). The desired fractions were combined and concentrated under reduced pressure by rotary evaporation (40 °C, 40 torr) until the desired product began to condense in the bump trap. The heating bath was removed and replaced with an ice-water bath, which induced freezing of the colorless oil to afford **14** as a lustrous white crystalline solid (8.4064 g, 73%). **^{1}H NMR** (400 MHz, $CDCl_3$) δ 5.29 (s, 1H), 1.33 (s, 12H); **^{13}C NMR** (101 MHz, $CDCl_3$) δ 85.6, 42.2 – 37.2 (m), 24.4, 24.3; **^{11}B NMR** (128 MHz, $CDCl_3$) δ 29; **HRMS** (APCI) calculated for $C_7H_{14}BBrClO_2$ $[M+H]^+$: 254.9953; found: 254.9953. **Note:** the first few column fractions often contain a significant

quantity of grease, which is detrimental to the physical properties of the substance. The crystalline product may be released from the walls of the flask by application of high vacuum (< 1 torr, room temperature). The product is stable for at least three hours in a sealed container under air but is hygroscopic and should be kept at -30 °C under inert atmosphere for long-term storage. The product could be kept at -80 °C for 6 months without any apparent decomposition.

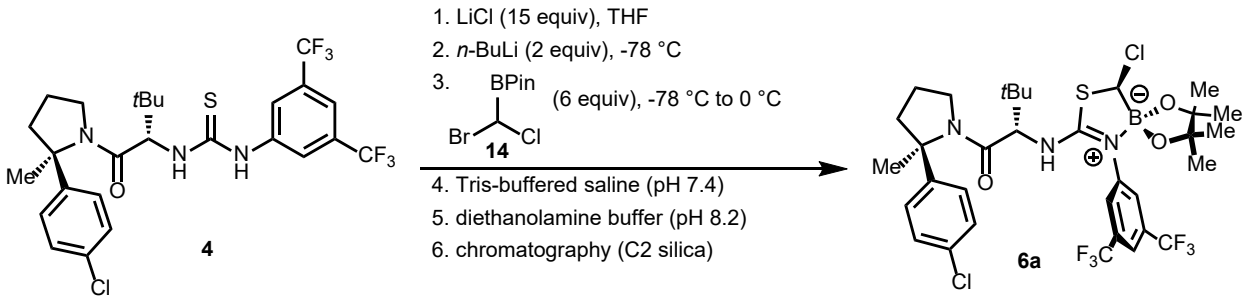

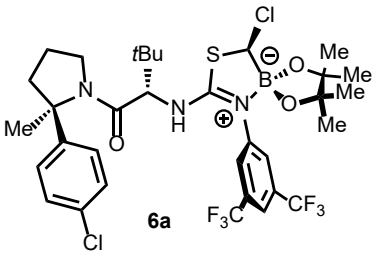

(*S*)-2-(((*S*)-1-(3,5-bis(trifluoromethyl)phenyl)-4-chloro-7,7,8,8-tetramethyl-6,9-dioxa-3-thia-1λ^4-aza-5λ^4-boraspiro[4.4]non-1-en-2-yl)amino)-1-((*R*)-2-(4-chlorophenyl)-2-methylpyrrolidin-1-yl)-3,3-dimethylbutan-1-one (6a):

Preparation of reagents and workup solutions:

Preparation of 0.1 M pH 8.2 diethanolamine buffer: Diethanolamine (10.5 g, 100 mmol) was dissolved in water (800 mL) in a 1 L graduated cylinder equipped with a magnetic stir bar. The stirring solution was adjusted to pH 8.2 using a pH meter with 10% aqueous H_2SO_4. The solution was diluted with water to 1 L in volume to afford 0.1 M pH 8.2 diethanolamine buffer.

Preparation of pH 7.4 tris-buffered saline: Commercially available 10x tris-buffered saline concentrate was diluted with water to afford a 20 mM solution of pH 7.4 tris-buffered saline.

Preparation of 0.5 M LiCl solution: A flame-dried 100 mL round-bottom flask equipped with a magnetic stir bar in a nitrogen-filled glovebox was charged with anhydrous LiCl (2.12 g, 50 mmol), sealed with a rubber septum, wrapped with electrical tape around the septum to ensure a tight seal, and removed from the glovebox. The flask was filled with THF (~ 100 mL) via cannula. The mixture was stirred rapidly under positive nitrogen pressure for 1 hour to dissolve the LiCl. **Note:** depending on the water content of the purportedly anhydrous THF, some of the LiCl may not dissolve; we have not encountered difficulties in the synthesis of **6a** using such solutions of slightly different molarity.

Simultaneous titration of *n*-butyllithium concentration and LiCl solution water content: *We have found it essential to account for the presence of water in the synthesis of **6a**, as it quenches n-butyllithium and lowers conversion.* An oven-dried 2-dram vial was charged with *N*-benzylbenzamide (84.5 mg, 0.4 mmol) and a magnetic stir bar and then sealed with a Teflon-coated septum cap and put under a nitrogen atmosphere. The vial was charged with **0.5 M LiCl solution** (6000 μL) (see above), and the reaction mixture was stirred until it formed a colorless, homogeneous solution. The solution was cooled to 0 °C and stirred for 5 minutes. A 250 μL microsyringe was flushed twice with a solution of *n*-butyllithium (~ 2.5 M in hexanes) and then charged with *n*-butyllithium (250 μL). The *n*-butyllithium solution was added dropwise to the rapidly stirring solution of LiCl and indicator, and addition was continued until a persistent blue/indigo color remained in the reaction mixture. The volume of *n*-butyllithium added was recorded and the remaining *n*-butyllithium and reaction mixture were discarded. This volume multiplied by 10 is denoted **V** in the following synthetic procedure. The theoretical value of **V** is 1600 μL. **Note:** this LiCl solution is highly hygroscopic and should be used within 5 hours of titration or stored in a nitrogen-filled glovebox for optimal results.

Synthesis of 6a: A flame-dried 250 mL round-bottom flask equipped with a magnetic stir bar was charged with thiourea **4** (1160.1 mg, 2 mmol, 1 equiv), sealed with a rubber septum, and put under a nitrogen atmosphere. The flask was charged with freshly prepared **0.5 M LiCl solution** (60.0 mL) (see above). The resulting reaction mixture was stirred until homogeneous, then cooled to -78 °C with rapid stirring. To the reaction flask was then added a solution of *n*-butyllithium (**V** µL [see titration above]) dropwise over 5 minutes. This deprotonated thiourea mixture was allowed to stir for an additional 5 minutes. Meanwhile, a flame-dried 50 mL round-bottom flask was charged with bromochloromethyl-BPin (**14**) (3064 mg, 12 mmol, 6 equiv) and put under a nitrogen atmosphere. To this flask was added THF (12 mL), and the mixture was cooled to -78 °C. This cold solution of bromochloromethyl-BPin was then cannulated as rapidly as possible into the cold deprotonated thiourea reaction mixture. The resulting combined reaction mixture was allowed to stir for an additional 5 minutes, after which time the cold bath was removed and the reaction mixture was allowed to stir at room temperature for 20 minutes. The reaction mixture was then diluted with Et_2O (50 mL) and quenched with **tris-buffered saline** (100 mL) (see above). The organic and aqueous layers were separated, and the aqueous layer was extracted with Et_2O (2 x 50 mL). The combined organic layers were dried over Na_2SO_4, filtered, and concentrated under reduced pressure in an oversized flask to minimize bumping. The residue was taken up in CH_2Cl_2 (100 mL), and the organic layer was washed with **diethanolamine buffer** (3 x 100 mL) (see above) to remove excess **14**. The organic layer was dried over Na_2SO_4, filtered, and concentrated under reduced pressure. Purification by flash column chromatography on C2 silica (0 to 20% EtOAc in hexanes) afforded **6a** as a colorless gum; repeated evaporation from pentane converted this material into a white foam that could be crushed into a dry powder (1.0017 g, 66%). **^{1}H NMR** (400 MHz, C_6D_6) δ 7.82 (s, 2H), 7.47 (s, 1H), 7.41 (d, J = 8.7 Hz, 2H), 6.80 (d, J = 8.7 Hz, 2H),

6.12 (d, J = 10.1 Hz, 1H), 4.92 (s, 1H), 3.89 (d, J = 10.1 Hz, 1H), 3.48 (dt, J = 9.7, 6.6 Hz, 1H), 3.02 (dt, J = 9.3, 6.6 Hz, 1H), 1.46 (s, 3H), 1.40 – 0.77 (m, 16H), 0.69 (s, 9H); **^{13}C NMR** (101 MHz, C_6D_6) δ 170.1, 167.0, 144.3, 140.6, 133.1 (q, J = 34.6 Hz), 132.9, 129.1, 129.0 – 128.6 (m), 126.3, 123.3 (q, J = 273.4 Hz), 121.6 (sept, J = 3.8 Hz), 80.7, 67.4, 64.2, 49.9, 43.9, 35.5, 26.3, 26.0, 24.4, 22.8 [*the carbon attached to boron was not observed due to quadrupolar relaxation*]; **^{11}B NMR** (128 MHz, C_6D_6) δ 11.8; **^{19}F NMR** (376 MHz, C_6D_6) δ -62.78; **HRMS** (ESI) calculated for $C_{33}H_{41}BCl_2F_6N_3O_3S$ $[M+H]^+$: 754.2237; found: 754.2248. $[\alpha]_D^{24}$ = -45.8° (c = 10 mg/mL, CH_2Cl_2). A crystal suitable for X-ray diffraction grew spontaneously upon allowing a saturated solution of **6a** in pentane to stand at 0 °C, allowing for the assignment of its structure and absolute configuration (see section **X-Ray Crystallography** for crystallographic details). **Note:** this compound can be handled in air and was found to be stable in a sealed vial in a desiccator cabinet for at least 3 months. Extended exposure to high levels of humidity, brief exposure to acidic conditions (including trace HCl in $CDCl_3$), or attempted purification on normal silica may result in epimerization of the chloride stereocenter and/or hydrolysis to thiourea **4**. Contamination of this compound by residual bromochloromethyl-BPin (**14**) has an adverse effect on its material properties and air stability. To the best of our knowledge, this is the first report of a molecule bearing a sulfur-boron-chlorine-hydrogen-substituted carbon stereocenter.

Figure 2.37 Approximately 1 gram of **6a**.

Synthesis and Characterization of Substrates

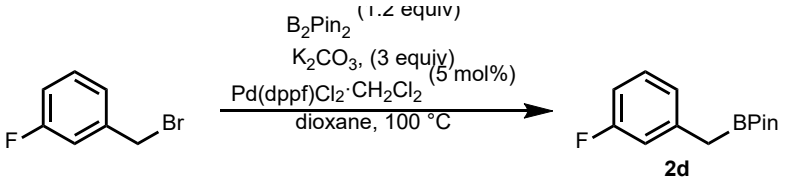

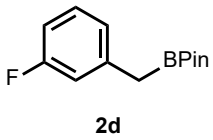

2-(3-fluorobenzyl)-4,4,5,5-tetramethyl-1,3,2-dioxaborolane (2d): A flame-dried 40 mL septum-top vial equipped with a magnetic stir bar was charged with anhydrous K_2CO_3 (1.66 g, 12 mmol, 3 equiv), bis(pinacolato)diboron (1.22 g, 4.8 mmol, 1.2 equiv), and $Pd(dppf)Cl_2 \cdot CH_2Cl_2$ (163 mg, 0.2 mmol, 5 mol%). The vial was capped, sealed with electrical tape, and put under a nitrogen atmosphere before being charged with dioxane (10 mL) and 3-fluorobenzyl bromide (491 μL, 4 mmol, 1 equiv). The nitrogen line was removed, and the reaction mixture was stirred at 100 °C for 24 hours. The reaction mixture was cooled to room temperature, diluted with EtOAc, and filtered through a pad of normal silica (~ 4 cm thick), rinsing with additional EtOAc until the filtrate was colorless. The filtrate was concentrated under reduced pressure, and the residue purified by flash column chromatography on normal silica (0 to 8% Et_2O/hexanes) to afford **2d** as a colorless liquid (637.9 mg, 68%). **^{1}H NMR** (400 MHz, $CDCl_3$) δ 7.18 (td, *J* = 8.0, 6.1 Hz, 1H), 6.99 – 6.86 (m, 2H), 6.81 (td, *J* = 8.6, 3.1 Hz, 1H), 2.29 (s, 2H), 1.24 (s, 12H); **^{13}C NMR** (101 MHz, $CDCl_3$) δ 163.0 (d, *J* = 244.1 Hz), 141.4 (d, *J* = 8.0 Hz), 129.6 (d, *J* = 8.4 Hz), 124.8 (d, *J* = 2.9 Hz), 116.0 (d, *J* = 21.1 Hz), 111.9 (d, *J* = 21.1 Hz), 83.7, 24.8 [*the carbon attached to boron was not observed due to quadrupolar relaxation*]; **^{19}F NMR** (376 MHz, $CDCl_3$) δ -114.31; **HRMS** (ESI) calculated for $C_{13}H_{19}BFO_2$ $[M+H]^+$: 237.1457; found: 237.1459. **Note: 2d** is susceptible to rapid oxidation under air and should be purified immediately before use.

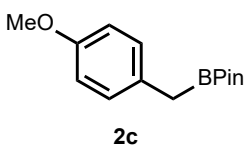

2c

2-(4-methoxybenzyl)-4,4,5,5-tetramethyl-1,3,2-dioxaborolane (2c): Prepared analogously to **2d** using 4-methoxybenzyl chloride (542 µL, 4 mmol, 1 equiv). Purification by flash column chromatography on normal silica (0 to 8% Et_2O in hexanes) afforded **2c** as a colorless liquid (813.0 mg, 82%). **^{1}H NMR** (400 MHz, $CDCl_3$) δ 7.10 (d, *J* = 8.8 Hz, 2H), 6.79 (d, *J* = 8.8 Hz, 2H), 3.77 (s, 3H), 2.23 (s, 2H), 1.23 (s, 12H); **^{13}C NMR** (101 MHz, $CDCl_3$) δ 157.2, 130.6, 129.9, 113.9, 83.5, 55.3, 24.9 [*the carbon attached to boron was not observed due to quadrupolar relaxation*]; **HRMS** (ESI) calculated for $C_{14}H_{22}BO_3$ $[M+H]^+$: 249.1657; found: 249.1662. **Note: 2c** is susceptible to rapid oxidation under air and should be purified immediately before use.

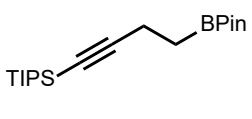

2e

triisopropyl(4-(4,4,5,5-tetramethyl-1,3,2-dioxaborolan-2-yl)but-1-yn-1-yl)silane (2e): A flame-dried 20 mL septum-top vial equipped with a magnetic stir bar was charged with 1-trimethylsilylpropyne (0.48 mL, 2 mmol, 1 equiv), capped, and put under a nitrogen atmosphere before being charged with THF (4 mL). The stirring reaction mixture was cooled to 0 °C for 5 minutes, after which a solution of *n*-butyllithium (~ 2.5 M in hexanes, 1 equiv) was added to the reaction mixture. After 5 minutes, the reaction mixture was cooled to -78 °C, and then neat (bromomethyl)boronic acid pinacol ester (0.44 mL, 2 mmol, 1 equiv) was added. The vial was removed from the cold bath and allowed to warm to room temperature over the course of 1 hour. After this time, the reaction mixture was diluted with hexanes (10 mL) and filtered through a pad of celite (~ 4 cm thick), rinsing with Et_2O (10 mL). The filtrate was concentrated under reduced pressure, and the residue purified by flash column chromatography on normal silica (0 to 5% Et_2O/hexanes) to afford **2e** as a colorless liquid (524.0 mg, 78%). **^{1}H NMR** (400 MHz, $CDCl_3$) δ 2.34 (t, J = 7.6 Hz, 2H), 1.24 (s, 12H), 1.10 – 0.96 (m, 23H); **^{13}C NMR** (101 MHz, $CDCl_3$) δ 111.0, 83.2, 79.0, 24.8, 18.7, 14.6, 11.3 [*the carbon*

attached to boron was not observed due to quadrupolar relaxation]; **^{11}B NMR** (128 MHz, $CDCl_3$) δ 34; **HRMS** (ESI) calculated for $C_{19}H_{38}BO_2Si$ $[M+H]^+$: 337.2734; found: 337.2729.

Reaction Scope and C–Cl Elaboration Reactions

General procedures for catalytic, enantioselective rearrangement reaction and telescoped sequential catalyzed and uncatalyzed rearrangement reactions:

General Procedure A provides the procedure for the enantioselective rearrangement reaction catalyzed by **Li-6a**. **General Procedure B** provides the procedure used to acquire NMR yields for the chloride products **5** generated by **General Procedure A**. **General Procedure C** provides the procedure for the telescoped stereospecific elaboration of crude chloride products **5** generated by **General Procedure A** with Grignard reagents to afford secondary boronic ester products **7**. **General Procedure D** provides a procedure for the synthesis of racemic chloride products. **General Procedure E** provides a procedure for the synthesis of racemic secondary boronic ester products.

General Procedure A (catalyzed rearrangement reaction):

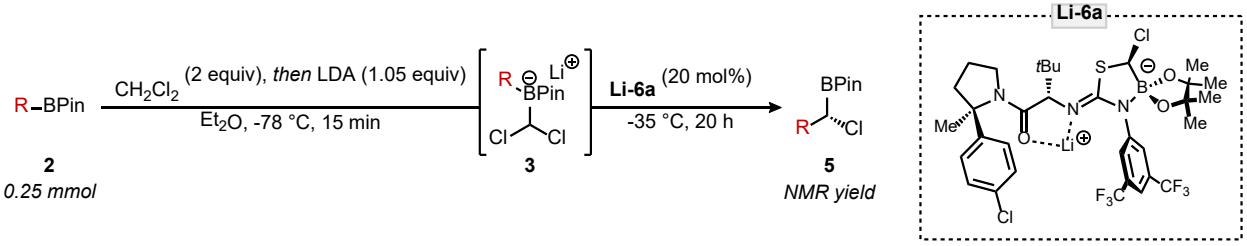

Preparation of LDA: An oven-dried 1-dram vial equipped with a magnetic stir bar and Teflon-coated septum cap under a nitrogen atmosphere was charged with diisopropylamine (370 µL, 2.64 mmol, 1.06 equiv) and Et_2O (1200 µL), then cooled with stirring to -78 °C. To this solution was added a solution of *n*-butyllithium (1000 µL, 2.5 M in hexanes, 2.5 mmol, 1 equiv) over 1 minute. The solution was removed from the cold bath and allowed to warm to room

temperature over 20 minutes. **Note:** once prepared, this solution of LDA should be used in the catalytic reaction within 12 hours; we have observed irreproducibility when using day-old LDA solution, even when re-titrated.

Titration of LDA: An oven-dried 2-dram vial was charged with *N*-benzylbenzamide (~ 100 mg, 0.473 mmol). The exact mass of *N*-benzylbenzamide used was recorded. The vial was then equipped with a magnetic stir bar and a septum cap and then was put under a nitrogen atmosphere. The vial was charged with THF (4 mL), and the reaction mixture was stirred until it formed a colorless, homogeneous solution. The vessel was cooled to 0 °C and stirred for 5 minutes. The LDA was taken up in a syringe and was added dropwise to the rapidly stirring indicator mixture, and addition was continued until a persistent blue/indigo color remained in the reaction mixture. The volume of LDA added was recorded, and the remaining LDA in the syringe and indicator mixture were discarded. The concentration of the LDA solution was calculated as (**mass of *N*-benzylbenzamide** / (211.26 g/mol)) / (**volume of LDA added**), affording a concentration typically between 0.90 and 1.05 M.

***In situ* preparation of lithium boronate (3):** An oven-dried 1-dram vial equipped with a magnetic stir bar was charged with a pinacol boronic ester substrate **2** (0.25 mmol, 1 equiv), sealed with a septum cap, and put under a nitrogen atmosphere (3 vacuum/nitrogen cycles). The vial was then charged with Et_2O (400 μL) and CH_2Cl_2 (32 μL, 0.50 mmol, 2 equiv). The reaction mixture was cooled to -78 °C and stirred at this temperature for 5 minutes. A titrated solution of LDA (~ 1.0 M in Et_2O/hexanes, 0.2625 mmol, 1.05 equiv) (see above) at room temperature was added dropwise to the center of the reaction mixture (rather than the vial walls) at a rate not exceeding 1 drop per 2 seconds. The reaction mixture was stirred at -78 °C to form a white or orange suspension of lithium boronate **3**. After aging for 15 minutes, this suspension of lithium

boronate was used in the catalyzed reaction as detailed in the "**Running the reaction**" section below. **Note:** low-boiling liquid boronic esters were added by microsyringe after putting the vial under a nitrogen atmosphere. We have *not* observed conversion of the boronate to product at -78 °C; 30 minutes of additional aging of the boronate before addition of catalyst does not lead to changes in reaction outcome.

Preparation of catalyst solution (Li-6a): An oven-dried 1-dram vial was charged with precatalyst **6a** (37.7 mg, 0.05 mmol, 20 mol%), sealed with a septum cap, and put under a nitrogen atmosphere. The vial was charged with Et_2O (300 μL) and CH_2Cl_2 (100 μL), then cooled to 0 °C and stirred at this temperature for 5 minutes. A solution of LiHMDS (50 μL, 1.0 M in toluene, 0.05 mmol, 20 mol%) was added to the vessel via microsyringe and the mixture was stirred for 1 minute to afford a solution of **Li-6a**. **Note:** this catalyst solution should be kept at 0 °C and used immediately for optimal results.

Running the reaction: After formation and aging of lithium boronate **3**, the cold solution of catalyst **Li-6a** was rapidly drawn into a nitrogen-flushed 1 mL disposable plastic syringe and injected directly into the suspension of **3** stirring at -78 °C. The catalyst solution vial was rinsed with Et_2O (140 μL), which was transferred using the same disposable syringe to the boronate solution. The reaction mixture was stirred for 1 minute at -78 °C, then placed in a -35 °C cryocool and stirred for 20 hours. After this time, the vial was removed from the cold bath and allowed to stir at room temperature for 15 minutes. The heterogeneous reaction mixture was diluted with Et_2O and quenched with saturated aqueous NH_4Cl (500 μL). The organic and aqueous layers were separated and the aqueous layer was extracted with Et_2O (2 x 2 mL). The combined organic layers were dried over $MgSO_4$, filtered, and concentrated under reduced pressure to afford the crude chloride product **5** as a yellow oil.

General Procedure B (acquiring NMR yields of α-chloro boronic esters): General Procedure A was followed to afford the crude chloride product **5**. To this crude chloride was added 1,3,5-trimethoxybenzene (14.0 mg, 0.0832 mmol, 0.333 equiv) as an internal standard. The mixture was taken up in $CDCl_3$ (750 μL) and transferred to an NMR tube. The NMR spectrum was acquired using an appropriately long NMR relaxation delay to achieve quantitative results (typically 12 seconds). The NMR yield was calculated by measuring the integral of an unobscured product proton peak with the 1,3,5-trimethoxybenzene aryl proton peak defined as 1, where % NMR yield = 100*(product peak integral) for products with a single proton measured or 50*(product peak integral) for products with two protons measured. The enantioenrichment of the product was measured by subjecting the crude mixture to GC analysis.

General Procedure C (addition of Grignard reagents to crude chloride products):

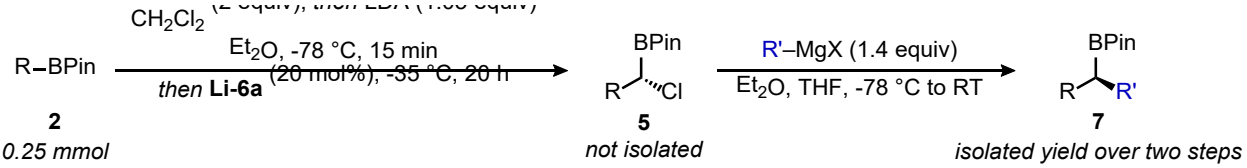

General Procedure A was followed to afford the crude chloride product **5**, which was transferred to an oven-dried 2-dram vial. The vial was equipped with a magnetic stir bar, sealed with a septum cap, and put under a nitrogen atmosphere. The vial was charged with Et_2O (1 mL), then cooled to -78 °C and stirred at this temperature for 5 minutes. A solution of a Grignard reagent (0.35 mmol, 1.4 equiv) was added dropwise over 2 minutes. The reaction mixture was stirred at -78 °C for 5 minutes, then removed from the cold bath and allowed to stir at room temperature for 1 hour. After this time, the heterogeneous reaction mixture was diluted with Et_2O (3 mL) and quenched with saturated aqueous NH_4Cl (500 μL) and water (500 μL) to afford two transparent layers. The organic and aqueous layers were separated, and the aqueous layer was

extracted with Et_2O (2 x 2 mL). The combined organic layers were dried over $MgSO_4$, filtered, and concentrated under reduced pressure to afford the crude secondary boronic ester product **7**. The products were purified by flash column chromatography on C2 silica.

General Procedure D (synthesis of racemic chloride products): An oven-dried 1-dram vial was charged with a pinacol boronic ester substrate **2** (0.25 mmol, 1 equiv) and a magnetic stir bar, sealed with a septum cap, and put under a nitrogen atmosphere (3 vacuum/nitrogen cycles). The vial was charged with Et_2O (1000 μL) and CH_2Cl_2 (32 μL, 0.50 mmol, 2 equiv), cooled to -78 °C, and stirred at this temperature for 5 minutes. A titrated solution of LDA (~ 1.0 M in Et_2O, 0.2625 mmol, 1.05 equiv) (see **General Procedure A**) at room temperature was added dropwise to the center of the reaction mixture (rather than the vial walls) at a rate not exceeding 1 drop per 2 seconds. The reaction mixture was stirred at -78 °C for 15 minutes to form a white or orange suspension of lithium boronate **3**. The cold bath was removed, and the reaction mixture was allowed to stir at room temperature for 1 hour. After this time, the heterogeneous reaction mixture was diluted with Et_2O and quenched with saturated aqueous NH_4Cl (500 μL). The organic and aqueous layers were separated and the aqueous layer was extracted with Et_2O (2 x 2 mL). The combined organic layers were dried over $MgSO_4$, filtered, and concentrated under reduced pressure to afford the crude racemic chloride product **5**. **Note:** low-boiling liquid boronic esters were added to the nitrogen-purged vial by microsyringe.

General Procedure E (addition of Grignard reagents to crude racemic chloride products): **General Procedure D** was followed to afford the crude racemic chloride product **5**, which was transferred to an oven-dried 2-dram vial. The vial was equipped with a magnetic stir bar, sealed with a Teflon-coated septum cap, and put under a nitrogen atmosphere. The vial was charged with Et_2O (1 mL), then cooled to -78 °C and stirred at this temperature for 5 minutes. A solution

of a Grignard reagent (0.275 mmol, 1.1 equiv) was added dropwise over 2 minutes. The reaction mixture was stirred at -78 °C for 5 minutes, then removed from the cold bath and allowed to stir at room temperature for 1 hour. The heterogeneous reaction mixture was diluted with Et_2O (3 mL) and quenched with saturated aqueous NH_4Cl (500 µL) and water (500 µL) to afford two transparent layers. The organic and aqueous layers were separated and the aqueous layer was extracted with Et_2O (2 x 2 mL). The combined organic layers were dried over $MgSO_4$, filtered, and concentrated under reduced pressure to afford the crude racemic secondary boronic ester product **7**.

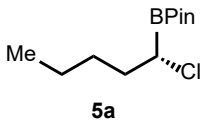

5a

(*S*)-2-(1-chloropentyl)-4,4,5,5-tetramethyl-1,3,2-dioxaborolane (5a): Prepared according to **General Procedure B** using **2a** (46.0 mg, 0.25 mmol, 1 equiv), affording crude **5a** as a yellow oil (77% NMR yield). **^{1}H NMR** (400 MHz, $CDCl_3$) δ 3.40 (dd, *J* = 8.2, 6.6 Hz, 1H, C**H**Cl); **^{11}B NMR** (128 MHz, $CDCl_3$) δ 31.

5a was determined to be of 95% ee by chiral GC analysis (CP-Chirasil-Dex CB, 75 to 100 °C, 1 °C/min, 20 PSI, t_R(minor) = 19.1 min, t_R(major) = 19.7 min).

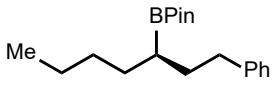

7m

(*R*)-4,4,5,5-tetramethyl-2-(1-phenylheptan-3-yl)-1,3,2-dioxaborolane (7m): Prepared according to **General Procedure C** using **2a** (46.0 mg, 0.25 mmol, 1 equiv) and phenethylmagnesium bromide (350 µL, 1.0 M in THF, 0.35 mmol, 1.4 equiv). Purification by flash column chromatography on C2 silica (0 to 2% Et_2O in hexanes) afforded **7m** as a colorless oil (46.0 mg, 61%). **^{1}H NMR** (400 MHz, $CDCl_3$) δ 7.39 – 7.30 (m, 2H), 7.28 – 7.19 (m, 3H), 2.84 – 2.45 (m, 2H), 1.96 – 1.65 (m, 2H), 1.62 – 1.42 (m, 2H), 1.38 –

1.35 (m, 3H), 1.34 (s, 12H), 1.32 (s, 1H), 1.11 (tt, J = 8.8, 5.9 Hz, 1H), 1.08 – 0.84 (m, 3H); **^{13}C NMR** (101 MHz, $CDCl_3$) δ 143.2, 128.4, 128.2, 125.5, 82.9, 35.7, 33.6, 31.5, 30.9, 24.9, 24.8, 23.0, 14.1 [*the carbon attached to boron was not observed due to quadrupolar relaxation*]; **^{11}B NMR** (128 MHz, $CDCl_3$) δ 30; **HRMS** (ESI) calculated for $C_{19}H_{35}NBO_2$ $[M+NH_4]^+$: 320.2761; found: 320.2755. **7m** was determined to be of 94% ee (100% e.s.) by chiral HPLC analysis of the secondary alcohol obtained by oxidation with sodium perborate (CHIRALPAK OJ-H, 2% *i*PrOH/hexanes, 1.0 mL/min, 210 nm, t_R(minor) = 12.6 min, t_R(major) = 13.6 min).

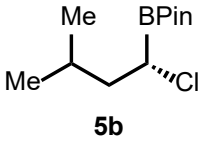

5b

(*S*)-2-(1-chloro-3-methylbutyl)-4,4,5,5-tetramethyl-1,3,2-dioxaborolane (5b): Prepared according to **General Procedure B** using **2b** (46.0 mg, 0.25 mmol, 1 equiv), affording crude **5b** as a yellow oil (81% NMR yield). **^{1}H NMR** (400 MHz, $CDCl_3$) δ 3.47 (dd, *J* = 9.9, 6.0 Hz, 1H, C**H**Cl); **^{11}B NMR** (128 MHz, $CDCl_3$) δ 31.

5b was determined to be of 97% ee by chiral GC analysis (CP-Chirasil-Dex CB, 65 to 80 °C, 0.3 °C/min, 21 PSI, t_R(minor) = 33.4 min, t_R(major) = 33.7 min).

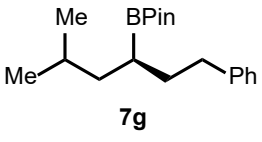

7g

(*S*)-4,4,5,5-tetramethyl-2-(5-methyl-1-phenylhexan-3-yl)-1,3,2-dioxaborolane (7g): Prepared according to **General Procedure C** using **2b** (46.0 mg, 0.25 mmol, 1 equiv) and phenethylmagnesium bromide (350 μL, 1.0 M in THF, 0.35 mmol, 1.4 equiv). Purification by flash column chromatography on C2 silica (0 to 2% Et_2O in hexanes) afforded **7g** as a colorless oil (60.0 mg, 79%). **^{1}H NMR** (400 MHz, $CDCl_3$) δ 7.38 – 7.31 (m, 2H), 7.28 – 7.18 (m, 3H), 2.67 (dt, *J* = 9.9, 6.3 Hz, 2H), 1.84 – 1.67 (m, 2H), 1.65 (ddd,

J = 12.9, 6.5, 2.2 Hz, 1H), 1.55 – 1.40 (m, 1H), 1.34 (s, 12H), 1.28 (dd, *J* = 7.5, 5.9 Hz, 1H), 1.25 – 1.15 (m, 1H), 0.94 (dd, *J* = 6.6, 4.2 Hz, 6H); **^{13}C NMR** (101 MHz, $CDCl_3$) δ 143.2, 128.4, 128.2, 125.6, 82.9, 40.5, 35.7, 33.8, 27.3, 24.9, 24.8, 23.1, 22.6 [*the carbon attached to boron was not observed due to quadrupolar relaxation*]; **^{11}B NMR** (128 MHz, $CDCl_3$) δ 29; **HRMS** (ESI) calculated for $C_{19}H_{32}BO_2$ $[M+H]^+$: 303.2490; found: 303.2497. **7g** was determined to be of 97% ee (100% e.s.) by chiral HPLC analysis of the secondary alcohol obtained by oxidation with sodium perborate (CHIRALPAK OJ-H, 2% *i*PrOH/hexanes, 1.0 mL/min, 210 nm, t_R(minor) = 11.7 min, t_R(major) = 12.4 min).

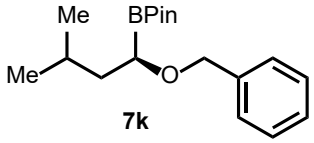

7k

(*R*)-2-(1-(benzyloxy)-3-methylbutyl)-4,4,5,5-tetramethyl-1,3,2-dioxaborolane (7k): Prepared according to **General Procedure C**, with modifications to the second chloride displacement reaction, using **2b** (46.0 mg, 0.25 mmol, 1 equiv) and benzyl alcohol (0.25 mmol, 26 μL, 1 equiv). To a 1-dram vial equipped with a magnetic stir bar and a septum top under a N_2 atmosphere was added benzyl alcohol and DMSO (0.5 mL). The reaction vessel was cooled to 0 °C and then charged with sodium hydride (10 mg, 60% by weight in mineral oil, 0.25 mmol, 1 equiv). The heterogeneous mixture was allowed to stir at room temperature for 30 minutes and was then added to a crude solution of **5b** (generated via **General Procedure A**) in THF (0.25 mL). The resulting reaction mixture was stirred at room temperature overnight. To the reaction mixture was added a saturated solution of ammonium chloride (1 mL), brine (0.5 mL), water (0.5 mL), and Et_2O (4 mL). The organic layer was removed, and the aqueous layer was extracted with Et_2O (3 x 2 mL). The combined organic layers were washed with brine (2 x 1 mL), dried over magnesium sulfate, filtered, and concentrated by rotary evaporation. The crude product was purified by flash column

chromatography on C2 silica (0 to 10% Et_2O in hexanes) to afford **7k** (30.2 mg, 40%). **^{1}H NMR** (400 MHz, $CDCl_3$) δ 7.29 – 7.19 (m, 4H), 7.18 – 7.13 (m, 1H), 4.49 (d, *J* = 11.8 Hz, 1H), 4.35 (d, *J* = 11.8 Hz, 1H), 3.26 (dd, *J* = 9.3, 5.2 Hz, 1H), 1.75 (dp, *J* = 13.2, 6.6 Hz, 1H), 1.58 (ddd, *J* = 14.9, 9.4, 5.7 Hz, 1H), 1.36 – 1.24 (m, 1H), 1.18 (s, 12H), 0.79 (dd, *J* = 20.4, 6.6 Hz, 6H); **^{13}C NMR** (101 MHz, $CDCl_3$) δ 139.2, 128.2, 127.9, 127.3, 83.7, 72.4, 40.4, 25.0, 24.6, 23.4, 22.0 [*the carbon attached to boron was not observed due to quadrupolar relaxation*]; **^{11}B NMR** (128 MHz, $CDCl_3$) δ 33; **HRMS** (ESI) calculated for $C_{18}H_{30}BO_3$ $[M+H]^+$: 305.2283; found: 305.2288. **7k** was determined to be of 97% ee (100% e.s.) by chiral GC analysis (CP-Chirasil-Dex CB, 90 to 110 °C, 0.1 °C/min, 20 PSI, t_R(minor) = 192.1 min, t_R(major) = 195.2 min).

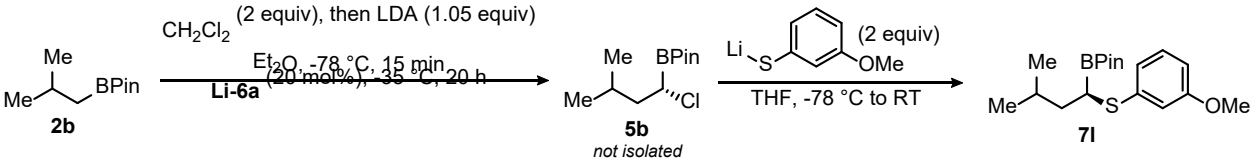

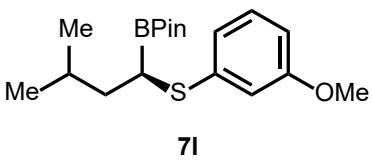

(*R*)-2-(1-((3-methoxyphenyl)thio)-3-methylbutyl)-4,4,5,5-tetramethyl-1,3,2-dioxaborolane (7l):

Crude isobutyl-substituted chloride product **5b** was prepared according to **General Procedure A** using **2b** (46.0 mg, 0.25 mmol). An oven-dried 1-dram vial equipped with a magnetic stir bar, Teflon tape-coated threads, and a Teflon-coated septum cap was put under a nitrogen atmosphere. The vial was charged with 3-methoxythiophenol (62 µL, 0.5 mmol, 2 equiv) and THF (600 µL), and the reaction mixture cooled with stirring to -78 °C. A solution of *n*-butyllithium (200 µL, 2.5 M in hexanes, 0.5 mmol, 2 equiv) was added over the course of 2 minutes, and the reaction mixture was allowed to stir for 5 minutes. The crude isobutyl-

substituted chloride product **5b** was transferred to an oven-dried 2-dram vial. The vial was equipped with a magnetic stir bar; the threads were wrapped with Teflon tape; the vial was sealed with a Teflon-coated septum cap; and the reaction mixture was put under a nitrogen atmosphere. The vial was charged with THF (300 μL), then cooled with stirring to -78 °C. The THF solution of **5b** was rapidly cannulated into the stirring thiophenol solution, and the vial rinsed with additional THF (300 μL). The reaction mixture was allowed to warm to room temperature over the course of 16 hours. The reaction mixture was diluted with Et_2O and quenched with saturated aqueous NH_4Cl (500 μL). The organic and aqueous layers were separated and the aqueous layer was extracted with Et_2O (2 x 2 mL). The combined organic layers were dried over $MgSO_4$, filtered, concentrated under reduced pressure, and purified by flash column chromatography on C2 silica (0 to 3% Et_2O in hexanes) to afford **7l** as a colorless oil (51.1 mg, 61%). **^{1}H NMR** (400 MHz, $CDCl_3$) δ 7.15 (t, *J* = 7.9 Hz, 1H), 6.96 (d, *J* = 9.6 Hz, 2H), 6.68 (d, *J* = 8.3 Hz, 1H), 3.78 (s, 3H), 2.80 (t, *J* = 8.0 Hz, 1H), 1.82 – 1.62 (m, 2H), 1.62 – 1.50 (m, 1H), 1.19 (s, 12H), 0.91 (t, *J* = 4.8 Hz, 6H); **^{13}C NMR** (101 MHz, $CDCl_3$) δ 159.8, 138.4, 129.5, 121.9, 114.7, 112.1, 84.0, 55.3, 40.3, 27.6, 24.76, 24.72, 22.9, 22.4 [*the carbon attached to boron was not observed due to quadrupolar relaxation*]; **^{11}B NMR** (128 MHz, $CDCl_3$) δ 32; **HRMS** (ESI) calculated for $C_{18}H_{30}BO_3S$ $[M+H]^+$: 337.2003; found: 337.2012. **7l** was determined to be of 95% ee (98% e.s.) by chiral SFC analysis (CHIRALPAK IF, 3% MeOH/CO_2, 5.0 mL/min, 222 nm, t_R(minor) = 2.0 min, t_R(major) = 1.8 min).

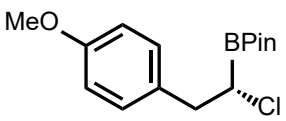

5c

(*S*)-2-(1-chloro-2-(4-methoxyphenyl)ethyl)-4,4,5,5-tetramethyl-1,3,2-dioxaborolane (5c): Prepared according to **General Procedure B** using **2c** (62.0 mg, 0.25 mmol, 1 equiv), affording crude **5c** as a yellow oil (73%

NMR yield). **^{1}H NMR** (400 MHz, $CDCl_3$) δ 3.55 (t, *J* = 8.1 Hz, 1H, C**H**Cl); **^{11}B NMR** (128 MHz, $CDCl_3$) δ 31.

5c was determined to be of 96% ee by chiral GC analysis (CP-Chirasil-Dex CB, 100 to 145 °C, 0.33 °C/min, 20 PSI, t_R(minor) = 104.5 min, t_R(major) = 106.1 min).

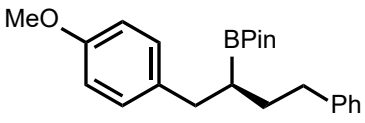

7n

(*S*)-2-(1-(4-methoxyphenyl)-4-phenylbutan-2-yl)-4,4,5,5-tetramethyl-1,3,2-dioxaborolane (7n): Prepared according to **General Procedure C** using **2c** (62.0 mg, 0.25 mmol, 1 equiv) and phenethylmagnesium bromide (350 µL, 1.0 M in THF, 0.35 mmol, 1.4 equiv). Purification by flash column chromatography on C2 silica (0 to 3% Et_2O in hexanes) afforded **7n** as a colorless oil (57.0 mg, 62%). **^{1}H NMR** (400 MHz, $CDCl_3$) δ 7.39 – 7.30 (m, 2H), 7.30 – 7.16 (m, 5H), 6.88 (d, *J* = 8.8 Hz, 2H), 3.86 (s, 3H), 2.87 – 2.59 (m, 4H), 1.92 – 1.71 (m, 2H), 1.56 – 1.44 (m, 1H), 1.28 (s, 6H), 1.26 (s, 6H); **^{13}C NMR** (101 MHz, $CDCl_3$) δ 157.8, 143.0, 134.3, 129.9, 128.5, 128.4, 125.7, 113.6, 83.2, 55.4, 36.4, 35.7, 33.2, 25.0, 24.9 [*the carbon attached to boron was not observed due to quadrupolar relaxation*]; **^{11}B NMR** (128 MHz, $CDCl_3$) δ 35; **HRMS** (ESI) calculated for $C_{23}H_{35}NBO_3$ $[M+NH_4]^+$: 384.2705; found: 384.2709. **7n** was determined to be of 96% ee (100% e.s.) by chiral SFC analysis of the secondary alcohol obtained by oxidation with sodium perborate (CHIRALPAK IH, 5% MeOH/CO_2, 5.0 mL/min, 210 nm, t_R(minor) = 5.4 min, t_R(major) = 6.0 min).

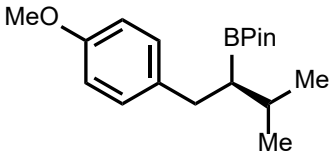

7f

(*R*)-2-(1-(4-methoxyphenyl)-3-methylbutan-2-yl)-4,4,5,5-tetramethyl-1,3,2-dioxaborolane (7f): Prepared according to **General Procedure C** on 2x scale using **2c** (124.1 mg, 0.5 mmol, 1

equiv) and isopropylmagnesium bromide (700 µL, 1.0 M in THF, 0.70 mmol, 1.4 equiv). Purification by flash column chromatography on C2 silica (0 to 3% Et_2O in hexanes) afforded **7f** as a colorless oil (78.5 mg, 52%). **^{1}H NMR** (400 MHz, $CDCl_3$) δ 7.17 – 7.08 (m, 2H), 6.83 – 6.73 (m, 2H), 3.77 (s, 3H), 2.70 (dd, *J* = 13.5, 6.5 Hz, 1H), 2.60 (dd, *J* = 13.6, 10.6 Hz, 1H), 1.82 – 1.66 (m, *J* = 6.6 Hz, 1H), 1.24 (dt, *J* = 10.5, 6.4 Hz, 1H), 1.13 (s, 6H), 1.08 (s, 6H), 0.98 (t, *J* = 6.9 Hz, 6H); **^{13}C NMR** (101 MHz, $CDCl_3$) δ 157.7, 134.9, 129.9, 113.6, 83.0, 55.4, 34.6, 29.8, 25.0, 24.9, 22.8, 21.6 [*the carbon attached to boron was not observed due to quadrupolar relaxation*]; **^{11}B NMR** (128 MHz, $CDCl_3$) δ 35; **HRMS** (ESI) calculated for $C_{18}H_{30}BO_3$ $[M+H]^+$: 305.2283; found: 305.2289. **7f** was determined to be of 96% ee (100% e.s.) by chiral HPLC analysis of derivatives **8b** and **8d** (see section **Scope of C–B Elaborations**).

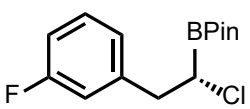

5d

(*S*)-2-(1-chloro-2-(3-fluorophenyl)ethyl)-4,4,5,5-tetramethyl-1,3,2-dioxaborolane (5d): Prepared according to **General Procedure B** using **2d** (59.0 mg, 0.25 mmol, 1 equiv), affording crude **5d** as a yellow oil (80% NMR yield). **^{1}H NMR** (400 MHz, $CDCl_3$) δ 3.57 (t, *J* = 8.1 Hz, 1H, C**H**Cl); **^{11}B NMR** (128 MHz, $CDCl_3$) δ 31; **^{19}F NMR** (376 MHz, $CDCl_3$) δ -62.83.

5d was determined to be of 97% ee by chiral GC analysis (CP-Chirasil-Dex CB, 70 to 140 °C, 1.0 °C/min, 14 PSI, t_R(minor) = 63.7 min, t_R(major) = 64.2 min).

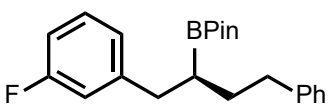

7a

(*S*)-2-(1-(3-fluorophenyl)-4-phenylbutan-2-yl)-4,4,5,5-tetramethyl-1,3,2-dioxaborolane (7a): Prepared according to **General Procedure C** using **2d** (59.0 mg, 0.25 mmol, 1 equiv) and phenethylmagnesium bromide (350 µL, 1.0 M in THF, 0.35 mmol, 1.4 equiv). Purification by flash

column chromatography on C2 silica (0 to 2% Et_2O in hexanes) afforded **7a** as a colorless oil (73.5 mg, 83%). **^{1}H NMR** (400 MHz, $CDCl_3$) δ 7.40 – 7.20 (m, 6H), 7.05 (d, *J* = 7.8 Hz, 1H), 7.00 (dt, *J* = 10.1, 2.1 Hz, 1H), 6.93 (td, *J* = 7.9, 1.8 Hz, 1H), 2.90 – 2.61 (m, 4H), 1.93 – 1.72 (m, 2H), 1.57 – 1.45 (m, 1H), 1.29 (s, 6H), 1.26 (s, 6H); **^{13}C NMR** (101 MHz, $CDCl_3$) δ 162.9 (d, *J* = 244.9 Hz), 144.9 (d, *J* = 7.3 Hz), 142.8, 129.6 (d, *J* = 8.4 Hz), 128.5, 128.4, 125.8, 124.6 (d, *J* = 2.5 Hz), 115.8 (d, *J* = 20.7 Hz), 112.6 (d, *J* = 21.1 Hz), 83.3, 37.1 (d, *J* = 1.8 Hz), 35.6, 33.3, 25.0, 24.9 [*the carbon attached to boron was not observed due to quadrupolar relaxation*]; **^{11}B NMR** (128 MHz, $CDCl_3$) δ 34; **^{19}F NMR** (376 MHz, $CDCl_3$) δ -114.29; **HRMS** (ESI) calculated for $C_{22}H_{29}BFO_2$ $[M+H]^+$: 355.2239; found: 355.2244. **7a** was determined to be of 98% ee (101% e.s.) by chiral SFC analysis of the secondary alcohol obtained by oxidation with sodium perborate (CHIRALPAK IA, 5% MeOH/CO_2, 5.0 mL/min, 210 nm, t_R(minor) = 4.4 min, t_R(major) = 5.5 min).

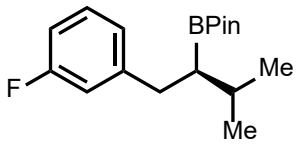

7b

(*R*)-2-(1-(3-fluorophenyl)-3-methylbutan-2-yl)-4,4,5,5-tetramethyl-1,3,2-dioxaborolane (7b): Prepared according to **General Procedure C** using **2d** (59.0 mg, 0.25 mmol, 1 equiv) and isopropylmagnesium bromide (350 μL, 1.0 M in THF, 0.35 mmol, 1.4 equiv). Purification by flash column chromatography on C2 silica (0 to 2% Et_2O in hexanes) afforded **7b** as a colorless oil (39.2 mg, 54%). **^{1}H NMR** (400 MHz, $CDCl_3$) δ 7.18 (td, *J* = 7.9, 6.1 Hz, 1H), 6.98 (d, *J* = 7.9 Hz, 1H), 6.93 (dt, *J* = 10.3, 2.2 Hz, 1H), 6.82 (td, *J* = 7.8, 1.8 Hz, 1H), 2.74 (dd, *J* = 13.5, 6.3 Hz, 1H), 2.66 (dd, *J* = 13.5, 10.6 Hz, 1H), 1.83 – 1.69 (m, *J* = 6.7 Hz, 1H), 1.30 – 1.20 (m, 1H), 1.13 (s, 6H), 1.10 (s, 6H), 0.99 (t, *J* = 6.9 Hz, 6H); **^{13}C NMR** (101 MHz, $CDCl_3$) δ 162.9 (d, *J* = 244.5 Hz), 145.6 (d, *J* = 7.3 Hz), 129.5 (d, *J* = 8.4 Hz), 124.7 (d, *J* = 2.5 Hz), 115.9 (d, *J* = 20.7 Hz), 112.4 (d, *J* = 21.1

Hz), 83.1, 35.3 (d, J = 1.8 Hz), 30.0, 25.0, 24.9, 22.7, 21.6 [*the carbon attached to boron was not observed due to quadrupolar relaxation*]; **^{11}B NMR** (128 MHz, $CDCl_3$) δ 34; **^{19}F NMR** (376 MHz, $CDCl_3$) δ -114.55; **HRMS** (ESI) calculated for $C_{17}H_{27}BFO_2$ $[M+H]^+$: 293.2083; found: 293.2087. **7b** was determined to be of 98% ee (102% e.s.) by chiral SFC analysis of the secondary alcohol obtained by oxidation with sodium perborate (CHIRALPAK ID, 1% MeOH/CO_2, 5.0 mL/min, 210 nm, t_R(minor) = 5.0 min, t_R(major) = 5.9 min).

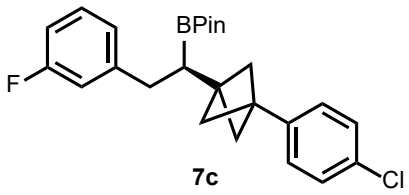

7c

(*R*)-2-(1-(3-(4-chlorophenyl)bicyclo[1.1.1]pentan-1-yl)-2-(3-fluorophenyl)ethyl)-4,4,5,5-tetramethyl-1,3,2-dioxaborolane (7c):

Preparation of (3-(4-chlorophenyl)bicyclo[1.1.1]pentan-1-yl)magnesium bromide: Prepared according to the following method, adapted from a literature procedure reported by Aggarwal and coworkers (*9*). A 50 mL pressure tube fitted with a J Young stopcock and equipped with a magnetic stir bar was put under an atmosphere of N_2. The stopcock was removed, and the tube was sequentially charged with [1.1.1]propellane (409 µL, 0.61 M solution in Et_2O, 0.25 mmol, 1 equiv) and 4-chlorophenylmagnesium bromide (250 µL, 1.0 M solution in Et_2O, 0.25 mmol, 1 equiv) while under strong positive N_2 pressure. The tube was tightly sealed with the stopcock and then placed in an oil bath at room temperature behind a blast shield. The reaction mixture was heated to 100 °C with stirring for 1 hour before being allowed to cool to room temperature. The solvent was then removed using high vacuum (taking care to not expose the reaction mixture to the atmosphere), after which a solution of anhydrous lithium chloride (10.6 mg, 0.25 mmol, 1 equiv, stored in a N_2-filled glovebox) in THF (1.5 mL) was added against a strong current of

positive N_2 pressure. The reaction mixture was then stirred for 20 minutes to afford a solution of (3-(4-chlorophenyl)bicyclo[1.1.1]pentan-1-yl)magnesium bromide in THF.

*Synthesis of **7c**:* Prepared according to **General Procedure C** using **2d** (59.0 mg, 0.25 mmol, 1 equiv) and the (3-(4-chlorophenyl)bicyclo[1.1.1]pentan-1-yl)magnesium bromide solution in THF (0.25 mmol, 1 equiv) described above, affording crude **7c** as a yellow oil (56% NMR yield relative to 1,3,5-trimethoxybenzene). **^{1}H NMR (aliphatic region only)** (400 MHz, $CDCl_3$) δ 2.79 – 2.73 (m, 2H), 2.00 – 1.93 (m, 6H), 1.73 – 1.66 (m, 1H), 1.19 (d, J = 6.9 Hz, 12H). This molecule was isolated and fully characterized as the alcohol as described immediately below due to difficulties in chromatographic purification of the boronic ester.

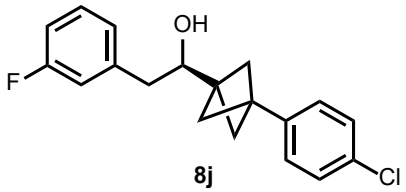

8j

(*R*)-1-(3-(4-chlorophenyl)bicyclo[1.1.1]pentan-1-yl)-2-(3-fluorophenyl)ethan-1-ol (8j): A 2-dram vial equipped with a magnetic stir bar was sequentially charged with crude **7c** (see directly above), THF (2 mL), water (2 mL), and sodium perborate tetrahydrate (192.3 mg, 1.25 mmol, 5 equiv relative to **2d**). The vial was then capped, and the reaction mixture was vigorously stirred overnight. After this time, the reaction mixture was diluted with Et_2O (2 mL) and water (1 mL), the organic layer separated, and the aqueous layer extracted with Et_2O (2 x 2 mL). The combined organic phases were dried over $MgSO_4$, filtered, and concentrated by rotary evaporation. Purification of the reaction mixture by flash column chromatography on normal silica (0 to 10% Et_2O in hexanes) afforded **8j** as a white solid (31.0 mg, 39% isolated yield over three steps). **^{1}H NMR** (400 MHz, $CDCl_3$) δ 7.31 – 7.23 (m, 3H), 7.17 – 7.12 (m, 2H), 7.05 – 6.89 (m, 3H), 3.94 (dt, J = 9.7, 3.1

Hz, 1H), 2.85 (dd, J = 13.9, 3.7 Hz, 1H), 2.63 (dd, J = 14.0, 9.6 Hz, 1H), 2.05 – 1.89 (m, 6H); **^{13}C NMR** (101 MHz, $CDCl_3$) δ 163.0 (d, J = 246.0 Hz), 141.2 (d, J = 7.3 Hz), 139.2, 132.4, 130.0 (d, J = 8.4 Hz), 128.3, 127.5, 124.9 (d, J = 2.7 Hz), 116.1 (d, J = 20.9 Hz), 113.4 (d, J = 20.9 Hz), 71.2, 50.1, 41.7, 40.9, 40.3 (d, J = 1.8 Hz); **^{19}F NMR** (376 MHz, $CDCl_3$) δ -113.33 (td, J = 9.3, 6.2 Hz). **HRMS** (ESI) calculated for $C_{19}H_{19}ClFO$ $[M+HCOO]^-$: 361.1012; found: 361.1013. **8j** was determined to be of 96% ee (99% e.s.) by chiral HPLC analysis (CHIRALPAK OD-H, 3% *i*PrOH/hexanes, 1.0 mL/min, 210 nm, t_R(minor) = 25.9 min, t_R(major) = 14.0 min).

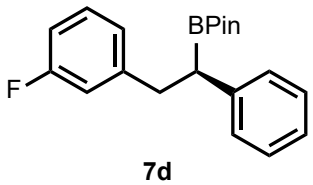

7d

(*R*)-2-(2-(3-fluorophenyl)-1-phenylethyl)-4,4,5,5-tetramethyl-1,3,2-dioxaborolane (7d): Prepared according to **General Procedure C** using **2d** (59.0 mg, 0.25 mmol, 1 equiv) and phenylmagnesium bromide (350 μL, 1.0 M in THF, 0.35 mmol, 1.4 equiv). Purification by flash column chromatography on C2 silica (0 to 2% Et_2O in hexanes) afforded **7d** as a colorless oil (39.5 mg, 48%). **^{1}H NMR** (400 MHz, $CDCl_3$) δ 7.32 – 7.23 (m, 4H), 7.23 – 7.13 (m, 2H), 6.97 (d, J = 7.6 Hz, 1H), 6.93 (dt, J = 10.1, 2.1 Hz, 1H), 6.85 (td, J = 8.3, 2.6 Hz, 1H), 3.17 (dd, J = 13.6, 9.7 Hz, 1H), 2.97 (dd, J = 13.5, 6.9 Hz, 1H), 2.67 (dd, J = 9.8, 6.9 Hz, 1H), 1.15 (s, 12H); **^{13}C NMR** (101 MHz, $CDCl_3$) δ 162.8 (d, J = 244.9 Hz), 144.5 (d, J = 7.3 Hz), 142.3, 129.5 (d, J = 8.4 Hz), 128.54, 128.48, 125.7, 124.7 (d, J = 2.5 Hz), 115.9 (d, J = 20.7 Hz), 112.7 (d, J = 21.1 Hz), 83.6, 38.7, 24.70, 24.65 [*the carbon attached to boron was not observed due to quadrupolar relaxation*]; **^{11}B NMR** (128 MHz, $CDCl_3$) δ 33; **^{19}F NMR** (376 MHz, $CDCl_3$) δ -114.30; **HRMS** (ESI) calculated for $C_{20}H_{25}BFO_2$ $[M+H]^+$: 327.1926; found: 327.1933. **7d** was determined to be of 97% ee (100% e.s.) by chiral SFC analysis of the secondary alcohol obtained by oxidation with sodium perborate (CHIRALPAK IB N-5, 5% MeOH/CO_2, 5.0 mL/min, 210 nm, t_R(minor) = 4.7 min, t_R(major) = 4.2 min).

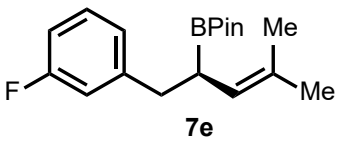

7e

(*R*)-2-(1-(3-fluorophenyl)-4-methylpent-3-en-2-yl)-4,4,5,5-tetramethyl-1,3,2-dioxaborolane (7e): Prepared according to **General Procedure C** using **2d** (59.0 mg, 0.25 mmol, 1 equiv) and 2-methyl-1-propenylmagnesium bromide (700 µL, 0.5 M in THF, 0.35 mmol, 1.4 equiv). Purification by flash column chromatography on normal silica (0 to 100% CH_2Cl_2 in hexanes) afforded **7e** as a colorless oil (46.0 mg, 60%). **^{1}H NMR** (400 MHz, $CDCl_3$) δ 7.18 (td, *J* = 7.9, 6.1 Hz, 1H), 6.96 (dt, *J* = 7.7, 1.3 Hz, 1H), 6.91 (dt, *J* = 10.3, 2.1 Hz, 1H), 6.87 – 6.78 (m, 1H), 5.07 (dt, *J* = 9.6, 1.5 Hz, 1H), 2.81 (dd, *J* = 13.6, 8.4 Hz, 1H), 2.65 (dd, *J* = 13.6, 7.8 Hz, 1H), 2.28 (q, *J* = 8.5 Hz, 1H), 1.67 (d, *J* = 1.4 Hz, 3H), 1.51 (d, *J* = 1.3 Hz, 3H), 1.16 (d, *J* = 1.9 Hz, 12H); **^{13}C NMR** (101 MHz, $CDCl_3$) δ 162.7 (d, *J* = 244.5 Hz), 144.8 (d, *J* = 7.2 Hz), 132.0, 129.3 (d, *J* = 8.3 Hz), 124.5 (d, *J* = 2.7 Hz), 123.9, 115.7 (d, *J* = 20.7 Hz), 112.4 (d, *J* = 21.1 Hz), 83.1, 37.3 (d, *J* = 1.6 Hz), 25.8, 24.7, 24.5, 18.1 [*the carbon attached to boron was not observed due to quadrupolar relaxation*]; **^{19}F NMR** (376 MHz, $CDCl_3$) δ -114.55 (td, *J* = 9.3, 6.0 Hz); **HRMS** (ESI) calculated for $C_{18}H_{27}BFO_2$ $[M+H]^+$: 305.2083; found: 305.2087. **7e** was determined to be of 98% ee (101% e.s.) by chiral HPLC analysis of the secondary alcohol obtained by oxidation with sodium perborate (CHIRALPAK OD-H, 2% *i*PrOH/hexanes, 1.0 mL/min, 210 nm, t_R(minor) = 13.1 min, t_R(major) = 16.0 min).

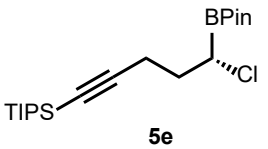

5e

(*S*)-(5-chloro-5-(4,4,5,5-tetramethyl-1,3,2-dioxaborolan-2-yl)pent-1-yn-1-yl)triisopropylsilane (5e): Prepared according to **General Procedure B** using **2e** (84.1 mg, 0.25 mmol, 1 equiv), affording crude **5e** as a yellow oil (88%

NMR yield). **^{1}H NMR** (400 MHz, $CDCl_3$) δ 3.60 (dd, *J* = 9.5, 5.4 Hz, 1H, C**H**Cl); **^{11}B NMR** (128 MHz, $CDCl_3$) δ 32.

5e was determined to be of 98% ee by chiral GC analysis (CP-Chirasil-Dex CB, 100 to 160 °C, 0.33 °C/min, 20 PSI, t_R(minor) = 143.6 min, t_R(major) = 144.9 min).

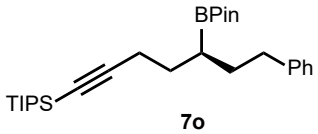

7o

(*R*)-triisopropyl(7-phenyl-5-(4,4,5,5-tetramethyl-1,3,2-dioxaborolan-2-yl)hept-1-yn-1-yl)silane (7o): Prepared according to **General Procedure C** using **2e** (84.1 mg, 0.25 mmol, 1 equiv) and phenethylmagnesium bromide (350 µL, 1.0 M in THF, 0.35 mmol, 1.4 equiv). Purification by flash column chromatography on C2 silica (0 to 2% Et_2O in hexanes) afforded **7o** as a colorless oil (81.8 mg, 72%). **^{1}H NMR** (400 MHz, $CDCl_3$) δ 7.38 – 7.29 (m, 2H), 7.29 – 7.19 (m, 3H), 2.68 (qdd, *J* = 13.5, 10.2, 6.3 Hz, 2H), 2.46 – 2.25 (m, 2H), 1.92 – 1.61 (m, 4H), 1.33 (s, 12H), 1.20 – 1.08 (m, 21H), 1.08 – 1.03 (m, 1H); **^{13}C NMR** (101 MHz, $CDCl_3$) δ 143.0, 128.4, 128.3, 125.6, 83.1, 80.0, 35.5, 33.1, 30.4, 24.9, 24.8, 19.5, 18.7, 11.3 [*the carbon attached to boron was not observed due to quadrupolar relaxation*]; **^{11}B NMR** (128 MHz, $CDCl_3$) δ 34; **HRMS** (ESI) calculated for $C_{28}H_{48}BO_2Si$ $[M+H]^+$: 455.3515; found: 455.3511. **7o** was determined to be of 98% ee (101% e.s.) by chiral HPLC analysis of the secondary alcohol obtained by oxidation with sodium perborate (CHIRALPAK AD-H, 1% *i*PrOH/hexanes, 1.0 mL/min, 210 nm, t_R(minor) = 23.1 min, t_R(major) = 26.3 min).

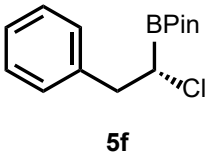

5f

(*S*)-2-(1-chloro-2-phenylethyl)-4,4,5,5-tetramethyl-1,3,2-dioxaborolane (5f): Prepared according to **General Procedure B** using **2f** (54.5 mg, 0.25 mmol, 1 equiv), affording crude **5f** as a yellow oil (80% NMR yield). **^{1}H NMR** (400 MHz, $CDCl_3$) δ 3.59 (t, *J* = 8.2 Hz, 1H, C**H**Cl); **^{11}B NMR** (128 MHz, $CDCl_3$) δ 31.

5f was determined to be of 98% ee by chiral GC analysis (CP-Chirasil-Dex CB, 90 to 125 °C, 0.33 °C/min, 14 PSI, t_R(minor) = 92.1 min, t_R(major) = 93.6 min).

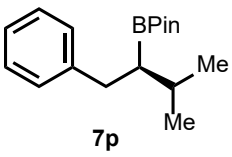

7p

(*R*)-4,4,5,5-tetramethyl-2-(3-methyl-1-phenylbutan-2-yl)-1,3,2-dioxaborolane (7p): Prepared according to **General Procedure C** on reduced scale using **2f** (54.5 mg, 0.2 mmol, 1 equiv) and isopropylmagnesium bromide (280 µL, 1.0 M in THF, 0.28 mmol, 1.4 equiv). Purification by flash column chromatography on C2 silica (0 to 2% Et_2O in hexanes) afforded **7p** as a colorless oil (31.0 mg, 57%). **^{1}H NMR** (400 MHz, $CDCl_3$) δ 7.32 – 7.22 (m, 4H), 7.21 – 7.14 (m, 1H), 2.81 (dd, J = 13.5, 6.4 Hz, 1H), 2.70 (dd, J = 13.5, 10.6 Hz, 1H), 1.80 (dq, J = 13.4, 6.7 Hz, 1H), 1.33 (dt, J = 10.8, 6.4 Hz, 1H), 1.14 (d, J = 18.8 Hz, 12H), 1.04 (t, J = 6.6 Hz, 6H); **^{13}C NMR** (101 MHz, $CDCl_3$) δ 142.7, 128.9, 128.0, 125.5, 82.9, 35.4, 29.8, 24.9, 24.8, 22.6, 21.5 [*the carbon attached to boron was not observed due to quadrupolar relaxation*]; **^{11}B NMR** (128 MHz, $CDCl_3$) δ 34; **HRMS** (ESI) calculated for $C_{17}H_{31}NBO_2$ $[M+NH_4]^+$: 292.2448; found: 292.2442. **7p** was determined to be of 98% ee (100% e.s.) by chiral HPLC analysis of the secondary alcohol obtained by oxidation with sodium perborate (CHIRALPAK OJ-H, 2% *i*PrOH/hexanes, 1.0 mL/min, 210 nm, t_R(minor) = 14.1 min, t_R(major) = 13.0 min).

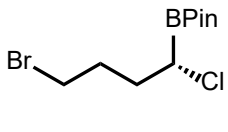

5g

(*S*)-2-(4-bromo-1-chlorobutyl)-4,4,5,5-tetramethyl-1,3,2-dioxaborolane (5g): Prepared according to **General Procedure B** using **2g** (62.2 mg, 0.25 mmol, 1 equiv), affording crude **5g** as a yellow oil (75% NMR yield). **^{1}H NMR** (400 MHz, $CDCl_3$) δ 3.45 – 3.38 (m, 3H, C**H**Cl+C**H$_2$**Br); **^{11}B NMR** (128 MHz, $CDCl_3$) δ 31.

5g was determined to be of 97% ee by chiral GC analysis (CP-Chirasil-Dex CB, 70 to 103 °C, 0.3 °C/min, 21 PSI, t_R(minor) = 100.4 min, t_R(major) = 102.3 min).

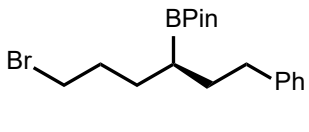

7q

(*S*)-2-(6-bromo-1-phenylhexan-3-yl)-4,4,5,5-tetramethyl-1,3,2-dioxaborolane (7q): Prepared according to **General Procedure C** using **2g** (62.2 mg, 0.25 mmol, 1 equiv) and phenethylmagnesium bromide (350 μL, 1.0 M in THF, 0.35 mmol, 1.4 equiv). Purification by flash column chromatography on C2 silica (0 to 2% Et_2O in hexanes) afforded **7q** as a colorless oil (40.3 mg, 44%). **^{1}H NMR** (400 MHz, $CDCl_3$) δ 7.38 – 7.18 (m, 5H), 3.46 (t, *J* = 6.9 Hz, 2H), 2.77 – 2.59 (m, 2H), 2.02 – 1.56 (m, 6H), 1.34 (s, 12H), 1.19 – 1.08 (m, 1H); **^{13}C NMR** (101 MHz, $CDCl_3$) δ 142.9, 128.5, 128.4, 125.8, 83.3, 35.6, 34.2, 33.4, 32.5, 29.8, 25.00, 24.98 [*the carbon attached to boron was not observed due to quadrupolar relaxation*]; **^{11}B NMR** (128 MHz, $CDCl_3$) δ 36; **HRMS** (ESI) calculated for $C_{18}H_{29}BBrO_2$ $[M+H]^+$: 367.1438; found: 367.1443. **7q** was determined to be of 97% ee (100% e.s.) by chiral SFC analysis of the secondary alcohol obtained by oxidation with sodium perborate (CHIRALPAK IE, 5% MeOH/CO_2, 5.0 mL/min, 210 nm, t_R(minor) = 4.7 min, t_R(major) = 5.2 min).

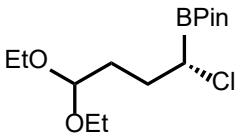

5h

(*S*)-2-(1-chloro-4,4-diethoxybutyl)-4,4,5,5-tetramethyl-1,3,2-dioxaborolane (5h): Prepared according to **General Procedure B** using **2h** (64.5 mg, 0.25 mmol, 1 equiv) with the following modification: the lithium boronate **3** was prepared using a solvent blend of Et_2O (100 μL) and CH_2Cl_2 (300 μL), rather than the previously described blend of Et_2O (400 μL) and CH_2Cl_2 (32 μL). Crude **5h** was obtained as a yellow oil (81% NMR yield). **^{1}H NMR** (400 MHz, $CDCl_3$) δ 4.48 (t, *J* = 5.4 Hz, 1H, C**H**$(OEt)_2$); **^{11}B NMR** (128 MHz, $CDCl_3$) δ 31.

5h was determined to be of 94% ee by chiral GC analysis (CP-Chirasil-Dex CB, 120 to 140 °C, 1.0 °C/min, 21 PSI, t_R(minor) = 15.0 min, t_R(major) = 15.3 min).

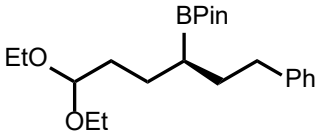

7r

(*S*)-2-(6,6-diethoxy-1-phenylhexan-3-yl)-4,4,5,5-tetramethyl-1,3,2-dioxaborolane (7r): Prepared according to **General Procedure C** using **2h** (64.5 mg, 0.25 mmol, 1 equiv) and phenethylmagnesium bromide (350 μL, 1.0 M in THF, 0.35 mmol, 1.4 equiv) with the following modification: the lithium boronate **3** was prepared using a solvent blend of Et_2O (100 μL) and CH_2Cl_2 (300 μL), rather than the previously described blend of Et_2O (400 μL) and CH_2Cl_2 (32 μL). Purification by flash column chromatography on C2 silica (0 to 3% Et_2O in hexanes) afforded **7r** as a colorless oil (70.1 mg, 75%). **^{1}H NMR** (400 MHz, $CDCl_3$) δ 7.38 – 7.19 (m, 5H), 4.54 (t, *J* = 5.6 Hz, 1H), 3.77 – 3.64 (m, 2H), 3.62 – 3.49 (m, 2H), 2.78 – 2.59 (m, 2H), 1.89 – 1.46 (m, 6H), 1.34 (s, 12H), 1.27 (t, *J* = 7.1 Hz, 6H), 1.16 – 1.07 (m, 1H); **^{13}C NMR** (101 MHz, $CDCl_3$) δ 143.1, 128.5, 128.3, 125.7, 103.2, 83.1, 61.0, 60.6, 35.7, 33.5, 33.1, 26.2, 25.0, 15.5 [*the carbon attached to boron was not observed due to quadrupolar relaxation*]; **^{11}B NMR** (128 MHz, $CDCl_3$) δ 34; **HRMS** (ESI)

calculated for $C_{22}H_{38}BO_4$ $[M+H]^+$: 377.2858; found: 377.2861. **7r** was determined to be of 94% ee (100% e.s.) by chiral SFC analysis of the secondary alcohol obtained by oxidation with sodium perborate (CHIRALPAK IB N-5, 5% MeOH/CO_2, 5.0 mL/min, 210 nm, t_R(minor) = 4.0 min, t_R(major) = 3.4 min).

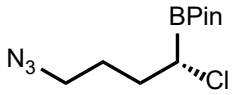

5i

(*S*)-2-(4-azido-1-chlorobutyl)-4,4,5,5-tetramethyl-1,3,2-dioxaborolane (5i): Prepared according to **General Procedure B** using **2i** (52.8 mg, 0.25 mmol, 1 equiv), affording crude **5i** as a yellow oil (52% NMR yield); **^{1}H NMR** (400 MHz, $CDCl_3$) δ 3.42 (dd, *J* = 8.5, 5.7 Hz, 1H, C**H**Cl); **^{11}B NMR** (128 MHz, $CDCl_3$) δ 31.

5i was determined to be of 98% ee by chiral GC analysis (CP-Chirasil-Dex CB, 90 to 125 °C, 0.33 °C/min, 14 PSI, t_R(minor) = 72.8 min, t_R(major) = 74.2 min).

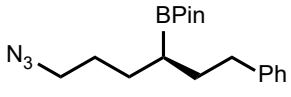

7s

(*S*)-2-(6-azido-1-phenylhexan-3-yl)-4,4,5,5-tetramethyl-1,3,2-dioxaborolane (7s): Prepared according to **General Procedure C** using **2i** (52.8 mg, 0.25 mmol, 1 equiv) and phenethylmagnesium bromide (350 µL, 1.0 M in THF, 0.35 mmol, 1.4 equiv). Purification by flash column chromatography on C2 silica (0 to 2% Et_2O in hexanes) afforded **7s** as a colorless oil (40.0 mg, 49%). **^{1}H NMR** (400 MHz, $CDCl_3$) δ 7.39 – 7.31 (m, 2H), 7.25 (d, *J* = 7.5 Hz, 3H), 3.31 (dt, *J* = 6.9, 3.2 Hz, 2H), 2.67 (tp, *J* = 13.5, 7.1, 6.4 Hz, 2H), 1.95 – 1.78 (m, 1H), 1.69 (dddd, *J* = 21.4, 8.7, 6.6, 4.6 Hz, 3H), 1.63 – 1.46 (m, 2H), 1.34 (s, 12H), 1.21 – 1.08 (m, 1H); **^{13}C NMR** (101 MHz, $CDCl_3$) δ 142.8, 128.4, 128.3, 125.7, 83.2, 51.7, 35.5, 33.4, 28.4, 28.2, 24.9 [*the carbon attached to boron was not observed due to*

quadrupolar relaxation]; **^{11}B NMR** (128 MHz, $CDCl_3$) δ 34; **HRMS** (ESI) calculated for $C_{18}H_{32}BN_4O_2$ $[M+NH_4]^+$: 347.2617; found: 347.2613. **7s** was determined to be of 98% ee (100% e.s.) by chiral HPLC analysis of the secondary alcohol obtained by oxidation with sodium perborate (CHIRALPAK OB-H, 4% *i*PrOH/hexanes, 1.0 mL/min, 210 nm, t_R(minor) = 17.4 min, t_R(major) = 20.7 min).

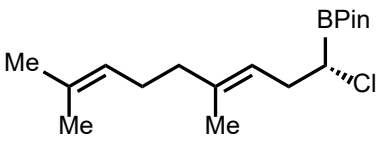

5j

(*S*,*E*)-2-(1-chloro-4,8-dimethylnona-3,7-dien-1-yl)-4,4,5,5-tetramethyl-1,3,2-dioxaborolane (5j): Prepared according to **General Procedure B** using **2j** (66.1 mg, 0.25 mmol, 1 equiv), affording crude **5j** as a yellow oil (75% NMR yield). **^{1}H NMR** (400 MHz, $CDCl_3$) δ 3.36 (t, *J* = 7.8 Hz, 1H, C**H**Cl); **^{11}B NMR** (128 MHz, $CDCl_3$) δ 31.

5j was determined to be of 94% ee by chiral GC analysis (CP-Chirasil-Dex CB, 120 to 160 °C, 0.8 °C/min, 21 PSI, t_R(minor) = 30.3 min, t_R(major) = 30.7 min).

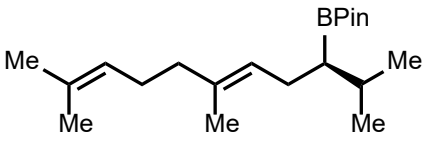

7t

(*R*,*E*)-4,4,5,5-tetramethyl-2-(2,6,10-trimethylundeca-5,9-dien-3-yl)-1,3,2-dioxaborolane (7t): Prepared according to **General Procedure C** using **2j** (66.1 mg, 0.25 mmol, 1 equiv) and isopropylmagnesium bromide (350 μL, 1.0 M in THF, 0.35 mmol, 1.4 equiv). Purification by flash column chromatography on C2 silica (0 to 2% Et_2O in hexanes) afforded **7t** as a colorless oil (50.3 mg, 63%). **^{1}H NMR** (400 MHz, $CDCl_3$) δ 5.16 – 5.01 (m, 2H), 2.15 – 1.99 (m, 4H), 2.00 – 1.90 (m, 2H), 1.76 – 1.69 (m, 1H), 1.67 (s, 3H), 1.60 (s, 3H), 1.58 (s, 3H), 1.26 (d, *J* = 6.4 Hz, 1H), 1.22 (s, 12H), 0.93 (t, *J* = 7.1 Hz, 6H); **^{13}C NMR** (101 MHz, $CDCl_3$) δ 134.7, 131.2, 124.6, 124.5, 82.8, 39.9, 29.5, 27.7, 26.7, 25.7, 24.89, 24.86, 22.4, 21.8, 17.6, 16.2 [*the carbon attached*

to boron was not observed due to quadrupolar relaxation]; **^{11}B NMR** (128 MHz, $CDCl_3$) δ 33; **HRMS** (ESI) calculated for $C_{20}H_{38}BO_2$ $[M+H]^+$: 321.2959; found: 321.2960. **7t** was determined to be of 87% ee (92% e.s.) by chiral SFC analysis of the secondary alcohol obtained by oxidation with sodium perborate (CHIRALPAK IF, 5% MeOH/CO_2, 5.0 mL/min, 222 nm, t_R(minor) = 1.5 min, t_R(major) = 1.8 min).

(5k): Prepared according to **General Procedure B** using **2k** (42.5 mg, 0.25 mmol, 1 equiv), affording crude **5k** as a yellow oil (63% NMR yield). *Note: **5k** is highly volatile.* **^{1}H NMR** (400 MHz, $CDCl_3$) δ 3.24 (d, *J* = 6.8 Hz, 1H, C**H**Cl); **^{11}B NMR** (128 MHz, $CDCl_3$) δ 31.

5k was determined to be of 89% ee by chiral GC analysis (CP-Chirasil-Dex CB, 70 to 92 °C, 1 °C/min, 14 PSI, t_R(minor) = 18.4 min, t_R(major) = 18.7 min).

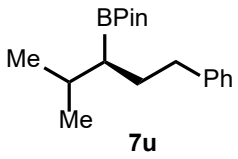

7u

(*S*)-4,4,5,5-tetramethyl-2-(4-methyl-1-phenylpentan-3-yl)-1,3,2-dioxaborolane (7u): Prepared according to **General Procedure C** using **2k** (42.5 mg, 0.25 mmol, 1 equiv) and phenethylmagnesium bromide (350 µL, 1.0 M in THF, 0.35 mmol, 1.4 equiv). Purification by flash column chromatography on C2 silica (0 to 2% Et_2O in hexanes) afforded **7u** as a colorless oil (18.0 mg, 25%). *Note: a-chloro intermediate **5k** is highly volatile.* **^{1}H NMR** (400 MHz, $CDCl_3$) δ 7.36 – 7.29 (m, 2H), 7.28 – 7.19 (m, 3H), 2.70 (ddd, *J* = 13.4, 10.9, 5.2 Hz, 1H), 2.57 (ddd, *J* = 13.5, 10.6, 6.3 Hz, 1H), 1.90 – 1.76 (m, 2H), 1.76 – 1.67 (m, 1H), 1.35 (s, 12H), 1.00 (dd, *J* = 6.8, 1.4 Hz, 6H), 0.98 – 0.93 (m, 1H); **^{13}C NMR** (101 MHz, $CDCl_3$) δ 143.2, 128.4, 128.2, 125.6, 82.9, 36.1, 31.5, 29.6, 25.1,

24.9, 22.3, 21.7 [*the carbon attached to boron was not observed due to quadrupolar relaxation*]; **^{11}B NMR** (128 MHz, $CDCl_3$) δ 34; **HRMS** (ESI) calculated for $C_{18}H_{33}NBO_2$ $[M+NH_4]^+$: 306.2606; found: 306.2599. **7u** was determined to be of 90% ee (102% e.s.) by chiral HPLC analysis of the secondary alcohol obtained by oxidation with sodium perborate (CHIRALPAK AD-H, 2% *i*PrOH/hexanes, 1.0 mL/min, 210 nm, t_R(minor) = 17.7 min, t_R(major) = 15.8 min).

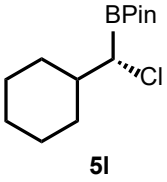

5l

(*S*)-2-(chloro(cyclohexyl)methyl)-4,4,5,5-tetramethyl-1,3,2-dioxaborolane (5l): Prepared according to **General Procedure B** using **2l** (52.5 mg, 0.25 mmol, 1 equiv), affording crude **5l** as a yellow oil (67% NMR yield). **^{1}H NMR** (400 MHz, $CDCl_3$) δ 3.22 (d, *J* = 7.4 Hz, 1H, C**H**Cl); **^{11}B NMR** (128 MHz, $CDCl_3$) δ 31; **5l** was determined to be of 89% ee by chiral GC analysis (CP-Chirasil-Dex CB, 90 to 145 °C, 0.5 °C/min, 7 PSI, t_R(minor) = 77.2 min, t_R(major) = 76.2 min).

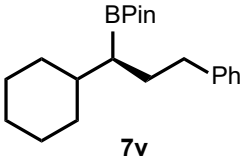

7v

(*S*)-2-(1-cyclohexyl-3-phenylpropyl)-4,4,5,5-tetramethyl-1,3,2-dioxaborolane (7v): Prepared according to **General Procedure C** using **2l** (52.5 mg, 0.25 mmol, 1 equiv) and phenethylmagnesium bromide (350 µL, 1.0 M in THF, 0.35 mmol, 1.4 equiv). Purification by flash column chromatography on C2 silica (0 to 2% Et_2O in hexanes) afforded **7v** as a clear crystalline solid (50.1 mg, 61%). **^{1}H NMR** (400 MHz, $CDCl_3$) δ 7.30 – 7.22 (m, 2H), 7.20 – 7.12 (m, 3H), 2.63 (ddd, *J* = 13.5, 10.8, 5.3 Hz, 1H), 2.50 (ddd, *J* = 13.5, 10.5, 6.3 Hz, 1H), 1.79 – 1.60 (m, 7H), 1.47 – 1.35 (m, 1H), 1.28 (s, 12H), 1.25 – 0.90 (m, 6H); **^{13}C NMR** (101 MHz, $CDCl_3$) δ 143.2, 128.4, 128.2, 125.5, 82.9, 39.7, 36.1, 32.8, 32.5, 31.1, 26.8, 26.8, 26.8, 25.1, 24.9 [*the carbon attached to boron was not observed due*

to quadrupolar relaxation]; **^{11}B NMR** (128 MHz, $CDCl_3$) δ 34; **HRMS** (ESI) calculated for $C_{21}H_{37}NBO_2$ $[M+NH_4]^+$: 346.2919; found: 346.2912. **7v** was determined to be of 87% ee (98% e.s.) by chiral HPLC analysis of the secondary alcohol obtained by oxidation with sodium perborate (CHIRALPAK AS-H, 2% *i*PrOH/hexanes, 1.0 mL/min, 210 nm, t_R(minor) = 8.3 min, t_R(major) = 9.0 min). A crystal suitable for X-ray diffraction grew spontaneously upon allowing a saturated solution of **7v** in pentane to stand at room temperature, allowing for the assignment of its structure and absolute configuration (see section **X-Ray Crystallography** for crystallographic details).

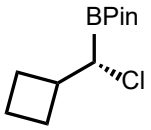

5m

(*S*)-2-(chloro(cyclobutyl)methyl)-4,4,5,5-tetramethyl-1,3,2-dioxaborolane (5m): Prepared according to **General Procedure B** using **2m** (45.5 mg, 0.25 mmol, 1 equiv), affording crude **5m** as a yellow oil (74% NMR yield). **^{1}H NMR** (400 MHz, $CDCl_3$) δ 3.35 (d, *J* = 9.3 Hz, 1H, C**H**Cl); **^{11}B NMR** (128 MHz, $CDCl_3$) δ 31.

5m was determined to be of 96% ee by chiral GC analysis (CP-Chirasil-Dex CB, 60 to 90 °C, 0.2 °C/min, 21 PSI, t_R(minor) = 72.6 min, t_R(major) = 75.0 min).

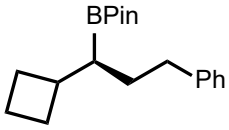

7w

(*S*)-2-(1-cyclobutyl-3-phenylpropyl)-4,4,5,5-tetramethyl-1,3,2-dioxaborolane (7w): Prepared according to **General Procedure C** using **2m** (45.5 mg, 0.25 mmol, 1 equiv) and phenethylmagnesium bromide (350 µL, 1.0 M in THF, 0.35 mmol, 1.4 equiv). Purification by flash column chromatography on C2 silica (0 to 2% Et_2O in hexanes) afforded **7w** as a colorless oil (46.2 mg, 62%). **^{1}H NMR** (400 MHz, $CDCl_3$) δ 7.38 – 7.20 (m, 5H), 2.70 (dt, *J* = 13.5, 8.4 Hz, 1H), 2.58 (dt, *J* = 13.5, 8.0 Hz, 1H), 2.49

– 2.35 (m, 1H), 2.20 – 2.00 (m, 2H), 1.95 – 1.62 (m, 6H), 1.33 (s, 12H), 1.20 – 1.09 (m, 1H); **^{13}C NMR** (101 MHz, $CDCl_3$) δ 143.3, 128.5, 128.4, 125.7, 83.0, 38.0, 36.1, 31.5, 29.7, 28.5, 25.0, 24.9, 18.6 [*the carbon attached to boron was not observed due to quadrupolar relaxation*]; **^{11}B NMR** (128 MHz, $CDCl_3$) δ 34; **HRMS** (ESI) calculated for $C_{19}H_{30}BO_2$ $[M+H]^+$: 301.2333; found: 301.2338. **7w** was determined to be of 96% ee (100% e.s.) by chiral SFC analysis of the secondary alcohol obtained by oxidation with sodium perborate (CHIRALPAK ID, 5% MeOH/CO_2, 5.0 mL/min, 210 nm, t_R(minor) = 2.4 min, t_R(major) = 3.0 min).

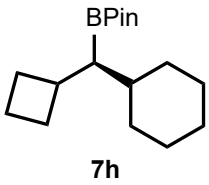

7h

(*R*)-2-(cyclobutyl(cyclohexyl)methyl)-4,4,5,5-tetramethyl-1,3,2-dioxaborolane (7h): Prepared according to **General Procedure C** on 2x scale using **2m** (91.0 mg, 0.5 mmol, 1 equiv) and cyclohexylmagnesium chloride (370 µL, 1.9 M in Et_2O, 0.70 mmol, 1.4 equiv) with the following modification: the crude chloride product was dissolved before Grignard reagent addition in a mixture of Et_2O (1300 µL) and THF (700 µL), rather than Et_2O (2 mL). Purification by flash column chromatography on C2 silica (0 to 2% Et_2O in hexanes) afforded **7h** as a colorless oil (76.3 mg, 55%). **^{1}H NMR** (400 MHz, $CDCl_3$) δ 2.54 – 2.34 (m, 1H), 2.13 – 1.90 (m, 2H), 1.86 – 1.72 (m, 1H), 1.72 – 1.55 (m, 8H), 1.39 – 1.28 (m, 1H), 1.23 (s, 6H), 1.23 (s, 6H), 1.19 – 0.89 (m, 6H); **^{13}C NMR** (101 MHz, $CDCl_3$) δ 82.9, 38.7, 36.2, 33.9, 32.4, 31.2, 29.1, 27.03, 26.95, 26.92, 25.2, 24.9, 18.9 [*the carbon attached to boron was not observed due to quadrupolar relaxation*]; **^{11}B NMR** (128 MHz, $CDCl_3$) δ 33; **HRMS** (APCI) calculated for $C_{17}H_{32}BO_2$ $[M+H]^+$: 279.2490; found: 279.2488. **7h** was determined to be of 96% ee (100% e.s.) by chiral SFC analysis of derivative **8i** (see section **Scope of C–B Elaborations**).

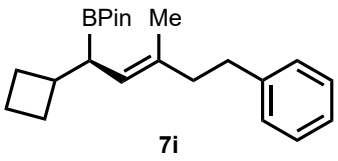

7i

(*R*,*E*)-2-(1-cyclobutyl-3-methyl-5-phenylpent-2-en-1-yl)-4,4,5,5-tetramethyl-1,3,2-dioxaborolane (7i):

Formation of (E)-(2-methyl-4-phenylbut-1-en-1-yl)magnesium bromide: To a flame-dried 2-dram vial equipped with a magnetic stir bar was added (*E*)-(4-bromo-3-methylbut-3-en-1-yl)benzene (78.8 mg, 0.35 mmol, 1.4 equiv). The vial was capped with a septum top and put under an atmosphere of N_2. THF (0.5 mL) was added, and the vial was cooled to -78 °C with stirring. To the reaction mixture was slowly added a solution of *tert*-butyllithium (411 μL, 1.7 M in pentane, 0.7 mmol, 2.8 equiv), after which the mixture was let stir for 30 minutes. To a separate vial in a N_2-filled glovebox was added $MgBr_2$ (64.4 mg, 0.35 mmol, 1.4 equiv) and THF (0.5 mL), and the vial was capped with a septum top and removed from the glovebox. Then, this magnesium bromide solution was transferred to the cold reaction mixture, after which the reaction mixture was let stir for an hour to afford (*E*)-(2-methyl-4-phenylbut-1-en-1-yl)magnesium bromide. *Note: use of the vinyl lithium species rather than the vinyl magnesium bromide led to prohibitively low yields of desired product.*

*Synthesis of **7i**:* Prepared according to **General Procedure C** using **2m** (45.5 mg, 0.25 mmol, 1 equiv) and (*E*)-(2-methyl-4-phenylbut-1-en-1-yl)magnesium bromide (THF solution as described above, 0.35 mmol, 1.4 equiv). Purification by flash column chromatography on normal silica (0 to 100% CH_2Cl_2 in hexanes) afforded **7i** as a colorless oil (40.0 mg, 47%). **^{1}H NMR** (400 MHz, $CDCl_3$) δ 7.37 – 7.29 (m, 2H), 7.28 – 7.20 (m, 3H), 5.10 (dd, *J* = 9.6, 1.4 Hz, 1H), 2.79 – 2.71 (m, 2H), 2.47 (dq, *J* = 9.8, 7.8 Hz, 1H), 2.42 – 2.33 (m, 2H), 2.13 – 1.98 (m, 3H), 1.93 – 1.76 (m,

3H), 1.74 (d, J = 1.4 Hz, 3H), 1.68 – 1.55 (m, 1H), 1.28 (d, J = 3.8 Hz, 12H); **^{13}C NMR** (101 MHz, $CDCl_3$) δ 142.5, 134.1, 128.4, 128.2, 125.5, 124.3, 82.9, 41.7, 37.8, 35.0, 28.8, 27.8, 24.8, 24.6, 18.4, 16.6 [*the carbon attached to boron was not observed due to quadrupolar relaxation*]; **^{11}B NMR** (128 MHz, $CDCl_3$) δ 33; **HRMS** (ESI) calculated for $C_{22}H_{34}BO_2$ $[M+H]^+$: 341.2646; found: 341.2651. **7i** was determined to be of 95% ee (99% e.s.) by chiral HPLC analysis of the secondary alcohol obtained by oxidation with sodium perborate (CHIRALPAK OD-H, 3% *i*PrOH/hexanes, 1.0 mL/min, 210 nm, t_R(minor) = 10.3 min, t_R(major) = 22.4 min).

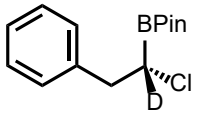

5f-d$_1$

(*S*)-2-(1-chloro-2-phenylethyl-1-*d*)-4,4,5,5-tetramethyl-1,3,2-dioxaborolane (5f-d$_1$): Prepared according to **General Procedure B** using **2f** (54.5 mg, 0.25 mmol, 1 equiv), with the following modification: CD_2Cl_2 (32 µL, 0.50 mmol, 2 equiv) was used instead of CH_2Cl_2 in the preparation of the lithium boronate. Crude **5f-d$_1$** was obtained as a yellow oil (80% NMR yield). **^{1}H NMR** (400 MHz, $CDCl_3$) δ 3.20 – 3.04 (m, 2H, PhC**H$_2$**). **^{11}B NMR** (128 MHz, $CDCl_3$) δ 31.

5f-d$_1$ was determined to be of 97% ee by chiral GC analysis (CP-Chirasil-Dex CB, 90 to 125 °C, 0.33 °C/min, 14 PSI, t_R(minor) = 92.1 min, t_R(major) = 93.6 min).

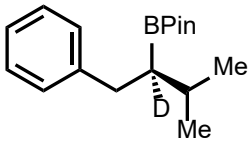

7p-d$_1$

(*R*)-4,4,5,5-tetramethyl-2-(3-methyl-1-phenylbutan-2-yl-2-*d*)-1,3,2-dioxaborolane (7p-d$_1$): Prepared according to **General Procedure C** using **2f** (43.6 mg, 0.2 mmol, 1 equiv) and isopropylmagnesium bromide

(280 μL, 1.0 M in THF, 0.28 mmol, 1.4 equiv), with the following modification: CD_2Cl_2 (25.5 μL, 0.40 mmol, 2 equiv) was used instead of CH_2Cl_2 in the preparation of the lithium boronate. Purification by flash column chromatography on C2 silica (0 to 2% Et_2O in hexanes) afforded **7p-d$_1$** as a colorless oil (38.0 mg, 69%). **^{1}H NMR** (400 MHz, $CDCl_3$) δ 7.32 – 7.23 (m, 4H), 7.17 (ddd, *J* = 5.5, 4.3, 2.4 Hz, 1H), 2.80 (d, *J* = 13.5 Hz, 1H), 2.70 (d, *J* = 13.5 Hz, 1H), 1.80 (p, *J* = 6.7 Hz, 1H), 1.17 (s, 6H), 1.12 (s, 6H), 1.04 (t, *J* = 6.4 Hz, 6H); **^{13}C NMR** (101 MHz, $CDCl_3$) δ 142.7, 128.9, 128.0, 125.5, 82.9, 35.4, 29.7, 24.9, 24.8, 22.6, 21.4 [*the carbon attached to boron was not observed due to quadrupolar relaxation*]; **^{11}B NMR** (128 MHz, $CDCl_3$) δ 34; **HRMS** (ESI) calculated for $C_{17}H_{30}NDBO_2$ $[M+NH_4]^+$: 293.2511; found: 293.2505. **7p-d$_1$** was determined to be of 95% ee (98% e.s.) by chiral HPLC analysis of the secondary alcohol obtained by oxidation with sodium perborate (CHIRALPAK OJ-H, 1% *i*PrOH/hexanes, 1.0 mL/min, 210 nm, t_R(minor) = 19.5 min, t_R(major) = 18.8 min).

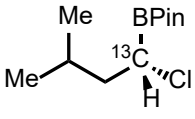

5b-^{13}C

(*S*)-2-(1-chloro-3-methylbutyl-1-^{13}*C*)-4,4,5,5-tetramethyl-1,3,2-dioxaborolane (5b-^{13}C): Prepared according to **General Procedure B** using **2b** (46.0 mg, 0.25 mmol, 1 equiv), with the following modification: $^{13}CH_2Cl_2$ (32 μL, 0.50 mmol, 2 equiv) was used instead of CH_2Cl_2 in the preparation of the lithium boronate. Crude **5b-^{13}C** was obtained as a yellow oil (86% NMR yield). **^{1}H NMR** (400 MHz, $CDCl_3$) δ 3.46 (ddd, *J* = 138.7, 9.9, 6.0 Hz, 1H, ^{13}C**H**Cl); **^{11}B NMR** (128 MHz, $CDCl_3$) δ 31.

5b-^{13}C was determined to be of 97% ee by chiral GC analysis (CP-Chirasil-Dex CB, 65 to 80 °C, 0.3 °C/min, 21 PSI, t_R(minor) = 32.5 min, t_R(major) = 33.2 min).

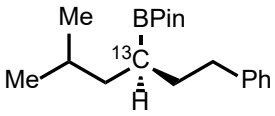

7g-^{13}C

(*S*)-4,4,5,5-tetramethyl-2-(5-methyl-1-phenylhexan-3-yl-3-^{13}*C*)-1,3,2-dioxaborolane (7g-^{13}C): Prepared according to **General Procedure C** using **2b** (46.0 mg, 0.25 mmol, 1 equiv) and phenethylmagnesium bromide (350 µL, 1.0 M in THF, 0.35 mmol, 1.4 equiv), with the following modification: $^{13}CH_2Cl_2$ (32 µL, 0.50 mmol, 2 equiv) was used instead of CH_2Cl_2 in the preparation of the lithium boronate. Purification by flash column chromatography on C2 silica (0 to 2% Et_2O in hexanes) afforded **7g-^{13}C** as a colorless oil (41.2 mg, 54%). **^{1}H NMR** (400 MHz, $CDCl_3$) δ 7.38 – 7.18 (m, 5H), 2.67 (dtt, *J* = 10.5, 6.9, 3.6 Hz, 2H), 1.85 – 1.58 (m, 3H), 1.52 – 1.42 (m, 1H), 1.42 – 1.35 (m, 1H), 1.34 (s, 12H), 1.31 – 1.25 (m, 1H), 0.94 (dd, *J* = 6.6, 4.1 Hz, 6H); **^{13}C NMR** (101 MHz, $CDCl_3$) δ 143.3 (d, *J* = 3.6 Hz), 128.5, 128.4, 125.7, 83.0 (d, *J* = 1.1 Hz), 40.7 (d, *J* = 31.2 Hz), 35.8, 33.9 (d, *J* = 30.5 Hz), 27.4, 25.03, 24.95, 23.2 (d, *J* = 2.9 Hz), 22.7 (d, *J* = 2.2 Hz), 23.99 – 19.50 (br s); **^{11}B NMR** (128 MHz, $CDCl_3$) δ 35; **HRMS** (ESI) calculated for $C_{18}{}^{13}CH_{32}BO_2$ $[M+H]^+$: 304.2523; found: 304.2529. **7g-^{13}C** was determined to be of 97% ee (100% e.s.) by chiral SFC analysis of the secondary alcohol obtained by oxidation with sodium perborate (CHIRALPAK IB N-5, 5% MeOH/CO_2, 5.0 mL/min, 210 nm, t_R(minor) = 2.8 min, t_R(major) = 2.4 min).

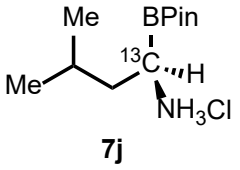

7j

(*R*)-chloro(3-methyl-1-(4,4,5,5-tetramethyl-1,3,2-dioxaborolan-2-yl) butyl-1-^{13}*C*)-λ^5-azane (7j): Prepared according to **General Procedure C**, with modifications to the workup for the second chloride displacement reaction, using **2b** (55.2 mg, 0.3 mmol, 1 equiv), $^{13}CH_2Cl_2$ (23 µL, 0.36 mmol, 1.2 equiv), and lithium bis(trimethylsilyl)amide (LiHMDS) (420 µL, 1.0 M solution in toluene, 0.42 mmol, 1.4 equiv). The modifications to the workup for the second chloride displacement step are as follows: the reaction mixture containing the crude product of the chloride displacement with

LiHMDS was concentrated by rotary evaporation, redissolved in hexanes (1 mL), let stir for 1 hour, and passed through a plug of celite eluting with hexanes (5 mL). The filtrate was concentrated by rotary evaporation, and the resulting yellow oil was placed under an N_2 atmosphere and dissolved in dioxane (1 mL). This reaction mixture was cooled to 0 °C with stirring before a solution of hydrogen chloride (1.0 mL, 1.0 M in Et_2O, 1.0 mmol, 4 equiv) was added at a rate of 1 drop per second. The resulting mixture was allowed to warm to room temperature and stirred for 2 hours. After this time, the reaction mixture was concentrated, resuspended in hexanes (2 mL), and stirred for 30 minutes. The suspension was filtered and the solid washed twice with hexanes (2 mL) and collected to afford pure **7j** as an off-white powder (53.1 mg, 71% yield). **^{1}H NMR** (400 MHz, $CDCl_3$) δ 8.08 (s, 3H), 2.94 (d, J = 131.6 Hz, 1H), 1.89 (s, 1H), 1.82 – 1.56 (m, 2H), 1.28 (s, 12H), 0.95 (d, J = 6.2 Hz, 6H) **^{13}C NMR** (101 MHz, $CDCl_3$) δ 85.0, 38.6 (d, J = 31.4 Hz), 36.0 (^{13}C-labeled carbon), 25.1, 25.0, 24.6, 22.5 (dd, J = 6.1, 2.8 Hz); **HRMS** (ESI) calculated for $C_{10}{}^{13}CH_{25}BNO_2$ $[M–Cl]^+$: 215.2006; found: 215.2009. **7j** was determined to be of 98% ee (101% e.s.) by chiral GC analysis of the *N*-pivalate obtained by acylation with pivaloyl chloride and triethylamine in CH_2Cl_2 (CP-Chirasil-Dex CB, 90 to 145 °C, 0.33 °C/min, 20 PSI, t_R(minor) = 71.0 min, t_R(major) = 72.1 min). A crystal suitable for X-ray diffraction was grown by vapor diffusion of hexanes into a saturated acetone solution of **7j**, allowing for the assignment of its structure and absolute configuration (see section **X-Ray Crystallography** for crystallographic details).

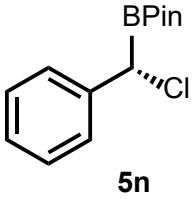

5n

(*S*)-2-(chloro(phenyl)methyl)-4,4,5,5-tetramethyl-1,3,2-dioxaborolane (5n): Prepared according to **General Procedure B** using **2n** (40.8 mg, 0.25 mmol, 1 equiv), affording crude **5n** as a yellow oil (49–76% NMR yield; spectrum

included shows 76% yield). **^{1}H NMR** (400 MHz, $CDCl_3$) δ 4.49 (s, 1H, C**H**Cl); **^{11}B NMR** (128 MHz, $CDCl_3$) δ 31. The enantioenrichment of **5n** varied between runs and was determined upon elaboration with 1.4 equivalents of isopropylmagnesium bromide followed by oxidation with sodium perborate as described directly below.

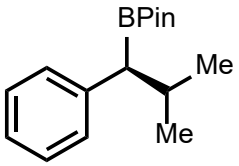

7x

(*S*)-4,4,5,5-tetramethyl-2-(2-methyl-1-phenylpropyl)-1,3,2-dioxaborolane (7x): Prepared according to **General Procedure C** using **2n** (40.8 mg, 0.25 mmol, 1 equiv) and isopropylmagnesium bromide (350 μL, 1.0 M in THF, 0.35 mmol, 1.4 equiv). Purification by flash column chromatography on C2 silica (0 to 2% Et_2O in hexanes) afforded **7x** as a colorless oil (27.0 mg, 42%). **^{1}H NMR** (400 MHz, $CDCl_3$) δ 7.33 – 7.22 (m, 4H), 7.20 – 7.15 (m, 1H), 2.17 (dp, *J* = 10.3, 6.5 Hz, 1H), 2.02 (d, *J* = 10.3 Hz, 1H), 1.24 (d, *J* = 9.0 Hz, 12H), 1.08 (d, *J* = 6.6 Hz, 3H), 0.78 (d, *J* = 6.5 Hz, 3H); **^{13}C NMR** (101 MHz, $CDCl_3$) δ 142.3, 129.1, 128.1, 125.2, 83.2, 31.0, 24.6, 24.6, 23.1, 22.0 [*the carbon attached to boron was not observed due to quadrupolar relaxation*]; **^{11}B NMR** (128 MHz, $CDCl_3$) δ 33; **HRMS** (ESI) calculated for $C_{16}H_{29}NBO_2$ $[M+NH_4]^+$: 277.2208; found: 277.2204.

Depending on the run, **7x** was determined to vary between 57–81% ee by chiral HPLC analysis of the secondary alcohol obtained by oxidation with sodium perborate (shown: 77% ee result; CHIRALPAK AD-H, 2% *i*PrOH/hexanes, 1.0 mL/min, 210 nm, t_R(minor) = 15.2 min, t_R(major) = 16.4 min).

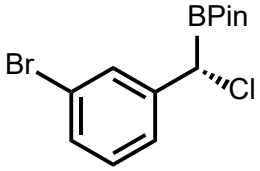

5o

(*S*)-2-((3-bromophenyl)chloromethyl)-4,4,5,5-tetramethyl-1,3,2-dioxaborolane (5o): Prepared according to **General Procedure B** using **2o** (70.8 mg, 0.25 mmol, 1 equiv), affording crude **5o** as a yellow oil (57–75% NMR yield; spectrum included shows product at 75% yield). **^{1}H NMR** (400 MHz, $CDCl_3$) δ 4.28 (s, 1H, C**H**Cl); **^{11}B NMR** (128 MHz, $CDCl_3$) δ 31. The enantioenrichment of **5o** varied between runs and was determined upon elaboration with 1.4 equivalents of isopropylmagnesium bromide followed by oxidation with sodium perborate as described directly below.

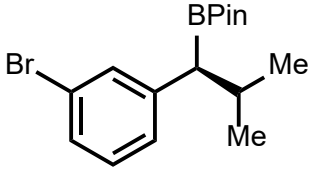

7y

(S)-2-(1-(3-bromophenyl)-2-methylpropyl)-4,4,5,5-tetramethyl-1,3,2-dioxaborolane (7y): Prepared according to **General Procedure C** on 0.5x scale using **2o** (35.4 mg, 0.125 mmol, 1 equiv) and isopropylmagnesium bromide (175 μL, 1.0 M in THF, 0.175 mmol, 1.4 equiv). Purification by flash column chromatography on C2 silica (0 to 2% Et_2O in hexanes) afforded **7y** as a colorless oil (17.0 mg, 40%). **^{1}H NMR** (400 MHz, $CDCl_3$) δ 7.50 (t, J = 1.8 Hz, 1H), 7.42 – 7.38 (m, 1H), 7.29 – 7.21 (m, 2H), 2.22 (dp, J = 10.3, 6.5 Hz, 1H), 2.07 (d, J = 10.4 Hz, 1H), 1.34 (s, 6H), 1.33 (s, 6H), 1.16 (d, J = 6.5 Hz, 3H), 0.87 (d, J = 6.6 Hz, 3H); **^{13}C NMR** (101 MHz, $CDCl_3$) δ 144.9, 132.0, 129.6, 128.3, 127.7, 122.3, 83.4, 31.0, 24.7, 24.5, 23.0, 22.0 [*the carbon attached to boron was not observed due to quadrupolar relaxation*]; **^{11}B NMR** (128 MHz, $CDCl_3$) δ 33; **HRMS** (ESI) calculated for $C_{16}H_{25}BBrO_2$ $[M+H]^+$: 339.1128; found: 339.1125. **7y** was determined to be of 82–93% ee by chiral HPLC analysis of the secondary alcohol obtained by oxidation with sodium perborate (shown: 92% ee result; CHIRALPAK AD-H, 2% *i*PrOH/hexanes, 1.0 mL/min, 210 nm, t_R(minor) = 18.4 min, t_R(major) = 20.6 min).

Scope of C–B Elaborations

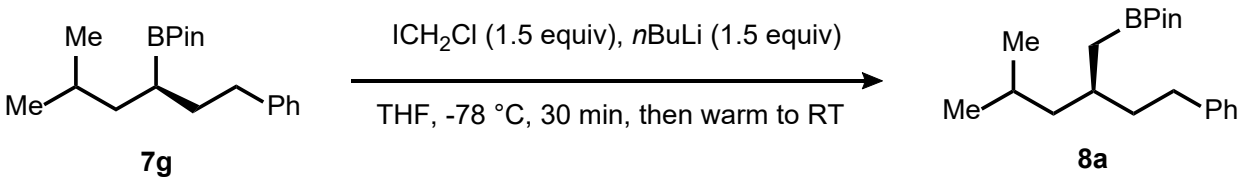

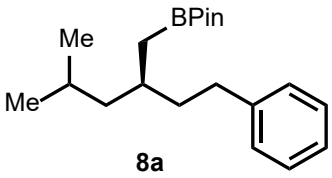

(*S*)-4,4,5,5-tetramethyl-2-(4-methyl-2-phenethylpentyl)-1,3,2-dioxaborolane (8a): To a 1-dram vial equipped with a magnetic stir bar was added **7g** (10.5 mg, 0.035 mmol, 1 equiv) before the vial was capped with a septum top and put under an atmosphere of N_2. To the vial was added iodochloromethane (4 µL, 0.52 mmol, 1.5 equiv) and THF (0.35 mL), and then the vessel was cooled to -78 °C. To the stirring reaction mixture was added a solution of *n*-butyllithium (21 µL, 2.5 M in hexanes, 0.052 mmol, 1.5 equiv), and the reaction mixture was stirred at this temperature for an additional 30 minutes. After this time, the vessel was warmed to room temperature, and saturated aqueous ammonium chloride (1 mL) and Et_2O (1 mL) were added to the reaction mixture. The organic layer was removed, and the aqueous layer was extracted with Et_2O (2 x 2 mL). The combined organic layers were dried with magnesium sulfate, filtered, and concentrated by rotary evaporation. The product was purified by flash column chromatography on C2 silica (0 to 2% Et_2O in hexanes) to afford **8a** as a colorless oil (8.0 mg, 72%). **^{1}H NMR** (400 MHz, $CDCl_3$) δ 7.25 (d, *J* = 6.8 Hz, 2H), 7.16 (dd, *J* = 13.9, 7.1 Hz, 3H), 2.68 – 2.51 (m, 2H), 1.75 (dp, *J* = 13.2, 6.6 Hz, 1H), 1.69 – 1.58 (m, 2H), 1.56 – 1.47 (m, 1H), 1.25 (s, 12H), 1.23 – 1.19 (m, 1H), 1.11 (dt, *J* = 13.7, 7.0 Hz, 1H), 0.86 (dd, *J* = 6.5, 5.1 Hz, 6H), 0.83 (dd, *J* = 6.7, 2.8 Hz, 2H); **^{13}C NMR** (101 MHz, $CDCl_3$) δ 143.5, 128.4, 128.2, 125.4, 82.9, 46.4, 38.8, 33.2, 31.9, 25.4, 24.9 (d, *J* = 1.6 Hz), 23.1, 22.9 [*the carbon attached to boron was not observed due to quadrupolar relaxation*]; **^{11}B NMR** (128

MHz, $CDCl_3$) δ 33; **HRMS** (ESI) calculated for $C_{20}H_{37}NBO_2$ $[M+NH_4]^+$: 334.2912; found: 334.2918. **8a** was determined to be of 96% ee (99% e.s.) by chiral HPLC analysis of the secondary alcohol obtained by oxidation with sodium perborate (CHIRALPAK AD-H, 2% *i*PrOH/hexanes, 1.0 mL/min, 210 nm, t_R(minor) = 14.6 min, t_R(major) = 16.0 min).

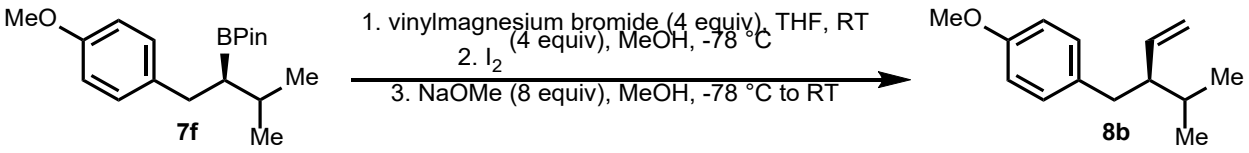

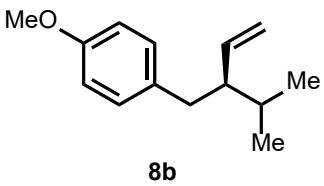

(*R*)-1-(2-isopropylbut-3-en-1-yl)-4-methoxybenzene (8b): Prepared according to the following method, adapted from a literature procedure reported by Aggarwal and coworkers. An oven-dried 2-dram vial was charged with **7f** (21.3 mg, 0.07 mmol, 1 equiv). The vial was equipped with a magnetic stir bar; the threads were wrapped with Teflon tape; the vial was sealed with a Teflon-coated septum cap; and the reaction was put under a nitrogen atmosphere. The vial was charged with THF (700 µL), and a solution of vinylmagnesium bromide (280 µL, 1.0 M in THF, 0.28 mmol, 4 equiv) was added at a rate of 1 drop per second with rapid stirring at room temperature. The reaction mixture was allowed to stir for 30 minutes, then cooled to -78 °C. A solution of iodine (71.1 mg, 0.28 mmol, 4 equiv) in MeOH (1 mL) was added over 5 minutes and the reaction mixture was allowed to stir for an additional 30 minutes. A solution of sodium methoxide (1120 µL, 0.5 M in MeOH, 0.56 mmol, 8 equiv) was added over 2 minutes. The reaction was removed from the cold bath and allowed to stir at room temperature for 1 hour. The reaction was quenched with water (1 mL) and diluted with Et_2O, and excess iodine was quenched with saturated aqueous $Na_2S_2O_3$. The organic and aqueous layers were separated and the aqueous layer was extracted with Et_2O (2 x 2 mL). The combined organic layers were dried over $MgSO_4$, filtered, concentrated under reduced pressure, and purified by flash column chromatography on normal silica (Et_2O/hexanes) to afford **8b** as a yellow oil (7.3

mg, 51%). **^{1}H NMR** (400 MHz, $CDCl_3$) δ 7.05 (d, *J* = 8.8 Hz, 2H), 6.80 (d, *J* = 8.6 Hz, 2H), 5.63 (ddd, *J* = 17.1, 10.3, 8.9 Hz, 1H), 4.96 (dd, *J* = 10.3, 2.2 Hz, 1H), 4.81 (ddd, *J* = 17.1, 2.1, 0.9 Hz, 1H), 3.78 (s, 3H), 2.70 (dd, *J* = 13.7, 5.9 Hz, 1H), 2.52 (dd, *J* = 13.8, 8.6 Hz, 1H), 2.11 (ddd, *J* = 14.3, 8.8, 5.4 Hz, 1H), 1.65 (m, 1H), 0.90 (dd, *J* = 14.6, 6.8 Hz, 6H); **^{13}C NMR** (101 MHz, $CDCl_3$) δ 157.7, 139.8, 133.4, 130.2, 115.9, 113.6, 55.3, 52.4, 37.9, 30.7, 21.1, 18.3; **HRMS** (ESI) calculated for $C_{14}H_{21}O$ $[M+H]^+$: 205.1587; found: 205.1589. **8b** was determined to be of 96% ee (100% e.s.) by chiral HPLC analysis (CHIRALCEL OD-H, 0.1% *i*PrOH/hexanes, 1.0 mL/min, 210 nm, t_R(minor) = 7.1 min, t_R(major) = 6.3 min).

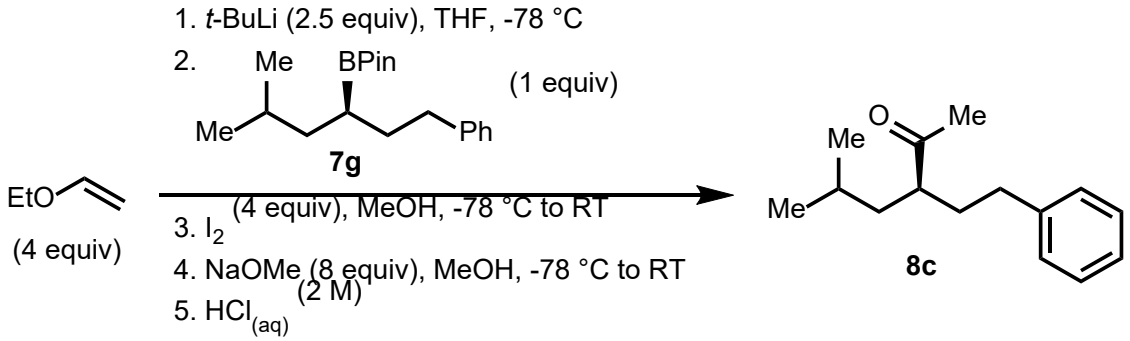

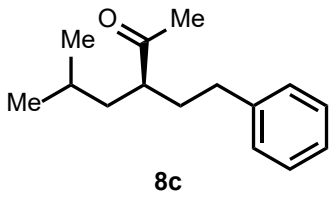

(*S*)-5-methyl-3-phenethylhexan-2-one (8c): Prepared according to the following method, adapted from a literature procedure reported by Aggarwal and coworkers. An oven-dried 2-dram vial equipped with a magnetic stir bar, Teflon tape-coated threads, and a Teflon-coated septum cap was put under a nitrogen atmosphere. The vial was charged with freshly distilled ethyl vinyl ether (44.3 μL, 0.4628 mmol, 4 equiv) and THF (1.3 mL) and cooled to -78 °C with stirring. A solution of *tert*-butyllithium (242 μL, 1.2 M in pentane, 0.2893 mmol, 2.5 equiv) was added at a rate of 1 drop per second and the reaction allowed to stir at -78 °C for an additional 30 minutes. The reaction was warmed to 0 °C, allowed to stir for 30 minutes, cooled to -78 °C, and charged with additional THF (700 μL). Neat **7g** (35.0 mg, 0.1157 mmol, 1 equiv) was added via microsyringe

at a rate of 1 drop per 5 seconds, and the reaction was allowed to stir at -78 °C for an additional 30 minutes. The reaction was warmed to 0 °C, allowed to stir for 10 minutes, then cooled to -78 °C. A solution of iodine (117.7 mg, 0.4628 mmol, 4 equiv) in MeOH (1.3 mL) was added over 5 minutes and the reaction mixture allowed to stir for an additional 30 minutes. The reaction was removed from the cold bath and allowed to stir at room temperature for 5 minutes, then cooled to -78 °C. A solution of sodium methoxide (1.85 mL, 0.5 M in MeOH, 0.9256 mmol, 8 equiv) was added over 2 minutes. The reaction was removed from the cold bath and allowed to stir at room temperature for 1 hour. The reaction was quenched with aqueous 2 M HCl (1 mL) and allowed to stir at room temperature for 15 minutes. The reaction mixture was diluted with Et_2O and neutralized with saturated aqueous $NaHCO_3$, and excess iodine was quenched with saturated aqueous $Na_2S_2O_3$. The organic and aqueous layers were separated and the aqueous layer was extracted with Et_2O (2 x 2 mL). The combined organic layers were dried over $MgSO_4$, filtered, concentrated under reduced pressure, and purified by flash column chromatography on normal silica (Et_2O/hexanes) to afford **8c** as a colorless oil (16.5 mg, 65%). **^{1}H NMR** (400 MHz, $CDCl_3$) δ 7.33 – 7.09 (m, 5H), 2.61 – 2.46 (m, 3H), 2.10 (s, 3H), 1.95 – 1.82 (m, 1H), 1.75 – 1.62 (m, 1H), 1.59 – 1.44 (m, 2H), 1.27 – 1.21 (m, 1H), 0.85 (dd, J = 9.4, 6.4 Hz, 6H); **^{13}C NMR** (101 MHz, $CDCl_3$) δ 212.8, 141.8, 128.6, 128.5, 126.1, 50.8, 41.0, 33.8, 33.7, 28.7, 26.2, 23.0, 22.6; **HRMS** (ESI) calculated for $C_{15}H_{23}O$ $[M+H]^+$: 219.1743; found: 219.1747. **8c** was determined to be of 96% ee (99% e.s.) by chiral GC analysis (CP-Chirasil-Dex CB, 70 to 120°C, 0.5 °C/min, 21 PSI, t_R(minor) = 76.7 min, t_R(major) = 75.5 min).

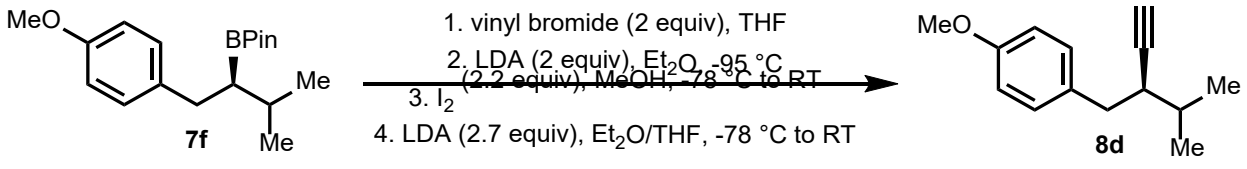

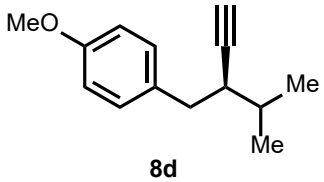

8d

(*R*)-1-(2-isopropylbut-3-yn-1-yl)-4-methoxybenzene (8d): Prepared according to the following method, adapted from a literature procedure reported by Aggarwal and coworkers. An oven-dried 1-dram vial was charged with **7f** (21.3 mg, 0.07 mmol, 1 equiv). The vial was equipped with a magnetic stir bar; the threads were wrapped with Teflon tape; the vial was sealed with a Teflon-coated septum cap; and the reaction was put under a nitrogen atmosphere. The vial was charged with Et_2O (470 μL) and a solution of vinyl bromide (140 μL, 1.0 M in THF, 0.14 mmol, 2 equiv). The reaction mixture was cooled to -95 °C (acetone/$N_{2(l)}$) with rapid stirring, and a solution of LDA (140 μL, 1.0 M in Et_2O, 0.14 mmol, 2 equiv) was added at a rate of 1 drop per 5 seconds. The reaction was allowed to stir at -95 °C for 1 hour. A solution of iodine (39.2 mg, 0.154 mmol, 2.2 equiv) in MeOH (470 μL) was added over 5 minutes. The reaction was removed from the cold bath and allowed to stir at room temperature for 1 hour. The reaction was quenched with water (1 mL) and diluted with Et_2O, and excess iodine was quenched with saturated aqueous $Na_2S_2O_3$. The organic and aqueous layers were separated and the aqueous layer was extracted with Et_2O (2 x 2 mL). The combined organic layers were dried over $MgSO_4$, filtered, concentrated under reduced pressure, and the residue transferred to an oven-dried 1-dram vial. The vial was sealed and put under inert atmosphere as described above. The vial was charged with THF (470 μL) and the reaction mixture was cooled with stirring to -78 °C. A solution of LDA (190 μL, 1.0 M in Et_2O, 0.19 mmol, 2.7 equiv) was added at a rate of 1 drop per second. The vial was removed from the cold bath and allowed to stir at room temperature for 1 hour. The reaction was quenched with saturated aqueous NH_4Cl (1 mL) and diluted with Et_2O. The organic and aqueous layers were separated and the aqueous layer was extracted with Et_2O (2 x 2 mL). The combined organic layers were dried over

$MgSO_4$, filtered, concentrated under reduced pressure, and purified by flash column chromatography on normal silica to yield **8d** as a colorless oil (8.5 mg, 60%). **^{1}H NMR** (400 MHz, $CDCl_3$) δ 7.16 (d, *J* = 8.8 Hz, 2H), 6.84 (d, *J* = 8.6 Hz, 2H), 3.79 (s, 3H), 2.80 – 2.64 (m, 2H), 2.50 (dddd, *J* = 8.6, 6.6, 4.4, 2.4 Hz, 1H), 2.05 (d, *J* = 2.4 Hz, 1H), 1.72 (m, 1H), 1.02 (d, *J* = 6.8 Hz, 6H); **^{13}C NMR** (101 MHz, $CDCl_3$) δ 158.2, 132.2, 130.1, 113.8, 85.7, 71.1, 55.4, 41.1, 38.3, 30.5, 21.5, 17.8; **HRMS** (ESI) calculated for $C_{14}H_{19}O$ $[M+H]^+$: 203.1430; found: 203.1433. **8d** was determined to be of 96% ee (100% e.s.) by chiral HPLC analysis (CHIRALCEL OD-H, 0.2% *i*PrOH/hexanes, 1.0 mL/min, 210 nm, t_R(minor) = 8.3 min, t_R(major) = 7.2 min).

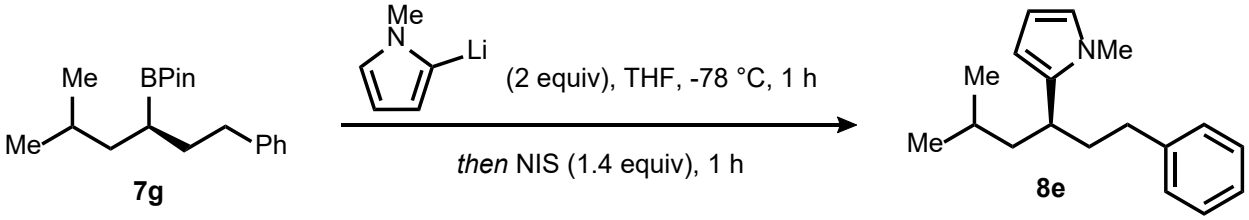

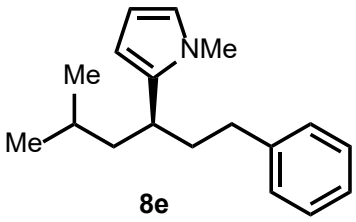

(*S*)-1-methyl-2-(5-methyl-1-phenylhexan-3-yl)-1*H*-pyrrole (8e): Prepared according to the following method, adapted from a literature procedure reported by Aggarwal and coworkers. To a 2-dram vial under an atmosphere of N_2 equipped with a magnetic stir bar and septum cap was added *N*-methylpyrrole (17.8 µL, 0.2 mmol, 2 equiv) and THF (0.8 mL). The reaction vessel was cooled to -78 °C, after which a solution of *sec*-butyllithium (160 µL, 1.25 M in hexane, 0.2 mmol, 2 equiv) was added dropwise to the stirring reaction mixture. After 5 minutes, the reaction mixture was allowed to stir at room temperature for 40 minutes, and then cooled back down to -78 °C. **7g** (30.2 mg, 0.1 mmol, 1 equiv) was added as a solution in THF (0.4 mL), and the reaction mixture was let stir at -78 °C for 1 hour. To the vessel was added a solution of *N*-iodosuccinimide (31.5 mg, 0.14 mmol, 1.4 equiv) in THF (0.8 mL), and the reaction mixture was let stir at -78 °C for 1 hour. A saturated aqueous solution of sodium thiosulfate (2 mL) was added

to the reaction mixture, and the vessel was removed from the cold bath and allowed to warm to room temperature with vigorous stirring. The reaction mixture was diluted with EtOAc (2 mL) and water (2 mL). The organic layer was removed, and the aqueous layer was extracted with EtOAc (2 x 3 mL). The combined organic layers were dried over magnesium sulfate, filtered, and concentrated by rotary evaporation. The crude mixture was purified by flash column chromatography on normal silica (0 to 2% Et_2O in hexanes) to afford **8e** as a yellow oil (16.1 mg, 63%, 82% based on recovered starting material) as well as recovered **7g** (7.0 mg, 23%). **^{1}H NMR** (400 MHz, $CDCl_3$) δ 7.29 – 7.23 (m, 2H), 7.16 (t, *J* = 7.4 Hz, 1H), 7.12 (d, *J* = 7.2 Hz, 2H), 6.52 – 6.39 (m, 1H), 6.10 (t, *J* = 3.1 Hz, 1H), 5.91 (dd, *J* = 3.4, 1.7 Hz, 1H), 3.45 (s, 3H), 2.71 (p, *J* = 7.6 Hz, 1H), 2.55 (pt, *J* = 9.4, 5.0 Hz, 2H), 1.97 – 1.75 (m, 2H), 1.61 – 1.40 (m, 3H), 0.85 (d, *J* = 6.2 Hz, 6H); **^{13}C NMR** (101 MHz, $CDCl_3$) δ 142.6, 137.3, 128.4, 128.3, 125.7, 120.6, 106.6, 104.3, 45.4, 37.9, 33.7, 33.6, 33.4, 25.6, 23.0, 22.7; **HRMS** (ESI) calculated for $C_{18}H_{26}N$ $[M+H]^+$: 256.2060; found: 256.2064. **8e** was determined to be of 96% ee (100% e.s.) by chiral HPLC analysis (CHIRALPAK OD-H, 0.2% *i*PrOH/hexanes, 0.2 mL/min, 210 nm, t_R(minor) = 9.8 min, t_R(major) = 12.1 min).

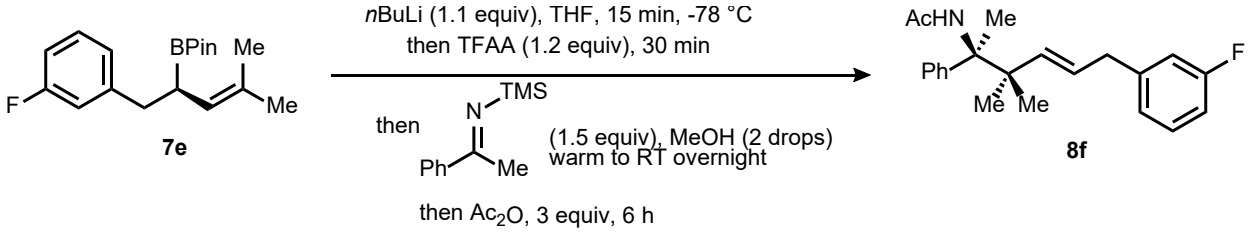

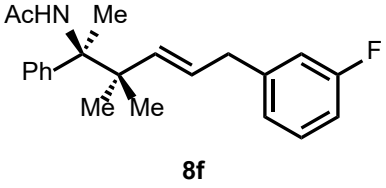

(*S*,*E*)-*N*-(6-(3-fluorophenyl)-3,3-dimethyl-2-phenylhex-4-en-2-yl)acetamide (8f): Prepared according to the following method, adapted from a literature procedure reported by Aggarwal and coworkers. To a 1-dram

vial equipped with a magnetic stir bar was added allylic boronic ester **7e** (30.0 mg, 0.0987 mmol, 1 equiv). The reaction vessel was fitted with a septum cap and put under an atmosphere of N_2. THF (1 mL) was added, and then the vessel was cooled to -78 °C. To the stirring reaction mixture was added a solution of *n*-butyllithium (44 µL, 2.5 M in hexanes, 0.109 mmol, 1.1 equiv), and the solution was allowed to stir for 15 minutes. To this mixture was added trifluoroacetic anhydride (16.4 µL, 0.118 mmol, 1.2 equiv) dropwise and the reaction was stirred for a further 30 minutes at -78 °C. 1-phenyl-*N*-(trimethylsilyl)ethan-1-imine (28 mg, 0.148 mmol, 1.5 equiv) and methanol (8 µL) were then added, and the mixture allowed to warm up to room temperature overnight. Acetic anhydride (28 µL, 0.296 mmol, 3 equiv) was then added and the mixture stirred for a further 6 hours. The reaction was quenched with a saturated aqueous solution of sodium bicarbonate (2 mL) and extracted with EtOAc (3 x 5 mL). The combined organic layers were washed with brine, dried over magnesium sulfate, filtered, concentrated by rotary evaporation, and purified by flash chromatography on normal silica (20 to 50% EtOAc in hexanes) to provide **8f** as an off-white powder (19.0 mg, 57%). **^{1}H NMR** (400 MHz, $CDCl_3$) δ 7.27 (dt, *J* = 7.7, 4.6 Hz, 3H), 7.22 – 7.14 (m, 3H), 7.00 – 6.87 (m, 3H), 5.91 (s, 1H), 5.69 (dt, *J* = 15.6, 6.8 Hz, 1H), 5.52 (d, *J* = 15.7 Hz, 1H), 3.39 (d, *J* = 6.8 Hz, 2H), 1.87 (d, *J* = 1.1 Hz, 6H), 1.08 (s, 3H), 0.85 (s, 3H) ; **^{13}C NMR** (101 MHz, $CDCl_3$) δ 168.8, 143.2, 141.9, 138.5, 130.2 (d, *J* = 8.3 Hz), 128.6, 127.5, 127.2, 126.4, 124.0 (d, *J* = 2.8 Hz), 115.3 (d, *J* = 21.0 Hz), 113.2 (d, *J* = 21.1 Hz), 62.5, 42.8, 39.1, 24.2, 23.1, 22.3, 21.1; **^{19}F NMR** (376 MHz, $CDCl_3$) δ -113.00 (td, *J* = 9.2, 6.1 Hz). **HRMS** (ESI) calculated for $C_{22}H_{27}FNO$ $[M+H]^+$: 340.2071; found: 340.2076. **8f** was determined to be of 92% ee (94% e.s.) by chiral HPLC analysis (CHIRALPAK AD-H, 5% *i*PrOH/hexanes, 1.0 mL/min, 220 nm, t_R(minor) = 10.1 min, t_R(major) = 11.6 min).

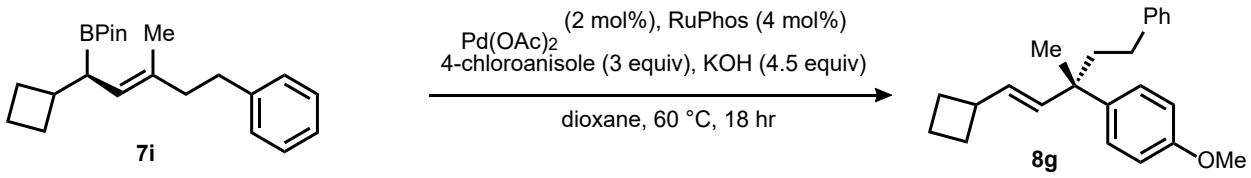

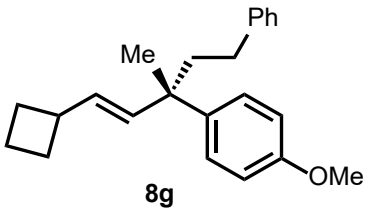

(*S*,*E*)-1-(1-cyclobutyl-3-methyl-5-phenylpent-1-en-3-yl)-4-methoxybenzene (8g): Prepared according to the following method, adapted from a literature procedure reported by Morken and coworkers. A 2-dram vial equipped with a magnetic stir bar was charged with allylic boronic ester **7i** (26.0 mg, 0.0765 mmol, 1 equiv). The vial was sealed with a septum cap and put under an atmosphere of N_2. Dioxane (0.2 mL) was added and the reaction was stirred. A solution of $Pd(OAc)_2$ (0.3 mg, 0.0015 mmol, 2 mol%) and RuPhos (1.4 mg, 0.003 mmol, 4 mol%) in dioxane (0.2 mL, sparged with N_2 for 10 minutes before use) was added to the reaction vial via syringe. 4-chloroanisole (36.4 µL, 0.30 mmol, 3 equiv) and 8.0 M aqueous KOH (43 µL, 0.344 mmol, 4.5 equiv, sparged with N_2 for 30 minutes before use) were added sequentially via syringe. The reaction vessel cap was wrapped with Teflon tape, and then the reaction mixture was heated to 60 °C for 18 hours. The reaction mixture was cooled to room temperature, diluted with Et_2O (2 mL), and filtered through a plug of silica eluting with additional Et_2O (10 mL). The filtrate was concentrated via rotary evaporation and purified by silica gel chromatography on normal silica (0 to 2% Et_2O in hexanes) to afford **8g** as a light yellow oil (20.0 mg, 82%, combined yield of both diastereomers) in 12:1 d.r. (determined by NMR of the crude and purified material; no change to observed d.r. during purification). **^{1}H NMR** (400 MHz, $CDCl_3$, major diastereomer only) δ 7.31 – 7.22 (m, 4H), 7.19 – 7.10 (m, 3H), 6.90 – 6.83 (m, 2H), 5.60 – 5.56 (m, 2H), 3.81 (s, 3H), 2.97 (dtd, *J* = 10.1, 7.8, 4.9 Hz, 1H), 2.49 (td, *J* = 12.9, 12.4, 5.2 Hz, 1H), 2.39 (td, *J* = 13.4, 12.9, 5.0 Hz, 1H), 2.11 (ddd, *J* = 9.6, 5.4, 2.6 Hz, 2H), 2.01 (ddd, *J* =

23.2, 12.1, 4.8 Hz, 2H), 1.93 – 1.74 (m, 4H), 1.41 (s, 3H); **^{13}C NMR** (101 MHz, $CDCl_3$, major diastereomer only) δ 157.5, 143.2, 140.1, 136.7, 132.2, 128.3, 127.7, 125.6, 113.4, 55.2, 44.0, 42.7, 38.6, 31.2, 29.0, 28.9, 25.9, 18.6; **HRMS** (ESI) calculated for $C_{23}H_{29}O$ $[M+H]^+$: 321.2213; found: 321.2215. **8g** was determined to be of 94% ee (99% e.s.) by chiral HPLC analysis (CHIRALPAK IB N-5, 0.3% *i*PrOH/hexanes, 1.0 mL/min, 210 nm, t_R(minor) = 8.2 min, t_R(major) = 7.9 min).

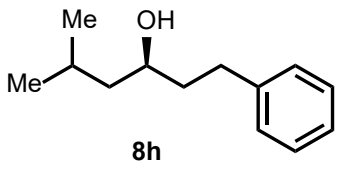

8h

(*S*)-5-methyl-1-phenylhexan-3-ol (8h): To a 1-dram vial equipped with a magnetic stir bar was added **7g** (8.0 mg, 0.026 mmol, 1 equiv), THF (0.2 mL), water (0.2 mL), and sodium perborate tetrahydrate (45 mg, 0.29 mmol, 11 equiv). The vial was capped and let stir at room temperature for 2 hours. Et_2O (1 mL) and water (1 mL) were added, the organic layer removed, and the aqueous layer extracted with Et_2O (2 x 1 mL). The combined organic phases were dried over magnesium sulfate, filtered, and concentrated by rotary evaporation. The crude product was purified using flash column chromatography on normal silica (0 to 30% Et_2O in hexanes) to afford **8h** as a clear oil (4.5 mg, 90% yield). **^{1}H NMR** (400 MHz, $CDCl_3$) δ 7.32 – 7.27 (m, 2H), 7.19 (dd, *J* = 12.4, 7.1 Hz, 3H), 3.72 (s, 1H), 2.80 (ddd, *J* = 15.7, 9.8, 5.9 Hz, 1H), 2.68 (ddd, *J* = 13.7, 9.7, 6.6 Hz, 1H), 1.84 – 1.66 (m, 3H), 1.47 – 1.37 (m, 1H), 1.32 – 1.27 (m, 2H), 0.91 (t, *J* = 6.4 Hz, 6H); **^{13}C NMR** (101 MHz, $CDCl_3$) δ 142.2, 128.4, 125.8, 69.5, 46.9, 39.7, 32.1, 24.7, 23.5, 22.1; **HRMS** (ESI) calculated for $C_{13}H_{21}O$ $[M+HCOO]^-$: 251.1653; found: 251.1654. **8h** was determined to be of 97% ee (100% e.s.) by chiral HPLC analysis (CHIRALPAK OJ-H, 2% *i*PrOH/hexanes, 1.0 mL/min, 210 nm, t_R(minor) = 11.7 min, t_R(major) = 12.4 min).

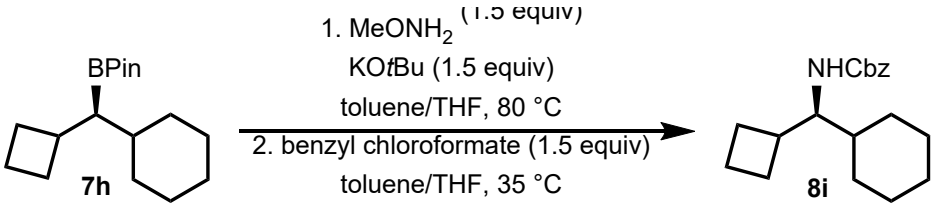

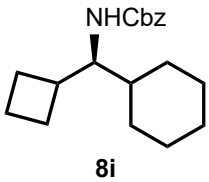

benzyl (*R*)-(cyclobutyl(cyclohexyl)methyl)carbamate (8i): Prepared according to the following method, adapted from a literature procedure reported by Morken and coworkers. An oven-dried 1-dram vial was charged with **7h** (16.7 mg, 0.06 mmol, 1 equiv). The vial was equipped with a magnetic stir bar; the threads were wrapped with Teflon tape; the vial was sealed with a Teflon-coated septum cap; and the reaction was put under a nitrogen atmosphere. The vial was charged with toluene (300 µL), neat (*19*) methoxyamine (5 µL, 0.09 mmol, 1.5 equiv), and a solution of potassium *tert*-butoxide (90 µL, 1 M in THF, 0.09 mmol, 1.5 equiv). The nitrogen line was removed and the vial top was wrapped with electrical tape. The reaction was stirred at 80 °C for 16 hours, then cooled to room temperature. Benzyl chloroformate (13 µL, 0.09 mmol, 1.5 equiv) and additional toluene (200 µL) were added and the reaction was stirred at 35 °C for 2 hours. The reaction mixture was diluted with Et_2O and quenched with 1:1 water:saturated aqueous $NaHCO_3$ (1 mL). The organic and aqueous layers were separated and the aqueous layer was extracted with Et_2O (2 x 2 mL). The combined organic layers were dried over $MgSO_4$, filtered, concentrated under reduced pressure, and purified by flash column chromatography on normal silica (5 to 10% Et_2O/hexanes) to afford **8i** as a white solid (10.4 mg, 58%). **^{1}H NMR** (400 MHz, $CDCl_3$) δ 7.40 – 7.28 (m, 5H), 5.20 – 5.01 (m, 2H), 4.62 – 4.19 (m, 1H), 3.57 – 3.33 (m, 1H), 2.54 – 2.28 (m, 1H), 1.99 – 1.84 (m, 2H), 1.81 – 1.67 (m, 5H), 1.62 (d, *J* = 13.5 Hz, 3H), 1.39 – 1.29 (m, 1H), 1.23 – 1.00 (m, 4H), 0.96 – 0.82 (m, 1H); **^{13}C NMR** (101 MHz, $CDCl_3$) δ 156.9, 136.9, 128.7, 128.2, 66.7, 60.5, 40.7, 38.0,

30.3, 29.9, 28.0, 26.6, 26.5, 26.4, 25.4, 18.1; **HRMS** (ESI) calculated for $C_{19}H_{28}NO_2$ $[M+H]^+$: 302.2115; found: 302.2117. **8i** was determined to be of 96% ee (100% e.s.) by chiral SFC analysis (CHIRALPAK IA, 5% MeOH/CO_2, 5.0 mL/min, 210 nm, t_R(minor) = 4.0 min, t_R(major) = 4.5 min).

Synthesis and Characterization of Other Catalyst Species

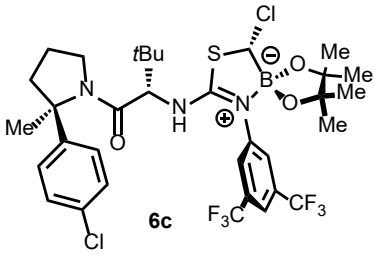

6c

(*S*)-2-(((*R*)-1-(3,5-bis(trifluoromethyl)phenyl)-4-chloro-7,7,8,8-tetramethyl-6,9-dioxa-3-thia-1λ^4-aza-5λ^4-boraspiro[4.4]non-1-en-2-yl)amino)-1-((*R*)-2-(4-chlorophenyl)-2-methylpyrrolidin-1-yl)-3,3-dimethylbutan-1-one (6c): following the procedure for the synthesis of the epimeric species **6a** also resulted in the isolation of **6c** as a white powder (351.0 mg, 23%). **^{1}H NMR** (400 MHz, C_6D_6) δ 7.83 (s, 2H), 7.60 (d, *J* = 8.8 Hz, 3H), 6.85 (dd, *J* = 8.5, 1.4 Hz, 2H), 6.24 (d, *J* = 9.9 Hz, 1H), 4.96 – 4.88 (m, 1H), 3.83 (dd, *J* = 10.2, 1.5 Hz, 1H), 3.37 (dd, *J* = 8.2, 5.2 Hz, 1H), 3.00 (dd, *J* = 8.4, 5.6 Hz, 1H), 1.54 (s, 3H), 1.52 – 0.69 (m, >16H), 0.65 – 0.61 (m, 9H); **^{13}C NMR** (101 MHz, C_6D_6) δ 169.5, 166.7, 143.9, 140.4, 133.4 – 132.2 (m), 128.9, 128.7, 126.0, 124.2, 121.5, 121.3, 80.5, 67.2, 63.1, 49.6, 43.4, 34.8, 26.0, 25.5, 24.2, 22.4; **^{19}F NMR** (376 MHz, C_6D_6) -62.86; **^{11}B NMR** (128 MHz, C_6D_6) δ 12. **HRMS** (ESI) calculated for $C_{33}H_{41}BCl_2F_6N_3O_3S$ $[M+H]^+$: 754.2237; found: 754.2242. $[a]_D^{25} = +47.1°$ (c = 11 mg/mL, CH_2Cl_2). **Note:** we propose that the ^{1}H NMR multiplet from 1.52 – 0.69 ppm integrates to greater than the expected 16H due to difficulties in spectrum baseline correction for this broad multiplet.

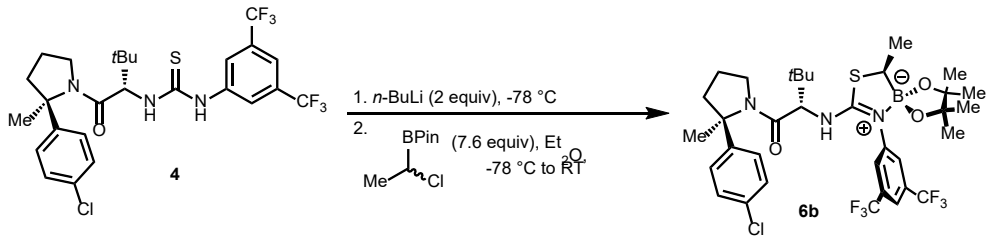

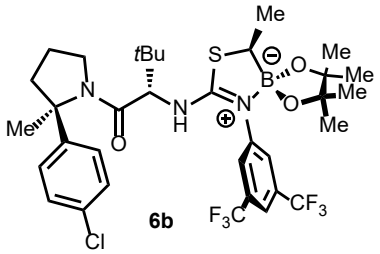

(*S*)-2-(((*R*)-1-(3,5-bis(trifluoromethyl)phenyl)-4,7,7,8,8-pentamethyl-6,9-dioxa-3-thia-1λ^4-aza-5λ^4-boraspiro[4.4]non-1-en-2-yl)amino)-1-((*R*)-2-(4-chlorophenyl)-2-methylpyrrolidin-1-yl)-3,3-dimethylbutan-1-one (6b):

An oven-dried 2-dram vial equipped with a magnetic stir bar, Teflon tape-coated threads, and a Teflon-coated septum cap was put under a nitrogen atmosphere. The vial was charged with dichloromethyl-BPin (**1**) (333 μL, 1.8 mmol, 7.8 equiv) and Et_2O (3 mL) and the reaction mixture was cooled to -78 °C with stirring. A solution of methyllithium (1.35 mL, 1.36 M in Et_2O, 1.83 mmol, 8.0 equiv) was added over 5 minutes, and the reaction mixture was allowed to stir at room temperature for 16 h. A flame-dried 20 mL septum-top vial equipped with a magnetic stir bar was charged with thiourea **4** (133.0 mg, 0.23 mmol, 1 equiv), sealed, and put under a nitrogen atmosphere. The vial was charged with Et_2O (5.75 mL), stirred at room temperature until all solids dissolved, and then cooled to -78 °C with stirring. A solution of *n*-butyllithium (184 μL, 2.5 M in hexanes, 0.46 mmol, 2 equiv) was added at a rate of 1 drop per 2 seconds. The reaction mixture was allowed to stir for 5 minutes. The crude heterogeneous boronic ester mixture at room temperature was cannulated rapidly into the cold thiourea mixture. The 20 mL vial was removed from the cold bath and allowed to stir at room temperature for 1 hour. The reaction mixture was filtered through a pad of normal silica (~ 4 cm thick), rinsing with copious Et_2O, and the filtrate

concentrated under reduced pressure to a yellow oil. Purification by flash column chromatography on normal silica (10 to 35% Et_2O in hexanes) afforded **6b** as a colorless gum; repeated evaporation from pentane converted this material into a white foam that could be crushed into a dry powder (138.0 mg, 82%). **^{1}H NMR** (400 MHz, $CDCl_3$) δ 7.79 (s, 1H), 7.69 (s, 2H), 7.33 – 7.27 (m, 2H), 7.00 – 6.91 (m, 2H), 5.65 (d, *J* = 9.9 Hz, 1H), 4.23 (d, *J* = 9.9 Hz, 1H), 3.92 (ddd, *J* = 9.8, 7.3, 5.3 Hz, 1H), 3.78 (dt, *J* = 9.8, 7.2 Hz, 1H), 2.72 (q, *J* = 7.3 Hz, 1H), 2.06 – 1.87 (m, 4H), 1.76 (s, 3H), 1.45 (d, *J* = 7.4 Hz, 3H), 0.93 (s, 9H), 0.93 – 0.86 (br s, 6H), 0.79 – 0.58 (br s, 6H); **^{13}C NMR** (101 MHz, $CDCl_3$) δ 172.2, 167.1, 143.6, 141.1, 133.2 (q, *J* = 34.0 Hz), 132.6, 128.8, 128.7, 125.8, 122.8 (q, *J* = 273.2 Hz), 121.7 (sept, *J* = 3.9 Hz), 79.4, 67.6, 63.1, 50.2, 44.2, 37.0, 26.7, 26.4, 25.8, 24.7, 22.8, 18.7 [*the carbon attached to boron was not observed due to quadrupolar relaxation*]; **^{11}B NMR** (128 MHz, $CDCl_3$) δ 12; **^{19}F NMR** (376 MHz, $CDCl_3$) δ -63.04; **HRMS** (ESI) calculated for $C_{34}H_{44}BClF_6N_3O_3S$ $[M+H]^+$: 734.2784; found: 734.2790. $[\alpha]_D^{24} = +131.6°$ (c = 10 mg/mL, CH_2Cl_2). A crystal suitable for X-ray diffraction grew spontaneously upon allowing a saturated solution of **6b** in pentane to stand at 0 °C, allowing for the assignment of its structure and absolute configuration (see section **X-Ray Crystallography** for crystallographic details).

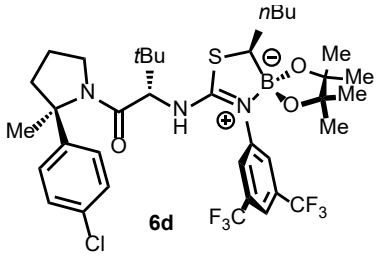

6d

(*S*)-2-(((*R*)-1-(3,5-bis(trifluoromethyl)phenyl)-4-butyl-7,7,8,8-tetramethyl-6,9-dioxa-3-thia-1λ^4-aza-5λ^4-boraspiro[4.4]non-1-en-2-yl)amino)-1-((*R*)-2-(4-chlorophenyl)-2-methylpyrrolidin-1-yl)-3,3-dimethylbutan-1-one (6d): To a round-bottom flask equipped with a magnetic stir bar was added *n*-butyl boronic acid pinacol ester (300 mg, 1.63 mmol, 5 equiv). The flask was capped with a rubber septum and put under an atmosphere of N_2. To the reaction vessel was added Et_2O (16 mL) and dichloromethane (125 μL, 1.96 mmol, 6

equiv), and then the reaction mixture was cooled to -78 °C. A solution of lithium diisopropylamide (1.63 mL, 1.0 M in Et_2O, 1.63 mmol, 5 equiv) was added slowly to the rapidly stirring reaction mixture. The flask was maintained at -78 °C for 5 minutes, then warmed to room temperature and let stir 30 minutes to yield a solution of racemic butyl rearrangement product **5a**. A separate round-bottom flask equipped with a magnetic stir bar was charged with thiourea **4** (189 mg, 0.326 mmol, 1 equiv), capped with a rubber septum, and put under an atmosphere of N_2. THF (3.3 mL) was added, and the reaction mixture was cooled to -78 °C. A solution of *n*-butyllithium (0.26 mL, 2.5M in hexanes, 0.625 mmol, 2 equiv) was slowly added to the stirring reaction mixture. To this solution of deprotonated thiourea at -78 °C was rapidly added the solution of **5a** via syringe. The combined reaction mixture was warmed to room temperature, let stir 30 minutes, and filtered through a pad of normal silica eluting with Et_2O. The filtrate was concentrated by rotary evaporation and purified by flash column chromatography on normal silica (0 to 15% Et_2O / hexanes) to afford diastereomerically pure **6d** as a yellow gum that turned into a white powder upon triple evaporation from pentane (205 mg, 81% yield). **^{1}H NMR** (400 MHz, $CDCl_3$) δ 7.80 (s, 1H), 7.68 (s, 2H), 7.30 (d, *J* = 8.5 Hz, 2H), 6.95 (d, *J* = 8.6 Hz, 2H), 5.62 (d, *J* = 9.9 Hz, 1H), 4.29 (d, *J* = 9.9 Hz, 1H), 3.98 – 3.87 (m, 1H), 3.86 – 3.76 (m, 1H), 2.63 (dd, *J* = 12.3, 2.0 Hz, 1H), 2.15 – 1.99 (m, 3H), 1.99 – 1.84 (m, 2H), 1.76 (s, 3H), 1.64 – 1.43 (m, 3H), 1.41 – 1.30 (m, 2H), 0.94 (s, 18H), 0.68 (s, 6H); **^{13}C NMR** (101 MHz, $CDCl_3$) δ 172.2, 167.0, 143.4, 141.0, 133.1 (q, *J* = 33.9 Hz), 132.5, 128.7, 128.6, 125.7, 122.7 (q, *J* = 273.0 Hz), 121.7, 79.3, 67.5, 63.0, 50.1, 44.1, 37.0, 33.6, 33.2, 26.6, 26.2, 25.7, 24.6, 22.7, 22.5, 14.1 [*the carbon attached to boron was not observed due to quadrupolar relaxation*]; **^{19}F NMR** (376 MHz, $CDCl_3$) δ -63.05; **^{11}B NMR** (128 MHz, $CDCl_3$) δ 12; **HRMS**

(ESI) calculated for $C_{37}H_{50}BClF_6N_3O_3S$ $[M+H]^+$: 776.3259; found: 776.3261. $[a]_D^{24} = +135.6°$ (c =10 mg/mL, CH_2Cl_2).

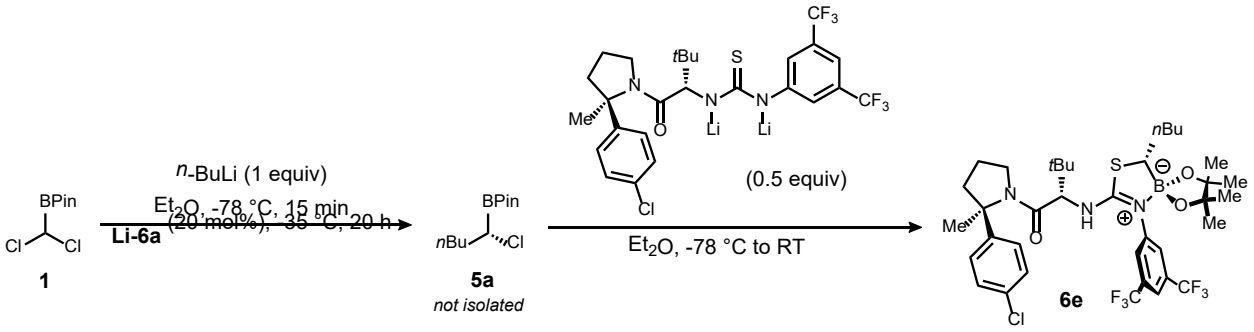

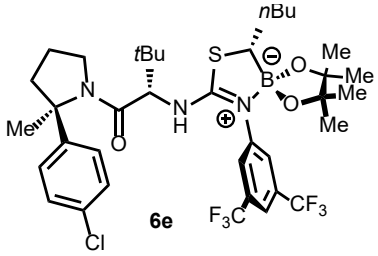

(*S*)-2-(((*S*)-1-(3,5-bis(trifluoromethyl)phenyl)-4-butyl-7,7,8,8-tetramethyl-6,9-dioxa-3-thia-1λ^4-aza-5λ^4-boraspiro[4.4]non-1-en-2-yl)amino)-1-((*R*)-2-(4-chlorophenyl)-2-methylpyrrolidin-1-yl)-3,3-dimethylbutan-1-one (6e): Crude *n*-butyl-substituted chloride product **5a** was prepared according to **General Procedure A** with the following modifications: the reaction was not quenched with NH_4Cl after stirring for 15 minutes at room temperature, and the lithium boronate was prepared as follows. An oven-dried 1-dram vial equipped with a magnetic stir bar, Teflon tape-coated threads, and a Teflon-coated septum cap was put under a nitrogen atmosphere. The vial was charged with dichloromethyl-BPin (**1**) (46.2 µL, 0.25 mmol, 1 equiv) and Et_2O (600 µL) and the reaction mixture was cooled with rapid stirring to -78 °C. A solution of *n*-butyllithium (100 µL, 2.5 M in hexanes, 0.25 mmol, 1 equiv) was added dropwise over 2 minutes. The reaction mixture was stirred at -78 °C for 15 minutes to afford a white suspension of the lithium boronate. The remainder of **General Procedure A** was followed as written. An oven-dried 2-dram vial was charged with thiourea **4** (72.5 mg, 0.125 mmol, 0.5 equiv). The vial was equipped with a magnetic stir bar; the threads were wrapped with Teflon tape; the vial was sealed with a Teflon-coated

septum cap; and the reaction was put under a nitrogen atmosphere. The vial was charged with Et_2O (3 mL) and stirred at room temperature to form a homogeneous solution before being cooled to -78 °C. A solution of *n*-butyllithium (100 µL, 2.5 M in hexanes, 0.25 mmol, 1 equiv) was added dropwise to the stirring thiourea solution over 2 minutes. The reaction mixture was stirred for an additional 5 minutes. The crude heterogeneous boronic ester mixture at room temperature was cannulated rapidly into the cold thiourea mixture. The reaction mixture was removed from the cold bath and allowed to stir at room temperature for 2 hours. The reaction mixture was diluted with Et_2O and quenched with saturated aqueous NH_4Cl (500 µL) and water (500 µL). The organic and aqueous layers were separated and the aqueous layer was extracted with Et_2O (2 x 2 mL). The combined organic layers were dried over $MgSO_4$, filtered, concentrated under reduced pressure, and purified by flash column chromatography on normal silica (EtOAc / hexanes) to afford **6e** as a white foam (26.1 mg, 27% yield relative to **4**). **^{1}H NMR** (400 MHz, $CDCl_3$) δ 7.79 (s, 1H), 7.69 (s, 2H), 7.29 – 7.22 (m, 2H), 7.03 – 6.94 (m, 2H), 5.66 (d, *J* = 9.9 Hz, 1H), 4.25 (d, *J* = 9.9 Hz, 1H), 4.13 – 4.01 (m, 1H), 3.82 (dt, *J* = 9.6, 6.9 Hz, 1H), 2.60 (dd, *J* = 11.9, 2.9 Hz, 1H), 2.23 – 2.08 (m, 1H), 2.06 – 1.91 (m, 4H), 1.78 (s, 3H), 1.64 – 1.38 (m, 5H), 0.97 – 0.91 (m, 12H), 0.90 – 0.65 (m, 12H); **^{13}C NMR** (101 MHz, $CDCl_3$) δ 172.3, 167.3, 143.8, 141.1, 133.1 (q, *J* = 34.5 Hz), 132.6, 128.8, 128.7, 125.7, 122.9 (q, *J* = 272.9 Hz), 121.5, 79.4, 67.5, 63.3, 50.2, 44.3, 36.4, 33.7, 33.2, 26.4, 26.2, 26.1, 24.7, 22.9, 22.6, 14.3 [*the carbon attached to boron was not observed due to quadrupolar relaxation*]; **^{11}B NMR** (128 MHz, $CDCl_3$) δ 12; **^{19}F NMR** (376 MHz, $CDCl_3$) δ -63.00; **HRMS** (ESI) calculated for $C_{37}H_{50}BClF_6N_3O_3S$ $[M+H]^+$: 776.3253; found: 776.3260. $[a]_D^{24} = 0.0°$ (c = 2.5 mg/mL, CH_2Cl_2).

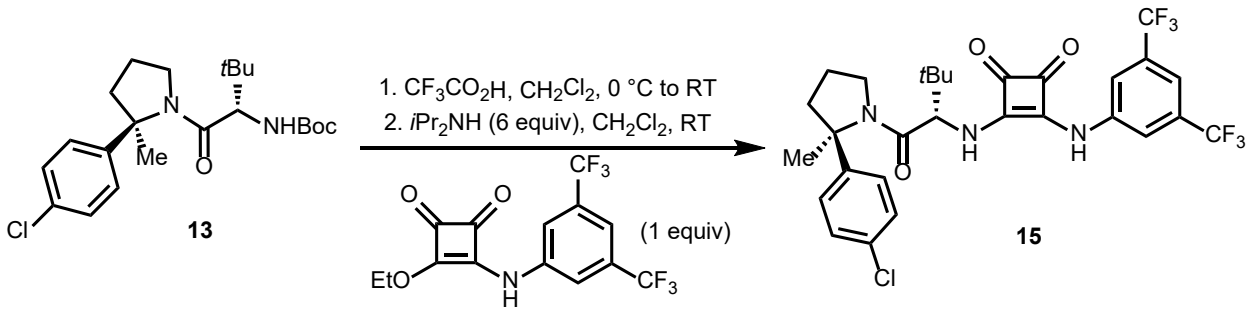

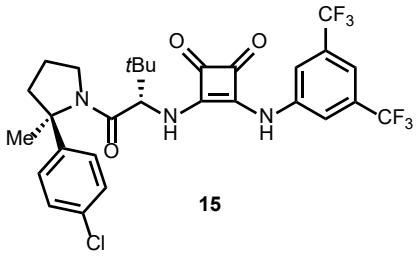

3-((3,5-bis(trifluoromethyl)phenyl)amino)-4-(((*S*)-1-((*R*)-2-(4-chlorophenyl)-2-methylpyrrolidin-1-yl)-3,3-dimethyl-1-oxobutan-2-yl)amino)cyclobut-3-ene-1,2-dione (15):

A 2-dram vial equipped with a magnetic stir bar was charged with **13** (102.2 mg, 0.25 mmol, 1 equiv) and CH_2Cl_2 (1 mL) and the stirring solution was cooled to 0 °C. Neat trifluoroacetic acid (360 µL) was added dropwise over 1 minute and the reaction mixture was allowed to stir at room temperature for 2 hours. The reaction mixture was concentrated under reduced pressure to remove excess trifluoroacetic acid and the residue redissolved in CH_2Cl_2 (1 mL). To the stirring solution of ammonium salt was added *N*,*N*-diisopropylethylamine (261 µL, 1.5 mmol, 6 equiv). The reaction mixture was allowed to stir for 5 minutes before addition of 3-((3,5-bis(trifluoromethyl)phenyl)amino)-4-ethoxycyclobut-3-ene-1,2-dione (88.3 mg, 0.25 mmol, 1 equiv). The reaction mixture was stirred at room temperature for 48 hours, then quenched with aqueous 1 M NaOH (1 mL) and stirred vigorously for 24 hours. The reaction mixture was diluted with CH_2Cl_2, the organic and aqueous layers were separated, and the aqueous layer was extracted with CH_2Cl_2 (2 x 2 mL). The combined organic layers were dried over Na_2SO_4, filtered, concentrated under reduced pressure, and purified by flash column chromatography on normal silica (Et_2O / hexanes) to afford **15** as a white powder (116.6 mg, 76%). **^{1}H NMR** (400 MHz, CD_3OD) δ 8.10 (s, 2H), 7.51 (s, 1H), 7.22 (s, 4H), 5.16 (s, 1H), 4.28 (ddd, *J* = 12.1, 7.4, 4.6 Hz,

1H), 3.91 (dt, J = 10.0, 7.4 Hz, 1H), 2.19 – 2.07 (m, 1H), 2.07 – 1.92 (m, 3H), 1.90 (s, 3H), 1.11 (s, 9H); **^{13}C NMR** (101 MHz, CD_3OD) δ 185.8, 182.3, 170.6, 169.8, 164.4, 146.0, 142.4, 133.9 (q, J = 33.6 Hz), 132.9, 129.2, 127.8, 124.6 (q, J = 271.8 Hz), 119.1 (d, J = 3.7 Hz), 116.5 (t, J = 3.5 Hz), 68.7, 63.6, 51.5, 45.4, 37.2, 26.5, 25.1, 23.5; **^{19}F NMR** (376 MHz, CD_3OD) δ -60.69; **HRMS** (ESI) calculated for $C_{29}H_{29}ClF_6N_3O_3$ $[M+H]^+$: 616.1796; found: 616.1798. $[a]_D^{24} = +9.2°$ (c =10 mg/mL, CH_2Cl_2).

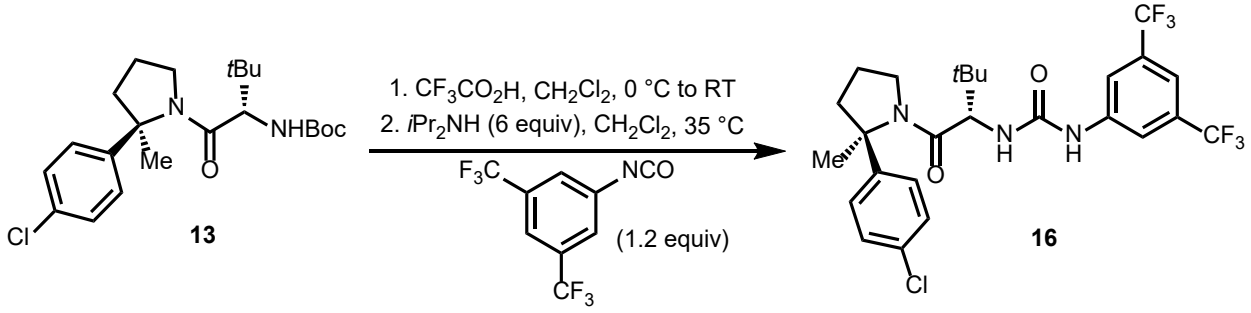

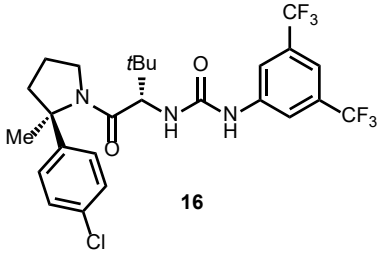

1-(3,5-bis(trifluoromethyl)phenyl)-3-((*S*)-1-((*R*)-2-(4-chlorophenyl)-2-methylpyrrolidin-1-yl)-3,3-dimethyl-1-oxobutan-2-yl)urea (16): A 2-dram vial equipped with a magnetic stir bar was charged with **13** (102.2 mg, 0.25 mmol, 1 equiv) and CH_2Cl_2 (1 mL) and the stirring solution was cooled to 0 °C. Neat trifluoroacetic acid (360 μL) was added dropwise over 1 minute and the reaction mixture was allowed to stir at room temperature for 2 hours. The reaction mixture was concentrated under reduced pressure to remove excess trifluoroacetic acid and the residue redissolved in CH_2Cl_2 (1 mL). To the stirring solution of ammonium salt was added *N*,*N*-diisopropylethylamine (261 μL, 1.5 mmol, 6 equiv). The reaction mixture was allowed to stir for 5 minutes before addition of 3,5-bis(trifluoromethyl)phenyl isocyanate (52 μL, 0.30 mmol, 1.2 equiv). The reaction mixture was stirred at 35 °C for 16 hours, then concentrated under reduced pressure. The residue was purified by flash column chromatography on normal silica (Et_2O / hexanes) to afford **16** as a white foam

(119.2 mg, 85%). **^{1}H NMR** (400 MHz, $CDCl_3$) δ 8.12 (s, 1H), 7.69 (s, 2H), 7.49 (s, 1H), 6.95 (s, 4H), 6.16 (s, 1H), 4.70 (d, *J* = 9.8 Hz, 1H), 4.29 – 4.09 (m, 1H), 3.88 (dt, *J* = 10.0, 7.0 Hz, 1H), 2.10 – 1.90 (m, 3H), 1.87 (s, 3H), 1.86 – 1.79 (m, 1H), 1.10 (s, 9H); **^{13}C NMR** (101 MHz, $CDCl_3$) δ 170.8, 155.7, 144.1, 140.6, 132.4 (q, *J* = 33.4 Hz), 132.0, 128.2, 126.1, 123.3 (q, *J* = 273.0 Hz), 119.4, 116.3, 67.4, 58.6, 50.5, 44.5, 35.5, 26.6, 25.0, 22.7; **^{19}F NMR** (376 MHz, $CDCl_3$) δ -62.92; **HRMS** (ESI) calculated for $C_{26}H_{29}ClF_6N_3O_2$ $[M+H]^+$: 564.1847; found: 564.1848. $[\alpha]_D^{24}$ = -61.4° (c = 10 mg/mL, CH_2Cl_2).

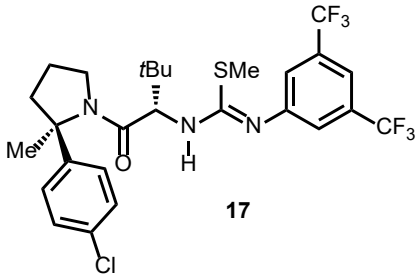

17

methyl (*Z*)-*N*'-(3,5-bis(trifluoromethyl)phenyl)-*N*-((*S*)-1-((*R*)-2-(4-chlorophenyl)-2-methylpyrrolidin-1-yl)-3,3-dimethyl-1-oxobutan-2-yl)carbamimidothioate (17): A round-bottom flask equipped with a magnetic stir bar was charged with thiourea **4** (99 mg, 0.17 mmol, 1 equiv), capped with a rubber septum, and put under an atmosphere of N_2. DMF (1.5 mL) was added, the rubber septum was briefly removed, potassium carbonate (46 mg, 0.33 mmol, 2 equiv) was added, and the rubber septum was replaced. Iodomethane (13 µL, 21 mmol, 1.2 equiv) was added to the stirring reaction mixture via syringe. The reaction mixture was warmed to room temperature and let stir overnight. To the reaction flask was added brine (5 mL) and Et_2O (10 mL). The organic phase was removed, and the aqueous phase was extracted with Et_2O (2 x 10 mL). The combined organic phases were washed with brine (2 x 5 mL), dried over magnesium sulfate, filtered, and evaporated to yield a yellow oil. Flash column chromatography on normal silica (5 to 13% EtOAc / hexanes) afforded **17** as a white powder (79 mg, 78% yield). **^{1}H NMR** (400 MHz, $CDCl_3$) δ 7.47 (s, 1H), 7.30 (s, 2H), 7.15 (d, *J* = 8.6 Hz, 2H), 7.06 (d, *J* = 8.6 Hz, 2H), 5.17 (d, *J* = 8.1 Hz, 1H), 4.68 (d, *J* = 7.3 Hz, 1H), 4.26 – 4.18 (m, 1H), 3.73 (q, *J* = 8.7 Hz, 1H), 2.27 (s, 3H), 1.94 (ddt, *J* = 23.5, 12.4, 6.1

Hz, 2H), 1.83 (s, 3H), 1.82 – 1.69 (m, 2H), 1.06 (s, 9H); **^{13}C NMR** (101 MHz, $CDCl_3$) δ 169.8, 155.9, 151.1, 144.4, 132.1 (q, J = 33.1 Hz), 132.0, 128.3, 126.2, 123.5 (q, J = 272.8 Hz), 122.6, 117.8 – 115.3 (m), 67.4, 60.3, 49.9, 44.4, 35.2, 26.7, 25.3, 22.4, 14.0; **^{19}F NMR** (376 MHz, $CDCl_3$) δ -62.83; **HRMS** (ESI) calculated for $C_{27}H_{31}ClF_6N_3OS$ $[M+H]^+$: 594.1781; found: 594.1782. $[a]_D^{24}$ = -105.4° (c =10 mg/mL, CH_2Cl_2).

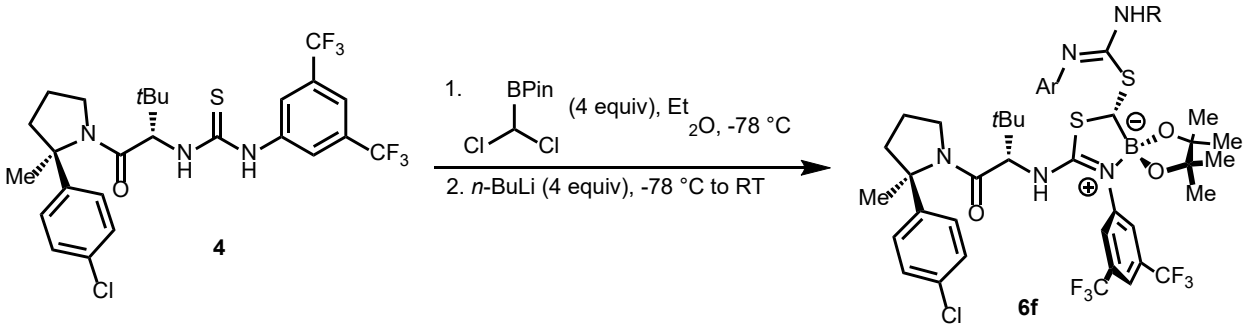

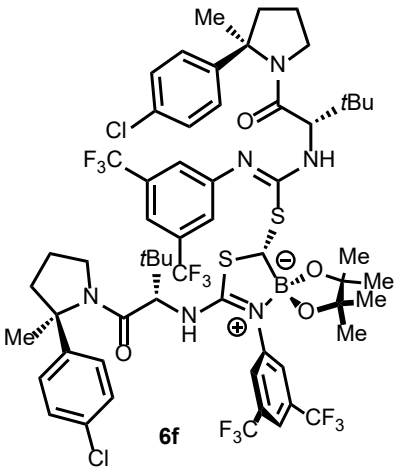

(*R*)-1-(3,5-bis(trifluoromethyl)phenyl)-2-(((*S*)-1-((*R*)-2-(4-chlorophenyl)-2-methylpyrrolidin-1-yl)-3,3-dimethyl-1-oxobutan-2-yl)amino)-7,7,8,8-tetramethyl-6,9-dioxa-3-thia-1λ^4-aza-5λ^4-boraspiro[4.4]non-1-en-4-yl (*Z*)-*N*'-(3,5-bis(trifluoromethyl)phenyl)-*N*-((*S*)-1-((*R*)-2-(4-chlorophenyl)-2-methylpyrrolidin-1-yl)-3,3-dimethyl-1-oxobutan-2-yl)carbamimidothioate (6f): A flame-dried 20 mL septum-top vial equipped with a magnetic stir bar was charged with thiourea **4** (200.0 mg, 0.345 mmol, 1 equiv), sealed, and put under a nitrogen atmosphere. The vial was charged with dichloromethyl-BPin (**1**) (255 µL, 1.38 mmol, 4 equiv) and Et_2O (9 mL), stirred at room temperature until all solids dissolved, and then cooled to -78 °C with stirring. A solution of *n*-butyllithium (563 µL, 2.45 M in hexanes, 1.38 mmol, 4 equiv) was added in one portion. The reaction mixture was removed from the cold bath and allowed to stir at room temperature for 30

minutes. The reaction mixture was filtered through a pad of normal silica (~ 4 cm thick), rinsing with copious Et_2O, and the filtrate concentrated to a yellow oil. Purification by flash column chromatography on normal silica (EtOAc/hexanes) afforded crude **6f** as an inseparable mixture with several unidentified thiourea-derived compounds. A crystal suitable for X-ray diffraction grew spontaneously upon allowing a solution of this crude mixture in Et_2O to stand at 0 °C, allowing for the assignment of its structure and absolute configuration (see section **X-Ray Crystallography** for crystallographic details). **HRMS** (ESI) calculated for $C_{59}H_{68}BCl_2F_{12}N_6O_4S_2$ $[M+H]^+$: 1297.4016; found: 1297.4025.

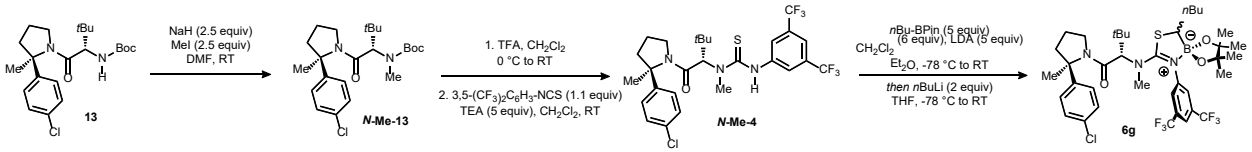

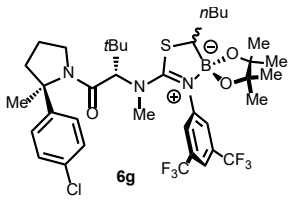

(2*S*)-2-((1-(3,5-bis(trifluoromethyl)phenyl)-4-butyl-7,7,8,8-tetramethyl-6,9-dioxa-3-thia-1λ^4-aza-5λ^4-boraspiro[4.4]non-1-en-2-yl)(methyl)amino)-1-((*R*)-2-(4-chlorophenyl)-2-methylpyrrolidin-1-yl)-3,3-dimethylbutan-1-one (6g):

A 2-dram vial equipped with a magnetic stir bar was charged with **13** (102 mg, 0.25 mmol, 1 equiv), capped with a septum top, and put under an atmosphere of N_2. To the vial was added DMF (2 mL) and sodium hydride (25 mg, 60% by weight in mineral oil, 0.625 mmol, 2.5 equiv), and the reaction mixture was let stir for 30 minutes. Iodomethane was added via syringe (39 µL, 0.625 mmol, 2.5 equiv), and the reaction was let stir overnight. The reaction was cooled to 0 °C, after which saturated aqueous ammonium chloride (1 mL), brine (1 mL), and Et_2O (4 mL) were added. The organic layer was separated, and the aqueous layer was extracted with Et_2O (2 x

2mL). The combined organic layers were washed with brine (2 x 2 mL), dried over magnesium sulfate, filtered, and concentrated by rotary evaporation to yield crude ***N*-Me-13** (87 mg).

A round-bottom flask equipped with a magnetic stir bar was charged with ***N*-Me-13** (87 mg, 0.206 mmol, 1 equiv) and CH_2Cl_2 (1 mL) and the stirring solution was cooled to 0 °C. Neat trifluoroacetic acid (0.3 mL) was added over 2 minutes and the reaction mixture was allowed to stir at room temperature for 2 hours. The reaction mixture was concentrated under reduced pressure to remove excess trifluoroacetic acid and the residue redissolved in CH_2Cl_2 (1 mL). The reaction mixture was cooled to 0 °C. To this stirring solution of ammonium salt was added triethylamine (140 µL, 0.725 mmol, 5 equiv). The reaction mixture was allowed to stir for 5 minutes before addition of 3,5-bis(trifluoromethyl)phenyl isothiocyanate (41 µL, 0.227 mmol, 1.1 equiv). The reaction mixture was stirred at room temperature for 16 hours, then quenched with 1:1 water:brine. The organic and aqueous layers were separated, and the aqueous layer was extracted with CH_2Cl_2 (3 x 2 mL). The combined organic layers were dried over magnesium sulfate, filtered, concentrated, and partially purified by flash column chromatography on normal silica (15% EtOAc / hexanes) to afford ***N*-Me-4** as a semi-crude powder (83 mg).

To a round-bottom flask equipped with a magnetic stir bar was added *n*-butyl boronic acid pinacol ester (149 µL, 0.7 mmol, 5 equiv). The flask was capped with a rubber septum and put under an atmosphere of N_2. To the reaction vessel was added Et_2O (1.4 mL) and dichloromethane (54 µL, 0.84 mmol, 6 equiv), and then the reaction mixture was cooled to -78 °C. A solution of lithium diisopropylamide (0.7 mL, 1.0 M in Et_2O, 0.7 mmol, 5 equiv) was added slowly to the rapidly stirring reaction mixture. The flask was maintained at -78 °C for 5 minutes, then warmed to room temperature and let stir 30 minutes to yield a solution of racemic butyl rearrangement product **5a**. A separate round-bottom flask equipped with a magnetic stir bar

was charged with semi-crude ***N*-Me-4** (83 mg, 0.14 mmol, 1 equiv), capped with a rubber septum, and put under an atmosphere of N_2. THF (1 mL) was added, and the reaction mixture was cooled to -78 °C. A solution of *n*-butyllithium (56 μL, 2.5 M in hexanes, 0.14 mmol, 1 equiv) was slowly added to the stirring reaction mixture. To this solution of deprotonated thiourea at -78 °C was rapidly added the solution of **5a** via syringe. The combined reaction mixture was warmed to room temperature, let stir 30 minutes, and filtered through a pad of normal silica eluting with Et_2O. The filtrate was concentrated by rotary evaporation, affording crude product in a 1.2:1 mixture of epimers at the carbon geminal to boron. Flash column chromatography on normal silica (0 to 15% Et_2O in hexanes) afforded diastereomerically pure **6g** as a yellow gum (26.5 mg, 24% yield; carbon stereochemistry geminal to boron unknown). **^{1}H NMR** (400 MHz, $CDCl_3$) δ 7.75 (d, *J* = 3.3 Hz, 3H), 7.24 (s, 2H), 7.05 (d, *J* = 8.6 Hz, 2H), 4.76 (s, 1H), 4.26 (dt, *J* = 10.4, 6.4 Hz, 1H), 3.90 – 3.78 (m, 1H), 2.63 (s, 3H), 2.59 – 2.48 (m, 1H), 2.00 (td, *J* = 13.0, 11.6, 7.1 Hz, 4H), 1.82 (s, 3H), 1.61 (s, 2H), 1.44 – 1.31 (m, 4H), 1.06 (s, 9H), 1.04 (s, 6H), 0.94 (t, *J* = 6.9 Hz, 3H), 0.71 (s, 6H); **^{13}C NMR** (101 MHz, $CDCl_3$) δ 174.8, 165.8, 145.1, 144.4, 132.2, 131.8 (q, *J* = 33.6 Hz), 128.5, 128.4, 125.8, 122.9 (q, *J* = 272.8 Hz), 120.1, 79.7, 68.1, 50.2, 44.3, 40.2, 38.8, 33.4, 33.3, 29.7, 27.8, 26.8, 26.2, 24.2, 22.9, 22.6, 14.1; **^{19}F NMR** (376 MHz, $CDCl_3$) δ -82.86; **^{11}B NMR** (128 MHz, $CDCl_3$) δ 14; **HRMS** (ESI) calculated for $C_{38}H_{52}BClF_6N_3O_3S$ $[M+H]^+$: 790.3410; found: 790.3419. $[\alpha]_D^{24} = +119.6°$ (c = 10 mg/mL, CH_2Cl_2).

Catalyst Optimization Studies

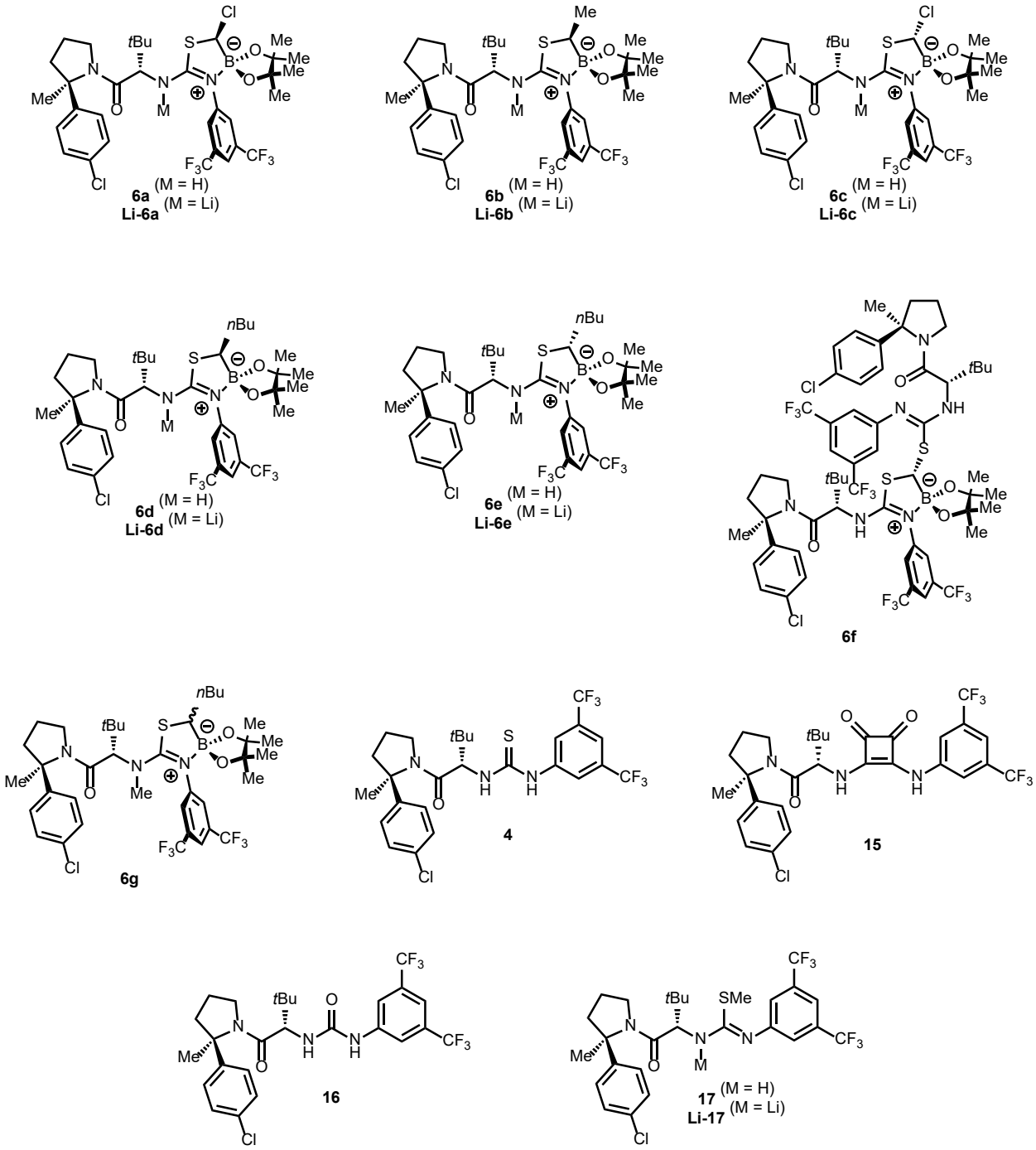

Figure 2.38 All catalyst species synthesized in this work.

General Procedure F: An oven-dried 1-dram vial equipped with a magnetic stir bar and a Teflon-coated septum cap was put under a nitrogen atmosphere. The vial was charged with dichloromethyl-BPin (**1**) (23.1 μL, 0.125 mmol, 1 equiv) and Et_2O (375 μL) and the reaction mixture was cooled with rapid stirring to -78 °C. A solution of *n*-butyllithium (2.5 M in hexanes, **X** equiv) was added in one portion over 15 seconds. The reaction mixture was stirred at -78 °C for **T** minutes to afford a white suspension of lithium boronate **3a**. A solution of **catalyst** (20 mol%) in Et_2O (250 μL) at 0 °C was added to the cold suspension of **3a** and the reaction mixture was stirred for 5 minutes before being transferred to a -35 °C cryocool to stir for 16 hours. The reaction vial was removed from the cold bath and allowed to stir at room temperature for 15 minutes. Dodecane (25 μL) was injected into the reaction vial as internal standard and the heterogeneous mixture shaken to mix thoroughly. The reaction vial was opened and the mixture was diluted with hexanes (1 mL), filtered through a syringe filter to afford a clear solution, and subjected to chiral GC analysis to assess conversion of **1**, yield of **5a**, and ee of **5a**.

General Procedure G: An oven-dried 1-dram vial was charged with solid **catalyst** (20 mol%). The vial was equipped with a magnetic stir bar and a Teflon-coated septum cap and put under a nitrogen atmosphere. The vial was charged with dichloromethyl-BPin (**1**) (23.1 μL, 0.125 mmol, 1 equiv) and Et_2O (625 μL) and the reaction mixture was cooled with rapid stirring to -78 °C. A solution of *n*-butyllithium (2.5 M in hexanes, **X** equiv) was added dropwise over 2 minutes. The reaction mixture was stirred at -78 °C for **T** minutes to afford a white suspension of lithium boronate **3a**. The reaction vial was transferred to a -35 °C cryocool and allowed to stir for 16 hours. The reaction vial was removed from the cold bath and allowed to stir at room temperature for 15 minutes. Dodecane (25 μL) was injected into the reaction vial as internal standard and the heterogeneous mixture shaken to mix thoroughly. The reaction vial was opened and the mixture

was diluted with hexanes (1 mL), filtered through a syringe filter to afford a clear solution, and subjected to chiral GC analysis to assess conversion of **1**, yield of **5a**, and ee of **5a**.

General Procedure H: General Procedure A was followed using **2a** (26.6 µL, 0.125 mmol, 1 equiv), 1 equivalent of LDA, and a specified **catalyst** (20 mol%) up until the reaction vial was removed from the -35 °C cooling bath. After stirring at room temperature for 15 minutes, dodecane (25 µL) was injected into the reaction vial as internal standard and the heterogeneous mixture shaken to mix thoroughly. The reaction vial was opened and the mixture was diluted with hexanes (1 mL), filtered through a syringe filter to afford a clear solution, and subjected to chiral GC analysis to assess conversion of **2a**, yield of **5a**, and ee of **5a**.

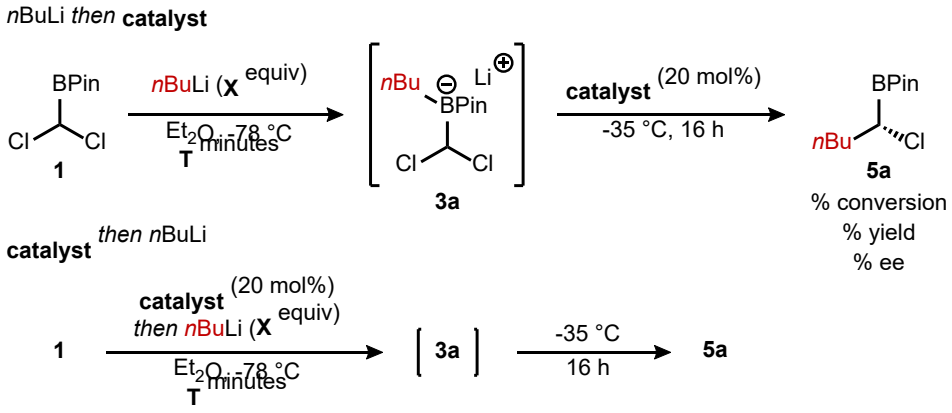

Table 2.4 Catalyst optimization using *n*-butyllithium to form boronate. For the order of addition "*n*BuLi *then* **catalyst**", **General Procedure F** was followed. For the order of addition "**catalyst** *then* *n*BuLi", **General Procedure G** was followed.

entry	order of addition	catalyst	X	T	% conversion	% yield	% ee
1	*n*BuLi *then* **catalyst**	**4**	0.96	0.33	88	78	66
2	*n*BuLi *then* **catalyst**	**4**	0.96	5	93	78	48
3	**catalyst** *then* *n*BuLi	**4**	0.96	5	88	68	92
4	**catalyst** *then* *n*BuLi	**4**	1.20	5	97	62	94

5	*n*BuLi *then* **catalyst**	**16**	0.96	5	98	89	48
6	*n*BuLi *then* **catalyst**	**15**	0.96	5	99	89	5
7	*n*BuLi *then* **catalyst**	**6a**	0.96	5	86	86	26
8	*n*BuLi *then* **catalyst**	**6a**	1.00	15	90	83	21
9	**catalyst** *then* *n*BuLi	**6a**	1.00	5	91	74	94
10	*n*BuLi *then* **catalyst**	**6d**	0.96	15	93	88	10
11	*n*BuLi *then* **catalyst**	**6g**	0.96	15	87	71	0
12	*n*BuLi *then* **catalyst**	**Li-6a**	1.00	15	97	86	94

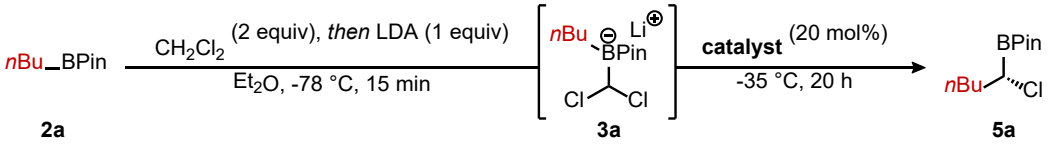

Table 2.5. Catalyst optimization using dichloromethyllithium to form boronate. All reactions were conducted according to **General Procedure H**.

entry	catalyst	% conversion	% yield	% ee
1	**Li-6a**	89	76	95
2	**Li-6b**	90	79	87
3	**Li-6c**	90	75	91
4	**Li-6d**	95	81	88
5	**Li-6e**	80	45	24
6	**Li-17**	94	88	6

Gutmann–Beckett Analysis

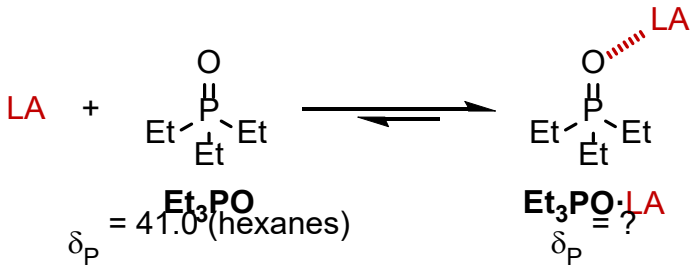

Figure 2.39 Gutmann–Beckett analysis

Preparation of solutions of Et_3PO in Et_2O: In a nitrogen-filled glovebox, a flame-dried 2-mL volumetric flask was charged with the appropriate amount of triethylphosphine oxide (Et_3PO) (*note: Et_3PO is very hygroscopic/deliquescent*), and the flask was capped with a septum top and removed from the glovebox. The flask was put under positive nitrogen pressure, and Et_2O was added via syringe to bring the total volume to 2 mL.

Preparation of capillary tube standard: To a capillary tube with one end sealed was added by syringe a solution of triphenylphosphine in C_6D_6 to fill the tube ¾ of the way. The open end of the tube was then sealed using a blowtorch. The tubes were tested for full closure by placing under high vacuum; capillary tubes that did not leak were used as pseudo-internal standards for locking/shimming NMR samples and for referencing the phosphorus spectra in the Gutmann–Beckett NMR experiments.

General details: NMR samples were locked and shimmed using C_6D_6 as a reference signal; spectra were acquired using ^{1}H-decoupled ^{31}P experiments using 16 scans with 5 second relaxation delays on a Bruker AVANCE NEO 400. Spectra were referenced to triphenylphosphine at -5.3 ppm. Spectra were acquired at various ratios of Lewis acid (LA) to Et_3PO; the acceptor number calculated for each Lewis acid was derived from the sample

featuring the largest downfield shift in the phosphorus spectrum (*note: concentration and ratio had minimal impact on calculated acceptor number so long as [LA] ≥ [Et_3PO]*) and rounded to the closest integer. The acceptor number (AN) formula is as follows, where $\delta_{P(new)}$ is the measured chemical shift of the Lewis acid-triethylphosphine oxide complex:

$$AN = 2.22 * (\delta_{P(new)} - 41.0)$$

Equation 1. Acceptor number formula

Analysis of Li-6a: A flame-dried 1-mL volumetric flask was charged with **6a** (53.2 mg, 0.0721 mmol), capped with a septum top, and put under an atmosphere of N_2. Et_2O was added until the total volume reached 1 mL, yielding a 0.072 M solution of **6a**. A 0.072 M solution of Et_3PO in Et_2O was prepared as described above. A flame-dried NMR tube equipped with a septum top and a capillary tube containing triphenylphosphine in C_6D_6 was placed under a N_2 atmosphere and charged with varying amounts of the **6a** solution (0.072 M in Et_2O), Et_3PO solution (0.072 M in Et_2O), and LiHMDS solution (1.0 M in toluene) to reach the desired concentrations with a total volume of 500 μL. The NMR tube was then sealed by melting the end with a blowtorch to minimize contamination by air or water during the course of the experiment. The spectra were then acquired as described above.

Table 2.6 Gutmann–Beckett analysis of **Li-6a**

[**Li-6a**] (mM)	[Et_3PO] (mM)	$\delta_{P(new)}$	AN
36	**36**	**57.5**	**37**
36	9.0	57.4	36
36	4.5	57.4	36

Analysis of $LiB(C_6F_5)_4$: In a nitrogen-filled glovebox, a flame-dried 1-mL volumetric flask was charged with $LiB(C_6F_5)_4$ (40.8 mg, 0.0468 mmol), capped with a septum top, and removed from the glovebox. Et_2O was added until the total volume reached 1 mL, yielding a 0.0468 M solution of $LiB(C_6F_5)_4$. A 0.156 M solution of Et_3PO in Et_2O was prepared as described above. A flame-dried NMR tube equipped with a septum top and a capillary tube containing triphenylphosphine in C_6D_6 was placed under a N_2 atmosphere and charged with varying amounts of the $LiB(C_6F_5)_4$ solution (0.156 M in Et_2O), Et_3PO solution (0.156 M in Et_2O), and Et_2O to reach the desired concentrations with a total volume of 650 μL. The NMR tube septum top was then wrapped in a layer of parafilm and the spectra were acquired as described above.

Table 2.7 Gutmann–Beckett analysis of $LiB(C_6F_5)_4$

$[LiB(C_6F_5)_4]$ (mM)	$[Et_3PO]$ (mM)	$\delta_{P(new)}$	AN
36	**36**	**59.0**	**40**
36	9.0	59.0	40

Analysis of $LiNTf_2$: In a nitrogen-filled glovebox, a flame-dried 1-mL volumetric flask was charged with $LiNTf_2$ (13.4 mg, 0.0468 mmol), capped with a septum top, and removed from the glovebox. Et_2O was added until the total volume reached 1 mL, yielding a 0.0468 M solution of $LiNTf_2$. A 0.156 M solution of Et_3PO in Et_2O was prepared as described above. A flame-dried NMR tube equipped with a septum top and a capillary tube containing triphenylphosphine in C_6D_6 was placed under a N_2 atmosphere and charged with varying amounts of the $LiNTf_2$ solution (0.156 M in Et_2O), Et_3PO solution (0.156 M in Et_2O), and Et_2O to reach the desired concentrations with a total volume of 650 μL. The NMR tube septum top was then wrapped in a layer of parafilm and the spectra were acquired as described above.

Table 2.8 Gutmann–Beckett analysis of $LiNTf_2$

[$LiNTf_2$] (mM)	[Et_3PO] (mM)	$\delta_{P(new)}$	AN
36	36	57.1	36
36	**9.0**	**57.2**	**36**

Analysis of LiHMDS: In a nitrogen-filled glovebox, a flame-dried 5-mL volumetric flask was charged with LiHMDS (39.1 mg, 0.234 mmol), capped with a septum top, and removed from the glovebox. Et_2O was added until the total volume reached 5 mL, yielding a 0.0468 M solution of LiHMDS. A 0.156 M solution of Et_3PO in Et_2O was prepared as described above. A flame-dried NMR tube equipped with a septum top and a capillary tube containing triphenylphosphine in C_6D_6 was placed under a N_2 atmosphere and charged with varying amounts of the LiHMDS solution (0.0468 M in Et_2O), Et_3PO solution (0.156 M in Et_2O), and Et_2O to reach the desired concentrations with a total volume of 650 μL. The NMR tube septum top was then wrapped in a layer of parafilm and the spectra were acquired as described above.

Table 2.9 Gutmann–Beckett analysis of LiHMDS

[LiHMDS] (mM)	[Et_3PO] (mM)	$\delta_{P(new)}$	AN
36	36	54.8	31
180	36	55.7	33
36	**9.0**	**55.8**	**33**
36	4.5	55.6	32
36	2.3	55.6	32

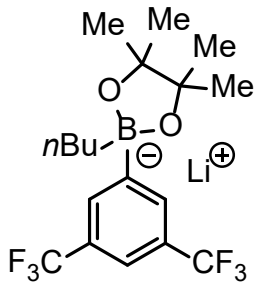

Li-9

Analysis of lithium boronate substrate mimic Li-9: A flame-dried 1-mL volumetric flask was charged with 2-(3,5-bis(trifluoromethyl)phenyl)-4,4,5,5-tetramethyl-1,3,2-dioxaborolane (15.9 mg, 0.0468 mmol), capped with a septum top, and put under an atmosphere of N_2. Et_2O (0.5 mL) was added, followed by a solution of *n*-butyllithium (18.7 μL, 2.5 M in hexanes, 0.0468 mmol), and additional Et_2O until the total volume reached 1 mL, yielding a 0.0468 M solution of boronate **Li-9**. A 0.156 M solution of Et_3PO in Et_2O was prepared as described above. A flame-dried NMR tube equipped with a septum top and a capillary tube containing triphenylphosphine in C_6D_6 was placed under a N_2 atmosphere and charged with varying amounts of the **Li-9** solution (0.156 M in Et_2O), Et_3PO solution (0.072 M in Et_2O), and Et_2O to reach the desired concentrations with a total volume of 650 μL. The NMR tube septum top was then wrapped in a layer of parafilm and the spectra were acquired as described above.

Table 2.10 Gutmann–Beckett analysis of lithium boronate substrate mimic **Li-9**

[**Li-9**] (mM)	[Et_3PO] (mM)	$\delta_{P(new)}$	AN
36	36	56.0	33
36	9.0	57.8	37
36	**4.5**	**58.1**	**38**
36	2.3	57.9	38

ReactIR study. Procedure: A heatgun-dried three-necked 25-mL round-bottom flask equipped with a magnetic stir bar and a ReactIR probe was put under an atmosphere of argon. The vessel was charged with Et_2O (1.5 mL) and cooled to 0 °C with stirring. A blank spectrum was acquired, and then sample data acquisition was begun, with scans taken 15 seconds apart. A

solution of **6a** (71.0 mg, 0.094 mmol, 1 equiv) in Et_2O (188 µL) was added to the reaction vessel 75 seconds into the experiment. A solution of LiHMDS (190 µL, 0.5 M in Et_2O, 0.095 mmol, 1.01 equiv) was added 285 seconds into the experiment. A solution of HCl (47.5 µL, 2.0 M in Et_2O, 0.095 mmol, 1.01 equiv) was added 690 sec into the experiment.

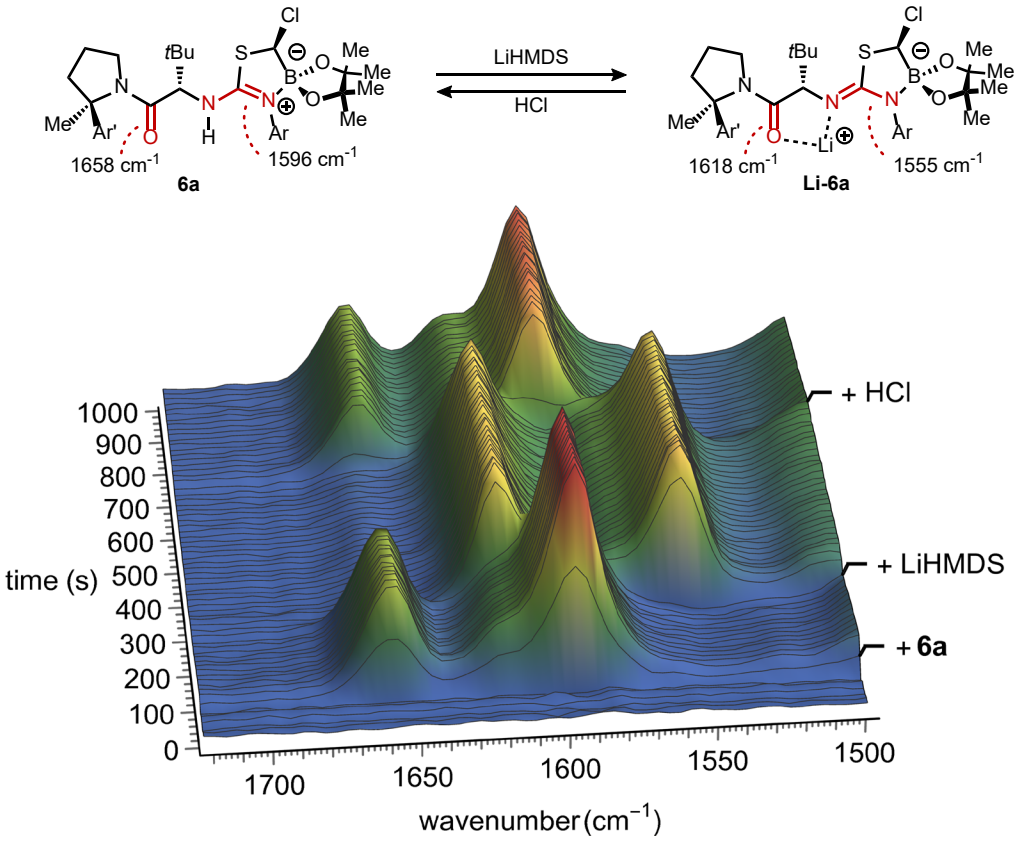

Figure 2.40 3D plot of ReactIR study of the deprotonation and reprotonation of **6a**.

X-Ray Crystallography

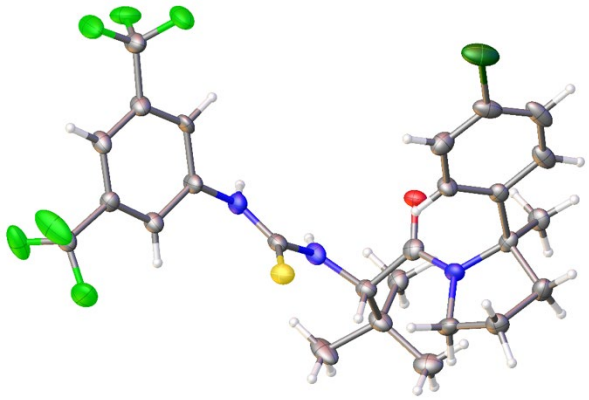

Figure 2.41 Crystal structure of **4a**

X-ray Crystallography: A crystal mounted on a diffractometer was collected data at 100 K. The intensities of the reflections were collected by means of a Bruker APEX II CCD diffractometer ($Mo K_\alpha$ radiation, λ=0.71073 Å), and equipped with an Oxford Cryosystems nitrogen flow apparatus. The collection method involved 0.5° scans in ω at 28° in 2θ. Data integration down to 0.78 Å resolution was carried out using SAINT V8.37A with reflection spot size optimization. Absorption corrections were made with the program TWINABS. The structure was solved by the Intrinsic Phasing methods and refined by least-squares methods again F^2 using SHELXT-2014 and SHELXL-2014 with OLEX2 interface. Non-hydrogen atoms were refined anisotropically, and hydrogen atoms were allowed to ride on the respective atoms. Crystal data as well as details of data collection and refinement are summarized in Table S8, geometric parameters are shown in Table S9, and hydrogen-bond parameters are listed on Table S10. The Ortep plots were produced with the SHELXL-2014 program, and the other drawings were produced with Accelrys DS Visualizer 2.0.

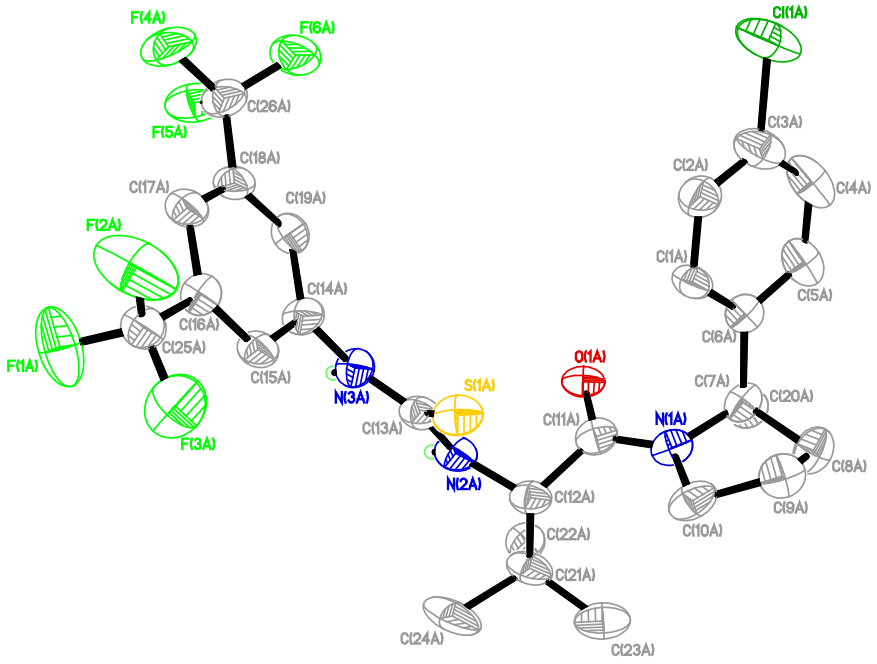

Figure 2.42 Perspective views showing 50% probability displacement

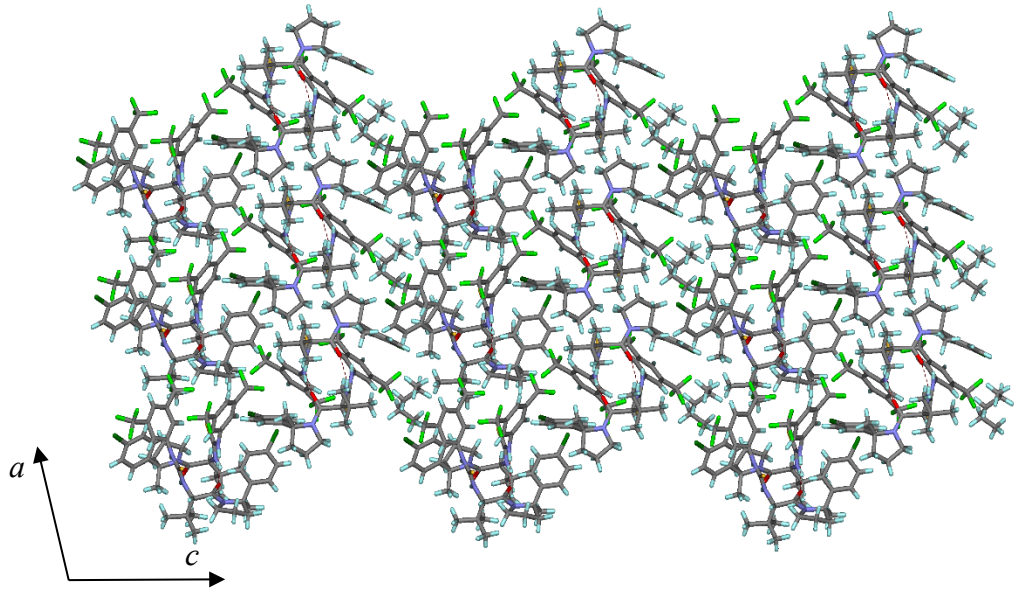

Figure 2.43 Three-dimensional supramolecular architecture viewed along the *b*-axis direction.

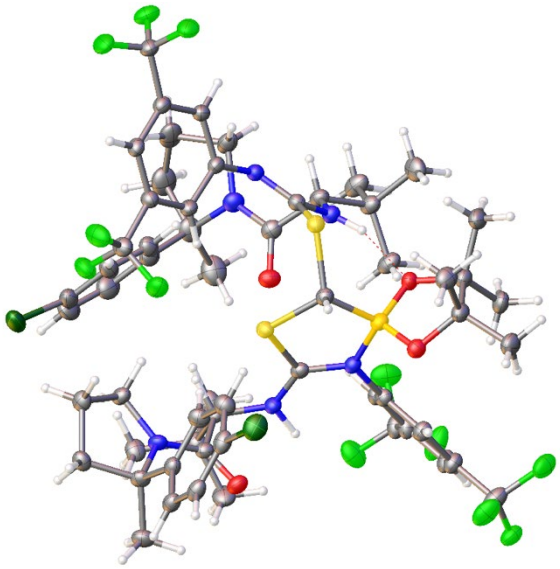

Figure 2.44 Crystal structure of **6f**

X-ray Crystallography: A crystal mounted on a diffractometer was collected data at 100 K. The intensities of the reflections were collected by means of a Bruker APEX DUO CCD diffractometer ($Cu_{K\alpha}$ radiation, λ=1.54178 Å), and equipped with an Oxford Cryosystems nitrogen flow apparatus. The collection method involved 1.0° scans in ω at -30°, -55°, -80°, 30°, 55°, 80° and 115° in 2θ. Data integration down to 0.84 Å resolution was carried out using SAINT V8.37A with reflection spot size optimization. Absorption corrections were made with the program TWINABS. The structure was solved by the Intrinsic Phasing methods and refined by least-squares methods again F^2 using SHELXT-2014 and SHELXL-2014 with OLEX2 interface. Non-hydrogen atoms were refined anisotropically, and hydrogen atoms were allowed to ride on the respective atoms. Crystal data as well as details of data collection and refinement are summarized in Table S11, geometric parameters are shown in Table S12, and hydrogen-bond parameters are listed in Table S13. The Ortep plots produced with SHELXL-2014 program, and the other drawings were produced with Accelrys DS Visualizer 2.0.

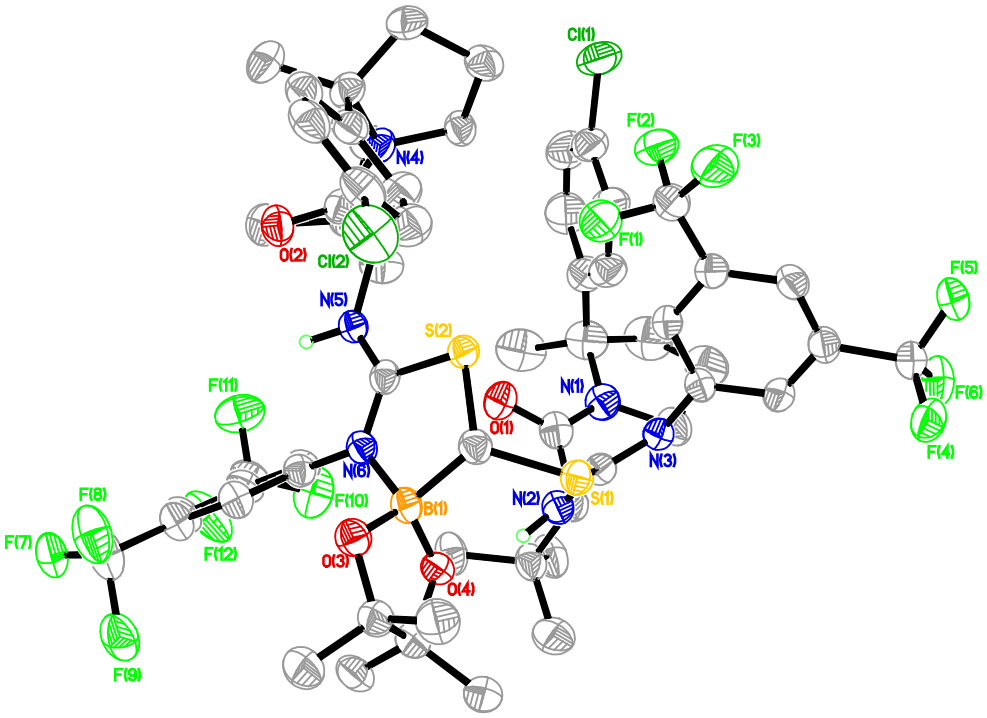

Figure 2.45 Perspective views showing 50% probability displacement

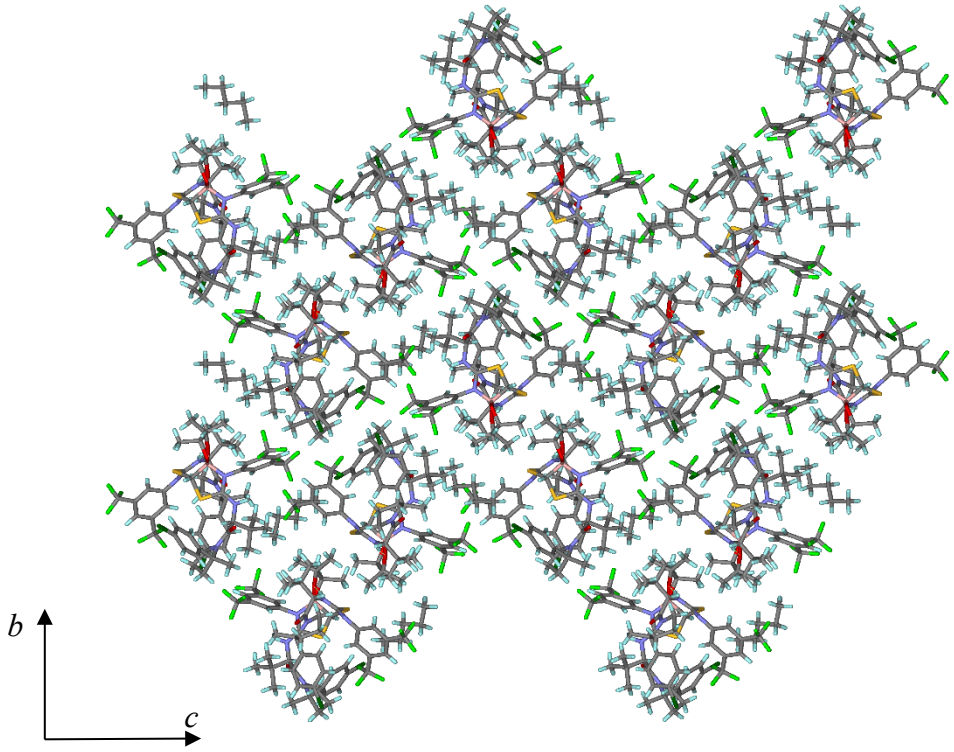

Figure 2.46 Three-dimensional supramolecular architecture viewed along the *a*-axis direction.

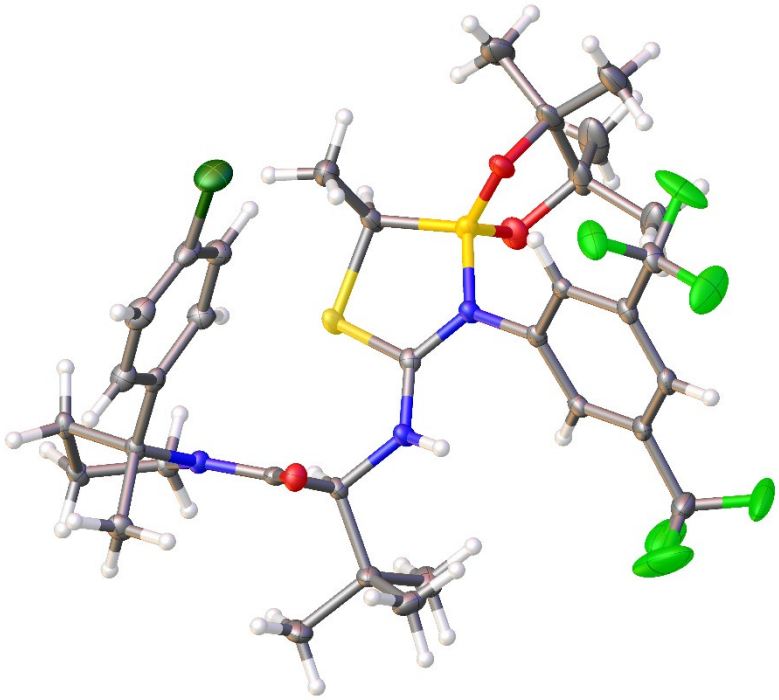

Figure 2.47 Crystal structure of **6b**

X-ray Crystallography: A crystal mounted on a diffractometer was collected data at 100 K. The intensities of the reflections were collected by means of a Bruker APEX II CCD diffractometer ($Mo_{K\alpha}$ radiation, λ=0.71073 Å), and equipped with an Oxford Cryosystems nitrogen flow apparatus. The collection method involved 0.5° scans in ω at 28° in 2θ. Data integration down to 0.78 Å resolution was carried out using SAINT V8.37A with reflection spot size optimization. Absorption corrections were made with the program SADABS. The structure was solved by the Intrinsic Phasing methods and refined by least-squares methods again F^2 using SHELXT-2015 and SHELXL-2014 with OLEX2 interface. Non-hydrogen atoms were refined anisotropically, and hydrogen atoms were allowed to ride on the respective atoms. Crystal data as well as details of data collection and refinement are summarized in Table S14, and geometric parameters are shown in Table S15. The Ortep plots were produced with the SHELXL-2014 program, and the other drawings were produced with Accelrys DS Visualizer 2.0.

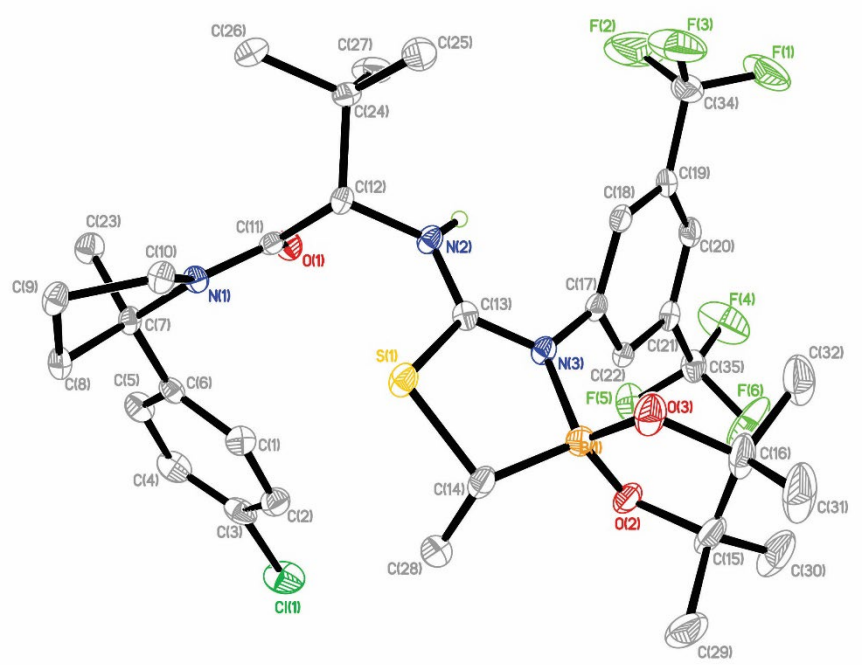

Figure 2.48 Perspective views showing 50% probability displacement

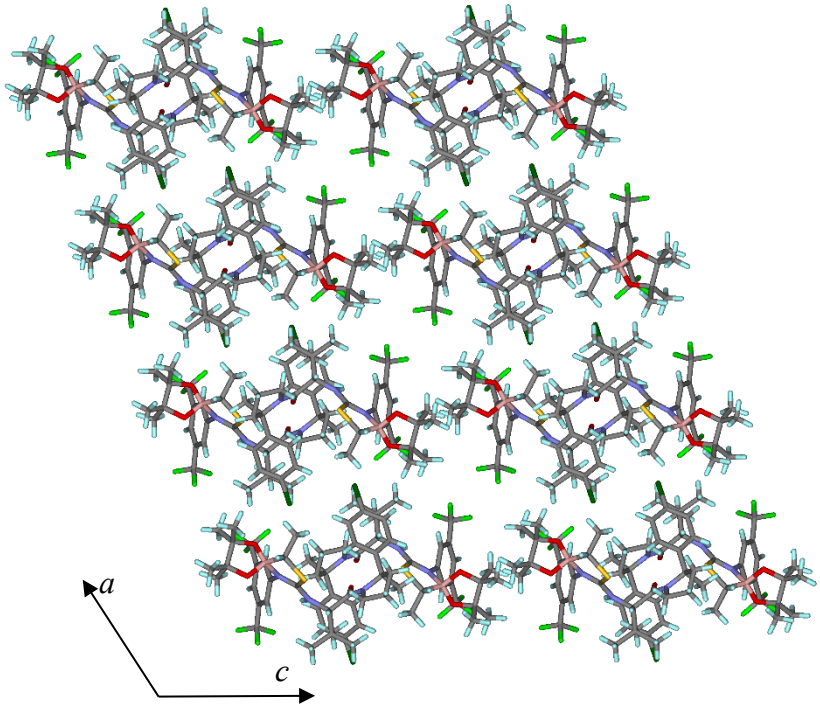

Figure 2.49 Three-dimensional supramolecular architecture viewed along the *b*-axis direction.

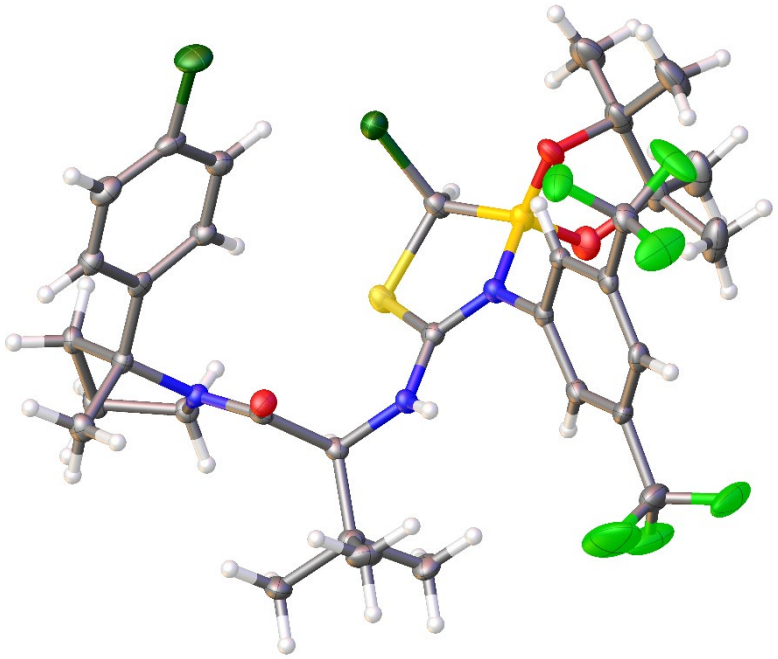

Figure 2.50 Crystal structure of **6a**

X-ray Crystallography: A crystal mounted on a diffractometer was collected data at 100 K. The intensities of the reflections were collected by means of a Bruker APEX DUO CCD diffractometer ($Cu_{K\alpha}$ radiation, λ=1.54178 Å), and equipped with an Oxford Cryosystems nitrogen flow apparatus. The collection method involved 1.0° scans in ω at -30°, -55°, -80°, 30°, 55°, 80° and 115° in 2θ. Data integration down to 0.84 Å resolution was carried out using SAINT V8.37A with reflection spot size optimization. Absorption corrections were made with the program SADABS. The structure was solved by the Intrinsic Phasing methods and refined by least-squares methods again F^2 using SHELXT-2014 and SHELXL-2014 with OLEX2 interface. Non-hydrogen atoms were refined anisotropically, and hydrogen atoms were allowed to ride on the respective atoms. Crystal data as well as details of data collection and refinement are summarized in Table S16, and geometric parameters are shown in Table S17. The Ortep plots were produced with the SHELXL-2014 program, and the other drawings were produced with Accelrys DS Visualizer 2.0.

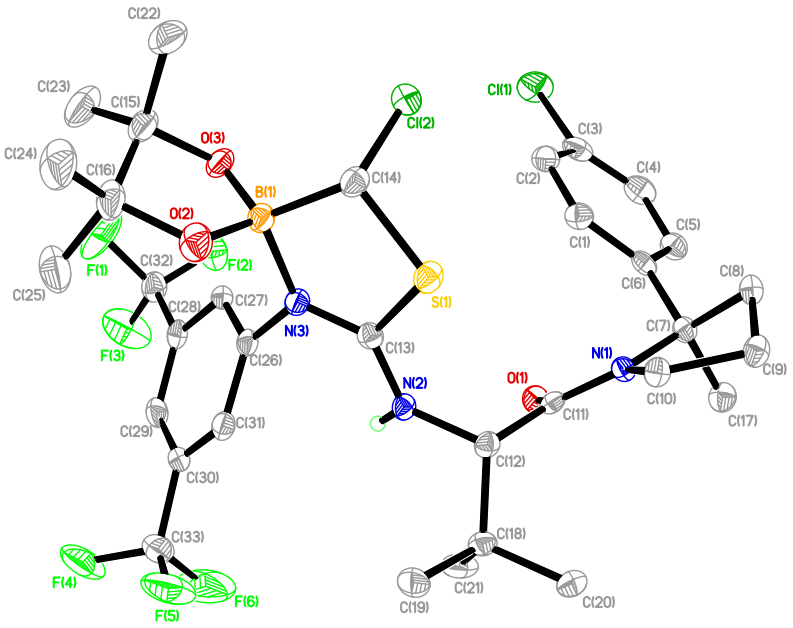

Figure 2.51 Perspective views showing 50% probability displacement

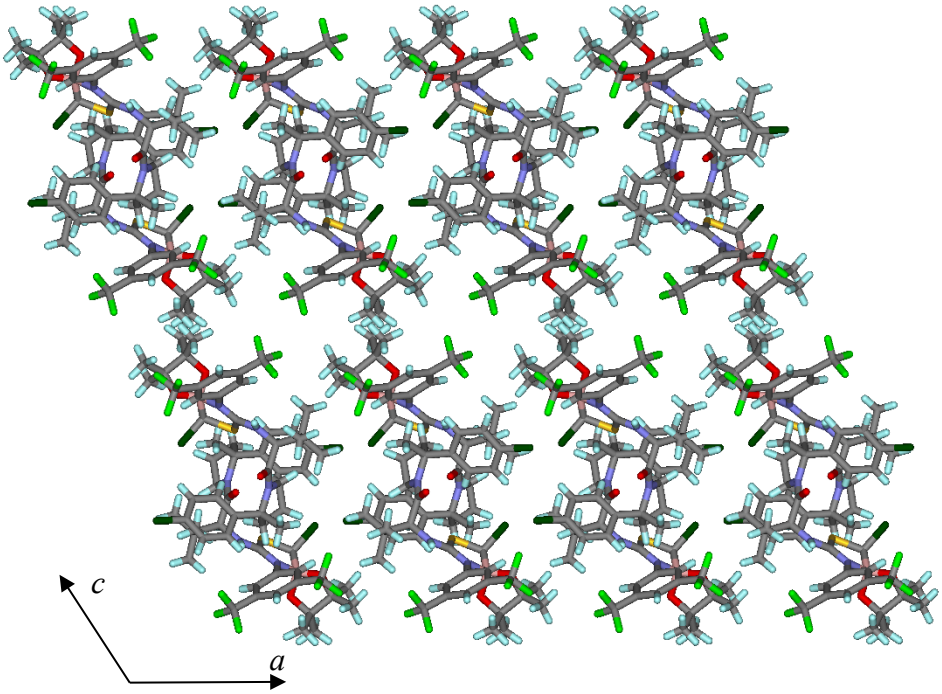

Figure 2.52 Three-dimensional supramolecular architecture viewed along the *b*-axis direction.

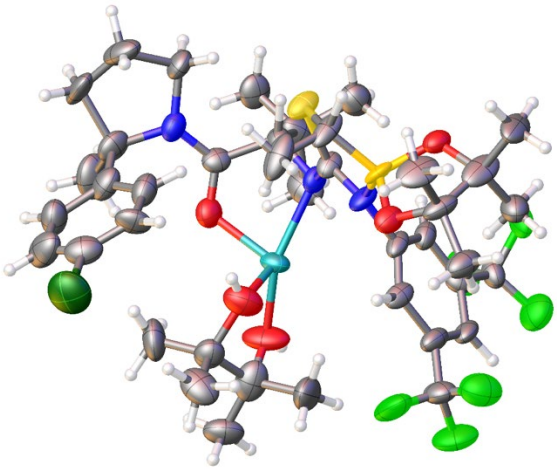

Figure 2.53 Crystal structure of **Li-6b**

Sample preparation: A mixture of **6b** (1 equiv) and LiHMDS (1 equiv) was prepared in Et_2O under a nitrogen atmosphere before being concentrated to dryness by vacuum transfer. A crystal suitable for X-ray diffraction grew spontaneously upon allowing a solution of this crude mixture in *tert*-butyl methyl ether to stand at 0 °C.

X-ray Crystallography: A crystal mounted on a diffractometer was collected data at 100 K. The intensities of the reflections were collected by means of a Bruker APEX II CCD diffractometer ($Mo_{K\alpha}$ radiation, λ=0.71073 Å), and equipped with an Oxford Cryosystems nitrogen flow apparatus. The collection method involved 0.5° scans in ω at 28° in 2θ. Data integration down to 0.84 Å resolution was carried out using SAINT V8.37A with reflection spot size optimization. Absorption corrections were made with the program TWINABS. The structure was solved by the Intrinsic Phasing methods and refined by least-squares methods again F^2 using SHELXT-2014 and SHELXL-2014 with OLEX2 interface. Non-hydrogen atoms were refined anisotropically, and hydrogen atoms were allowed to ride on the respective atoms. Crystal data as well as details of data collection and refinement are summarized in Table S18, geometric parameters are shown in Table S19, and hydrogen-bond parameters are listed in Table S20. The Ortep plots were

produced with the SHELXL-2014 program, and the other drawings were produced with Accelrys DS Visualizer 2.0.

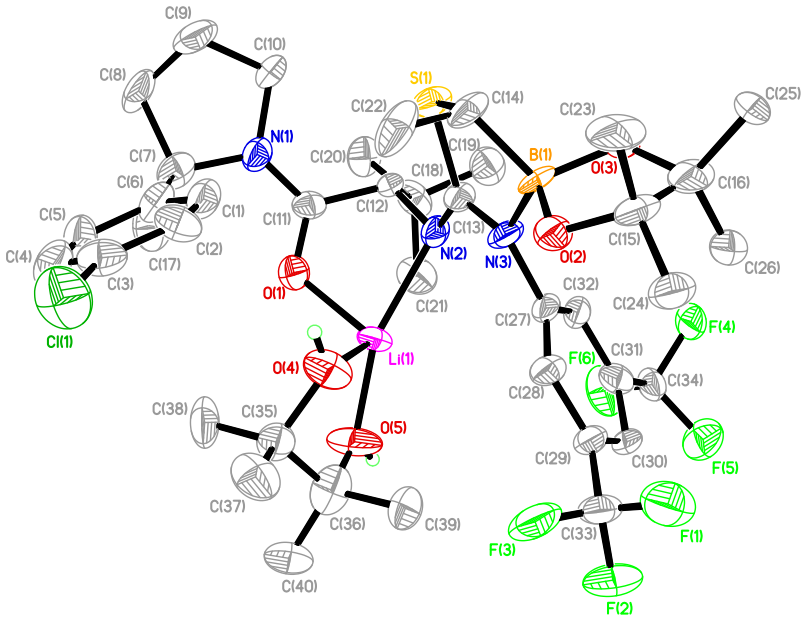

Figure 2.54 Perspective views showing 50% probability displacement

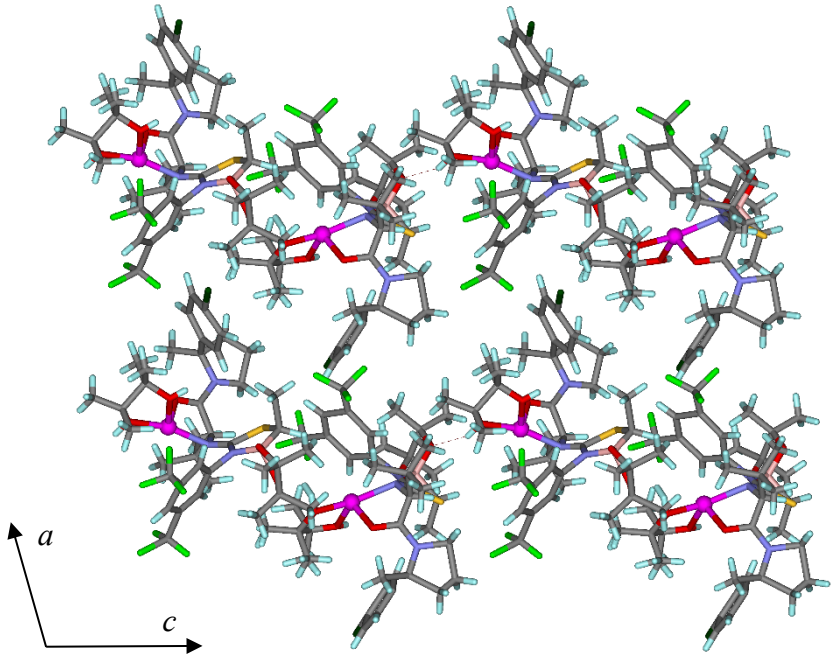

Figure 2.55 Three-dimensional supramolecular architecture viewed along the *b*-axis direction.

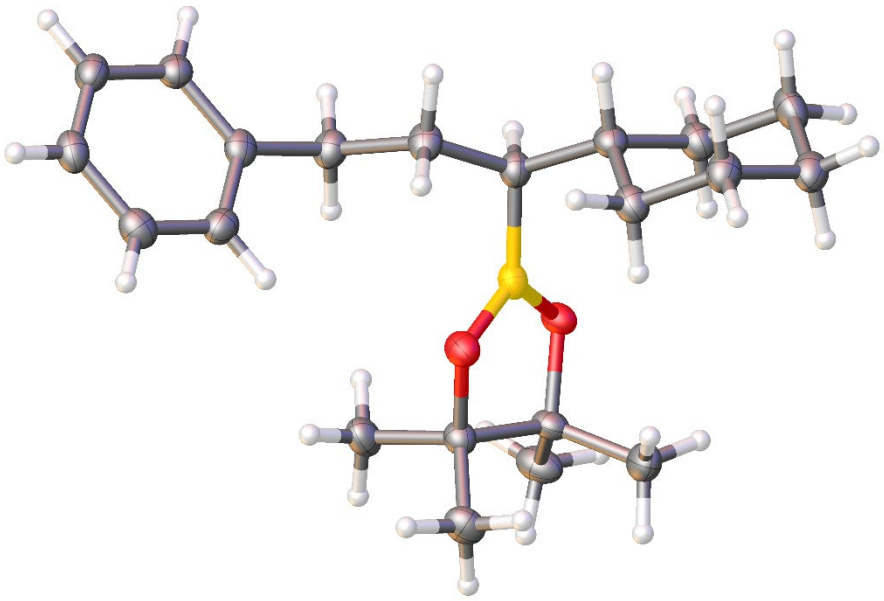

Figure 2.56 Crystal structure of **7v**

X-ray Crystallography: A crystal mounted on a diffractometer was collected data at 100 K. The intensities of the reflections were collected by means of a Bruker APEX DUO CCD diffractometer ($Cu_{K\alpha}$ radiation, λ=1.54178 Å), and equipped with an Oxford Cryosystems nitrogen flow apparatus. The collection method involved 1.0° scans in ω at -30°, -55°, -80°, 30°, 55°, 80° and 115° in 2θ. Data integration down to 0.84 Å resolution was carried out using SAINT V8.37A with reflection spot size optimization. Absorption corrections were made with the program SADABS (*33*, *38*). The structure was solved by the Intrinsic Phasing methods and refined by least-squares methods again F^2 using SHELXT-2014 and SHELXL-2014 with OLEX2 interface. Non-hydrogen atoms were refined anisotropically, and hydrogen atoms were allowed to ride on the respective atoms. Crystal data as well as details of data collection and refinement are summarized in Table S21, and geometric parameters are shown in Table S22. The Ortep plots were produced with the SHELXL-2014 program, and the three-dimensional supramolecular architecture drawing was produced with Accelrys DS Visualizer 2.0.

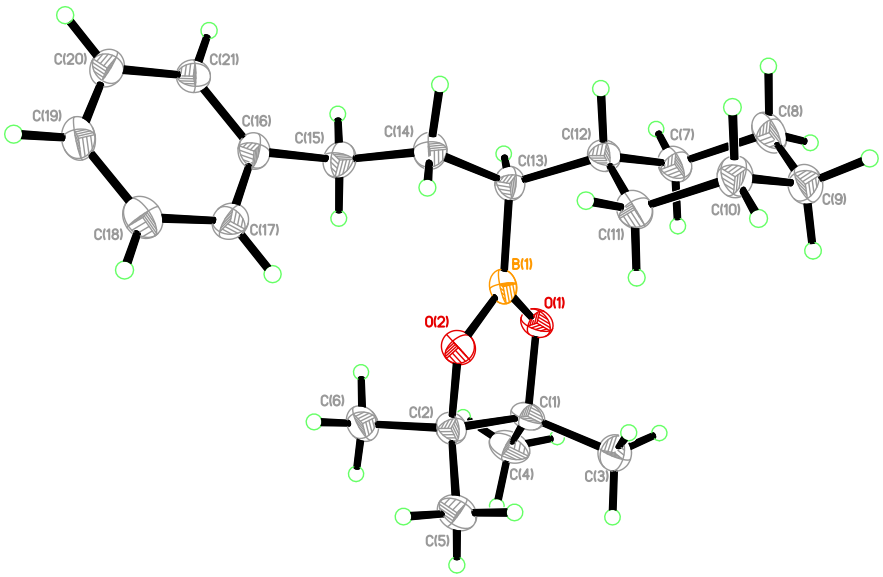

Figure 2.57 Perspective views showing 50% probability displacement

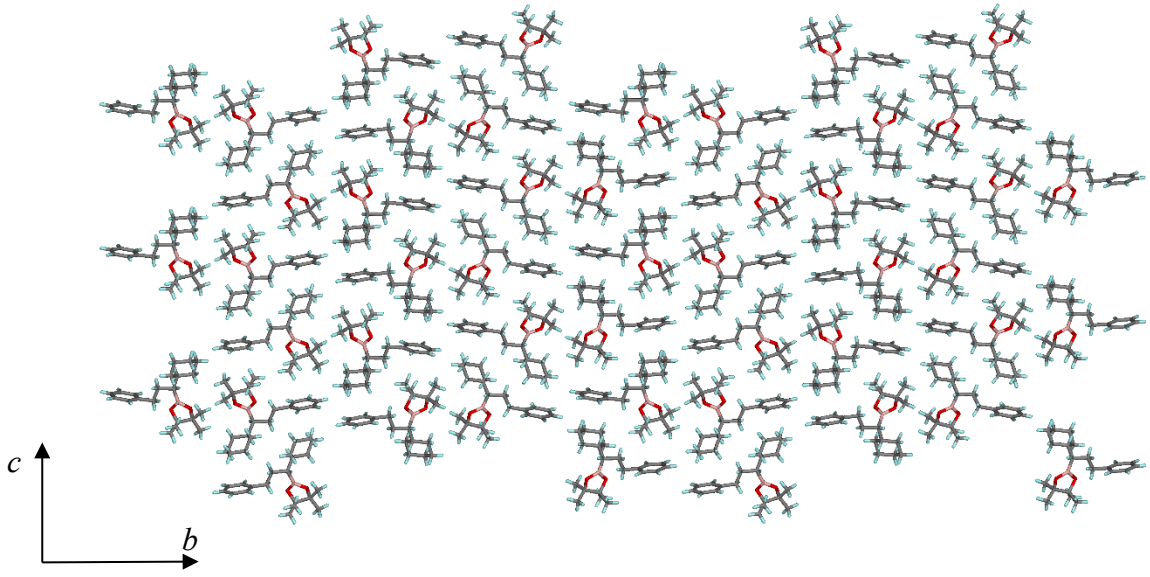

Figure 2.58 Three-dimensional supramolecular architecture viewed along the *a*-axis direction.

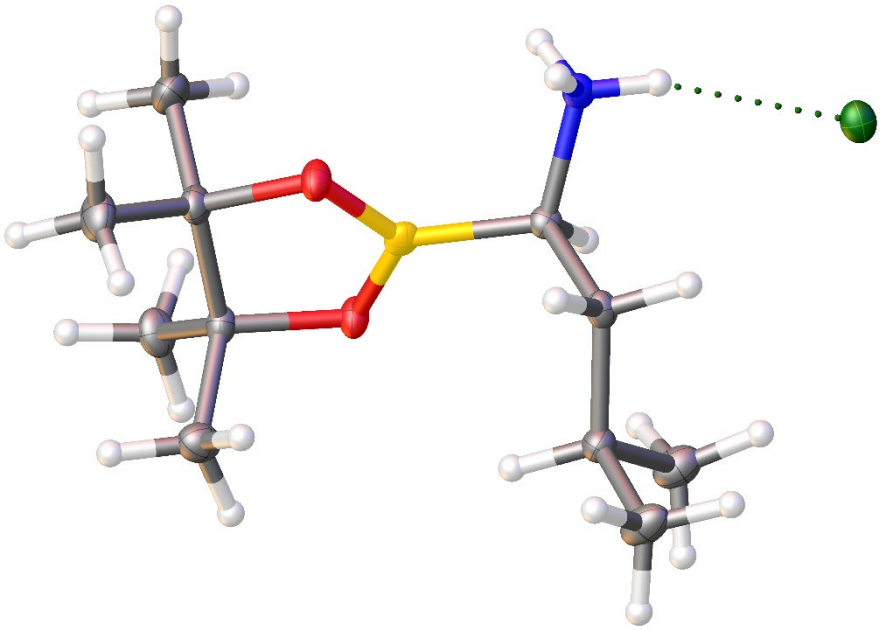

Figure 2.59 Crystal structure of **7j**

X-ray Crystallography: A crystal mounted on a diffractometer was collected data at 100 K. The intensities of the reflections were collected by means of a Bruker APEX II CCD diffractometer (MoK_α radiation, λ=0.71073 Å), and equipped with an Oxford Cryosystems nitrogen flow apparatus. The collection method involved 0.5° scans in ω at 28° in 2θ. Data integration down to 0.77 Å resolution was carried out using SAINT V8.37A with reflection spot size optimization. Absorption corrections were made with the program SADABS (*33*, *38*). The structure was solved by the Intrinsic Phasing methods and refined by least-squares methods again F^2 using SHELXT-2014 and SHELXL-2014 with OLEX2 interface. Non-hydrogen atoms were refined anisotropically, and hydrogen atoms were allowed to ride on the respective atoms. Crystal data as well as details of data collection and refinement are summarized in Table S23, geometric parameters are shown in Table S24, and hydrogen-bond parameters are listed in Table S25. The Ortep plots were produced with the SHELXL-2014 program, and the three-dimensional supramolecular architecture drawing was produced with Accelrys DS Visualizer 2.0.

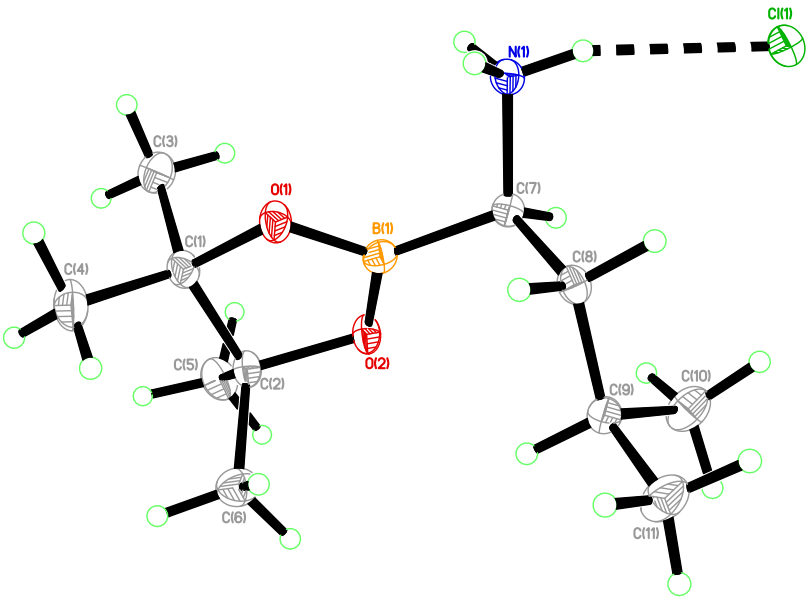

Figure 2.60 Perspective views showing 50% probability displacement

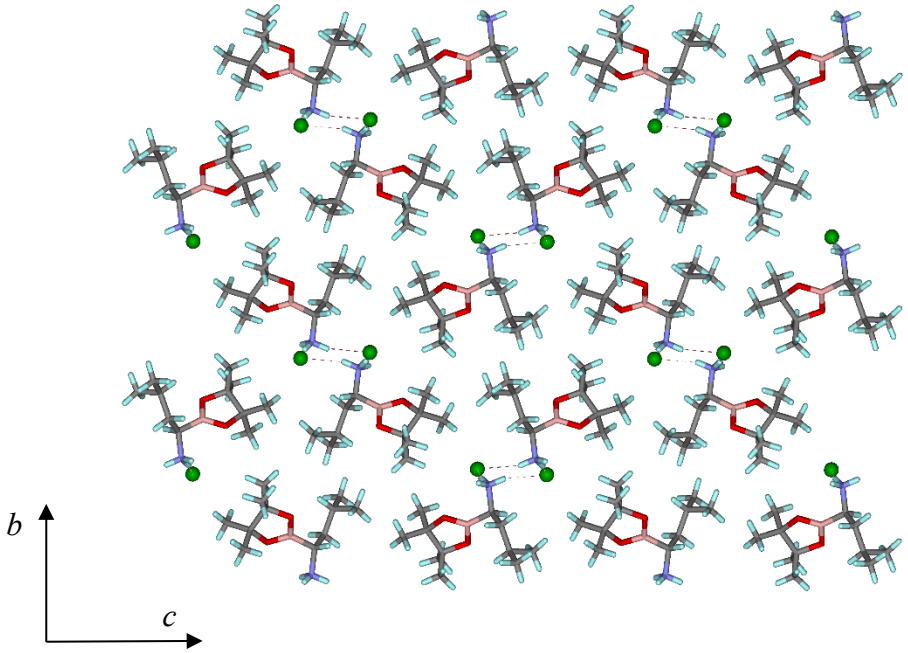

Figure 2.61 Three-dimensional supramolecular architecture viewed along the *a*-axis direction.

Chapter 3

Precise Natural Abundance ^{13}C Kinetic Isotope Effect Measurements Enabled by Single Quantum Suppression[1]

3.1 Introduction

Kinetic Isotope Effect (KIE) experiments are fundamentally important tools for mechanistic analysis of chemical reactions.[2] Of particular utility are carbon KIE experiments, which measure the difference in rate between reactants bearing ^{13}C or ^{14}C atoms at one or more specific sites vs reactants bearing ^{12}C atoms at the same site(s).[3] In this work, a new, highly precise

[1] This work was done in collaboration with Eugene Kwan, Ron Rhamsubhag, Yuwen Zeng, and Dongtao Cui. Eugene was uniquely responsible for the conception of the project, development of the requisite NMR pulse sequences, and all coding. Ron and Yuwen provided initial validation of the tool. Dongtao helped optimize the procedure for the n400B.

[2] Westheimer, F. H. The Magnitude of the Primary Kinetic Isotope Effect for Compounds of Hydrogen and Deuterium. *Chem. Rev.* **1961**, *61*, 265–273.

[3] DelMonte, A. J.; Haller, J.; Houk, K. N.; Sharpless, K. B.; Singleton, D. A. Strassner, T.; Thomas, A. A. Experimental and Theoretical Kinetic Isotope Effects for Asymmetric Dihydroxylation. Evidence Supporting a Rate-Limiting "(3 + 2)" Cycloaddition. *J. Am. Chem. Soc.* **1997**, *119*, 41, 9907–9908.

and efficient method for measurement of ^{13}C KIE at natural abundance termed SQUASH, or Single QUAntum Suppression ^{1}H, is applied to the study of three distinct reactions: phenol methylation, benzaldehyde reduction, and cinnamate epoxidation. The developed method enables quantification of the ratio of molecules bearing ^{12}C vs ^{13}C centers using integrations of the ^{12}C–H parent peak and ^{13}C–H satellite peaks from the proton spectrum, rather than using the ^{13}C peaks from the carbon spectrum. Specifically, single quantum suppression enables the precise integration of ^{13}C–H satellite peaks by suppressing the main, ^{12}C–H proton peak. As ^{1}H NMR sensitivity is approximately 64-fold greater than that of ^{13}C, this method potentially enables up to a 4,096-fold reduction in acquisition time, potentially transforming natural abundance carbon KIE experiments into a routine experiment.

3.2 Background

Carbon KIEs provide a measurement of the substrate-committing transition state geometries relative to those in the ground state, thus giving a snapshot of these otherwise difficult to probe structures. As such, KIE values can be used to rule out mechanisms (as exemplified in the WM study) and to corroborate the geometries of computed structures. As a striking example of this latter use, Singleton has shown that predicted KIEs correlate with calculated forming C–O bond distances, specifically in the TS of the epoxidation of 2-methyl-2-butene with oxaziridines (Fig. 3.1).[4] Applying this predicted KIE-bond distance relationship, experimental KIEs of 1.013 and 1.008 were shown to correspond to TS bond lengths of 2.11 Å and 2.26 Å, respectively. In

[4] Hirschi, J. S.; Takeya, T.; Hang, C.; Singleton, D. A. Transition-State Geometry Measurements from 13C Isotope Effects. The Experimental Transition State for the Epoxidation of Alkenes with Oxaziridines. *J. Am. Chem. Soc.* **2009**, *131*, 2397–2403.

this manner, tandem DFT and ^{13}C KIE analysis can enable the construction of highly precise pictures of transition states.

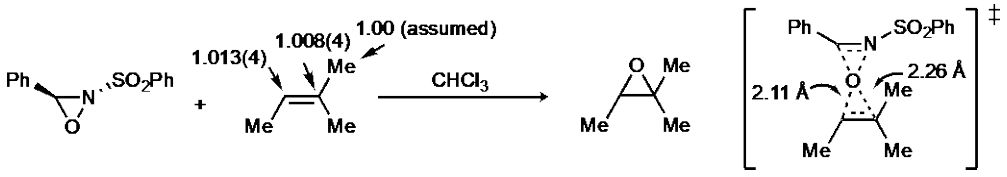

Figure 3.1 KIE study on the oxidation of 2-methyl-2-butene

The most common way ^{13}C KIEs are acquired is via natural abundance KIE experiments, which take advantage of the ~1% of all carbons that have atomic masses of 13. In principle, one experiment can afford KIE measurements on all carbons in a molecule, as any given labeled molecule is likely to bear only a single heavy carbon atom at any site. This approach obviates the need to synthesize labeled starting material, which is often prohibitively challenging, tedious, and/or expensive. The first use of natural abundance ^{13}C KIE experiments was reported by Singleton in 1995[5] involving the measurement of KIEs arising from the Diels–Alder cycloaddition of isoprene and maleic anhydride (Fig. 3.2). Using the ^{13}C NMR spectrum, ^{13}C:^{12}C ratios were determined for each carbon by dividing the area of the peak of the carbon of interest by the area of the peak of a carbon with an expected KIE of 1.00 (e.g. the methyl peak of isoprene). The KIE was calculated as a function of the ^{13}C:^{12}C ratio of starting material isolated from a high conversion reaction "R", the conversion F, and the ^{13}C:^{12}C ratio of unreacted starting material "R_0" (Equation 1.1). Since this report, Singleton and a few others have applied this tool to the study of innumerous reaction mechanisms.

[5] Singleton, D. A.; Thomas, A. A. High-Precision Simultaneous Determination of Multiple Small Kinetic Isotope Effects at Natural Abundance. *J. Am. Chem. Soc.* **1995**, *117*, 9357–9358.

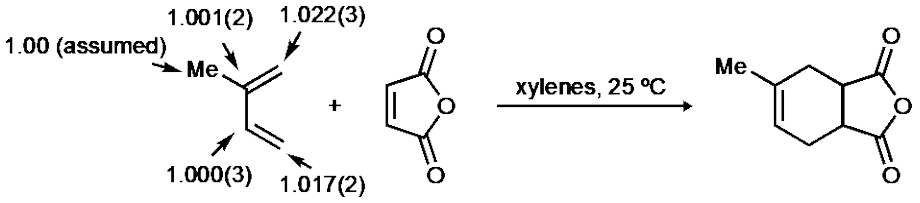

Figure 3.2 Experimental KIEs for the 4+2 cycloaddition of isoprene and maleic anhydride

$$KIE = \frac{\ln(1-F)}{\ln[(1-F)^{\frac{R}{R_0}}]}$$

Equation 1.1 Calculation of KIE values from conversion (F) and fractionation at partial (R) or zero percent (R_0) conversion

While natural abundance ^{13}C KIE experiments are powerful tools, fractionation measurements on naturally labeled material are hampered by the low sensitivity of the ^{13}C nucleus in NMR spectroscopy. Thus, to achieve accurate and precise measurements, reactions must be carried to either very high or very low conversion, which limits analysis to reactions that can be run on multi-gram-scale, and long NMR experiment times (days to weeks) must be used. Recent advances reported by the Jacobsen Lab have begun to surmount these limitations. In 2017, Kwan and Jacobsen reported the use of polarization transfer from ^{1}H to ^{13}C to enhance the signal of ^{13}C peaks with attached protons.[6] This technique increases the sensitivity of measured ^{13}C integrations by three- to four-fold, enabling a 9–16x reduction in instrument time. More recently, Kwan and Jacobsen have reported the use of multiple quantum filtration (MQF) to enable the accurate and precise measurement of ^{13}C:^{12}C ratios using the ^{19}F NMR spectrum. Specifically, this approach quantifies the relative amount of ^{12}C-labeled material by integrating the ^{12}C–^{19}F peak and the

[6] Kwan, E. E.; Park, Y.; Besser, H. A.; Anderson, T. L.; Jacobsen, E. N. Sensitive and Accurate ^{13}C Kinetic Isotope Effect Measurements Enabled by Polarization Transfer. *J. Am. Chem. Soc.* **2017**, *139*, 43–46.

amount of ^{13}C-labeled material by integrating the ^{13}C–^{19}F satellites.[7] Accurate satellite integrations could be obtained from the multiple-quantum-filtered spectrum, which suppresses the ^{12}C–^{19}F peaks to minimize interference to the flanking ^{13}C–^{19}F peaks. As the signal-to-noise of the fluorine satellites is theoretically 13.6x larger than the corresponding carbon peaks in the ^{13}C spectrum, this approach enables an approximately 185x reduction in acquisition time. As MQF requires fluorine substitution on the carbon of interest, application is limited to a narrow range of reactions involving introduction/removal of fluoride or that happen at a fluorine-substituted carbon center. We envisioned that a similar strategy that utilizes the proton spectrum rather than the fluorine spectrum would increase the generality of this tool.

3.3 Results

The SQUASH method is analogous to the MQF method except for the titular changes of using proton NMR as well as single (rather than multiple) quantum filtration. SQUASH was first tested on the methylation of *p*-cresol. The methyl ether product provides an ideal substrate for initial assessment of the developed method as the carbon of interest bears three hydrogens that correspond to a singlet in the ^{1}H spectrum. Four unique NMR experiments were conducted in duplicate (Fig. 3.3) to compare the results from SQUASH to state-of-the-art methodology (DEPT) and to assess the sensitivity of the technique with minimal solute quantities. Both the DEPT replicates using 100mg of material (in 350μL of $CDCl_3$) and the SQUASH experiment using 20mg of material (in 550μL of $CDCl_3$) afforded highly precise KIE measurements, with the SQUASH method arriving at the same answer with 1/5 of the material and a 10-fold reduction in acquisition

[7] Kwan, E. E.; Zeng, Y.; Besser, H. A.; Jacobsen, E. N. Concerted nucleophilic aromatic substitutions. *Nat. Chem.* **2018**, *10*, 917–923.

time relative to the DEPT method. Analysis of more dilute samples (1mg or 0.1mg in 550µL of $CDCl_3$) with longer acquisition times afforded similar KIE numbers, albeit with a moderate loss in precision and accuracy.

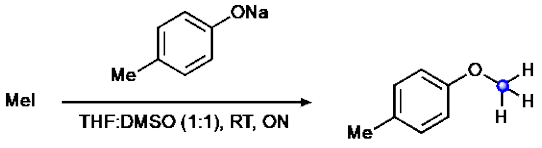

Replicate	acq time (h)	KIE rep1	KIE rep2
DEPT (100mg)[n]	14	1.065(2)	1.067(2)
SQUASH (20mg)[n]	1.1	1.065(2)	1.064(2)
SQUASH (1mg)[n]	10	1.071(6)	1.070(6)
SQUASH (0.1 mg)*	10	1.063(6)	1.070(8)

*acquired on an 800 mHz machine equipped with a cryoprobe

Figure 3.3 Methylation of *p*-cresol and KIE analysis

SQUASH was then applied to benzaldehyde reduction reactions as a showcase of the ease of consecutively analyzing multiple reactions in a short window of machine time. Three different benzaldehyde reduction reactions (using 9-Borabicyclo[3.3.1]nonane (9BBN), sodium triacetoxyborohydride (STAB), or sodium borohydride ($NaBH_4$)) were conducted. These reactions were run in duplicate, with the exception of the STAB reductions, which were conducted in quadruplicate (two using the Bruker n400B, two using the Varian i500B). For the purposes of analysis, the benzyl alcohol product was benzoylated to afford benzyl benzoate, which features a sharper singlet than benzyl alcohol for the benzylic protons in the ^1H NMR spectrum. Each sample was analyzed for <1h to give a total of ~7 hours of machine time on the n400B for the six partial conversion and two full conversion samples. High precision and excellent to good agreement was obtained between replicates, including the STAB experiments measured on the Bruker and Varian instruments (Fig. 3.4).

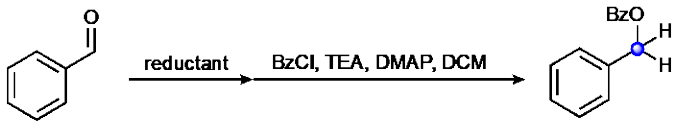

Experiment	KIE rep1	KIE rep2
9BBN	1.008(2)	1.009(2)
STAB	1.035(2)	1.037(2)
STAB*	1.034(3)	1.035(2)
$NABH_4$	1.034(2)	1.039(3)

*conducted on a 500 MHz Varian instrument

Figure 3.4 Reduction of benzaldehyde and KIE analysis

The epoxidation of alkenes provides an interesting and useful tool with which to assess this methodology, as these reactions can occur through multiple mechanistic pathways and feature starting material with increased complexity (i.e. protons with non-singlet splitting patterns). We selected the epoxidation of cis-isopropyl cinnamate with Mn[salen] as the initial model system, in part due to the multitude of mechanistic proposals (Fig. 3.5) and the prominence of this reaction in Jacobsen group history. In particular, this alkene functionalization has been proposed to proceed via concerted 2+1 (**A**), stepwise radical-based (**B**), and concerted 2+2 pathways (**C**), which correspond to 6+ unique potential selectivity-determining steps (SDS's) depending on the reversibility of any given bond formation. The SDS proffered by Jacobsen, **B1**, is expected to have a unique set of KIEs arising from rehybridization of C_α but not C_β in the TS, giving rise to expected KIEs of greater than 1.01 for C_α and near 1.00 for C_β. In contrast, both **A** and **C1** involve significant rehybridization of both alkene carbons C_α and C_β in the SDS and should have large KIEs on both carbons. **B2**, **C2**, and **C3** occur as the second of two steps in the rate-determining span. These pathways involve rehybridization of only the benzylic carbon C_β in the SDS, although C_α undergoes a change in bond strength between a C–C double bond in the ground-state cinnamate and a C–O single bond in the pre-SDS intermediate, and thus a large KIE is expected for C_β and an EIE is expected for C_α. While KIE analysis is unable to distinguish between every pathway, it can be used to corroborate or rule out favored pathway **B1**.

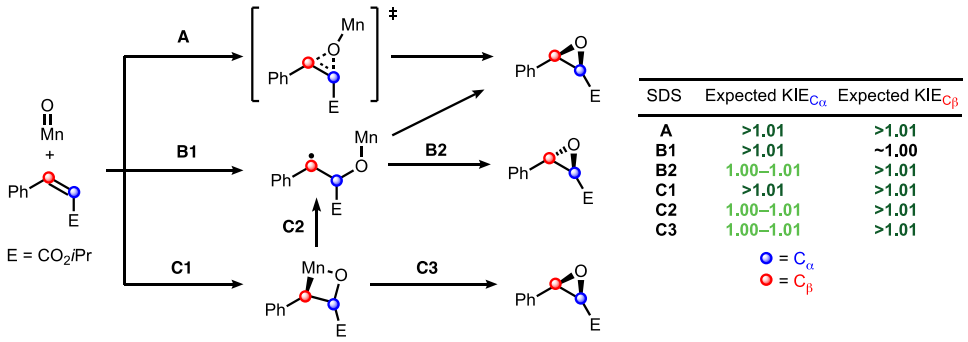

Figure 3.5 Hypothetical mechanisms for cinnamate epoxidation and expected KIEs

With these considerations in mind, SQUASH was conducted on the Mn[salen]-catalyzed epoxidation reaction (Fig. 3.6). Experiments were conducted using 30mg (0.16 mmol) of cinnamate in 550 mL $CDCl_3$ with two hours of acquisition time. Integrations (Fig. 3.7) were acquired for three of the four cis-isopropyl cinnamate alkene satellite peaks (doublets between 5.7 and 6.8 ppm) and both of the isopropyl methine satellite peaks (heptets in between 4.8 and 5.3 ppm). Excellent agreement was obtained between all four replicates to give average numbers of 1.045 for $KIE_{C\alpha}$ and 1.006 for $KIE_{C\beta}$. The most precise data was acquired using the n400B (Fig. 3.6, replicates 3–4), although both machines afforded meaningful measurements. The observation of a KIE near unity for the methine carbon, which is not involved in the SDS, provides further indication of the accuracy of these measurements. These results are consistent only with pathway **B1** and are inconsistent with the other proposed pathways.

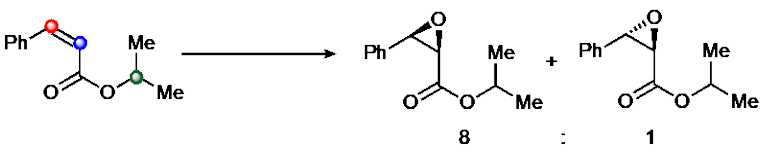

Replicate	$KIE_{C\alpha}$	$KIE_{C\beta}$	$KIE_{Cmethyne}$
1 (Varian)	1.048 (4)	1.007 (4)	-
2 (Varian)	1.044 (5)	1.005 (3)	-
3 (Bruker)	1.045 (1)	1.007 (1)	0.998 (1)
4 (Bruker)	1.045 (1)	1.006 (1)	0.998 (1)

Figure 3.6 KIE measurements for epoxidation of cis-isopropyl cinnamate

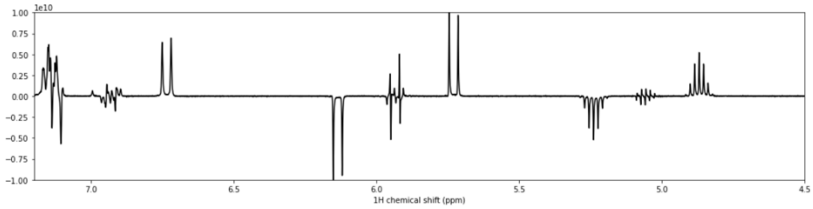

Figure 3.7 SQUASH spectrum of cis-isopropyl cinnamate

3.4 Conclusion

This chapter details the application of a new technology for the measurement of natural abundance ^{13}C KIEs. Highly precise and accurate KIE measurements on phenol methylation, benzaldehyde reduction, and cinnamate epoxidation reactions were achieved with small amounts of material (30–50mg) and short experiment times (1–2h/sample). As SQUASH makes the measurement of ^{13}C KIEs significantly easier than before, this technology has the potential to generalize the use of ^{13}C KIEs as tools for mechanistic analysis.

3.5 SQUASH for Dummies in the Harvard CCB NMR Facility

3.5.1 Reaction and Substrate Selection

When considering whether to apply SQUASH to measuring KIEs, it is necessary for 1) the carbon(s) of interest to bear one or more hydrogens where 2) the corresponding $^{12}C–H$ and $^{13}C–H$ peaks do not overlap with other peaks in the spectrum. As most carbons in molecules either naturally bear a hydrogen or can be hydrogenated/protonated to introduce hydrogen substitution, this first requirement allows for relatively widespread application and only prohibits analysis on fully-substituted or *ipso* carbons. The latter requirement is potentially more limiting, particularly for the analysis of complex molecules, although the ability to manipulate chemical shifts by varying the NMR solvent provides a partial workaround.

3.5.2 Experiment Setup

Each SQUASH experiment requires a unique set of parameters, namely the TOF_{1H} (chemical shift in Hz of the proton of interest; if there are multiple protons of interest, choose a chemical shift in between them), $T1_{1H}$, J_{1CH} (the carbon-proton coupling constant in Hz), TOF_{13C}, and the 90º pw. Most of these values should be acquired prior to the day of SQUASH. The TOF_{1H} can obviously be acquired from the ^{1}H spectrum. The T1 can be measured by conducting the T1 experiment in the n400B queue and analyzing the data in MNova (https://www2.chemistry.msu.edu/courses/Cem845/FS20/Data%20Analysis%20For%20T1%20Measurements%20Using%20Mnova.pdf). The TOF_{13C} and J_{1CH} can be measured using data from a carbon NMR experiment and a proton-coupled and a proton-decoupled HSQC experiment (note: the proton-coupled HSQC experiments need to be added to the list of approved experiments by Dongtao before use). To measure the 90º pw:

1. Enter manual mode on n400B
2. Insert sample, then run lock, tune, shim, prosol, and gain in order
3. Acquire 1 scan proton (ds=0)
4. Type and enter “pulsecal” into the command line
    a. This command generates two numbers, with the number at the higher power representing the desired 90º pw
5. Enter in the command “wrpa #” to copy the experiment to number “#”
6. Setup and acquire carbon spectrum
7. Use command “Pulsecal c13” to measure ^{13}C pulsecal, which can be entered into the SQUASH parameters but does not appear crucial.

3.5.3 NMR Spectra Acquisition

1. Once the n400B has been put into manual mode, create new proton and SQUASH experiments by making duplicates of old proton/SQUASH experiments.
2. Enter in appropriate acquired parameters (based on T1, 90º pw, $J_{1CH,}$ TOF_{1H}, and TOF_{13C})
3. Type “edpy” into command line (to edit python program)
4. Click “edit”
5. Change lines 23, 24, 26, and 42-46 to enter in the names of the experiments and the positions of the sample in the holder. Make sure to not duplicate file names if this is not the first acquisition.
6. File—>Save
7. Execute

3.5.4 Data Workup and Calculation of Fractionation

3.5.4.1 Topspin: Peak Referencing and Shimming

Download topspin for free. Load acquired data into topspin. Begin processing the first block of data. First, appropriately reference the solvent peak. Then, phase the spectrum using the following instructions for phasing arrays in topspin:

1. Pull up one spectrum from the array using the command “Rsr #” where “#” is the spectrum number. As all spectra in the array are likely to be phased similarly, the specific spectrum used is not important.
2. Enter the command “.ph” to bring up the phasing tool.
3. Click and hold 0 on toolbar to begin phasing peaks; drag the mouse while still holding to phase.
    a. The triangle buttons change phase increments

b. The phasing tool is initially set to ph0. Click 1 (instead of 0) to change first order phase instead. It is likely that only zero order shimming will be necessary, unless multiple peaks of interest with very different chemical shifts are being analyzed.

4. Click the disk (with nd) to save the phase
5. Click return arrow (without the save button on it)
6. Close out from the individual spectrum by pressing the "x" at the top right of the spectrum. This temporarily discards the phase, but worry not—the phase is still saved!
7. Enter the command "Xf2" to apply the phase to all spectra in the array.
8. Repeat for all blocks of spectra for all samples.

3.5.4.2 Using Python in Jupyter Lab

In order to process the referenced and shimmed data, it will be necessary to download and run a few separate pieces of software. The next set of instructions will walk through this process.

1. Running for the first time:
    a. Download Anaconda, which is used to create a virtual environment that can run python (https://www.anaconda.com/products/individual).
    b. Open a terminal window and type the following commands (only the words between the quotation marks):
        i. "conda create -n nmr python=3.9"
        ii. "y"
        iii. "conda activate nmr", which puts you into a new virtual environment
        iv. "pip install nmrglue jupyterlab jupyternotebook pandas matplotlib", which installs 1) the proper libraries to process NMR data and 2) jupyter lab and jupyter notebook, both which provide a local host on which the python

scripts are run (note: jupyter lab or jupyter notebook have identical functions, and as such either can be used, depending on preference).

v. "ipython kernel install --name nmr --user"

vi. "jupyter lab" or “jupyter notebook” (note: this opens the local host in a new window)

vii. To quit jupyter, type “cc jupyter notebook” or “cc jupyter lab”; to deactivate the virtual environment, type: “conda deactivate”

2. Running any time after setup, launch terminal and type:

   a. “conda activate nmr”

   b. "jupyter lab" or “jupyter notebook”

   c. To quit jupyter notebook, type “cc jupyter notebook” or “cc jupyter lab”; to deactivate the virtual environment, type: “conda deactivate”

If the preceding instructions were followed properly, the screen captured in Fig. 3.8 should appear after typing “jupyter lab” into the terminal.

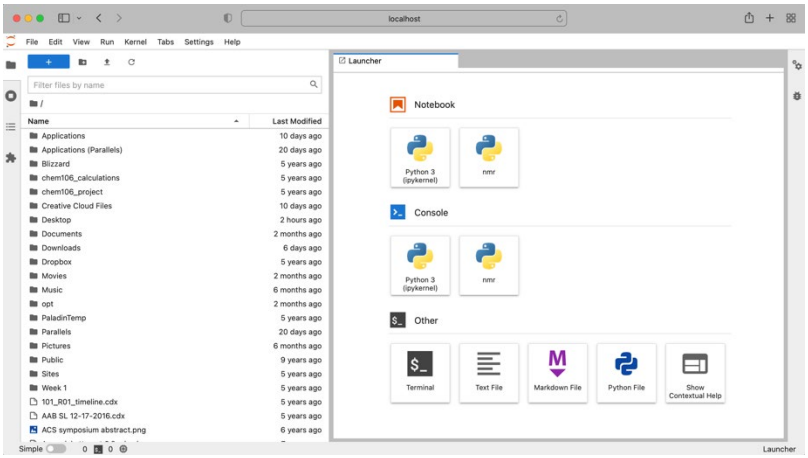

Figure 3.8 Jupyter lab main window

After this screen is loaded, navigate to the folder containing all of the NMR data folders of experiments and follow these instructions:

1. Copy the python notebooks into one folder containing all the NMR data folders for one sample (one for 1H, one for SQUASH; ask me for them. Alternatively, they should be posted in an online repository and soon to be github https://drive.google.com/drive/folders/1A8aUEuywxkS66qg-_-qTyhHk_myaeRwC)
2. Double click the .ipynb file for either the 1H or SQUASH (this will run the kernel; a kernel is something that allows for the cells of the python script to be run in the notebook). This will open a window such as that in Fig 3.9.

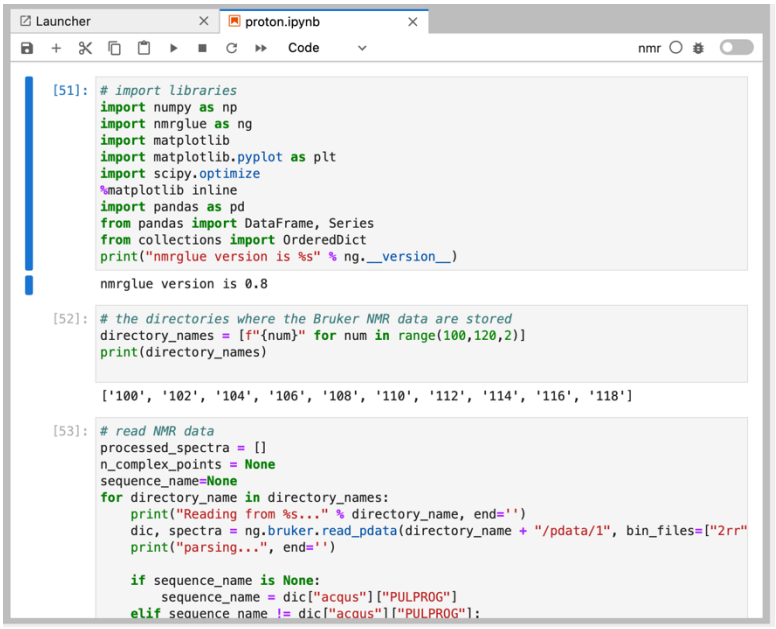

Figure 3.9 Initial window after beginning kernel

3. Run the first cell. (Note: Each grey box is a “cell”. Each cell contains code that performs a function. Cells are run by pressing “shift + enter” and waiting. Running the first cell imports the proper package/library into the kernel.)

4. Run the second cell: the directories where the Bruker NMR data are stored. (Note: this cell chooses what NMR data to upload for analysis. The range(x,y,z) function selects for all numbers between x–y with a step of z, including x but not y. As seen below, all even-numbered experiments 100–118 are loaded. This is why it is helpful to save different blocks of data as iteratively increasing numbers)

```
# the directories where the Bruker NMR data are stored
directory_names = [f"{num}" for num in range(100,120,2)]
print(directory_names)
```

```
['100', '102', '104', '106', '108', '110', '112', '114', '116', '118']
```

Fig. 3.10 Cell two

5. Continue to run cells. Each cell performs a certain task denoted by the first line that has been #'d out.
6. The next important cell begins with "# define peaks and phases here." This cell will define the integration region for all peaks of interest. Here, 11 peaks of interest have been selected and defined. Choose the range for each peak of interest that fully captures the peak.

```
# define peaks and phases here
# (larger chemical shift, smaller chemical shift)
peak_names = ["aryl 1", "aryl 2",   "chloroform",    "beta olefin left", "beta olefin", "beta olefin right",
              "alpha olefin left", "alpha olefin", "alpha olefin right",
              "isopropyl methine", "isopropyl methyl"]
peaks = [(7.67,7.50),  (7.43,7.276), (7.276,7.24),     (7.08,7.03),        (7.06,6.777),   (6.765,6.705),
         (6.172,6.096), (6.04,5.77), (5.766,5.70),
         (5.177,4.939),       (1.26,1.19)]
phases = [0.0 for i in peaks]
cphases = [ cphase(i) for i in phases ]
```

Figure 3.11 Peak integration area cell

7. The following cell (# check phasing and integration range for each peak) allows for a double-checking of the peak integration area. Each individual peak of interest can be examined for each block of spectra by defining the peak_number and spectrum_number, respectively. The close-up window of the peak will be printed below. The width of the X

axis can be changed using the "x_axis_range = max(peak[0]-peak[1]+0.3,0.3)" command, and the Y axis can be changed using the "plt.ylim(y_min-y_range*0.001,y_min+y_range*0.01)" command. (Note: the list of spectra/peaks starts at *0*, not *1*. As such, the final spectrum/peak is N – 1, where N is the number of spectra/peaks.)

8. The next important cell (def compute_baseline) defines the baseline, which is crucial for accurate integration. The "clip_below" tool tells the program where to stop integrating data (e.g. 3e7 for example in Fig. 3.12), and the "clip_above" tool defines the highest points above the noise (e.g. 6e7 for example in Fig. 3.12). Enter the appropriate values, and then run the cell.

Figure 3.12 Zoomed-in spectrum and baseline correction cell

9. The "# overlay spectra" cell prints the stacked array, which enables an assessment of the congruity of the peaks. The line "for i in range(0,len(subtracted_spectra),X):" controls the number of spectra included in the overlay, with "X" defining the step. To overlay all spectra, define X as 1.
10. The next cell (def compute_signal_to_noise(spectrum, noise=(x,y), plot=False):) computes the signal to noise. Define the noise region (x,y) as an area with no peaks or excessive noise. Running the cell will print the S/N for each defined peak.
11. Continue to run cells—you're almost done! The key results cell begins with "print("n = %d" % len(integrations))." This cell prints the integration and standard deviation for each

peak, as well as a variety of other measurements. Copy the integration and standard deviation into the excel workbook as noted below.

12. Run the final two cells. The final cell will print out graphs charting normalized integrations for each set by spectra. This enables a visual assessment of data drift within and between blocks of acquisition.
13. Save the kernel by pressing the save button. If using jupyter notebook, close and halt the kernel after saving it in order to exit the kernel.
14. Complete this process for SQUASH spectra if initially done on proton spectra, or vice versa.
15. Once both proton and SQUASH have been analyzed for one sample, copy the python notebooks from this sample into the folders of the other samples. This will carry over the peak integration area, baseline, and other variables, and thus will ensure that the same values are being used for all samples.
16. Complete the data workup process for each sample, which should be simpler now that all of the variables have been defined. For each sample, double check the quality of each set of spectra using the overlay tool (in bullet point "9") to ensure that there is no "funny business" (to quote Dennis A. Kutateladze).

3.5.4.3 Excel

1. Download an KIE-calculating excel workbook from Eugene's website, or email me for one.
2. Make sure to use the correct workbook for analyzing recovered SM or product.

3. Enter in the integrations and standard deviations for the proper peaks by sample. If analyzing multiple peaks, multiple excel sheets can be used, or one sheet can be modified to include data and analysis for multiple peaks (Fig. 3.13).
4. Enter in the total. number of blocks used, which is (the number of times the sample was acquired)*(the number of blocks within each sample acquisition). (Note: a block is a set of typically 16 or 32 scans. Anywhere between 1–8 blocks are run per sample acquisition. For the excel shown below, four blocks were run per sample acquisition, and the sample was acquired four times to give a total of 16 blocks.)
5. Enter in the calculated conversion and conversion error measurements.
6. The experimental KIE and error will be calculated by the formulas in the sheet and displayed in bold. Congratulations, you measured a KIE!

production run									1H	SQUASH		
Cinnamate epoxidation run 2								**line broadening**				
								baseline order				
sample A con	0.77							**blocks**	16	16		
sample B con	0.75							**transients/block**				
est. error(con	0.01											
	beta olefin			**alpha olefin**								
	1H	**SQUASH**		**1H**	**SQUASH**				beta		alpha	
INTEGRALS	12C	13C		12C	13C			STDEV	12C	13C	12C	13C
108-0p-1	176342.0655	11600.4		176425.1604	10073.1926			pure_A	536.704	41.4906	232.037	37.1188
108-0p-2	181920.1577	11898.3		181698.0505	10359.2830			pure_B	207.731	47.6991	200.323	38.0847
108A	187913.7382	12439		187745.6939	11410.7026			partial_A	266.865	37.4629	220.162	37.3174
108B	184143.0821	12198.9		183769.6194	11128.3336			partial_B	331.155	37.8664	167.153	39.3238
AVERAGES	12C	13C		12C	13C			68% ERR	12C	13C	12C	13C
108A	187913.7382	12438.9807		187745.6939	11410.7026			pure_A	138.0044	10.6686	59.6645	9.5445
108B	184143.0821	12198.9100		183769.6194	11128.3336			pure_B	53.4144	12.2650	51.5098	9.7928
108-0p	179131.1116	11749.3737		179061.6055	10216.2378			partial_A	68.6198	9.6330	56.6108	9.5955
								partial_B	85.1509	9.7367	42.9807	10.1114
FRACTIONAT	R	R0	R/R0	R	R0	R/R0		AVG 68% ERR	12C	13C	12C	13C
108A	0.0662	0.0656	1.0092	0.0608	0.0571	1.0653		partial A	68.6198	9.6330	56.6108	9.5955
108B	0.0662	0.0656	1.0100	0.0606	0.0571	1.0614		partial B	85.1509	9.7367	42.9807	10.1114
								pure	104.6382	11.4946	55.7365	9.6694
KIE	KIE	std err		KIE	std err							
108A	**1.006**	**0.001**		**1.045**	**0.001**			ln(1-F) / ln((1 - F) R/R0)				
108B	**1.007**	**0.001**		**1.045**	**0.001**			sqrt((A/B - 1/C)^2 * deltaF^2 + D/E)				
average	**1.007**			**1.045**								

Figure 3.13 Example excel worksheet; light blue denotes manually entered data

3.6 Supporting Experiments

Full conversion methylation reactions

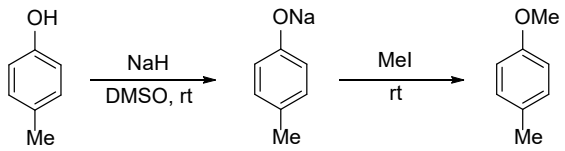

To a dry 100 mL flask equipped with a stir bar was added NaH (600 mg, 60%, 15 mmol, 1.5 equiv) and DMSO (20 mL, anhydrous). A solution of p-cresol (1.622 g, 15 mmol, 1.5 equiv) in DMSO (20 mL, anhydrous) was added dropwise into the flask and the reaction mixture was stirred at room temperature for 1 hour. After that, MeI (1.419 g, 10 mmol, 1.0 equiv) was added dropwise (>15 min) and the reaction was stirred at room temperature for another 2 hours. The reaction mixture was diluted with Et_2O (500 mL) and washed with NaOH (1 M, 100 mL) and water (3x300 mL). The organic phase was dried over MgSO4 and concentrated to give the crude product. The product was purified by silica gel chromatography (eluent: hexane to 10% Et_2O in hex) to yield the methylation product as a colorless oil (reaction A: 1.144 g, 94%; reaction B: 1.1315 g, 93%). After the reaction was done, a small aliquot (0.1 mL) of the reaction mixture was taken and analyzed by 1H NMR (in CDCl3). No MeI peak was found in the crude spectrum, thus indicating a 100% conversion.

Partial conversion reactions

To a dry 100 mL flask equipped with a stir bar was added NaH (~400 mg, 60%, 10 mmol, 0.25 equiv) and DMSO (15 mL, anhydrous). A solution of p-cresol (~1.298 g, 12 mmol, 0.30 equiv) in DMSO (15 mL, anhydrous) was added dropwise into the flask and the reaction mixture was stirred at room temperature for 1 hour. After that, this mixture was transfered dropwise (>15 min) into a solution of MeI (~5.678 g, 40 mmol, 1.0 equiv) in DMSO (15 mL, anhydrous). The reaction was stirred at room temperature for another 2 hours.

Conversion determination (by 1H NMR):

After the reaction was done, a certain amount of DCM (~770 mg, determined by weight) was added into the reaction mixture, then a small aliquot (0.1 mL) was taken and analyzed by 1H NMR (in CDCl3). In the crude spectrum, a ratio of DCM/MeO (in the product) was obtained after phase correction and baseline correction. After a correction factor was applied, a conversion could be calculated from this integral ratio.

Reaction A: NaH (402.6 mg), p-cresol (1.3199 g), MeI (5.682 g), and DCM (774.8 mg); integral ratio: DCM/MeO = 100.00/145.46; conversion: 21.4%

Reaction B: NaH (409.8 mg), p-cresol (1.3475 g), MeI (5.695 g), and DCM (780.9 mg); integral ratio: DCM/MeO = 100.00/146.14; conversion: 21.6%

Benzaldehyde reductions

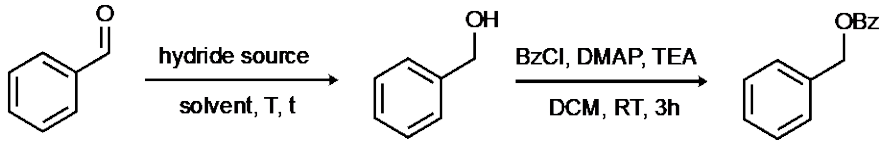

Full conversion benzaldehyde reductions

To a dry 50 mL flask under an atmosphere of N_2 was added benzaldehyde (400 μL, 3.92 mmol, 1 equiv) and methanol (12 mL). The reaction mixture was let stir, and then sodium borohydride (445 mg, 11.76 mmol, 3 equiv (12 equiv H–)) was added in three portions in 2-minute intervals. After stirring for three hours, the reaction reached full consumption of benzaldehyde as observed by NMR analysis of an aliquot. The reaction was diluted with diethyl ether (20 mL) and quenched with NH_4Cl (aq) (10 mL). The organic phase was removed, and the aqueous phase was extracted with diethyl ether (2x20 mL). The combined organic phases were dried over $MgSO_4$,

filtered, and concentrated by rotary evaporation. Purification via flash chromatography (0 to 25% Et_2O in hex) afforded pure benzyl alcohol.

Benzoylation procedure (both full and partial conversion reactions)

The benzyl alcohol product was dissolved in DCM (0.4M) and transferred to a 20-dram vial equipped with a stir bar. To this solution was sequentially added triethylamine (3 equiv), DMAP (0.05 equiv), and benzoyl chloride (1.4 equiv). The vial was capped and the reaction let stir overnight. The reaction was quenched via addition of NH_4Cl (aq). The phases were separated, and the aqueous phase extracted with DCM (2x20 mL). The combined organic phases were dried over $MgSO_4$, filtered, and concentrated by rotary evaporation. Purification via flash chromatography (0 to 2% Et_2O in hex) afforded pure benzyl benzoate.

Partial conversion benzaldehyde reduction reactions

9-Borabicyclo[3.3.1]nonane

To a dry 25 mL flask under an atmosphere of N_2 was added benzaldehyde (203 μL, 2 mmol, 1 equiv), THF (5 mL), and dodecane (100 μL). The reaction mixture was let stir, and then an aliquot (15 μL) was removed, diluted with 1 mL of Et_2O, and analyzed by GC (HP-5, 40→200 ºC, 8 min, 6.3 psi). 9-Borabicyclo[3.3.1]nonane (0.5M in THF, 1 mL, 0.5 mmol, 0.25 equiv) was added and the reaction mixture let stir overnight. An aliquot (15 μL) was removed and diluted for GC analysis, and then the reaction mixture was diluted with diethyl ether (20 mL) and quenched with water (5 mL). The organic phase was removed, and the aqueous phase was extracted with diethyl ether (2x20 mL). The combined organic phases were dried over $MgSO_4$, filtered, and concentrated by rotary evaporation. Purification via flash chromatography (0 to 25% Et_2O in hex) afforded pure benzyl alcohol. The benzyl alcohol was benzoylated as described above.

Conversion calculations for partial reductions with 9-Borabicyclo[3.3.1]nonane:

Table 3.1 Measured ratios of benzaldehyde:dodecane on GC before (t0) and after (tf) reaction for 9BBN reduction replicate 1

	9BBN Rep 1		
	benzaldehyde	dodecane	
t0-rep1	6367	2815	2.261811723
t0-rep2	6355	2801	2.26883256
t0-rep3	6335	2800	2.2625
t0-rep4	6349	2811	2.258626823
t0-rep5	6389	2822	2.263997165
		avg	2.263153654
		std dev	0.003731009
	benzaldehyde	dodecane	
tf-rep1	4986	2884	1.728848821
tf-rep2	5032	2917	1.725059993
tf-rep3	5041	2951	1.708234497
tf-rep4	4973	2920	1.703082192
tf-rep5	5054	2989	1.690866511
		avg	1.711218403
		std dev	0.015745812
Calculation	**Conv**	**0.243878824**	
	Low bar	0.235661279	0.008217545
	High bar	0.252069319	0.008190495

Table 3.2 Measured ratios of benzaldehyde:dodecane on GC before (t0) and after (tf) reaction for 9BBN reduction replicate 2

	9BBN Rep 2		
	benzaldehyde	dodecane	
t0-rep1	6556	3124	2.098591549
t0-rep2	6563	3123	2.101504963
t0-rep3	6662	3175	2.098267717
t0-rep4	6615	3161	2.092692186
t0-rep5	6639	3159	2.101614435
		avg	2.09853417
		std dev	0.003623421
	benzaldehyde	dodecane	
tf-rep1	4655	2888	1.611842105
tf-rep2	4688	2909	1.611550361
tf-rep3	4681	2937	1.593803201
tf-rep4	4701	2966	1.584962913
tf-rep5	4711	2978	1.581934184
		avg	1.596818553
		std dev	0.014264697
Calculation	**Conv**	**0.239079079**	
	Low bar	0.230953753	0.008125326
	High bar	0.247176395	0.008097316

Sodium triacetoxyborohydride

To a dry 25 mL flask under an atmosphere of N_2 was added benzaldehyde (203 μL, 2 mmol, 1 equiv), THF (4 mL), and dodecane (100 μL). The reaction mixture was let stir, and then an aliquot (15 μL) was removed, diluted with 1 mL of Et_2O, and analyzed by GC (HP-5, 40→200 ºC, 8 min, 6.3 psi). Sodium triacetoxyborohydride (127.2 mg, 0.6 mmol, 0.3 equiv) was added and the reaction mixture let stir overnight. An aliquot (15 μL) was removed and diluted for GC analysis, and then the reaction mixture was diluted with diethyl ether (20 mL) and quenched with NH_4Cl (aq) (5 mL). The organic phase was removed, and the aqueous phase was extracted with diethyl ether (2x20 mL). The combined organic phases were dried over $MgSO_4$, filtered, and concentrated by rotary evaporation. Purification via flash chromatography (0 to 25% Et_2O in hex) afforded pure benzyl alcohol. The benzyl alcohol was benzoylated as described above.

Conversion calculations for partial reductions with sodium triacetoxyborohydride:

Table 3.3 Measured ratios of benzaldehyde:dodecane on GC before (t0) and after (tf) reaction for STAB reduction replicate 1

STAB Rep 1			
	benzaldehyde	dodecane	
t0-rep1	6681	2865	2.331937173
t0-rep2	6653	2853	2.3319313
t0-rep3	6636	2841	2.335797254
t0-rep4	6649	2853	2.330529267
t0-rep5			
		avg	2.332548749
		std dev	0.002264683

	benzaldehyde	dodecane	
tf-rep1	5711	3429	1.665500146
tf-rep2	5783	3432	1.68502331
tf-rep3	5780	3454	1.673422119
tf-rep4	5736	3435	1.669868996
tf-rep5	5782	3414	1.693614528
		avg	1.67748582
		std dev	0.011566493
Calculation	**Conv**	**0.280835686**	
	Low bar	0.275173213	0.005662474
	High bar	0.286487175	0.005651489

Table 3.4 Measured ratios of benzaldehyde:dodecane on GC before (t0) and after (tf) reaction for STAB reduction replicate 2

STAB Rep 2			
	benzaldehyde	dodecane	
t0-rep1	8490	3956	2.146107179
t0-rep2	8391	3905	2.148783611
t0-rep3	8383	3909	2.144538245
t0-rep4	8331	3881	2.146611698
t0-rep5			
		avg	2.146510183
		std dev	0.001754017
	benzaldehyde	dodecane	
tf-rep1	7889	5020	1.571513944

tf-rep2		7782	4960	1.568951613
tf-rep3		7845	4995	1.570570571
tf-rep4		7802	4937	1.58031193
tf-rep5		7832	4987	1.570483256
			avg	1.572366263
			std dev	0.004535696
Calculation	**Conv**	**0.267477846**		
	Low bar	0.264763993	0.002713853	
	High bar	0.270187267	0.002709421	

Partial reductions with sodium borohydride

To a dry 25 mL flask under an atmosphere of N_2 was added benzaldehyde (203 μL, 2 mmol, 1 equiv), methanol (6 mL), and dodecane (100 μL). The reaction mixture was let stir, and then an aliquot (15 μL) was removed, diluted with 1 mL of Et_2O, and analyzed by GC (HP-5, 40→200 ºC, 8 min, 6.3 psi). Sodium borohydride (4.5 mg, 0.12 mmol, 0.06 equiv (0.24 equiv H–)) was added and the reaction mixture let stir overnight. An aliquot (15 μL) was removed and diluted for GC analysis, and then the reaction mixture was diluted with diethyl ether (20 mL) and quenched with NH_4Cl (aq) (5 mL). The organic phase was removed, and the aqueous phase was extracted with diethyl ether (2x20 mL). The combined organic phases were dried over $MgSO_4$, filtered, and concentrated by rotary evaporation. Purification via flash chromatography (0 to 25% Et_2O in hex) afforded pure benzyl alcohol. The benzyl alcohol was benzoylated as described above.

Conversion calculations for partial reductions with sodium borohydride:

Table 3.5 Measured ratios of benzaldehyde:dodecane on GC before (t0) and after (tf) reaction for $NABH_4$ reduction replicate 1

	NABH4 Rep 1		
	benzaldehyde	dodecane	
t0-rep1	6511	3148	2.068297332
t0-rep2	6632	3202	2.071205497
t0-rep3	6681	3223	2.072913435
t0-rep4	6621	3191	2.074898151
t0-rep5	6592	3178	2.074260541
		avg	2.072314991
		std dev	0.002654646
	benzaldehyde	dodecane	
tf-rep1	6741	3829	1.760511883
tf-rep2	6744	3847	1.753054328
tf-rep3	6757	3865	1.748253558
tf-rep4	6766	3879	1.744263986
tf-rep5	6758	3882	1.740855229
		avg	1.749387797
		std dev	0.007706059
Calculation	**Conv**	**0.155829203**	
	Low bar	0.151023084	0.030842222
	High bar	0.160623025	0.030763305

Table 3.6 Measured ratios of benzaldehyde:dodecane on GC before (t0) and after (tf) reaction for $NABH_4$ reduction replicate 2

NABH4 Rep 2			
	benzaldehyde	dodecane	
t0-rep1	5105	2359	2.164052565
t0-rep2	5149	2378	2.165264929
t0-rep3	5099	2347	2.172560716
t0-rep4	5211	2404	2.167637271
t0-rep5	5105	2351	2.171416419
		avg	2.16818638
		std dev	0.003724674
	benzaldehyde	dodecane	
tf-rep1	6800	3762	1.807549176
tf-rep2	6880	3807	1.807197268
tf-rep3	6757	3750	1.801866667
tf-rep4	6814	3780	1.802645503
tf-rep5	6837	3795	1.801581028
		avg	1.804167928
		std dev	0.002954462
Calculation	**Conv**	**0.167890756**	
	Low bar	0.16509385	0.016659087
	High bar	0.17067807	0.016601949

Partial conversion cinnamate epoxidation reaction

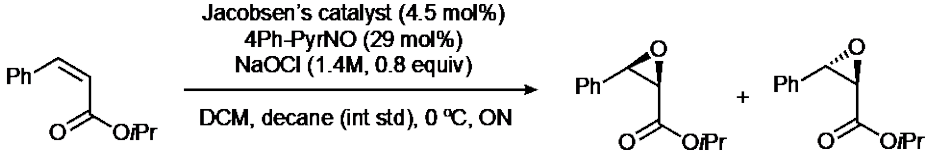

A 20-dram vial was equipped with a stir bar and charged with cis-isopropyl cinnamate (500 mg, 2.63 mmol, 1 equiv), 4-phenylpyridine-N-oxide (130 mg, 0.76 mmol, 29 mol%), dichloromethane (6 mL), and dodecane (125 μL). A 15 μL aliquot was removed, diluted with 1 mL of Et_2O, and subjected to GC analysis (HP-5, 40→200 ºC, 8 min, 6.3 psi). To the reaction medium was then added Jacobsen's catalyst (75 mg, 0.118 mmol, 4.5 mol%). The resulting brown solution was cooled to 0 ºC and then combined with a precooled bleach solution (1.4M, 1.5 mL, 2.1 mmol, 0.8 equiv). The two-phase mixture was vigorously stirred for 12 h at 4 ºC. After this point, a 15 μL aliquot was removed, diluted with 1 mL of Et_2O, and subjected to GC analysis (HP-5, 40→200 ºC, 8 min, 6.3 psi) to determine the conversion. The reaction mixture was diluted with Et_2O (40 mL) and the organic phase was separated, washed with water (2x40 mL), brine (1x40mL), and then dried over $MgSO_4$. Solvents were removed under reduced pressure, and the resulting residue was purified by flash chromatography (0 to 10% Et_2O in hex; care was taken to only collect middle fractions) to afford recovered cinnamate.

Table 3.7 Measured ratios of benzaldehyde:dodecane on GC before (t0) and after (tf) reaction for cinnamate epoxidation replicate 1

Cinnamate epoxidation replicate 1			
	alkene	dodecane	
t0-rep1	3961	1349	2.936249073
t0-rep2	4131	1364	3.028592375
t0-rep3	4142	1349	3.070422535
t0-rep4	4148	1344	3.086309524
t0-rep5	4163	1356	3.070058997
		avg	3.038326501
		std dev	0.060938558

	alkene	dodecane	
tf-rep1	309.5	435.1	0.711330729
tf-rep2	316.9	446.7	0.70942467
tf-rep3	374.8	550.9	0.68034126
tf-rep4	393	560.9	0.700659654
tf-rep5	393.2	559.7	0.702519207
		avg	0.700855104
		std dev	0.01231667
Calculation	**Conv**	0.769328575	
	Low bar	0.757741693	
	High bar	0.779561559	

Table 3.8 Measured ratios of benzaldehyde:dodecane on GC before (t0) and after (tf) reaction for cinnamate epoxidation replicate 2

Cinnamate epoxidation replicate 2			
	alkene	dodecane	
t0-rep1	6143	1961	3.132585416
t0-rep2	6378	2007	3.177877429
t0-rep3	6352	1994	3.18555667
t0-rep4	6464	2025	3.192098765
t0-rep5	6475	2032	3.186515748
		avg	3.174926806
		std dev	0.02420575
	alkene	dodecane	
tf-rep1	535.5	688.9	0.777326172
tf-rep2	610.2	771	0.791439689
tf-rep3	753.3	962.8	0.782405484

tf-rep4	776.7	984.2	0.789168868
tf-rep5	761.5	962.9	0.79084017
		avg	0.786236077
		std dev	0.006142808

Conv	0.752360881
Low bar	0.747352559
High bar	0.756484298

2.6.3 Pulse Sequence Codes

Proton

```
;eek_multi_proton
;Eugene Kwan (06/27/19)
;repeated proton spectra in blocks for KIE measurements
;
;$CLASS=HighRes
;$DIM=2D
;$TYPE=
;$SUBTYPE=
;$COMMENT=



#include <Avance.incl>


"d11=30m"
"acqt0=-p1*2/3.1416"
```

```
d12
1 ze
2 d1
  p1 ph1
  go=2 ph31
  d11 wr #0 if #0
  lo to 1 times td1
exit

;ph1=0 2 2 0 1 3 3 1
;ph31=0 2 2 0 1 3 3 1

ph1=0 1 2 3
ph31=0 1 2 3


;pl1 : f1 channel - power level for pulse (default)
;p1 : f1 channel -  90 degree high power pulse
;p2 : f1 channel - 180 degree high power pulse
;d1 : relaxation delay; 1-5 * T1
;d11: delay for disk I/O                  [30 msec]
;d12: pre-acquisition delay
;ns: number of scans per block
;td1: number of blocks
;FnMODE: undefined
```

```
;this pulse program produces a ser-file (PARMOD = 2D)



;$Id: eek_multi_proton 2019/06/27 10:44:00am $
```

SQUASH

```
; SQUASH
; single quantum supression of hydrogens bound to 12C
; Eugene Kwan, 2019
;
;$CLASS=HighRes
;$DIM=2D
;$TYPE=
;$SUBTYPE=
;$COMMENT=

#include <Avance.incl>
#include <Grad.incl>
#include <Delay.incl>

"p2=p1*2"
"p4=p3*2"
"d6=1s/(cnst13*4)"
"DELTA1=d6-larger(p2,p14)/2-4u"
;"DELTA3=DELTA1-p28"
"acqt0=0"
baseopt_echo
```

```
1 ze
2 d1

  ; generate antiphase
3 (p1 ph1)
  DELTA1 pl0:f2
  4u
  (center (p2 ph2) (p14:sp3 ph2):f2 )
  4u
  DELTA1 pl2:f2 UNBLKGRAD
  ;DELTA3 pl2:f2 UNBLKGRAD
  ;(p28 ph3) ; trim

          ; INEPT
  (p1 ph3)
  p16:gp3   ; purge
  d16       ; stabilization
  (p3 ph4):f2

          ; retro-INEPT
          (center (p1 ph5) (p3 ph6):f2 )

  4u BLKGRAD
  go=2 ph31
  30m wr #0 if #0
lo to 1 times td1
exit
```

```
ph1  = 0 0 0 0 1 1 1 1 2 2 2 2 3 3 3 3   0 0 0 0 1 1 1 1 2 2 2 2 3 3 3 3
ph2  = 0 0 0 0 1 1 1 1 2 2 2 2 3 3 3 3   3 3 3 3 0 0 0 0 1 1 1 1 2 2 2 2
ph3  = 3 3 3 3 0 0 0 0 1 1 1 1 2 2 2 2   3 3 3 3 0 0 0 0 1 1 1 1 2 2 2 2
ph4  = 0 0 2 2 1 1 3 3 2 2 0 0 3 3 1 1   0 0 2 2 1 1 3 3 2 2 0 0 3 3 1 1
ph5  = 0 0 0 0 1 1 1 1 2 2 2 2 3 3 3 3   0 0 0 0 1 1 1 1 2 2 2 2 3 3 3 3
ph6  = 0 2 2 0 1 3 3 1 2 0 0 2 3 1 1 3   2 0 0 2 3 1 1 3 0 2 2 0 1 3 3 1
ph31 = 0 2 0 2 1 3 1 3 2 0 2 0 3 1 3 1   0 2 0 2 1 3 1 3 2 0 2 0 3 1 3 1

;pl0 : 0W
;pl1 : f1 channel - power level for pulse (default)
;pl2 : f2 channel - power level for pulse (default)
;sp3: f2 channel - shaped pulse 180 degree for inversion
;spnam3: Crp60,0.5,20.1
;p1 : f1 channel -  90 degree high power pulse
;p2 : f1 channel - 180 degree high power pulse
;p3 : f2 channel -  90 degree high power pulse
;p4 : f2 channel - 180 degree high power pulse
;p14: f2 channel - 180 degree shaped pulse for inversion
;     = 500usec for Crp60,0.5,20.1
;p16: purge pulse duration
;d16: gradient stabilization time
;d1 : relaxation delay; > 5 * T1
;cnst13: one bond carbon-proton coupling constant
;ns: scans per block (multiple of 32)
;ds: dummy scans (set to zero)
;td1: number of blocks
;FnMODE: undefined
```

;for z-only gradients:

;gpz3: 30%

;use gradient files:

;gpnam3: SMSQ10.100

;$Id: SQUASH $

Sample Preparation

For methylation reactions, three sets of four samples of anisole were prepared (100 mg in 500 μL of CDCl3, 20 mg in 550 μL of CDCl3, 1 mg in 550 μL of CDCl3, and 0.1 mg in xx μL of CDCl3). Two of the samples in each set were full conversion samples (F = 100%) with respect to the methyl iodide starting material and two were partial conversion samples (F = 21.4%, 21.6%) with respect to the methyl iodide starting material. The samples were prepared in Wilmad 528-PP-9 NMR tubes and subsequently hermetically sealed under air at room temperature.

For reduction reactions, eight samples of cinnamate were prepared (30 mg in 550μL of CDCl3). Two of the samples were starting material samples (F = 0%) and six were high conversion samples (9BBN: F = 24.4%, 23.9% STAB: 28.1%, 26.7% $NaBH_4$: 15.6%, 16.8%). Those samples were prepared in Wilmad 528-PP-9 NMR tubes and subsequently hermetically sealed under N_2 at room temperature.

For Mn[salen]-catalyzed epoxidation reactions, four samples of cinnamate were prepared (30 mg in 550μL of CDCl3). Two of the samples were starting material samples (F = 0%) and two were high conversion samples (F = 76.9% and 75.2%). Those samples were prepared in Wilmad 528-PP-9 NMR tubes and subsequently hermetically sealed under N_2 at room temperature.

Calculation of KIE and Error Bars

KIE was calculated according to:

$$\frac{\log(1-F)}{\log\left(1-F\frac{R}{R_0}\right)}$$

where F is the fractional conversion, R is the 13C/12C ratio in the product, R0 is the ratio in the starting material, and log refers to the natural logarithm. R0 is experimentally determined by taking the reaction to 100% conversion and quantitating product because this minimizes errors caused by deviations in response factors. The propagated error in this formula was calculated in Mathematica (using https://github.com/FlashTek/mathematica-error-propagation): TeXForm[FullSimplify[ErrorProgataionPrintFormula[Log[1 - F]/Log[1 - F*R/Subscript[R, 0]], {F, R, Subscript[R, 0]}]]]

$$\sqrt{\frac{(F-1)^2F^2R^2\log^2(1-F)\sigma_{R_0}^2+(F-1)^2F^2R_0^2\log^2(1-F)\sigma_R^2+R_0^2\sigma_F^2\left((F-1)R\log(1-F)+(R_0-FR)\log\left(1-\frac{FR}{R_0}\right)\right)^2}{(F-1)^2R_0^2(R_0-FR)^2\log^4\left(1-\frac{FR}{R_0}\right)}}$$

2.6.6 KIE data

Methylation reactions

Table 3.9 KIE measurements and calculations for 0.1mg methylation reactions

	1H	SQUASH
INTEGRALS	12C	13C
full_A	10.0523	9.3690
full_B	10.0639	9.4677
partial_A	7.7971	6.9185
partial_B	9.7207	8.5744

AVERAGES	12C	13C
partial A	7.7971	6.9185
partial B	9.7207	8.5744
full	10.0581	9.4184

FRACTIONATION	R	R0	R/R0
sample A	0.8873	0.9364	0.9476
sample B	0.8821	0.9364	0.9420

KIE	KIE	std err
sample A	**1.063**	**0.006**
sample B	**1.070**	**0.008**
average	**1.066**	**0.005**

Table 3.10 KIE error measurements and calculations for alkene in cinnamate epoxidation

STDEV	12C	13C
full_A	0.0040	0.1370
full_B	0.0019	0.1742
partial_A	0.0035	0.1262
partial_B	0.0026	0.1978

68% ERR	12C	13C
full_A	0.0015	0.0284
full_B	0.0007	0.0361
partial_A	0.0013	0.0262
partial_B	0.0010	0.0410

AVG 68% ERR	12C	13C
partial A	0.0013	0.0262

partial B	0.0010	0.0410
full	0.0012	0.0325

Reduction reactions

Table 3.11 KIE measurements and calculations for benzaldehyde reduction with STAB

	1H	SQUASH	
INTEGRALS	12C	13C	
full_A	326548.6026	20138.0675	
full_B	330981.4533	20404.8612	
partial_A	309767.5875	18970.3703	
partial_B	255565.9577	15641.0267	
AVERAGES	12C	13C	
partial A	309767.5875	18970.3703	
partial B	255565.9577	15641.0267	
full	328765.0280	20271.4644	
FRACTIONATION	R	R0	R/R0
sample A	0.0612	0.0617	0.9932
sample B	0.0612	0.0617	0.9926
KIE	KIE	std err	
sample A	**1.008**	**0.002**	
sample B	**1.009**	**0.003**	
average	**1.008**		

Table 3.12 KIE error measurements and calculations for benzaldehyde reduction with STAB

STDEV	12C	13C
full_A	300.9564	47.4434
full_B	172.0804	48.0044
partial_A	327.849	40.9894
partial_B	416.2644	39.5621

68% ERR	12C	13C
full_A	178.9078	28.2034
full_B	102.2957	28.5369
partial_A	194.8945	24.3667
partial_B	247.4543	23.5183

AVG 68% ERR	12C	13C
partial A	194.8945	24.3667
partial B	247.4543	23.5183
full	145.7265	28.3706

Table 3.13 KIE measurements and calculations for benzaldehyde reduction with 9BBN

	19F	**MQF**
INTEGRALS	12C	13C
full_A	326548.6026	20138.0650
full_B	330981.4533	20404.8600
partial_A	222473.0723	13325.8328
partial_B	324252.709	19348.8477

AVERAGES	12C	13C
partial A	222473.0723	13325.8328
partial B	324252.7090	19348.8477

full	328765.0280	20271.4625

FRACTIONATION	R	R0	R/R0
sample A	0.0599	0.0617	0.9714
sample B	0.0597	0.0617	0.9678

KIE	KIE	std err
sample A	**1.035**	**0.004**
sample B	**1.039**	**0.003**
average	**1.037**	

Table 3.14 KIE error measurements and calculations for benzaldehyde reduction with 9BBN

STDEV	12C	13C
full_A	300.9564	47.4434
full_B	172.0804	48.0044
partial_A	355.4645	49.2950
partial_B	283.5845	40.9168

68% ERR	12C	13C
full_A	178.9078	28.2034
full_B	102.2957	28.5369
partial_A	211.3110	29.3041
partial_B	168.5809	24.3236

AVG 68% ERR	12C	13C
partial A	211.3110	29.3041
partial B	168.5809	24.3236

full	145.7265	28.3706

Table 3.15 KIE measurements and calculations for benzaldehyde reduction with $NaBH_4$

	1H	SQUASH
INTEGRALS	12C	13C
full_A	326548.6026	20138.0650
full_B	330981.4533	20404.8600
partial_A	324777.0451	19418.1902
partial_B	334156.5357	19903.0508

AVERAGES	12C	13C
partial A	324777.0451	19418.1902
partial B	334156.5357	19903.0508
full	328765.0280	20271.4625

FRACTIONATION	R	R0	R/R0
sample A	0.0598	0.0617	0.9697
sample B	0.0596	0.0617	0.9660

KIE	KIE	std err
sample A	**1.034**	**0.002**
sample B	**1.039**	**0.003**
average	**1.036**	

Table 3.16 KIE error measurements and calculations for benzaldehyde reduction with $NaBH_4$

STDEV	12C	13C
full_A	300.9564	47.4434

full_B	172.0804	48.0044
partial_A	132.0535	46.0552
partial_B	390.6843	64.2400
68% ERR	12C	13C
full_A	178.9078	28.2034
full_B	102.2957	28.5369
partial_A	78.5011	27.3782
partial_B	232.2479	38.1884
AVG 68% ERR	12C	13C
partial A	78.5011	27.3782
partial B	232.2479	38.1884
full	145.7265	28.3706

Epoxidation reactions

Table 3.17 KIE measurements and calculations for alkene in cinnamate epoxidation

	beta olefin			**alpha olefin**		
	1H	**SQUASH**		**1H**	**SQUASH**	
INTEGRALS	12C	13C	R or R0	12C	13C	R or R0
0% conv rep 1	176342.0655	11600.4233	0.0658	176425.1604	10073.1926	0.0571
0% conv rep 2	181920.1577	11898.324	0.0654	181698.0505	10359.2830	0.0570
Part conv rep 1	187913.7382	12438.9807	0.0662	187745.6939	11410.7026	0.0608
Part conv rep 2	184143.0821	12198.91	0.0662	183769.6194	11128.3336	0.0606
AVERAGES	12C	13C		12C	13C	
Part conv rep 1	187913.7382	12438.9807		187745.6939	11410.7026	
Part conv rep 2	184143.0821	12198.9100		183769.6194	11128.3336	

0% conv	179131.1116	11749.3737		179061.6055	10216.2378	
FRACTIONATION	R	R0	R/R0	R	R0	R/R0
Part conv rep 1	0.0662	0.0656	1.0092	0.0608	0.0571	1.0653
Part conv rep 2	0.0662	0.0656	1.0100	0.0606	0.0571	1.0614
KIE	KIE	std err		KIE	std err	
Part conv rep 1	**1.006**	**0.001**		**1.045**	**0.001**	
Part conv rep 2	**1.007**	**0.001**		**1.045**	**0.001**	
average	**1.007**			**1.045**		

Table 3.18 KIE error measurements and calculations for alkene in cinnamate epoxidation

	beta		alpha	
STDEV	12C	13C	12C	13C
pure_A	536.704	41.4906	232.0373	37.1188
pure_B	207.7306	47.6991	200.3234	38.0847
partial_A	266.8646	37.4629	220.1615	37.3174
partial_B	331.1549	37.8664	167.1533	39.3238
68% ERR	12C	13C	12C	13C
pure_A	138.0044	10.6686	59.6645	9.5445
pure_B	53.4144	12.2650	51.5098	9.7928
partial_A	68.6198	9.6330	56.6108	9.5955
partial_B	85.1509	9.7367	42.9807	10.1114
AVG 68% ERR	12C	13C	12C	13C
partial A	68.6198	9.6330	56.6108	9.5955
partial B	85.1509	9.7367	42.9807	10.1114

pure	104.6382	11.4946	55.7365	9.6694